STUDY OF MODIFIED SIMULATED MOVING BED SYSTEMS FOR TERNARY SEPARATION

KURUP ANJUSHRI SREEDHAR

NATIONAL UNIVERSITY OF SINGAPORE

2005

STUDY OF MODIFIED SIMULATED MOVING BED
SYSTEMS FOR TERNARY SEPARATION

KURUP ANJUSHRI SREEDHAR
(B. Chem. Engg., UDCT, India)

A THESIS SUBMITTED

FOR THE DEGREE OF DOCTOR OF PHILOSOPHY

DEPARTMENT OF CHEMICAL & BIOMOLECULAR ENGINEERING

NATIONAL UNIVERSITY OF SINGAPORE

2005

Dedicated to

my beloved parents, sister

&

Hari…..

Acknowledgements

Table of Contents

Summary

Simulated Moving Bed (SMB) Technology has been one of the most popular separation techniques widely used in the petroleum and sugar industries, at least for the last few decades. Of late, the superior separating power of SMB has been a motivating factor for the researchers to enhance the performance of SMB at minimal operating costs. This has led to the development of systems such as Varicol, SMB with variable section flow rates, etc. The separating potential of SMB has also been exploited to improve the conversion of reactants and product purity of some reversible reactions. The SMB system is basically a binary separator and can aid in the separation of a feed containing two or more components into only two product streams. Hence, lately, research is also being done to bring about a multi-component (ternary or quaternary) separation using the SMB technology.

There are many parameters that influence the performance of the SMB systems. The selection of the optimal operating parameters is, thus, not straightforward and is subject to various separation / reaction requirements and constraints that are usually conflicting. The scope of this research work is two fold. Firstly, this study aims at performing a thorough and comprehensive optimization study of the SMB and its modifications such as Varicol and SMB with variable flow rates for two industrially important systems, the separation of C_8 aromatics to recover *p*-xylene and the reaction-separation system involving the biochemical reaction, Inversion of Sucrose yielding Fructose and Glucose. A robust, state-of-the-art non-traditional global optimization technique known as the elitist Non-dominated Sorting Genetic Algorithm with Jumping Genes (NSGA-II with JG) was used in this investigation to perform multi-objective optimization study. For both the separation systems, it was seen that systematic optimization resulted in higher performance of

the system in terms of recovering more of the desired product while consuming less desorbent. Optimization studies on Varicol and SMB with a variable flow mode showed considerable improvement in the performance.

After dealing with these binary separation systems, the study focuses on the application of SMB technology for ternary separation – the main aim of this thesis. Three configurations, a five-zone SMB, a four-zone SMB and a novel system called as the Pseudo-SMB, reported in the literature for ternary separations and which can be easily modified from the conventional SMB, are studied systematically. Performance comparisons of these systems are done under the effect of different separation conditions such as low adsorption selectivities, high mass transfer resistance, non-linearity in the adsorption isotherm, etc. These systems are also compared for the industrial-scale separation of C_8 aromatics containing the three xylene isomers (*o*, *m*, and *p*-xylene) and ethyl benzene. The objective of this study is to recover the two industrially important chemicals *p*-xylene and ethyl benzene in a single SMB unit. All the comparisons are done at the optimal conditions by performing multi-objective optimization studies. The studies revealed that the five-zone SMB system is preferable to the four-zone SMB for systems with non-ideal separation conditions. However, with this system simultaneous recovery of all the three components with high purity is not possible and in that case it has to be coupled with another SMB in series. With Pseudo-SMB system, however, it was seen that, it is possible to achieve high purities of all the three components even for difficult separations such as the C_8 aromatics, but at the cost of high adsorbent and desorbent consumption.

NOMENCLATURE

B   Langmuir adsorption constant (cm^3/g)

Bi_m mass Biot number

C   concentration in mobile phase (g/cm^3 or kg/m^3)

D   desorbent

D_{ax} axial diffusivity (cm^2/s or m^2/s)

d_{col} diameter of the column (cm or m)

d_p particle diameter (cm)

E   axial dispersion coefficient, solvent flow rate

Ex   extract

F   error (objective) function for optimization, feed (m^3/min or ml/min)

H   height equivalent of a theoretical plate (HETP) (cm), Henry constant

I   objective function

J   theoretical number of cells, objective function

K   reaction equilibrium constant (mol/l), linear adsorption equilibrium constant, Langmuir adsorption constant (m^3/kg or q^*/C or cm^3/g)

K'   adsorption constant for a homogeneous adsorbent particle

k_a mass-transport coefficient (LDF) (min^{-1})

K_e linear adsorption constant of the enzyme

k_f film mass-transport coefficient (m/s)

K_{fi} lumped mass transfer coefficient (min^{-1})

k_h mass-transport coefficient (LDF) (s^{-1} or min^{-1})

K_{mm} Michaelis-Menten constant

k_p mass-transport coefficient in the pores (s^{-1})

k_r reaction rate constant (s^{-1})

k_μ mass-transport coefficient in the micro-particles (s^{-1})

L   length (cm or m)

L_{col} column length (cm or m)

m   fluid to solid velocity ratios

MC   modified configuration

M_F mass flow rate of fructose (kg/h)

N   number, saturation capacity of the adsorbent (g/cm^3)

N_{col} number of columns

P   purity, section, bed phase ratio

p   vector of parameters tuned, number of columns in section P

Pe   Peclet number

PR   productivity (kg/m^3 solid/h)

Pur   purity (%)

q   adsorbed phase concentration (g/cm^3), number of columns in section Q

$\bar{q}$ adsorbed concentration averaged over the particle volume (kg/m^3)

$\bar{q}^*$ concentration at the particle surface in equilibrium with bulk fluid (kg/m^3)

Q   flow rate (m^3/min or m^3/h or cm^3/min), section

Q_F feed flow rate (m^3/min or ml/min)

Q_D desorbent flow rate (m^3/min or ml/min)

Q_{Ex} extract flow rate (m^3/min or ml/min)

Q_{Ra} raffinate flow rate (m^3/min or ml/min)

q_m adsorbed phase saturation concentration (g/cm^3 or kg/kg of solid)

r   number of columns in section R

R   reaction rate (mol/l –cat/min), section

Ra   raffinate

Rec   recovery (%)

R_p radius of the pore (m)

s   number of columns in section S

S   selectivity, section, bed cross section

SMB   simulated moving bed

SMBR   simulated moving bed reactor

T   temperature (K)

t   time (min)

TMB   true moving bed

t_p product collection time within a switching interval (min)

t_s switching period (min)

T_{step} step duration (min)

u   superficial column velocity (cm/min or m/min)

U_F fluid interstitial velocity (cm/min or m/min)

u_g fluid phase velocity (cm/min or m/min)

u_s solid velocity (cm/min or m/min)

u_{sol} solute migration velocity

u_{wi} linear velocity of the concentration wave of component i

V   volume (ml), velocity (cm/min)

Varicol   variable column system

x   length (cm or m)

X   conversion

Y   yield

z   axial coordinate (cm or m)

ΔP pressure Drop (bar)

Greek Symbols

α number of mass-transfer units for a homogeneous adsorbent particle (LDF)

ε bed porosity

ε^* overall void fraction of the bed

ε_p intra-particle porosity

χ dimensionless length

Ω column configuration

ρ density of adsorbent (g/cm^3)

ρ_B bed density (g/cm^3)

ρ_f feed density (g/cm^3)

ψ dimensionless velocity

ζ pseudo solid velocity (m/h)

ν solid to fluid volume ratio

γ dimensionless concentration, flow ratio parameter between solid and fluid

     phase

ρ_f feed density (g/cm^3)

τ dimensionless time

θ dimensionless time

σ relative carrying capacity, reaction stoichiometric coefficient

η feed composition

ϕ section, adsorption selectivity

ξ   dimensionless length

Subscripts and Superscripts

1   step 1

2   step 2

A, B, C   components or species in the feed mixture

b   bed

col   column

D   desorbent, eluent, solvent

e, eqm   equilibrium, effective

EB   ethylbenzene

Enz   enzyme

Ex   extract

exp   experiment

F   feed, fructose

f   feed

G   glucose

h   homogeneous particle

i   species i

k   column k

mX   m-xylene

NC   number of components

o   initial, pre-exponential, standard

oX   o-xylene

P,Q,R,S   sections of the SMB system

pDEB   paradiethylbenzene

pX   p-xylene

Ra   raffinate

s   switching, solid

Suc   sucrose

SucF   sucrose in feed

List of Figures

List of Tables

Chapter 1   Introduction

1.1 Simulated Moving Bed system

In Chemical Industry, the life science based products are regarded to have the most promising market in the near future. Since pharmaceuticals, food products and fine & specialty chemicals are subject to stringent restrictions on their quality, and at the same time as these products are sensitive to the processing conditions, efficient methods for separation of these products are necessitated. In particular, chromatographic separation is a suitable technology for tasks of such nature. To improve the economic viability of chromatographic processes, a continuous counter-current operation is often desirable. However, the real counter-current movement of solids, i.e., the adsorbent, leads to serious operating problems. Therefore, the Simulated Moving Bed (SMB) technology is an interesting alternative since it provides the advantages of a continuous counter-current operation while avoiding the technical problems associated with the operation of a True Moving Bed (TMB). The process was first realized in the family of SORBEX processes by Universal Oil Products (UOP) (Broughton & Gerhold, 1961) and is increasingly used in a wide range of industries. Some of the recent technical applications of SMB are in the separation of cyclic hydrocarbons, sugars, enantiomers, etc. These recent developments spur researchers to further optimize SMB processes, in order to improve the quality of the chemicals (purity of the products) and achieve better economics.

Quite a lot of research articles on SMB have been reported especially in the last couple of decades, which are indispensable in understanding the principles of

SMB operation and in designing the SMB process for binary separation. To mention a few SMB design strategies are the McCabe-Thiele method (Ruthven and Ching, 1989), the Triangle theory (Storti et al., 1993) and the Standing Wave concept (Ma and Wang, 1997). These strategies stem from the analytical solutions for an equivalent TMB model and are very much accurate and convenient especially for the cases wherein the mass transfer resistances are quite negligible and the adsorption is described by a linear isotherm. However, these approaches do not involve any systematic and rigorous mathematical optimization and as a result might prove inadequate in designing SMB systems under conditions such as severe column dispersion, complex adsorption isotherms or the existence of reaction.

1.2 Developments in SMB

The integration of reaction and separation in a single unit is quite a promising area in Chemical Engineering, which improves the economics and efficiency of the both processes. Similar to Reactive Distillation and Membrane Reactors, which couples chemical reaction & distillation together in one process and reaction & membrane separation in a single unit respectively, the Simulated Moving Bed Reactor (SMBR) technology combines the more powerful and energy-saving separation technology, SMB, with a reversible chemical reaction in a single set up. Apart from its economic viability, SMBR also enhances the conversion, yield, selectivity, and purity of the desired product beyond those predicted by thermodynamics of equilibrium limited (reversible) reactions. Recent investigations have proved successfully the high efficiency of SMBR that preserves the separation power and inherent advantages of SMB process. However, in spite of being acknowledged for its

superior separation power that has triggered several investigations on the performance of SMBR, reports on its industrial applications are not quite flattering. The reason probably can be the complexity of the process and the difficulties in the design. The design strategies available for SMB cannot be used directly for SMBR because of the complexity in obtaining analytical solutions from the TMB model due to the introduction of reaction kinetics. Hence, a rigorous optimal design of SMBR would be necessary and helpful in further understanding of this technology and thereby increasing its competitiveness.

In case of a conventional SMB system, during some part of its operation, the solids (stationary phase) in some of the columns are completely free of solutes, or in other words there is not an effective utilization of the solids, so that the separation capacity is significantly reduced. The novel process, Varicol, reported by Ludemann-Hombourger et al. (2000; 2002), which uses a non-synchronous switching pattern as against the synchronous switching of SMB is one method to improve the efficiency of SMB without introducing any additional fixed cost. Varicol is actually a conceptual innovation to SMB for a given multi-column set-up. Unlike the SMB, in which input/output ports shift simultaneously and equally along a series of fixed beds, Varicol is based on a non-synchronous switch of the input/output ports, either forward or even in backward direction. As a result, in Varicol, the column number and the length of each section may vary with time; the pseudo solid velocity is no longer constant with respect to the input/output lines. Varicol process could, therefore, have several different column configurations during one global switching period, which endow it more flexibility than the SMB. This very advantage can make the design of this process more cumbersome since then one has to explore all the possibilities of the

different column configurations. A rigorous mathematical optimization becomes a must in such cases.

A conventional SMB has constant flow rates during each switching period. An alternative option that could improve the effective utilization of adsorbent phase would be to vary the section flow rates of the fluid during a global switching interval. Strategies such as the partial feed (feed introduced during a part of the switching period), variable feed, variable desorbent or varying all the section flow rates simultaneously during a switching period have been reported in the literature and have been shown to perform more efficiently compared to the conventional SMB with fixed fluid flow rates. However, similar to Varicol, this flexibility in changing the section flow rates again makes the designing of these systems difficult since such a change in fluid flow rates would affect all concentration profiles in the process and may even lead to decreased performance. Therefore a rigorous optimization study on SMB/SMBR process model is required, taking into consideration all these interdependencies.

1.3 Ternary separation with SMB

A conventional (four-zone) SMB is a binary separator, which means a feed stream containing two or more components can be split only in two fractions. However, sometimes in industry, a multi-component mixture may have two or more than two components that have to be recovered with the best possible purity. Even in case of binary mixtures, sometimes a third component that acts like an impurity may be present and has to be completely eliminated from the two product streams. In such a scenario, performing multi-component separation (such as ternary or quaternary)

becomes essential. To mention a few of such industrial systems where multi-component separation becomes important, we have examples such as purification of biomass hydrolyzate to produce sugar mixture, separation of complex sugar molecules, production of raffinose from beet molasses, separation of C_8 aromatics containing p-xylene, m-xylene, o-xylene and ethyl benzene, etc. Several concepts have, thereby, been proposed and developed in order to perform such multi-component separations using SMB. To achieve a ternary separation, the concepts mentioned in the literature range from simplest ones, such as using two conventional SMBs in series, to the ones which are more intricate in operation such as the pseudo SMB process. A few other concepts to facilitate ternary separation, such as using different adsorbents or desorbents in different sections, using different operating conditions such as varying the section flow rates or using five or more than five sections instead of the conventional four-section SMB, etc., have also been proposed and developed. A review of the same can be found in the second chapter. However, these systems, due to the addition of more sections and/or product streams (compared to conventional SMB used for binary separation), tend to be more complicated and have more design variables. As a result the design and consequently optimization of these systems becomes rather difficult. Also most of these systems are designed for components described by linear isotherms and the performances of these systems, in the presence of non-idealities such as non-linearity in the adsorption isotherm, high mass transfer resistances, etc., are not dealt much in the literature.

1.4 Optimization of SMB systems

There are a few works in the open literature that report on the optimization of SMB systems (Storti et al., 1988; Proll and Kusters, 1998; Karlsson et al., 1999;

Dünnebier et al., 2000). However, most of these studies involve single (scalar) objective functions, incorporating several objectives with weightage factors, which are not efficient as they lose out certain optimal solutions due to the high non-convexity of the problem (Bhaskar et al., 2000). The application of multi-objective optimization with objective functions that are vectors provides a much better scenario of the process and allows for a more accurate decision on the optimal operating point (Bhaskar et al., 2000). In the case of multi-objective optimization problems, an entire set of optimal solutions, that are *equally* good when the objectives are conflicting by nature, can exist. These solutions are known as Pareto-optimal (or non-dominated) solutions. None of the non-dominated solutions in the Pareto set is superior to any other, and hence, any one of them is an acceptable solution. The choice of one solution over the other requires additional knowledge of the problem, and often, this knowledge is intuitive and non-quantifiable. The Pareto set, however, is extremely useful since it narrows down the choices and helps to guide a decision-maker in selecting a desired operating point (called the *preferred* solution) from among the (restricted) set of Pareto-optimal points, rather than from a much larger number of possibilities (Deb, 1995; 2001; Zhang et al., 2002b).

The ε-Constraint Method (Chankong and Haimes, 1983), the Goal Attainment Method (Fonseca and Fleming, 1998) and the Non-dominated Sorting Genetic Algorithm (NSGA) (Srinivas and Deb, 1995) are some of the recent developments to tackle multi-objective optimization problems. For NSGA, several merits have been realized: (a) its efficiency is relatively insensitive to the shape of the Pareto-optimal front; (b) problems with uncertainties, stochasticities, and discrete search spaces can be handled efficiently; (c) the 'spread' of the Pareto set obtained is excellent; and (d) one run is sufficient to obtain the entire Pareto set (as compared to other methods such

as the ε-Constraint Method which needs to be applied several times over and over again to hit the optima). A comprehensive description of the application of NSGA in Chemical Engineering was reported by Bhaskar et al. (2000). Elitist non-dominated sorting genetic algorithm (NSGA-II) with Jumping Genes (JG) is a further improvement to this optimization algorithm. This algorithm was reported to be faster thereby reducing the computational load in the cases of computationally-intensive problems. A short note about the same is given in Appendix A. In the presence of complicated problems such as optimizing SMB, which involves variables that are continuous as well as discrete, and which might have many objectives to be optimized such as the purity of the products, their recoveries etc., using such robust algorithms (Bhaskar et al., 2000) for optimization becomes important. Moreover, emphasis on the modified SMB systems such as Varicol or the ones used for ternary separation is increasing. The optimization procedure for these systems becomes even more complicated compared to SMB, since the number of decision variables further increases in these cases.

1.5 Scope & Organization of the thesis

This dissertation can be broadly divided into two parts. In the first part, a systematic and comprehensive multi-objective optimization study of non-reactive and reactive SMB systems and its modifications such as the Varicol and SMB with variable feed flow is performed. The optimization algorithm used in the study is NSGA-II with JG. Simulations and optimization studies are carried out for two representative cases: (a) an industrially important separation system which deals with the recovery of p-xylene from the C_8 aromatics mixture and (b) a reaction-separation

system for the inversion of sucrose to fructose and glucose. The method of optimization used in this study is very general and can be applied to other modified SMB systems. In this part of the thesis, the procedure to be used for multi-objective optimization is illustrated, and the solutions of few double objective optimization problems with few constraints are discussed. It should be noted that a whole variety of other problems can, indeed, be formulated and solved, depending upon one's interest. These simulation and optimization studies, which involved writing intensive simulation algorithms for each separation problem, helped in achieving a good understanding of the otherwise difficult concept of SMB and its different modifications. This part of the thesis addresses, for the *first time ever*, new concepts such as operation of SMBR with variable flow rates for sucrose inversion and application of Varicol for C_8 aromatics. In addition, these studies on binary separation also serve as excellent warm-up exercises to handle more intricate SMB systems for ternary separation, which is the central theme of this thesis.

The second part of the thesis deals with the application of SMB technology for ternary separation. Three configurations reported in the literature that are used for ternary separations are studied. Performances of these systems are studied and compared under the effect of different conditions ranging from the most ideal separation conditions to increasing non-ideality in the separation conditions. The performance of these systems is also compared by applying them on the industrial-scale problem for ternary separation of C_8 aromatics. The objective in this case was to recover both p-xylene and ethyl benzene in one pass, since among the four isomers these two are the most attractive chemicals and are gaining increasing importance in the market. All the comparisons are done at the optimal conditions. It should be noted that the emphasis of this study was to explore the performance of systems that are

relatively easy in operation from the practical point of view and can be easily modified from the conventional SMB (as will be explained in the later chapters). The other complicated systems with more intricate designs can theoretically give the best performance but the practical operation of these configurations is more difficult and hence these are not considered in this study.

This dissertation is organized into eight chapters. Following this short introduction to the SMB systems, in the subsequent chapter (Chapter 2), the background and applications of SMB technology is discussed; several SMB design strategies, optimization works and recent developments in the SMB technology are reviewed. This is followed by a review on the application of SMB to effect ternary separation and designing these modified SMB systems.

In Chapter 3, a methodical multi-objective optimization study of SMB and Varicol for the recovery of p-xylene from the mixture of C_8 aromatics is elaborately discussed. This is an industrial scale process and the operating conditions are obtained from the work of Minceva and Rodrigues (2002). A few double-objective optimization problems were solved to determine the optimum number of columns, their length and distribution in different zones. Optimization study was also extended to Varicol. The objective in this study was to maximize the recovery of p-xylene while consuming less desorbent. Results are presented and discussed in detail and the optimum results are also explained using equilibrium theory by locating them in the pure separation region.

In Chapter 4, a comprehensive optimization study is carried out to evaluate the performance of a reactive Simulated Moving Bed (SMBR) system and reactive Varicol, for an industrially important biochemical reaction-separation problem, the

inversion of sucrose and the in-situ separation of the products, viz., glucose and fructose. In addition, the concept of a variable feed mode is studied. The reaction and adsorption parameters for this reaction-separation problem reported in the work of Azevedo and Rodrigues (2001b) are used in this study. The chapter contains a comparison of the optimal performances that can be achieved by the reactive SMB, reactive Varicol and reactive SMB with a variable flow mode (both discrete and continuous as explained in the chapter). The objective in this study is to maximize the productivity of fructose (more desired in the industry) while minimizing the water consumption, which is a major concern in the sugar industries since the product streams are very dilute and consequently more energy is spent in concentrating them.

Chapter 5 deals with the study of modified SMB systems for ternary separation. In this chapter, two configurations were studied systematically and their performance in the presence of different kinetic and adsorption parameters is studied and compared. All these studies are done at optimal conditions and again in these cases multi-objective optimization is performed using NSGA-II with JG. The objective of the optimization exercise is to maximize the purities of all three components. In Chapter 6, some modifications are suggested to the configurations mentioned in Chapter 5 and these modified configurations are applied for the industrial-scale problem of simultaneous recovery of both p-xylene and ethyl benzene from the mixture of C_8 aromatics.

In Chapter 7, an unconventional and innovative system called as pseudo-simulated moving bed (SMB) is studied. The effect of different conditions, viz. different mass transfer rates, non-linearity in the adsorption isotherms and different feed composition, on the system performance is studied at optimal operation. This process is then applied for the separation of C_8 aromatics. Again, the focus is to obtain

p-xylene and ethyl benzene simultaneously with the best possible purity and recovery. A comparison of all the SMB configurations for ternary separation studied in this work on the basis of separation of C_8 aromatics is also presented in this chapter.

All the inferences and conclusions made from this research work and the directions for future work are summarized in the Chapter 8.

Chapter 2   Simulated Moving Bed Systems – A review

2.1 Counter-current chromatographic systems

In the last few decades, counter-current chromatographic systems have been developed extensively and implemented. As the name suggests, in this class of chromatographic systems the solid phase and the fluid phase move counter-currently to each other. The counter-current motion between the solid phase and the fluid phase can be achieved in two ways. Either, the column (that contains the solid phase) or the entire packed bed is physically moved or else the solid phase movement is simulated by some mechanical means. One of the primary and inherent disadvantages with the counter-current system is that it is suitable for performing only a two-component or two fraction separation at a time. In other continuous chromatographic systems such as co-current or cross-current chromatographic systems, a multi-component separation can be performed. For the simple type of continuous counter-current separation that involves sorption of a single component or a family of similar species, several results have been reported (Ruthven, 1984; Ruthven and Ching, 1989). Based on the methodology adopted to obtain counter-current motion of the two phases, a number of counter-current processes have been developed namely: Moving Bed Systems, Moving Column Systems and Simulated Moving Bed (SMB) Systems.

2.2 Moving Bed/Column Systems

The continuity of operation and the process advantages of counter-currency could theoretically be obtained in an adsorptive process by actually conveying the adsorbent through the system counter to the fluid streams. This is known as the True Moving Bed (TMB) process. A typical TMB system is illustrated in Figure 2.1 for

binary separation of component A and B, with component A being the more selectively adsorbed species. The input (feed & desorbent) and the output (extract & raffinate) ports divide the bed into four different zones/sections P, Q, R, S. Though these zones are not physically separated, they are distinct since they have different mobile phase flow rates due to either injection of feed or withdrawal of products. The liquid desorbent, D, supplied and recycled through the desorbent port, flows counter-currently to the solid motion.

The key to this process is the appropriate selection of fluid and solid flow rates in different sections to ensure that each section performs its specific separation task. The required migration direction for components A and B to facilitate separation in the four sections is shown in Figure 2.1. The net flow of the strongly adsorbed species, A, should be downward in the sections Q, R and S, while upward in section P, which enables the recovery of A at the extract port. On the other hand, B, the weakly adsorbed species, should travel upward in the sections P, Q and R, and downwards in the section S, making it easier for its collection at the raffinate port. The feed F gets split up into two streams namely, the extract containing A and D (the desorbent) with very little of B and the raffinate containing B and D with very little of A. Thus a single difficult separation of A & B is transformed into two easier separations – A & D and B & D.

The Hyper-sorption Process (Berg, 1946; Kehde et al., 1948) is supposed to be the earliest known large-scale moving bed process. Although there has been reasonable work done on moving bed systems (Fitch et al., 1962) and also a few of the large-scale systems have been successfully implemented in industries, the physical movement of the solid still poses a major problem, in fact, nullifying the potential
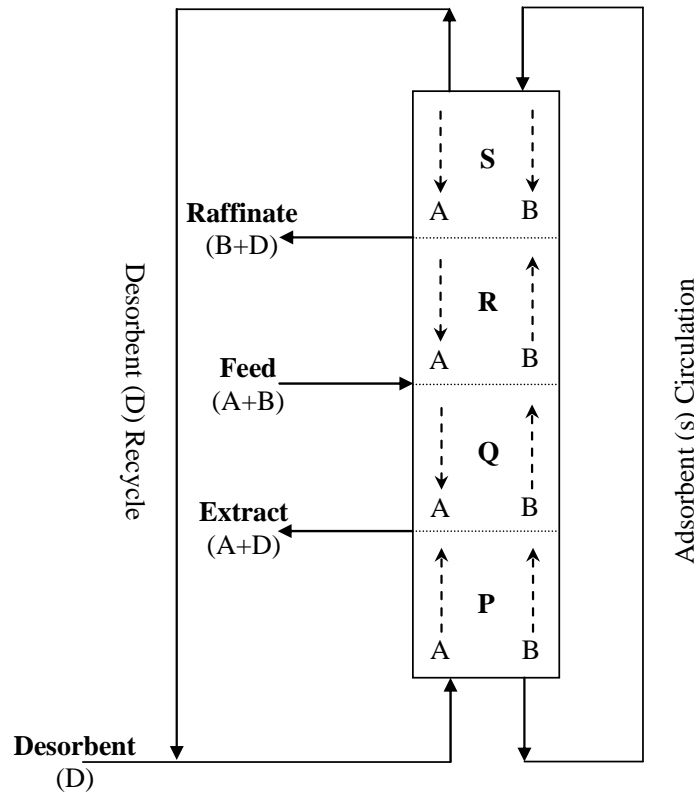
Figure 2.1 Four-zone True Moving Bed (TMB) for binary separation of A & B

merits of adsorption. Particle attrition, problems associated with the movement of the solid by mechanical means, difficulty in maintaining uniform plug flow of solid and fluid over the entire cross-section of the columns of large diameter, the axial dispersion induced by non-uniform flow leading to the deterioration of stage efficiencies are a few problems to mention.

To overcome the aforesaid problems, researchers made an attempt to switch from moving bed systems to moving column systems, wherein a circular array of packed columns interconnected in parallel, is rotated past fixed inlet and outlet ports at a controlled speed (Barker and Ganetsos, 1993).Three principal design approaches were developed and reported (Glasser, 1966; Luft, 1962; Barker and Huntington, 1966). However, the use of the cam-operated valve and its seal appears to be difficult

for scale-up, and hence are not yet known to have achieved extensive applications especially due to introduction of the Simulated Moving Bed (SMB) technology.

2.3 Simulated Moving Bed Systems

In SMB systems, most of the benefits of continuous counter-current operation can be achieved without the problems associated with moving the solid adsorbent. In this case, the system comprises of a multiple column (or multiple-section) fixed-bed with an appropriate sequence of column switching designed to simulate a counter flow system. The basic principle of this system is illustrated in Figure 2.2. At each switch, a fully generated column is added at the outlet of the regeneration train. In this way, the adsorbent is seen to be in effect moving counter-current to the fluid flow direction in both adsorption and regeneration trains. With sufficiently small elemental beds switched with appropriate frequency, such a system indeed becomes a perfect analog of a counter-current flow system. However, it has been shown both theoretically and experimentally that most of the benefits of counter-current flow can be achieved by a rather modest degree of subdivision of the bed (Ruthven and Ching, 1989).

Generally the operation of SMB is represented by a hypothetical moving bed operation for easy understanding. The concentration transition in SMB due to the shifting of inlet/outlet ports makes it difficult for the operation of SMB to be visualized. Hence, in order to understand SMB clearly, the operation of a True Moving Bed (TMB) shown in Figure 2.1 is considered. Assuming one-dimensional flow of solid and fluid, instant adsorption equilibrium, and negligible axial dispersion
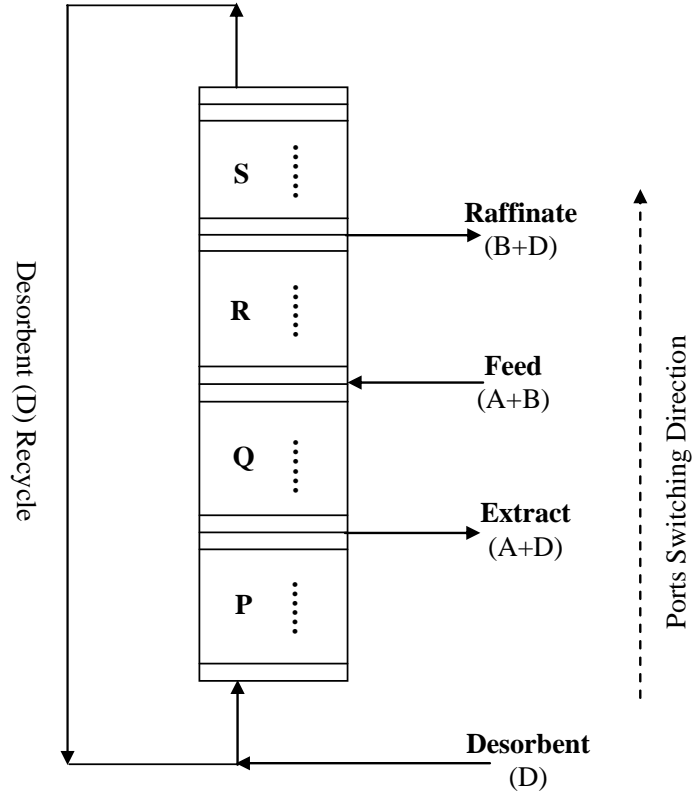
Figure 2.2 Four-zone Simulated Moving Bed (SMB) for binary separation of A and B

and other mass transfer resistances, the overall differential transient mass balance (Ray, 1992) for component i in any section is given by

$$\varepsilon \frac{\partial C_i}{\partial t} + (1-\varepsilon)\frac{\partial q_i}{\partial t} + \varepsilon u_g \frac{\partial C_i}{\partial x} - (1-\varepsilon)u_s \frac{\partial q_i}{\partial x} = 0 \tag{2.1}$$

where, u_s and u_g represent the velocities of the solid and the fluid phases in the respective sections. We can assume (for example) that the mobile phase concentration C_i is related to solid phase concentration q_i by the Langmuir isotherm

$$q_i = \frac{NK_iC_i}{1+K_iC_i} \tag{2.2}$$

Applying the dimensionless parameters given below,

$$\gamma_i = K_i C_i; \alpha_i = \frac{1-\varepsilon}{\varepsilon} NK_i; \sigma_i = \alpha_i \frac{u_s}{u_g} \qquad (2.3)$$

the mass balance equations are reduced to:

$$\left[1 + \frac{\alpha_i}{(1+\gamma_i)^2}\right]\frac{\partial \gamma_i}{\partial t} + u_g\left[1 - \frac{\sigma_i}{(1+\gamma_i)^2}\right]\frac{\partial \gamma_i}{\partial x} = 0 \qquad (2.4)$$

After rearrangement, the following equation is obtained

$$-\frac{dx}{dt} = V_{i,s} = \frac{u_g\left[1 - \dfrac{\sigma_i}{(1+\gamma_i)^2}\right]}{\left[1 + \dfrac{\alpha_i}{(1+\gamma_i)^2}\right]} \qquad (2.5)$$

where, $V_{i,s}$ is the velocity of a point of concentration γ_i describing the location of a particular concentration as time proceeds. In other words, $V_{i,s}$ is the effective velocity with which a solute travels within the column and for a given set of operating conditions, it is a function of γ_i only. At low concentration, $\gamma_i \ll 1$, $V_{i,s}$ reduces to

$$V_{i,s} = \frac{u_g(1-\sigma_i)}{(1+\alpha_i)} \qquad (2.6)$$

Eq. 2.6 shows that for systems described by linear isotherm, the velocity of the species traveling through the column is independent of the concentration, but dependent on parameter σ_i which was first defined by Petroulas and co-workers (1985). If $\sigma_i < 1$, $V_{i,s}$ will be positive and the species will always travel up the column in the direction of fluid flow regardless of the concentration of species. However, if $\sigma_i > 1$, the species will travel down the column with the solid phase. Therefore, complete separation of binary mixtures A and B can be accomplished in the true moving bed system by adjusting the fluid flow rates in the four sections and solid

17

phase flow rates u_s, such that for component A, $\sigma_A<1$ in section P and $\sigma_A>1$ in sections Q, R and S; and for component B, $\sigma_B<1$ in sections P, Q and R and $\sigma_B>1$ in section S.

The above example shows the principle of TMB operation for linear binary systems under ideal conditions where complete separation can be achieved. The same strategy is still valid in an equivalent SMB process, except that solid phase flow rate u_s in TMB should be replaced by the ratio between switching distance and switching time in SMB. However, in practical preparative and productive SMB systems, operation is usually conducted at higher concentrations (non-linear condition) and also in non-ideal packed columns (axial dispersion and other mass transfer resistances play a significant role in the column's performance). For most of these cases, no analytical solution (such as Eq. 2.6) to the mass balance equations is available and hence, the design procedure is much more complicated. For these real systems, several methodologies have been proposed to guide the design of SMB either theoretically or empirically.

2.4 Industrial applications of SMB technology

In the last few decades, SMB has been used for large-scale separations, notably the Parex process by UOP for extraction of p-xylene from C_8 aromatic mixture. In the past, major applications were in the petrochemical industry (Broughton and Gerhold, 1961; Broughton, 1968; Broughton et al., 1970; Rosset et al., 1976; Seko et al., 1982; Broughton and Gembicki, 1984), the corn wet milling industry (Lefevre, 1962; Hongisto, 1977a and b), and the sugar industry (Buckley and Norton, 1991). However, recently, SMB has found its new life in pharmaceutical industry due to the introduction of stricter drug quality requirements and rapid

development in life sciences, in which SMB has become one of the most popular separation techniques. A review of application of SMB in various industrial systems can be found in Ruthven and Ching (1989) and Blehaut and Nicoud (1998). In the pharmaceutical industry, SMB has found relevance in the preparation and separation of chiral drugs. Compared to stereo-selective synthesis methods such as asymmetric hydrogenation and enzyme synthesis, SMB was found to be more efficient in both production time and cost (McCoy, 2000). However, the success of SMB in pharmaceutical industry is the result of the recent development in chiral stationary phase (CSP), especially the pioneering works of Pirkle et al. (1980) and Okamoto and co-workers (Shibata et al, 1986; Yashima and Okamoto, 1995). It is possible to generate chromatographic columns with efficiency high enough for enantiomeric separation. The advancement in non-linear chromatography theory makes it possible for SMB to operate at preparative and productive scale as well. A review of various applications of SMB for the separation of chiral compounds is given in Schulte and Strube (2001).

2.5 Design strategies for SMB

Over the past few decades, many design strategies have been developed for SMB systems. The three important design methods that are widely known are the McCabe-Thiele method, the Triangle method and the Standing Wave concept. This section is dedicated for a brief explanation of these three methods.

2.5.1 McCabe-Thiele method

The McCabe-Thiele method is quite similar to that used for designing distillation processes. The McCabe-Thiele diagram can be applied to the SMB

systems and aids in choosing the optimal operating conditions that guarantee specified separation. Ruthven and Ching (1989) have elaborated the basic features of the design and operation of a typical four-section SMB system using McCabe-Thiele diagram, with an equivalent TMB configuration, shown in Figure 2.3 (a).Q_P, Q_Q, Q_R, Q_S, F, D, Ra, Ex and Q_s are the column flow rates in the sections P, Q, R and S, feed, desorbent, raffinate, extract flow rates and solid circulation flow rate, respectively.

In order to have a good separation in the equivalent TMB setup, the flow rates in the four sections have been proposed to be adjusted such that the net flow of A (more strongly adsorbed component) is downward in sections Q, R and S and upward in section P, while the net flow of B (less strongly adsorbed component) is downward in section S and upward in sections P, Q and R. Pure A and B thus get accumulated and are collected from the extract point and raffinate point respectively. Similar to σ_i (Petroulas et al., 1985), a flow ratio parameter γ_i was defined as the ratio between the solid flow rate Q_s and fluid flow rate Q_ϕ in section ϕ, i.e., $\gamma_i = K_i \dfrac{Q_s}{Q_\phi}$ (K_i is the equilibrium constant of component *i*).To achieve the preset separation tasks of all the 4 sections, the following inequalities are called for:

Section

S	$\gamma_A > 1.0$, $\gamma_B > 1.0$	(2.7a)
R	$\gamma_A > 1.0$, $\gamma_B < 1.0$	(2.7b)
Q	$\gamma_A > 1.0$, $\gamma_B < 1.0$	(2.7c)
P	$\gamma_A < 1.0$, $\gamma_B < 1.0$	(2.7d)

The above inequalities result in the following constraints on the flow rate ratios

$$(Q_P - D)/Q_s < K_B \tag{2.8a}$$
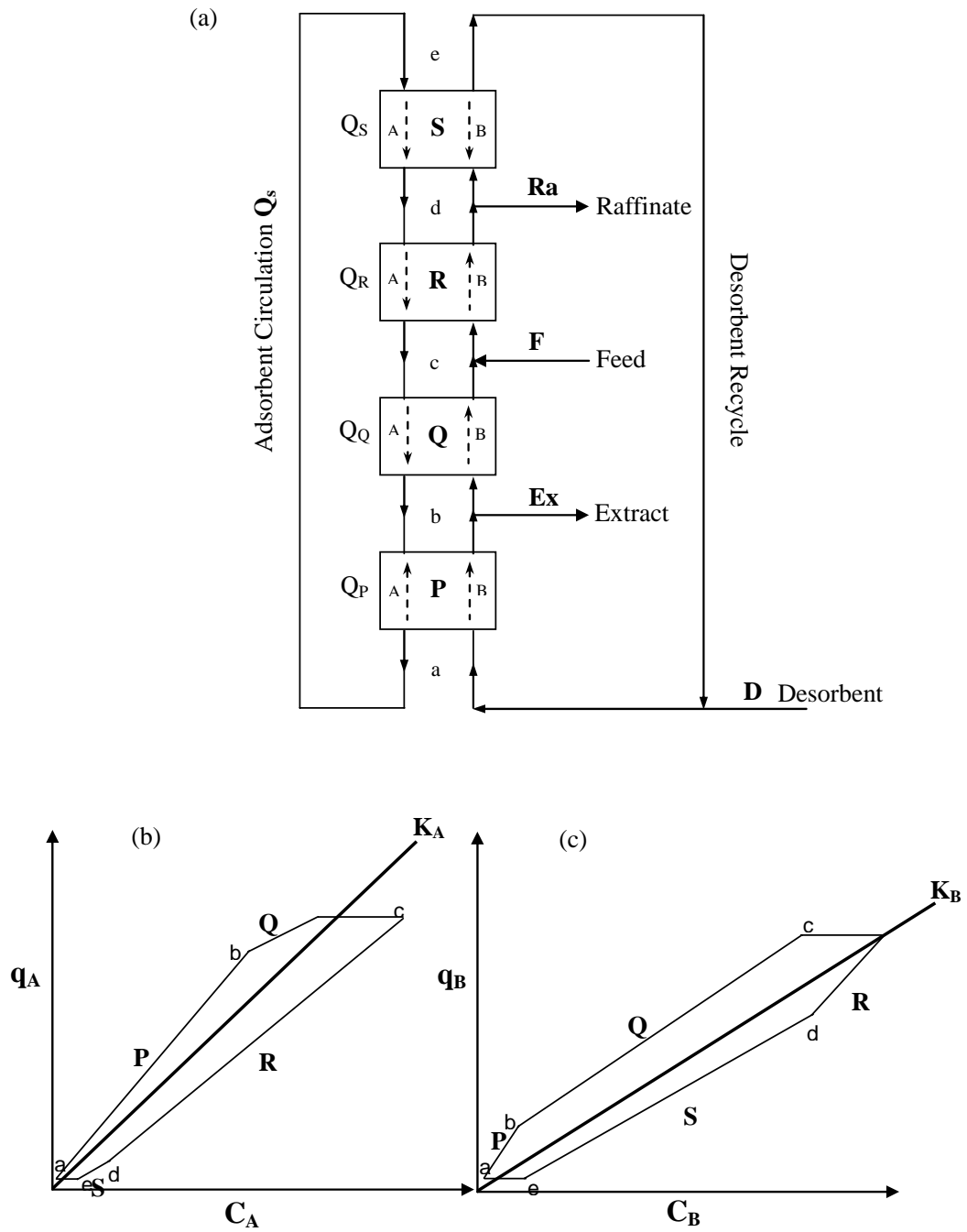
Figure 2.3 Four-zone TMB system and the corresponding McCabe-Thiele Operating Diagram for component A (b) and B (c) (Ruthven and Ching, 1989)

$$K_A > (Q_P - Ex + F)/Q_s > (Q_P - Ex)/Q_s > K_B \tag{2.8b}$$

$$Q_P/Q_s > K_A \tag{2.8c}$$

These constraints on the flow rates can be reflected in McCabe-Thiele diagram shown in Figures 2.3 (b) & (c), for components A and B respectively. The operating lines cross the equilibrium line at the feed port and at the desorbent re-circulation port because there is a sudden change in the liquid composition with no accompanying change in adsorbed phase concentration. The operating lines in sections P & Q must lie above the equilibrium line while those in the sections R & S must be below it. It can be observed from the operating lines that for the extract product (A), most of the separation takes place in the sections P & R, while that for the raffinate product (B) occurs mainly in the sections Q & S.

The McCabe-Thiele diagram can be used to determine the theoretical stage number for each section, as in distillation. Furthermore, the trade-off between the number of stages and the feed input or/and desorbent usage is evident from the diagram. However, such an approach is based on the assumption of equilibrium operations for the equivalent TMB process at steady state. Although zone lengths can be roughly determined from the height of an equivalent theoretical plate (HETP), the optimal operating conditions for certain separation tasks cannot be determined a priori and have to be found only by trial and error. Furthermore, this method cannot be used directly for the SMB process design, due to the cyclic concentration transition caused by port shift in SMB.

2.5.2 Triangle theory

A novel triangle theory was proposed by a research group at ETH, Zurich, to ascertain the operating conditions of the SMB to achieve a preset separation task (Storti et al., 1993; Mazzotti et al., 1997a). A triangle region, which denotes the complete separation area, is formed by an m_2-m_3 plane (described later) for linear or non-linear isotherm, with or without mass-transfer resistance.

The triangle theory is based on the analytical solution of an equivalent TMB model, which is used to predict the periodic steady state separation performances of the SMB unit. It has been proven that the two systems, viz., the TMB & SMB, are equivalent if the following conversion rules are obeyed

$$V_\phi = N_\phi V_{col} \tag{2.9}$$

$$\frac{V_{col}}{t_s} = \frac{Q_s}{1-\varepsilon} \tag{2.10}$$

$$Q_\phi^{SMB} = \left[Q_\phi^{TMB} + \frac{Q_s \varepsilon}{1-\varepsilon} \right] \tag{2.11}$$

where V_ϕ and V_{col} are the volume of section ϕ of the TMB unit and that of a single column of the SMB unit respectively; N_ϕ is the number of columns in section ϕ of the SMB unit; t_s is the switch time; ε is the bed void fraction; Q_s is the volumetric solid flow rate in the TMB unit; Q_ϕ^{SMB} and Q_ϕ^{TMB} are the volumetric flow rates of section ϕ in the SMB unit and in the equivalent TMB unit respectively. For the SMB unit (given its geometric and packing parameters and the adsorption equilibrium properties of the components to be separated), the design parameters are the internal flow rates, Q_ϕ^{SMB} and the switch time t_s; while Q_ϕ^{TMB} and solid flow rate Q_s, are those in an equivalent TMB unit as shown in Figure 2.3 (a) according to above relationships.

An Equilibrium TMB model, neglecting axial dispersion and mass transport resistances, was considered first for binary system of A and B (with A being the more strongly adsorbed species).In section φ, the mass balance simplifies to:

$$\frac{\partial}{\partial \tau}\left[\varepsilon^* C_i + \left(1-\varepsilon^*\right)q_i\right] + \left(1-\varepsilon_p\right)\frac{\partial}{\partial \xi}\left[m_\phi C_i - q_i\right] = 0 \qquad (i = A, B) \tag{2.12}$$

$$m_\phi = \frac{net\ \ fluid\ \ flow\ \ rate}{adsorbed\ \ phase\ \ flow\ \ rate} = \frac{Q_\phi^{TMB} - Q_s\varepsilon_p}{Q_s\left(1-\varepsilon_p\right)} \tag{2.13}$$

where, τ and ξ are the dimensionless time and space coordinates; $\varepsilon^* = \varepsilon + \varepsilon_p\left(1-\varepsilon\right)$ is the overall void fraction of the bed, whereas ε_p is the intra-particle porosity. The composition of component i in the adsorbed phase, q_i, is related to fluid phase composition C_i by either a linear or non-linear isotherm.

From the above relationships (Eqs. 2.12-2.13), in the case of given feed composition, the design of TMB or SMB unit gets reduced to developing a criteria for selection of values of the m_ϕ parameters. As defined earlier, m_ϕ is a ratio of the net fluid flow rate over the solid phase flow rate in each section of TMB unit (Eq. 2.13). In terms of the operating parameters of an equivalent SMB unit, using the conversion rules given by Eqs. 2.9-2.11, m_ϕ can be also defined as:

$$m_\phi = \frac{Q_\phi^{SMB}t_s - V_{col}\varepsilon^*}{V_{col}\left(1-\varepsilon^*\right)} \tag{2.14}$$

The differential mass balance equations were solved and the analytical solutions were obtained for both linear and non-linear type adsorption isotherm, and a complete separation region was mapped in the (m_2, m_3) plane (Storti et al., 1993; Mazzotti et al., 1994).

For a system described by the linear adsorption isotherm:

$$q_i = H_i C_i \quad (i = A, B) \tag{2.15}$$

where, H_i is the Henry constant for i^{th} component. It was proven (Mazzotti et al., 1997a) that the necessary and sufficient conditions for complete separation are the following inequalities,

$$H_A < m_P < \infty \tag{2.16a}$$

$$H_B < m_Q < H_A \tag{2.16b}$$

$$H_B < m_R < H_A \tag{2.16c}$$

$$\frac{-\varepsilon_p}{\left(1 - \varepsilon_p\right)} < m_S < H_B \tag{2.16d}$$

An additional constraint, $m_R > m_Q$, required by positive feed flow rate, combines constraints on m_Q (Eq. 2.16b) and m_R (Eq. 2.16c) into one,

$$H_B < m_Q < m_R < H_A \tag{2.16e}$$

This inequality (Eqs. 2.16e) defines the projection of the four-dimensional region of complete separation zone to the (m_Q, m_R) plane show in Figure 2.4, if the constraints on m_P (Eq. 2.16a) and m_S (Eq. 2.16d) are fulfilled. The whole region of the (m_Q, m_R) plane is divided into three regions. The triangle-shaped region in the middle of the diagram indicates the complete separation region, where 100% pure products can be collected both in the extract and raffinate. However, in the pure extract region in Figure 2.4, the third constraint is not fulfilled ($m_R > H_A$), consequently, the strong component A is carried upwards from section R into section S, thus polluting the raffinate stream, whereas extract is still 100% pure. Similarly, in

the pure raffinate region, $m_Q < H_B$, only 100% pure raffinate can be obtained. The region in the top-left corner where both $m_R > H_A$ and $m_Q < H_B$ corresponds to operating conditions under which none of the 100% pure products could be collected either in extract or in the raffinate stream. Thus for a system with linear adsorption it is very convenient to design a SMB system with the procedure mentioned above.

Similarly for non-linear systems such as that described by competitive Langmuir isotherms, the separation regimes were obtained (Storti et al., 1993; Mazzotti et al., 1994; Mazzotti et al, 1996a). However, in this case the method becomes more complicated and probably a trial and error strategy has to be employed. This procedure was also extended to other non-linear systems, for example, modified Langmuir isotherm (Charton and Nicoud, 1995; Mazzotti et al., 1997a) and bi-Langmuir isotherm (Gentilini et al., 1998). In these, different sets of constraints on m_ϕ were obtained, which describe different shapes of complete separation regions in (m_2, m_3) plane.

The procedures employed for binary separation were further applied to the design of multi-component systems that are characterized by the Langmuir isotherm (Storti et al., 1993; Mazzotti et al., 1996a, b; Mazzotti et al., 1997b) and to the design of SMB under non-ideal conditions, i.e. the effect of axial dispersion and mass transfer resistances were taken into account (Migliorini et al., 1999a; Biressi et al., 2000).
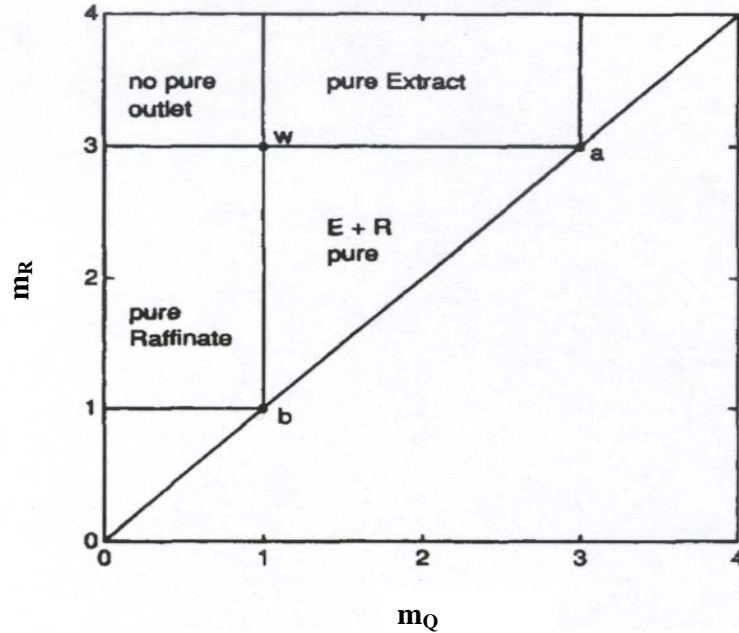
Figure 2.4 Triangle theory: Regions of the (m_Q, m_R) plane with different separation regimes in terms of purity of the outlet streams for a system described by a Linear Adsorption isotherm (Storti et al., 1993; Mazzotti et al., 1996a; 1997a)

2.5.3 Standing Wave Concept

A research group of Purdue University, US, has proposed another novel design procedure, the Standing Wave Concept. They derived a series of explicit algebraic equations to link the product purity and recovery to axial dispersion, a lumped mass transfer coefficient, section lengths, linear fluid velocities and solid movement velocity. The standing wave method was explained by applying it to investigate the separation of Raffinose and Fructose (Ma and Wang, 1997), Fructose and Glucose (Mallmann et al., 1998), and Paclitaxel Separations (Wu et al., 1999).

Similar to the principles used in establishing the McCabe-Thiele diagram, the standing wave concept was also based on the idea that each section should perform its

own specific separation role to ensure product purities by making certain concentration waves *stand* in a particular section. By proper choices of the four flow rates and solid movement velocity in the TMB (or equivalent port switching time in SMB), the advancing front (or adsorption wave) of the fast migrating solute (B) can be made standing in section S and its desorption wave standing in section Q (Figure 2.3). The adsorption wave of the slow migrating solute (A) is made standing in section R and its desorption wave standing in section P, as shown in Figure 2.5 for linear systems with mass transfer resistance (Wu et al., 1999).

Similar to triangle theory, an equivalent true moving bed (TMB) model was also used to derive the standing wave equations. For example, in section P, the transport equations for a solute in the mobile phase and in the pore phase are:

$$\frac{\partial C_i}{\partial t} = E_i^P \frac{\partial^2 C_i}{\partial x^2} - u_P^{TMB} \frac{\partial C_i}{\partial x} - P K_{fi}^P \left(C_i - C_i^* \right) \tag{2.17}$$

$$\varepsilon_p \frac{\partial C_i^*}{\partial t} + \left(1 - \varepsilon_p\right)\frac{\partial q_i^*}{\partial t} = K_{fi}^P \left(C_i - C_i^* \right) + u_s \varepsilon_p \frac{\partial C_i^*}{\partial x} + \left(1 - \varepsilon_p\right) u_s \frac{\partial q_i^*}{\partial x} \tag{2.18}$$

where C_i, C_i^* and q_i^* are the mobile phase, average pore phase and solid phase concentrations of the ith component respectively. P is the bed phase ratio, $(1-\varepsilon)/\varepsilon$, ε and ε_p are the bed and intra-particle void fraction respectively. u_P^{TMB} and u_s are the interstitial linear mobile phase velocity in section P and the adsorbent movement velocity respectively. E_i^P and K_{fi}^P are axial dispersion coefficient and lumped mass-transfer coefficient of component i in section P, respectively. The equivalent SMB interstitial velocity, u_P^{SMB}, is related to the TMB interstitial velocity u_P^{TMB} by:

$$u_P^{SMB} = u_P^{TMB} + u_s \tag{2.19}$$
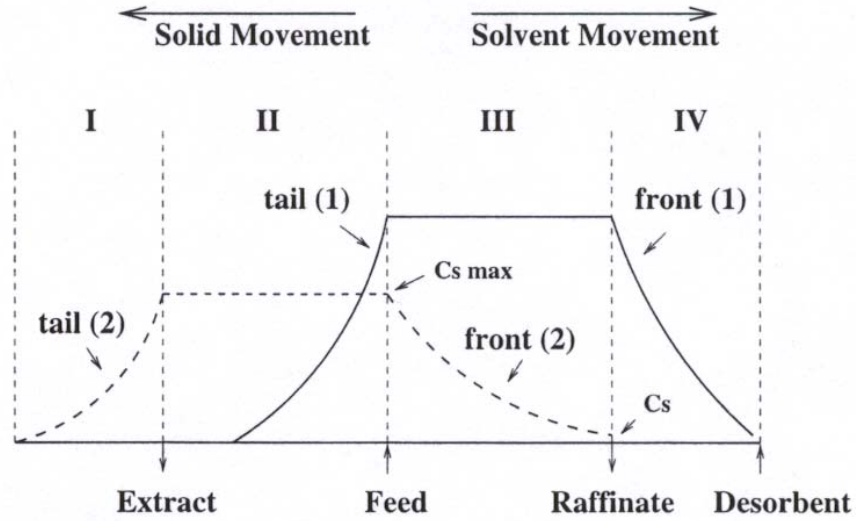
Figure 2.5 Standing Wave in a linear TMB system (Wu et al., 1999)

For a linear system with negligible axial dispersion and mass transfer resistance, the following equation was derived from Eqs.2.17 and 2.18 (Ma and Wang, 1997):

$$(1 + P\delta_i)\frac{\partial C_i}{\partial t} + \left[u_P^{SMB} - u_s(1 + P\delta_i)\right]\frac{\partial C_i}{\partial x} = 0 \tag{2.20}$$

where $\delta_i = \varepsilon_p + (1 - \varepsilon_p)K_i$; K_i is the linear equilibrium constant of component i.

From Eq. 2.20, the linear velocity of the concentration wave of component i, u_{wi}, relative to the feed point is

$$u_{wi} = -\frac{dx}{dt} = \frac{u_P^{SMB}}{1 + P\delta_i} - u_s = u_{sol,i} - u_s \tag{2.21}$$

Therefore, u_{wi} is determined by two independent linear velocities: the solid movement velocity, u_s, and the solute migration velocity, $u_{sol,i}$. In order to have separation, the migration velocity wave of the more retained solute (A) should be less than u_s in section R and that of the less retained solute (B) should be less than u_s in section S; the desorption wave of solute A should be greater than u_s in section P and

that of solute B should be greater than u_s in section Q. In conclusion, the following conditions for the velocities in each section were proposed to be satisfied for a complete separation.

Section P: $u_{sol,A} - u_s > 0$ (2.22a)

Section Q: $u_{sol,B} - u_s > 0$ (2.22b)

Section R: $u_{sol,A} - u_s < 0$ (2.22c)

Section S: $u_{sol,B} - u_s < 0$ (2.22d)

The following equations corresponding to the boundary values defined in Eqs.2.22a-d, were chosen as the optimum section flow rates, because they result in highest feed flow rate and lowest solvent flow rate for a given system.

$$u_P^{SMB} = (1 + P\delta_A)u_s$$ (2.23a)

$$u_Q^{SMB} = (1 + P\delta_B)u_s$$ (2.23b)

$$u_R^{SMB} = (1 + P\delta_A)u_s$$ (2.23c)

$$u_S^{SMB} = (1 + P\delta_B)u_s$$ (2.23d)

These equations imply that the adsorption wave of solute A is standing still in section R. Separation occurs because the adsorption wave of solute B travels faster than that of solute A, moving past the raffinate port and entering section S. Similarly, the desorption wave of solute B is standing still in section Q and the desorption wave of solute A passes the extract port and enters section P, because the migration velocity of solute A is slower than that of solute B. Furthermore, the adsorption wave of solute B stands in section S and the desorption wave of solute A stands in section P. As a result, the two concentration waves are confined in their respective sections so as to prevent them from contaminating each other.

If one more condition, either the feed flow rate, *F*, or solvent flow rate, *E*, is given, all the fluid and solid phase movement velocities can be obtained from Eqs. 2.23a-d and one of the following mass balance equations:

$$\frac{F}{\varepsilon S} = u_R^{SMB} - u_Q^{SMB}$$ (2.24a)

$$\frac{E}{\varepsilon S} = u_P^{SMB} - u_S^{SMB}$$ (2.24b)

where *S* is the bed cross section.

When mass transfer effects were taken into account, the authors used steady-state model to derive the analytical solutions, i.e., the time derivative term in the mass balance Eqs. 2.17 and 2.18 was omitted (Ma and Wang, 1997; Wu et al., 1999). The standing wave concept was further developed for non-linear systems, but without mass-transfer effects (Mallmann et al., 1998).

It is obvious that the triangle theory and the standing wave concept based on the TMB model, are very convenient and effective for the systems that are described by a few relatively simple adsorption isotherms (such as linear, Langmuir or modified Langmuir isotherm) provided the mass transfer resistances are not significant. The results obtained from these design principles (based on TMB process) might deviate from what happens in real SMB process, especially when the total number of columns is less. However, for real systems, triangle theory or standing wave concept can provide relatively close initial operating conditions in order to search for the optimal ones.

2.6 Numerical Optimization Methods for SMB

Quite a few studies have been reported in the open literature on optimization of SMB systems (Storti et al., 1988; Proll and Kusters, 1998; Karlsson et al., 1999; Dünnebier et al., 2000; Zhang et al., 2002a; 2002b, Subramani et al. 2003, Yu et al., 2003). In the work by Dünnebier et al. (2000), single objective optimization was reported, the objective being the specific separation cost C_{spec} (\$/kg). Five decision variables that were related to system flow rates (t_s, Ex, D, Q_S and F), were optimized. The following requirements on the product purities and maximum column flow rates act as constraints in the optimization problem:

Minimum extract purity:	$PurEx \geq PurEx_{min}$	(2.25a)
Minimum raffinate purity:	$PurRa \geq PurRa_{min}$	(2.25b)
Maximum column flow rate:	$Q_P \leq Q_{max}$	(2.25c)

A standard successive quadratic programming (SQP) algorithm was used to search for the optimal operation conditions in the optimization loop (Dünnebier and Klatt, 1999; Klatt et al., 2000). The approach had been applied to optimize *reactive-SMB* (SMBR) on two reaction systems: the inversion of Sucrose to produce Fructose and Glucose, and production of β-Phenethyl Acetate. In both cases, significant potential savings were obtained using their optimization program, in comparison to the original operating results in the literature.

However, in real chemical processes, there are usually two or more objectives that should be optimized at the same time. For example, in the case of SMB process for chiral separation, both raffinate and extract product purities should be maximized and consequently two objectives exist. The two objectives are of conflicting nature if operating under the same set-up (solid phase usage), solvent usage, throughput etc.

The previous optimization studies involve single (scalar) objective functions, incorporating several objectives with weightage factors. This parametric approach is not efficient and also has the drawback of possibly losing certain optimal solutions when the non-convexity of the objective function gives rise to a duality gap (Bhaskar et al., 2000), something that is very difficult to check out for complex, real-life problems. The use of multi-objective optimization with the objective functions that are vectors provides a much better picture of the processes. Zhang et al. (2002a; 2002b) reported a couple of multi-objective optimization studies on SMB & SMBR systems using a robust non-traditional optimization technique called *Non-dominated Sorting Genetic Algorithm* (NSGA). While one of these articles concentrated on the application of SMB system on chiral separation (1,2,3,4-tetrahydro-1-naphthol racemate separation) and also exemplified the merits of using a modified SMB (Varicol) for this separation, the other article focused on the applicability of SMB for reaction systems using the direct synthesis of Methyl Tertiary Butyl Ether (MTBE) from Tertiary Butyl Alcohol (TBA) and Methanol as a model reaction. In both cases, quite a few *double objective optimization problems* were formulated and solved to obtain *Pareto-optimal solutions*. Also recently, Yu et al. (2003) have reported multi-objective optimization studies on SMBR and Varicol for the synthesis of Methyl acetate using Genetic Algorithm.

Very recently, a method called the standing wave annealing technique (SWAT) was introduced (Cauley et al., 2004). A non-linear mathematical programming model that simultaneously optimizes the design variables and the operating costs of SMB system is formulated and solved by the optimization algorithm, simulated annealing. The system is represented by the standing wave equations used for designing the SMB systems to obtain the desired purity and yield

(as explained in the earlier section). The authors have claimed that this method can be extended to solve either single or multi-objective optimization problems. The application of this technique on two systems, the separation of glucose from sulfuric acid and the separation of insulin from an impurity was also shown.

2.7 Developments in SMB Technology

For long, SMB has been successfully implemented in the petroleum and sugar industries and has been found to be extremely beneficial and superior to other conventional separation processes. But then, the demand for the value-added products such as the pharmaceuticals and the fine chemicals at economical prices is increasing. These products also have stringent restrictions imposed on their quality by the food and drugs regulatory bodies. These factors have necessitated researchers to improve the SMB into a more economically viable, more flexible and more productive process. Moreover, researchers are also aiming at improving the whole separation process by combining SMB with other separation techniques.

2.7.1 Varicol

Varicol is a novel separation process patented by Adam et al. (1998). It shows a notable improvement over the SMB process without introducing any additional cost. Varicol is based on a non-simultaneous and unequal shift of the inlet/outlet ports as against the synchronous port switching in SMB. The principle of operation of Varicol system was described, for the first time, in the work of Ludemann-Hombourger et al. (2000; 2002). The principle of Varicol (four-subinterval switching) operation during one switching period t_s is explained in this section and illustrated in Figure 2.6, together with an equivalent SMB operation for comparison.
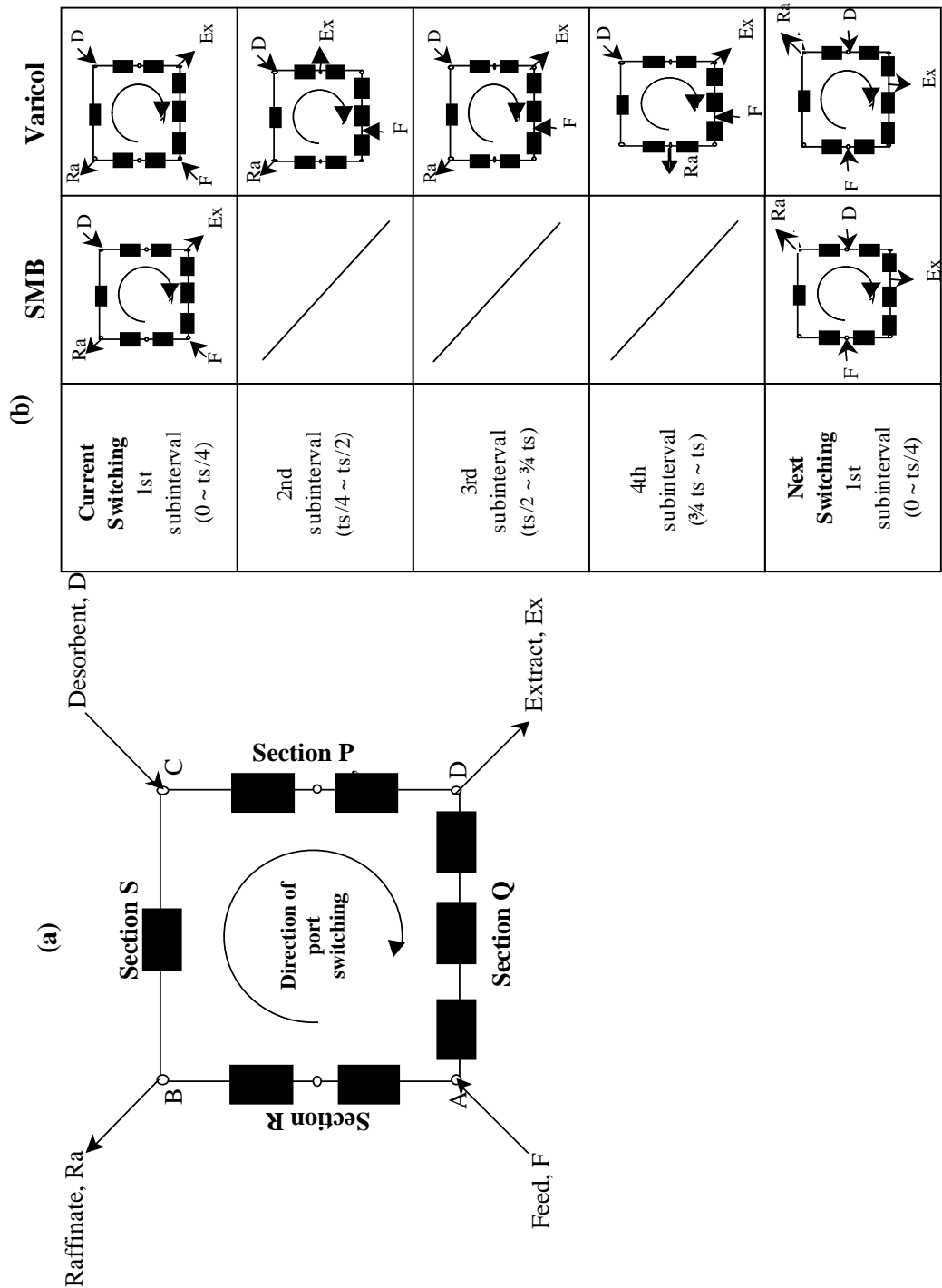
Figure 2.6 (a) Schematic diagram of an 8-column SMB system, (b) Principle of operation of the 8-column SMB and an equivalent 4-subinterval Varicol (port switching schedule)

Figure 2.6(a) depicts a conventional four-section SMB setup, with eight columns distributed as 2/3/2/1, meaning 2, 3, 2 and 1 column(s) in section P, Q, R and S, respectively. During a single switching period from 0 to t_s, in Figure 2.6(a), there is only one column configuration in the case of the SMB process, because all the input/output ports stand still before there is a simultaneous and equal shift of all the ports by one column. However, in Varicol operation, input/output ports may shift non-simultaneously and unequally, as shown in Figure 2.6(b) for a four-subinterval Varicol process, where the column configuration changes from 2/3/2/1 ($0 \sim t_s/4$) to 1/3/3/1 ($t_s/4 \sim t_s/2$) by shifting extract port and feed port one column backward, then to 2/2/3/1 ($t_s/2 \sim 3/4 \ t_s$) by shifting extract port one column forward, and then to 2/2/2/2 ($3/4 \ t_s \sim t_s$) by shifting raffinate port one column backward. As a result, there can be four different column configurations for the four time intervals during one global switching period of the Varicol system. After the fourth sub-interval, the column configuration reverts back to the original 2/3/2/1 configuration by shifting the feed and raffinate ports two column forward and extract and desorbent ports one column forward, and once again another global switching begins and the four sub-switching schedules repeated.

Thus, input/output ports in Varicol are shifted neither simultaneously nor equally. Furthermore, every port may shift more than once during one switching, either forward or even backward. This is quite different from SMB. As a result, Varicol process can have several column configurations which endows Varicol more flexibility than SMB. It is quite easy for one to imagine how flexible Varicol would be, if there were ten subintervals for a ten-column setup. SMB could be regarded as a special and also the most rigid case of Varicol, where the column configurations in all subintervals happen to be same.

In the open literature, only a couple of studies have been reported on Varicol process: for the enantio-separation of 1,2,3,4-tetrahydro-1-naphthol (Ludemann-Hombourger et al., 2000) and for the enantio-separation of SB-553261 (Ludemann-Hombourger et al., 2002). In both cases Chiralpak AD 20 μm (Chiral Technologies Europe, France) as the Chiral Stationary Phase (CSP) was used. Their simulation and experiment results did show that Varicol is indeed superior to SMB in terms of product purity and productivity. For example, they showed an 18.5% improvement in productivity using Varicol at the same desorbent consumption, same product purity and on the same 5-column setup (Ludemann-Hombourger et al., 2000). In their most recent article, the authors were able to show that a 4-column Varicol set-up was able to perform on par with a 6-column SMB for a given separation task but at the expense of slightly higher desorbent consumption rate (Ludemann-Hombourger et al., 2002).

There are also few works on the optimization of Varicol reported in the literature. Toumi (2002) have discussed the strategy for obtaining the optimal operating conditions of Varicol on two systems, separation of amino acids, Trytophan and Phenylamine, and separation of sugars, fructose and glucose. Zhang et al. (2002b); Subramani et al. (2003a) and Wongso et al. (2004) have presented results of multi-objective optimization procedure using genetic algorithm on the separation of a chiral drug, separation of glucose-fructose and enantio-separation of SB-553261 racemate respectively. Yu et al. (2003) and Subramani et al. (2003b) have also used genetic algorithm for the optimization of reactive separation systems, synthesis of Methyl Acetate and synthesis of Methyl Tertiary Butyl Ether respectively.

2.7.2 Simulated Moving Bed Reactor

The economics of many industrial chemical processes are unfavorably influenced by the equilibrium limitations of the reactions involved, subsequent separation of non-converted reactants from the reactor outlet product and their recycling to the reactor inlet. The advantages of coupling chemical reaction and separation have been exploited for a long time in the petrochemical industry with reactive distillation processes. Similarly, the non-reactive SMB system with superior separating power could be coupled with reactive systems to drive the reaction beyond the reaction equilibrium. This triggered off the advent of the novel Simulated Moving Bed Reactors (SMBR) also known as the Simulated Counter-current Moving Bed Chromatographic Reactor (SCMCR) and studies have been carried out in this direction in the last few decades. Similar to reactive distillation that couples distillation and chemical reaction together in one process, SMBR technology combines the more powerful and energy-saving separation technology, SMB, with reversible reaction in a single reactor set-up.

Like SMB, SMBR also consists of a (or a series) packed column(s) where chemical reaction and separation take place simultaneously. The behavior of counter-currency between the solid phase and the fluid phase is simulated by periodically switching the input and output ports sequentially along the column(s) in the same direction as the fluid flows. Proper catalyst and adsorbent, towards which products and reactants have different adsorption affinities, are packed in column(s) as the stationary phase. The reactor improves product purities and conversions by separating the desired product from the final product mixture or from reactants at the site of reaction. So, it offers a solution to the thermodynamically limited reactions by pushing forward their equilibrium conversions to nearly unity. For the kinetically

constrained reactions as well, SMBR provides an opportunity for higher conversion and purer products within a given time frame. This allows one to carry out endothermic reactions at lower temperatures than normally would be employed due to the low equilibrium constant. A decrease in temperature will usually suppress side reactions and improve product quality, avoiding the need for further purification steps. Also, exothermic reactions with unacceptably low reaction rates at temperatures where the equilibrium yield is large could be run at higher temperatures and not be limited by low equilibrium conversions. Highly purified products can be obtained from an appropriately designed SMBR that eliminates the use of conventional separating units that are indispensable in traditional chemical processes.

In the last couple of decades, quite a few studies have been carried out to evaluate the applicability of SMB to *in situ* reaction and separation processes. This might probably be due to the fact that SMB had gained an upper hand over the other conventional separation processes both in the petroleum and sugar industries owing to its superior separating power. Various classes of important reactions, both chemical and biochemical, have been studied using a SMBR. A review of the same is beyond the scope of this work. Some of the most explored reactions are Oxidative coupling of Methane (Tonkovich et al., 1993; Kruglov et al., 1994), Inversion of Sucrose (Ganestos and Barker, 1993; Meurer et al., 1996; Ching and Lu, 1997; Azevedo and Rodrigues, 2001b; Dünnebier et al., 2000) and Methyl Acetate synthesis (Lode et al., 2001; Yu et al., 2003). Strategies for the effective design of SMBR were also studied (Meurer et al., 1997; Fricke et al., 1999a; Migliorini et al., 1999a & b; Huang and Carr, 2001).

2.7.3 SMB with Variable flow rates

One of the limitations of the SMB system is that during much of the operation, the stationary phase in some of the columns are completely free of solutes, or in other words there is not an effective utilization of the solids and hence the separation capacity is significantly reduced. One way to improve SMB efficiency is to use non-synchronous switching as in Varicol (described earlier). An alternative option that could improve the effective utilization of adsorbent phase would be to vary the section flow rates of the fluid during a global switching interval. Most of the SMB studies reported in the open literature use constant flow rates during each switching period. However, there are few exceptions such as the study by Kloppenburg and Giles (1999), in which all flow rates were varied and an optimization method was used to find the optimal operating conditions. Zang and Wankat (2002a) explained a different strategy of variable flow called "partial feed" where the feed is introduced only during a part of the total switching time. This concept was applied to both three zone (Zang and Wankat, 2002a) and four zone (Zang and Wankat, 2002b) SMB and was found to be more efficient than the conventional SMB. Zang and Wankat (2003) discuss an optimization technique for the same. Yu et al. (2003) have applied the concept of varying the feed flow rate within the switching period for a reactive SMB system for the synthesis of Methyl Acetate. Zhang et al. (2003) have introduced a concept called "power feed" which again deals with changing the internal and the external flow rates in SMB. All the studies mentioned above show that the desorbent consumption can be reduced substantially for a given feed throughput by operating in a variable flow mode. Alternatively, the purity of the product streams can be increased while keeping both the desorbent consumption and the throughput constant. The advantages obtained by using such a variable flow mode as explained by

Kloppenburg and Giles (1999) can be understood by considering the fact that purity

and yield of a SMB/SMBR process vary with time as shown in Figure 2.7. The

periodic shape of the curves is due to movement of the spatial concentration profiles

with respect to the withdrawal points. The relevant performance indicator values for

the operation of SMB are the integral of purity and yield, which is actually the purity

and yield of the accumulated withdrawn fluid during a switching interval. These are

of course not the median / mean values.
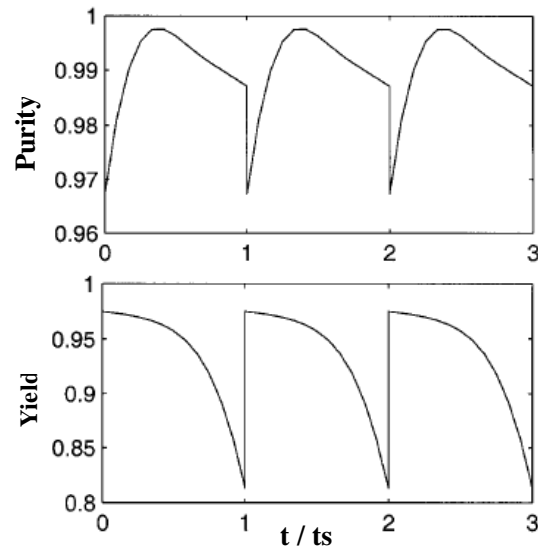
Figure 2.7 Typical time trajectories for Purity and Yield for an SMB process

Looking at Figure 2.7, with an aim to increase the SMB performance one

could think of lowering the extract flow rate (for example) when the purity is low and

increasing the flow rate when it is high. As a result, the integral purity is increased

while keeping the total volume withdrawn constant. Similarly with an aim to increase

the throughput/ productivity of the system, we can also think of introducing more feed

during the phase when the solids are most devoid of the adsorbates (probably in the

initial phase) and then reducing it. This can probably increase the efficiency of the

process for the same desorbent consumption. Unfortunately, such a change in fluid flow rates would affect all concentration profiles in the process and may even lead to decreased yield, which obviously is not acceptable. Therefore a rigorous optimization study on SMB/SMBR process model is required, taking into consideration all these interdependencies. Nevertheless, with efficient design and optimization, this concept indeed gives better performance than the conventional SMB with fixed fluid flow rates, as reported in the studies mentioned above.

2.8 Ternary separation using SMB

As discussed earlier the major limitation of counter-current chromatographic systems is that they can only perform a binary separation, which means a feed stream containing two or more components can be split only in two fractions. SMB being a counter-current chromatographic system naturally has this limitation and as a result the conventional SMB system (with four or three zones) cannot perform multi-component separation (separation of more than two components) in a single pass. However, industrially there can be a situation where the separation into three or more components becomes necessary. In some cases all the components are probably important and should be recovered or sometimes the feed containing a binary mixture may also have some impurities that have to be removed from the product streams. In such a scenario, performing multi-component separations (such as ternary or quaternary) becomes essential. There are some industrially significant separation systems that can use a multi-component separation using SMB. For example, the purification of biomass hydrolyzate (Wooley et al., 1998) to produce sugar mixture, separation of complex sugar molecules, production of raffinose from beet molasses, separation of xylene isomers containing p-xylene, m-xylene, o-xylene and ethyl

benzene etc. As a consequence, several concepts have been proposed to achieve this goal trying to keep the advantages of SMB.

For the separation of a ternary mixture using SMB, the simplest idea that can be employed is to use two SMB in series. For example, if it is assumed that the feed consists of a ternary mixture with components, A, B and C, in which A is the most weakly adsorbed component, C the most strongly adsorbed while B is the intermediate of the two in terms of adsorption affinity, then one can think of separating this ternary mixture into two streams, one containing pure A and other containing B and C, or one containing A and B and the other containing pure C with the conventional four zone SMB unit. Then the stream containing either B & C or A & B can be further separated using another four zone SMB unit. Apart from this simple strategy quite a few systems have been developed, which are basically modified SMB systems for the purpose of such multi-component separations. Different strategies that were followed to effect a ternary separation using SMB can be categorized in few groups and are explained in the following sub-sections. Table 2.1 gives a comprehensive survey of the various works on such ternary separations using modified SMB systems, as reported in the literature.

2.8.1 SMB with different adsorbents

In order to effect the ternary separation with a conventional SMB system, one of the simplest strategies one can think of is to pack the section columns with two different adsorbents alternately. The adsorbents should have different selectivities to the adsorbate components that have to be separated. Figure 2.8 shows a schematic diagram of the simulated moving bed adsorber with two types of adsorbents, A_1 and A_2, whose functions are quite different from each other. The adsorber described here

Table 2.1 Different types of modified SMB systems found in literature for ternary separation

References	Type of SMB	Description
Hotier et al. (1990a)	SMB with two desorbents	Not clearly mentioned (patented technology)
Hotier et al. (1990b)	SMB with one desorbent but with different temperature or pressure	Not clearly mentioned (patented technology)
Hashimoto et al. (1993)	SMB columns packed with two adsorbents	Proposal of the system and application on separation of starch, glucose and NaCl
Navarro et al. (1997)	Five-zone SMB	Modeling and simulation of the system for separation of Mannitol-Sorbitol-Xylitol mixture
Wooley et al. (1998)	Nine-zone SMB	Simulation with a lumped mass transfer model and validation with experimental data for separation of Sugars from Acetic acid & Sulfuric acid produced from a biomass hydrolyzate
Mata and Rodrigues (2001)	Pseudo-SMB	Modeling and simulation of the system with sensitivity studies for an unknown separation system
Nicolaos et al. (2001a and b)	Two four-zone SMB in series, five-zone & four-zone SMB in series, eight-zone and nine-zone SMB	Comparison of these systems by designing their equivalent TMBs using equilibrium theory for both Linear and Langmuir adsorption isotherms for an unknown separation system
Wankat (2001)	Two four-zone SMB in series, ten-zone and twelve-zone	Design of these systems using the equilibrium theory and performance comparisons through simulations for a hypothetical separation system and for separation of Sulfuric acid, Glucose and Acetic acid
Beste and Arlt (2002)	Five-zone SMB	Derivation of separation rules for five-zone SMB with either two extract or two raffinate streams using triangle theory. Simulation and experimental validation of ternary separation of Dimethyl phthalate, Dibutyl phthalate and Dioctyl phthalate
Kim et al. (2003)	Five-zone and four-zone SMB	Design of these systems using equilibrium theory and sensitivity studies for a hypothetical separation system

is a three-zone SMB system and not four-zone SMB system. However, it is known that a three-zone performs the same separation task as that of the conventional four-zone SMB (Nicoud, 2000). It only differs with the latter in the sense that there is no section for the recovery of desorbent (section S in four-zone SMB). The sections I, II

and III correspond to the sections P, Q and R of the four-zone SMB. Three components, A, B and C can be separated with this special multi-adsorbent system shown in Figure 2.8. The resins should be chosen such that component A does not adsorb on both A_1 and A_2. Also component B should adsorb onto A_1 but never on A_2 and component C should adsorb onto A_2 but never on A_1. In such a case, component A is eluted from the raffinate stream. The A_1 and A_2 resins appear in zone II alternately and are desorbed in zone I. Therefore, components B and C are obtained alternately at the extract stream and thus three components are separated continuously by repeating this procedure.

A mixture of starch, glucose and NaCl has been separated successfully by this simulated moving bed adsorber using four columns packed with a cation-exchange resin and an ion-retardant resin (Hashimoto et al., 1993). This principle developed for a three-component system can be extended for the separation of multiple-component systems where suitable adsorbents are available.
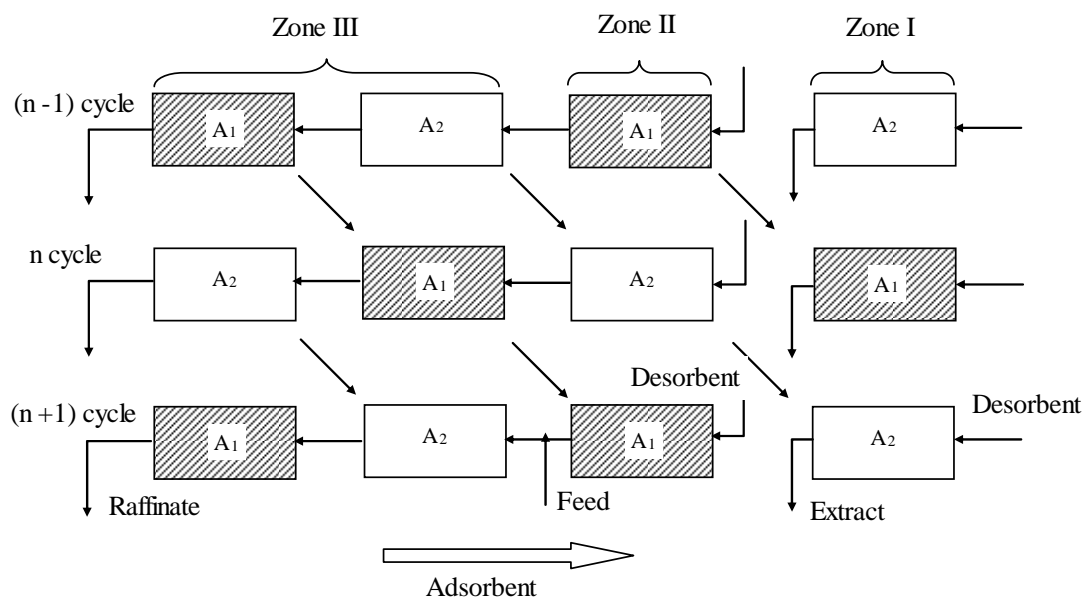
Figure 2.8 Ternary separation in SMB (three-zone) **with different adsorbents**
(Hashimoto et al., 1993)

2.8.2 SMB with different desorbents

In the earlier sub-section, separation of ternary mixture using two different adsorbents was discussed. Similarly one can think of exploiting the desorption selectivities of different desorbents on the adsorbate components. Separation of ternary mixture using two different desorbents is reported in a patented technology of Hotier et al. (1990a). The system used was a six zone SMB. Application of this system for the separation of xylene isomers and sugars are mentioned in the patent.

2.8.3 SMB with special operating techniques

Apart from the strategies discussed above, there exist few other ways to facilitate the ternary separation in SMB such as slightly modifying the operating techniques of a conventional four-zone SMB. Modifications such as having more than four sections or varying the section flow rates, etc. can effect ternary separation and are explained in the following sub-sections.

2.8.3.1 SMB with different arrangements of internal sections/zones

Five-zone SMB

If the feed of a four-zone SMB contains not two but three components A, B and C with adsorption affinity as described earlier, then the medium adsorbing component B will concentrate somewhere in the two separation sections (section Q and section R). This component could be withdrawn from a side stream introduced at the point of highest concentration. The introduction of the side stream in section Q would result in the division of that section. The separator would then have five sections in total and two extract streams, with the feed located between sections Q_2 and R (see Figure 2.9 (a)). Similarly, positioning the side stream in the raffinate

region would create a separator with two raffinate streams and a feed located between sections Q and R_1 (see Figure 2.9 (b)). Separation of ternary mixture with this five-zone SMB has been described in Kim et al. (2003), Beste and Arlt (2002) and Nicoud (2000).

In case of the system described in Figure 2.9 (a), for separation to be achieved between A, B and C, the component A should move at a higher velocity than u_s (velocity of solid = L_{col} / t_s) in sections Q_2 and R but at lower velocity than u_s in S. Component B should move at a higher velocity than u_s in section S but lower than u_s in Q_2 and R, while C should move at a higher velocity than u_s in section P but at lower velocity than u_s in sections Q_1 and R. Similarly for Figure 2.9 (b), component A should move at a higher velocity than u_s in sections Q to R_2 but at a lower rate in section S, B should move at a higher velocity in section R_2 but at a lower rate in sections R_1 and Q, and C should move at a lower rate in sections Q to R_2 but at a higher rate in section P.

If components B and C are the more desired products and A represents a contaminant that must be removed completely, then the SMB with two extract streams (Figure 2.9 (a)) is the only possible configuration because only it can produce a 100% yield of A in the raffinate (Beste and Arlt, 2002). It then has to be decided whether the side stream that consists of B contaminated with C can be usefully employed (returning it to the reactor) or has to be further separated. Purities of 60-90 % of B in the side stream and yields of 35-80 % of C in the extract stream are achievable (Beste and Arlt, 2002). Similarly, it can be said that if components A and B are more desired products then SMB with two raffinate streams (Figure 2.9 (b)) is the only possible configuration. A side-stream SMB is unsuitable if all three

components are equally valuable and have to be obtained at high purity and yield. In such cases, two binary SMBs or eight/nine zone SMB would be necessary.

(a)

(b)
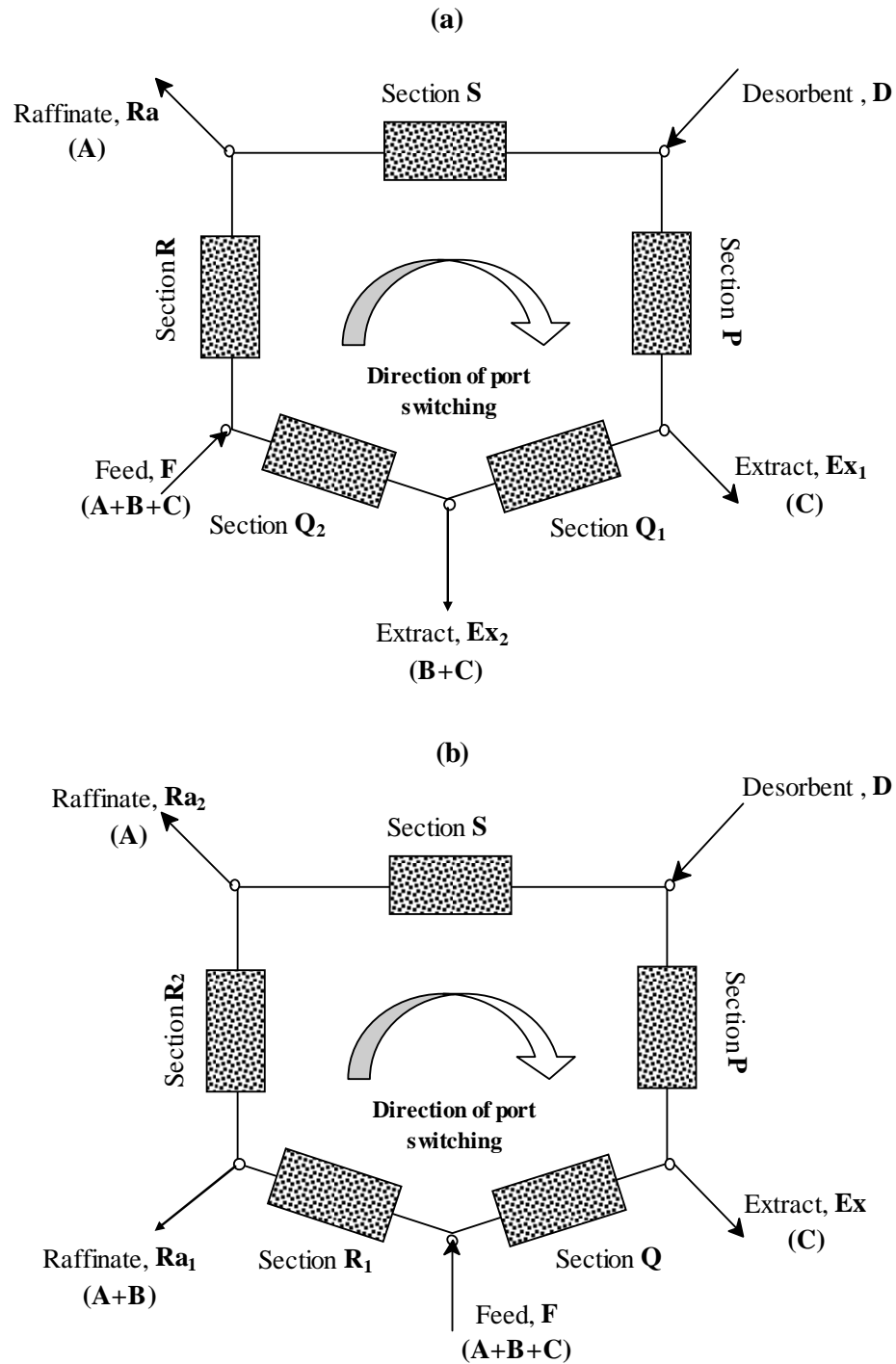
Figure 2.9 Five-zone SMB for ternary separation, (a) Five-zone SMB with two extract streams, (b) Five-zone SMB with two raffinate streams

Four-zone SMB

Figure 2.10 shows a four-zone SMB that can still effect ternary separation. It can be seen from the figure that this system differs from the conventional four-zone SMB due to a break between Section P and Q. This system is more like a batch chromatographic column since there is no recycle of desorbent within the system. However, even in this case, the solids do still move counter-currently due to the switching of the ports similar to the conventional SMB. The component with the least adsorption affinity (A) is collected in the raffinate as earlier. The product collection at the extract port is such that the component with intermediate adsorption capacity (B) is collected initially till time t_p ($t_p < t_s$) or till the time the most strongly adsorbed component (C) starts getting desorbed. After this time t_p the collection of B is stopped and C is collected till $t = t_s$. This process is repeated for every switching of the ports. This system is reported in Kim et al. (2003). However, in this system probably the products B and C will be more dilute compared to the five zone SMB system.
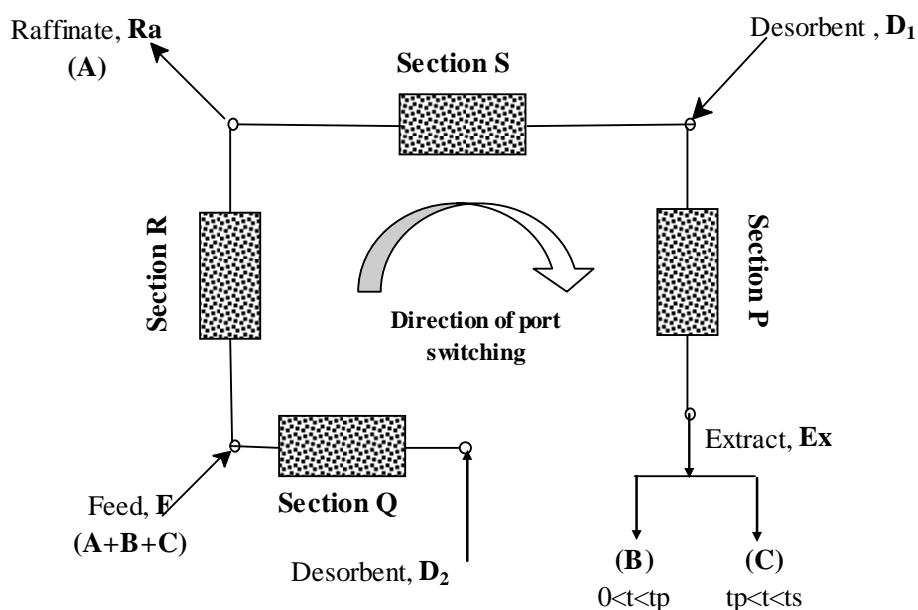
Figure 2.10 Four-zone SMB for ternary separation

Eight-zone and nine-zone SMB

These systems are basically obtained by coupling two SMBs in series into a single system. When two four-zone SMBs are coupled it forms the eight-zone system (Figure 2.11 (a)) and the coupling of a five and four-zone SMB results in the nine-zone system (Figure 2.11 (b)). The three inlet streams, feed and two desorbent inlets, three product outlet streams, and the bypass stream withdrawn from one point and added to another point splits the system into eight zones. In case of the nine-zone system an additional product outlet is available. Figure 2.11 shows the separation of ternary mixture by first splitting the feed into two streams containing pure A which is the Raffinate 1 (Ra1) and stream containing B and C which is the by pass stream. Similarly, another configuration of both eight and nine-zone system can be obtained by splitting into two streams one containing A and B and the other containing pure C. Eight-zone SMB has been reported in Chiang (1998) and Nicolaos et al. (2001a and b). The nine-zone system has been reported in Wooley et al. (1998), in which this system was used to recover two sugars, glucose and xylose from a biomass hydrolyzate. Sulfuric acid (least adsorbed component) is recovered in the Ra1. Acetic acid (most adsorbed) is partially recovered in the Ex1 which is the extract 1 stream. A mixture of sugars (intermediate adsorption affinity) and the remaining acetic acid are present in the bypass stream. Acetic acid is finally recovered in the second extract stream, Ex2 and the sugars are recovered in the second raffinate stream which is Ra2 (Wooley et al., 1998).

(a)

(b)
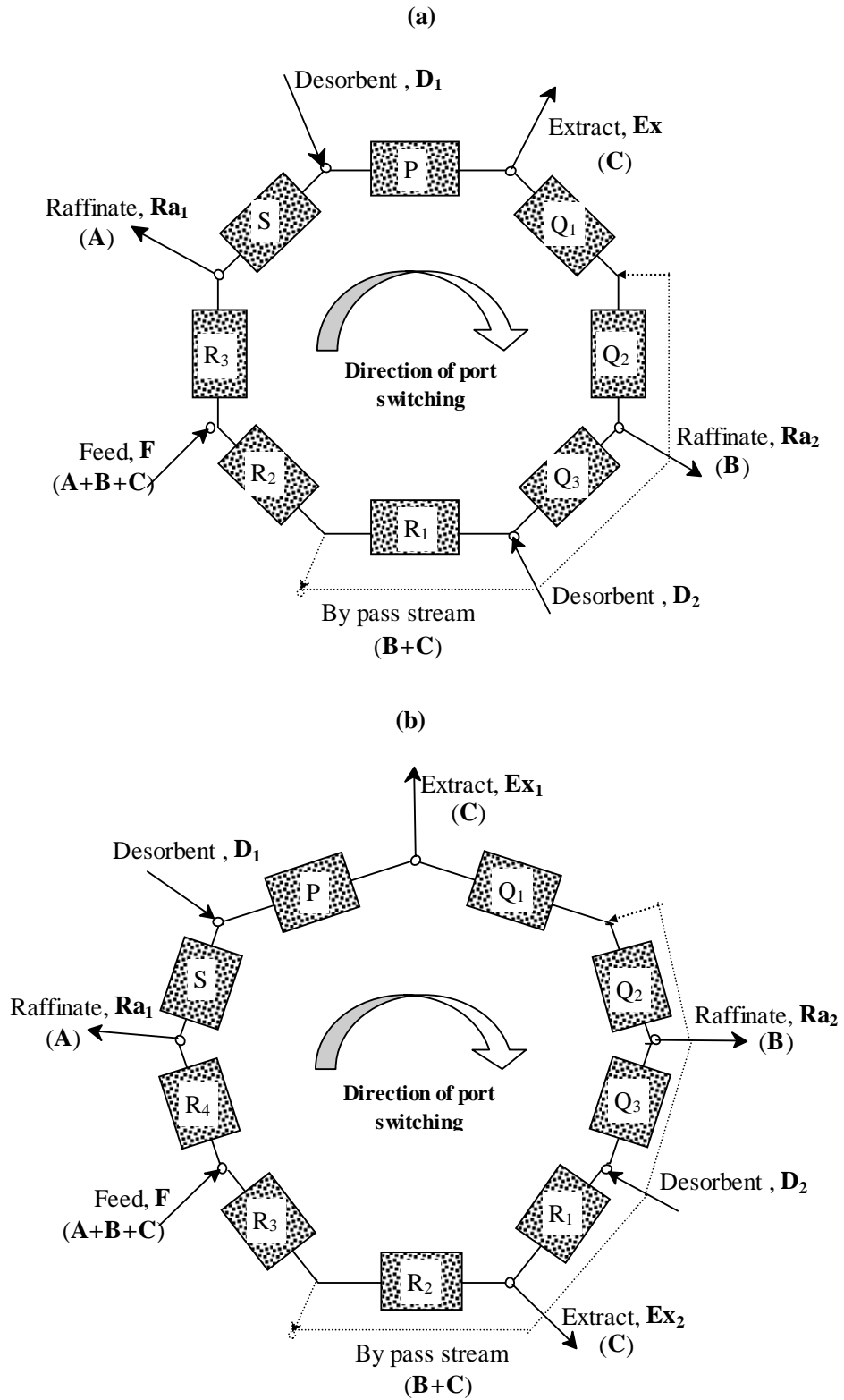
Figure 2.11 Eight-zone SMB (a) and Nine-zone SMB (b) systems for ternary separation

51

Twelve or more zones

This system consists of basically two or more SMB connected in series to separate the three components. Based on the analogy between distillation and SMB systems, Wankat (2001) has reported a few configurations for the purpose of ternary separation. It is based on the principle of easy split in distillation processes, that is, achieving the easiest separation first. Amongst the components A, B and C in the adsorption affinity described earlier, the easiest separation is between A and C while B can be allowed to distribute between the two product streams. Direct application of the analogy between such easy split distillation systems and SMB results in ten zone system shown in Figure 2.12 (a). In train 1, ternary feed is separated with the easiest split to form the AB and BC product streams. All the sections have the same functions as those in a conventional four-zone SMB used for binary separation. Section P must be operated so that all C is removed and section S so that all A is retained. Train 2 receives the two feeds and separates them into three product streams. Sections Q_1 and Q_2 separate B and C while sections R_1 and R_2 separate A and B. Section P' removes C from the adsorbent and section S' recovers A so that the desorbent can be recycled.

Similar to the 10 zone system many other configurations such as 12 zone easy split (Figure 2.12 (b)) and likes have been proposed in Wankat (2001).

(a)

(b)
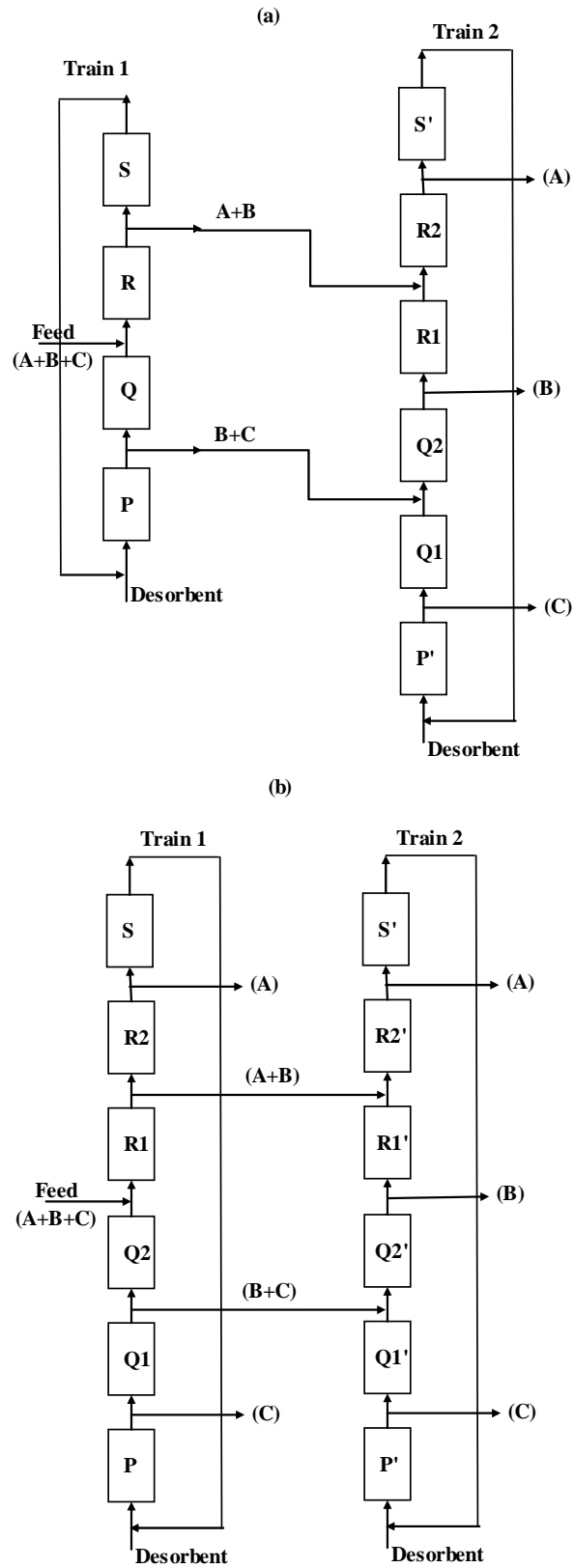
Figure 2.12 Ten-zone SMB (a) and Twelve-zone SMB (b) (Wankat, 2001)

2.8.3.2 SMB with different temperature/pressure in the internal sections

Varying the operating conditions such as temperature / pressure inside the columns to effect ternary separation has been mentioned in the patents by Hotier et al. (1990b) and Perrut et al. (1993). In the patented system described by Perrut et al. (1993) component mixtures are separated by adsorption in a simulated fluidized bed having three, four or five zones. The pressure in each of the zones is modulated. It is claimed that this method can be used to separate crude oil fractions.

2.8.3.3 Pseudo-SMB system

This system is invented by the Japan Organo Company (Ando et al., 1990 and Masuda et al., 1993). This system needs a shut-off valve which can cut the circulation flow and an additional outlet for component B, two features additional to that needed on the simulated moving-bed system. The operation of this system is basically a cyclic process in which a cycle consists of the following two steps (Figure 2.13).

Step 1: In the first step of the cycle, the circulation flow is stopped (shut-off valve closed), feed mixture is fed in, and, in a similar way to the fixed-bed mode, the component having an intermediate affinity (component B) to the adsorbent is withdrawn. During this process only the feed and desorbent streams enter the process while there is only one outlet. It should be noted that during this step the system operates in the fixed bed mode and hence no switching of the ports is followed.

Step 2: In the second step, there is only one inlet flow of desorbent. There is no input of feed and the shut-off valve is opened. During this step, the system operates in the same way as it does in simulated moving-bed mode, i.e. the desorbent feeding and the
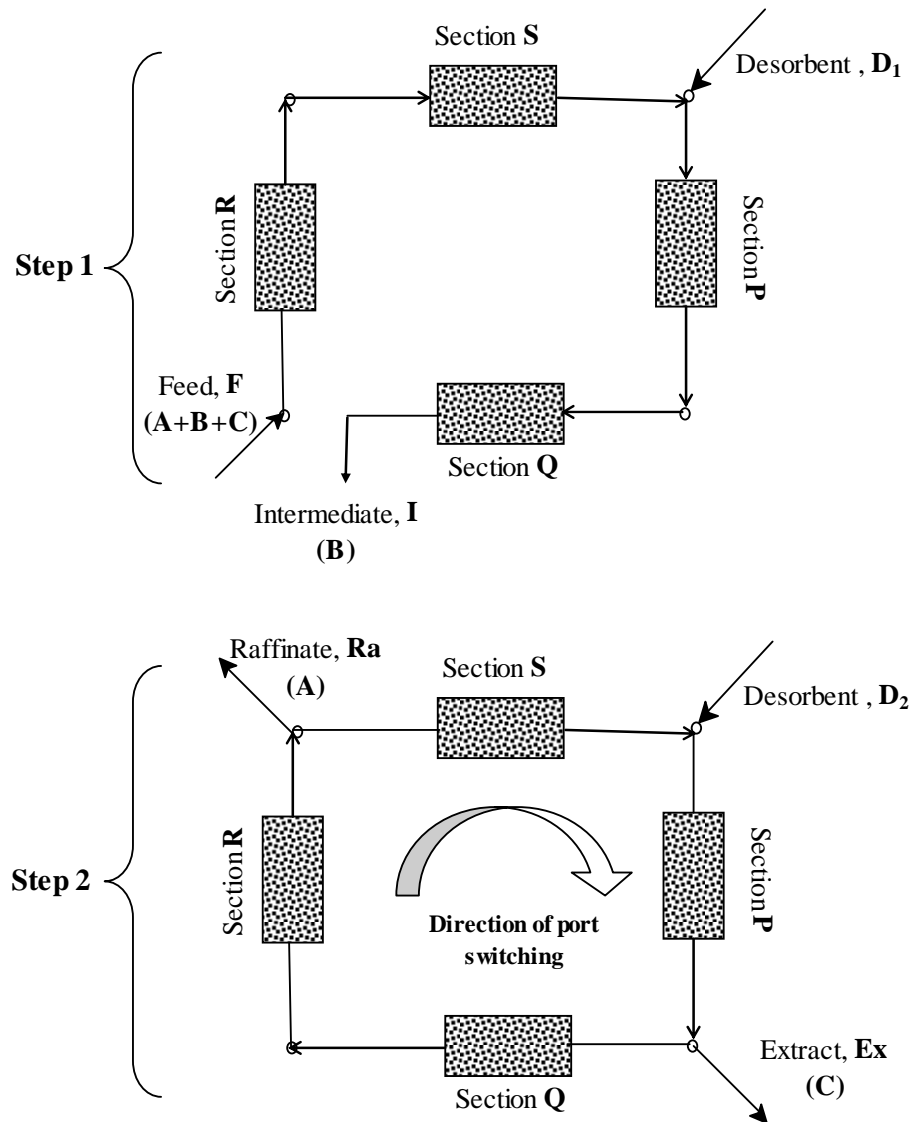
Figure 2.13 Pseudo-SMB system for ternary separation

product withdrawal ports are periodically moved as components A and C are continuously collected in the raffinate and extract port respectively.

During the second step, when there is no feed inlet, the migration rate of component B with the fluid phase and that with the solid phase become approximately equal ($\sigma=1$). As a result, components A and C move towards the front and rear of the intermediate affinity component B, and gradually a zone with only component B is formed. When the desorbent and the product outlet ports have been moved

periodically around until they are back to the same positions as in step 1, the circular flow is once again cut (shut-off valve closed), the feed mixture is fed, and component B is withdrawn. Through the repetition of this operation, components A and C can be simultaneously collected during step 2 while component B can be collected during step 1 thus enabling the continuous separation of a ternary mixture.

This strategy has been applied in the separation of complex multi-component mixtures, e.g. sucrose, glucose and betaine (Masuda et al., 1993) and in the production of raffinose from beet molasses (Sayama et al., 1992).

2.9 Design of modified SMB systems for ternary separation

The concept of triangle theory used for designing the conventional four-zone SMB systems (for binary separation) can be extended to configurations used for ternary separations. Beste and Arlt (2002) have obtained operating diagrams for the five zone SMB system with either two extract streams or two raffinate streams (as discussed earlier). If we consider the system with two raffinate streams (Figure 2.9 (b)), the aim of separation is to achieve an extract stream with a 100% yield of pure C, a raffinate stream with the greatest possible yield of pure A, and a side stream with a 100% yield of B and least possible contamination with A (since some amount of A in the side stream is inevitable). The desired separation is achieved if each component migrates through each section to its respective product outlet, a situation indicated by the arrows in the Figure 2.14 (a). If components A, B and C migrate as indicated by the heavy arrows, which represent the conditions sufficient to bring about the desired separation, then these components will also migrate in the directions indicated by the remaining or normal arrows. Similarly for the system with two extract streams (Figure 2.9 (a)), the conditions necessary for desired separation (100% yield of pure A in the

raffinate, pure C in the extract and a 100% yield of B in the side stream with minimum possible contamination from C) are represented in Figure 2.14 (b). The operating diagrams for both the configurations are shown in Figures 2.14 (c) & (d) respectively. The optimum point of operation is shown by the black point (OP). However this is only a theoretical optimum. To ensure a safe separation, the operating points should be chosen such that it lies well inside the shaded areas. Sections P and S in both the cases perform identical tasks. In both the cases component A must not be allowed to be recycled with the desorbent (section S), and C must not be transported from section P to section S. These conditions are also represented in Figures 2.14 (a) & (b).

This concept of designing the five-zone SMB system can be extended to higher zone SMBs such as eight-zone and nine-zone SMB. Nicolaos et al. (2001a) have obtained the operating diagrams for such systems using the similar concept. The required migration direction of each component in each of the zones were obtained and based on these the operating diagrams were drawn. Figures 2.15 (a) & (b) show the operating diagrams for eight-zone and nine-zone SMB systems respectively. The broken line represents the recycling flow rate. Similar to the earlier discussion, the first and the last sections of any configuration should meet similar constraints as to not allow component A to be recycled with the desorbent (section S), and C must not be transported from section P to section S.

All these design procedures are valid for only linear adsorption isotherms. For non linear isotherms the design procedure becomes more complicated. Nicolaos et al. (2001b) have obtained operating diagrams for these systems in case of the Langmuir adsorption isotherm. The design of other more complicated configurations used for ternary separation is probably more tedious and are case specific.

(a)

Hypothetical solid flow

A →   A →   A →   **A** →   **A** ←
B →   **B** →   B →   **B** ←   B ←
C →   C ←   **C** ←   C ←   C ←

$m_P > K_C$ $m_Q > K_B$ $m_{R1} < K_C$ $K_B > m_{R2} > K_A$ $m_S < K_A$

Recycle

Desorbent   Extract (C)   Feed (A,B,C)   Raffinate1 (B,A)   Raffinate2 (A)

(b)

Hypothetical solid flow

A →   A →   **A** →   A →   **A** ←
B →   **B** →   B ←   **B** ←   B ←
C →   C ←   C ←   C ←   C ←

$m_P > K_C$ $K_C > m_{Q1} > K_B$ $m_{Q2} > K_A$ $m_R < K_B$ $m_S < K_A$

Recycle

Desorbent   Extract1 (C)   Extract2 (B,C)   Feed (A,B,C)   Raffinate (A)

(c)

m_{R1}

K_C **OP**
K_B K_B

K_A

m_{Q1}, m_{R2}

m_Q m_{R2}

(d)

m_{Q2}

m_{Q1} m_R

K_B

K_A **OP** K_B K_C

m_R, m_{Q1}
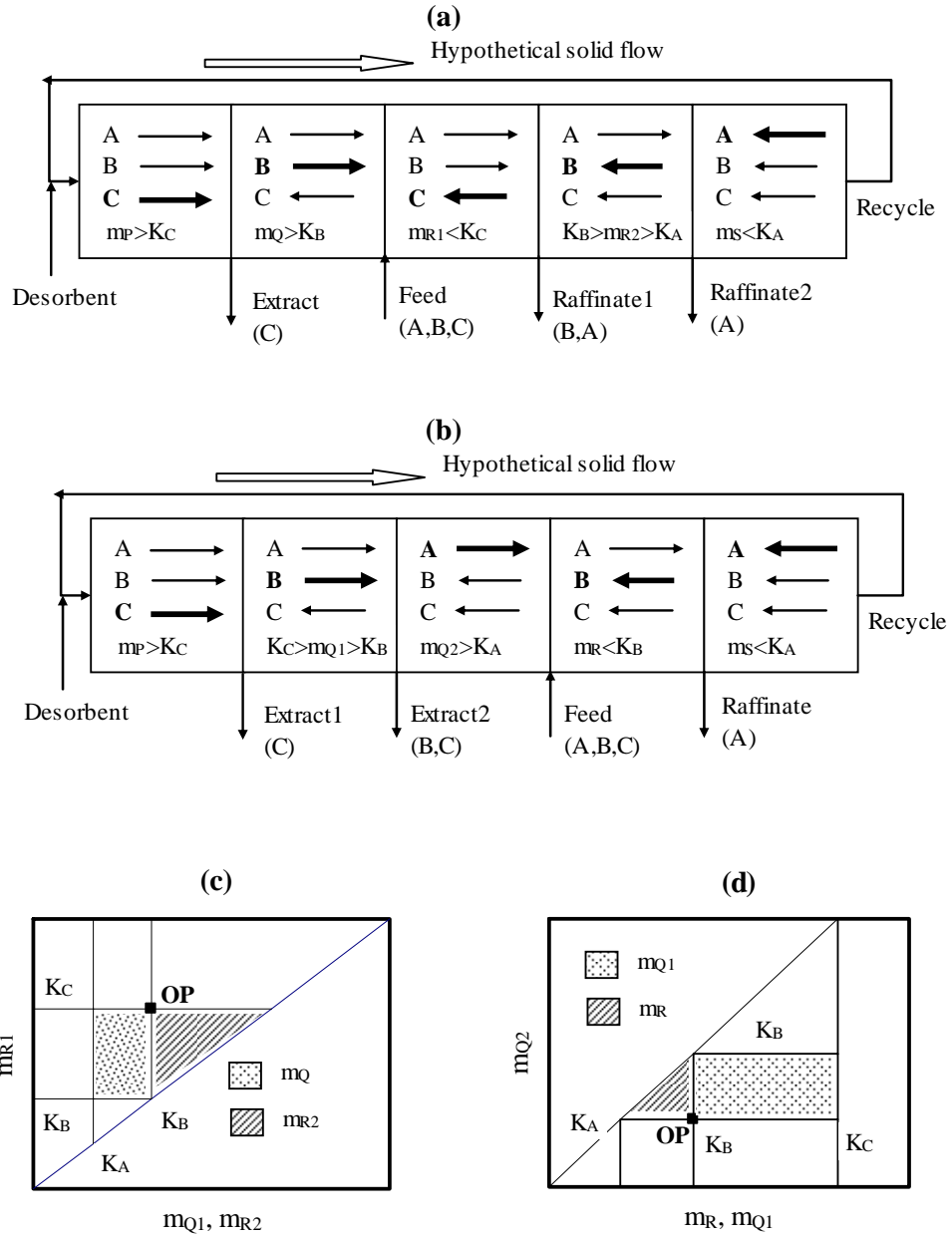
Figure 2.14 Design for Five-zone SMB: Migration directions for components A, B and C to ensure desired separation for the system with two raffinate streams **(a)** & two extract streams **(b).** Operating diagrams for system with two raffinate streams **(c)** & two extract streams **(d)** (Beste and Arlt, 2002)

(a)

(b)
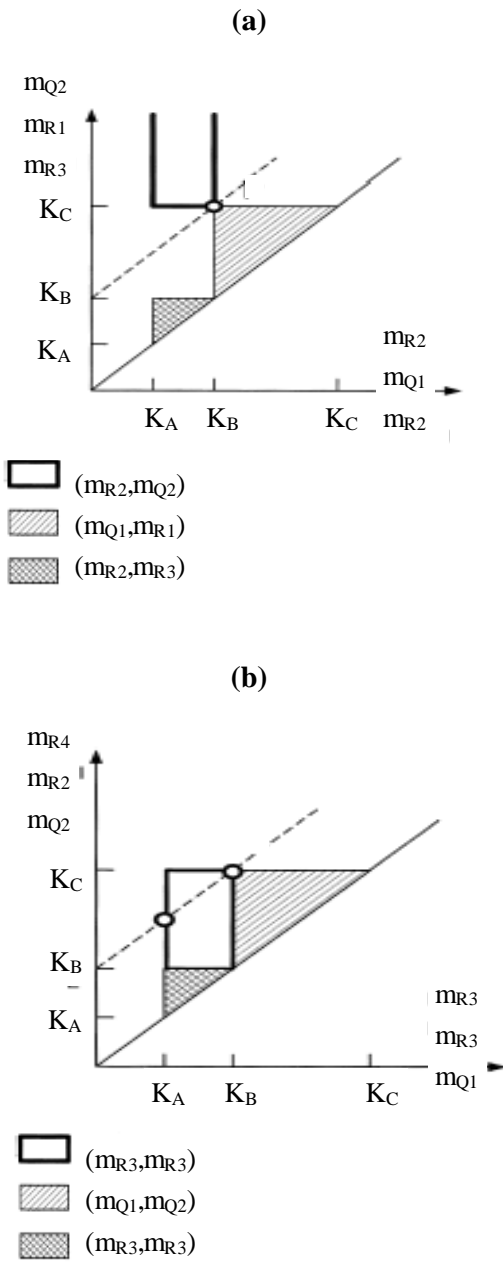
Figure 2.15 Operating diagrams for eight-zone (a) and nine-zone (b) SMB system
(Nicolaos et al., 2002a)

Chapter 3   Optimal Operation of an Industrial-Scale Parex Process for *p*-xylene recovery

3.1 Introduction

The Parex process is an innovative adsorptive separation method for the recovery of *p*-xylene (1,4-dimethyl benzene) from a mixture of C_8 aromatic isomers (consisting of ethyl benzene, and *o*-, *m*-, and *p*-xylene). These isomers boil so closely together that separating them by conventional distillation is not practical. The primary end use of *p*-xylene is for the production of films, resins and fibers including polyester fibers that are used for household fabrics, carpets, and clothing. Oxidation of *p*-xylene leads to terephthalic acid (TPA) or dimethyl terephthalate (DMT) that are then reacted with ethylene glycol to produce polyethylene terephthalate (PET). PET is the raw material for most of the polyesters. The use of polyester films and fibers is increasing rapidly, mainly in the Pacific Rim countries.

The Parex process is a continuous process based on Simulated Moving Bed (SMB) (Broughton and Gerhold, 1961) technology. SMB, as explained earlier, helps to achieve the separation performance of a true moving bed while avoiding the difficulties in movement of the solid phase. Separation is achieved by exploiting the differences in affinity of the adsorbent (e.g., zeolitic adsorbent) to feed components. In Parex process, the adsorbent is selective for *p*-xylene and it is generally aimed to recover best possible amount of *p*-xylene from the feed in a single pass while delivering high product purity (greater than 99.9 wt%). A schematic representation of a SMB system is illustrated in Figure 3.1, which consists of a number of packed (with adsorbent) columns of uniform cross-section connected in a circular array, each of length L_{col}. The two incoming streams (the feed, F, and the desorbent, D) and the two

outgoing streams (the raffinate, Ra, and the extract, Ex) divide the system into four sections (zones), namely P, Q, R and S, each of which comprises of p, q, r and s columns respectively. The flow rates in the section P, Q, R and S are designated as Q_P, Q_Q, Q_R and Q_S respectively while those of the feed, raffinate, desorbent and extract are designated as Q_F, Q_{Ra}, Q_D and Q_{Ex} respectively. However, only four of the above eight flow rates are independent, as the remaining four are determined from the mass balance at points (nodes) A, B, C and D (see Figure 3.1).

Even though the Parex process works on the same principle as shown in Figure 3.1, the actual configuration is somewhat different (see Figure 3.2). In this case, the adsorbent is not contained in discrete columns (beds) separated by switch valves but they are contained in a single bed that is divided into a number of segments. The introduction and withdrawal of fluid from each segment is done by specially designed flow distributors. A pump re-circulates fluid from the bottom to the top of the column. At any time only four of the connections to the packed bed are utilized. A rotary valve connected to each stream advances the two inlet and the two outlet points (feed, desorbent, extract and raffinate) by one segment in the direction of fluid flow and thus simulates the solid motion in the opposite direction. The valve also passes the extract and the raffinate streams to the respective ancillary distillation columns to remove the desorbent that is recycled back to the process (Ruthven and Ching, 1989). Several other industrial processes for the separation of these C_8 aromatic isomers have been developed in the past. The earliest separation processes were based on crystallization (Fabri et al., 2001). These separation processes are usually coupled with an isomerization process aimed to transform some or all of the other isomers into *p*-xylene. The adsorption of xylenes on ion-exchanged faujasite

Raffinate, **Ra**

Desorbent , **D**

Section S

D

A

Section R

Section P

**Direction of port
switching**

C

B

Section Q

Feed, **F**

Extract, **Ex**
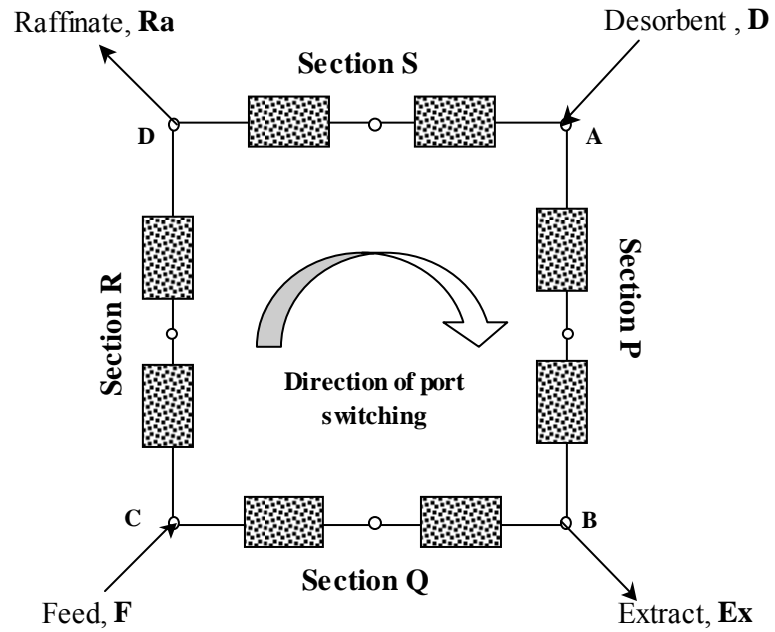
Figure 3.1 Schematic diagram of 8-column simulated moving bed (SMB) system
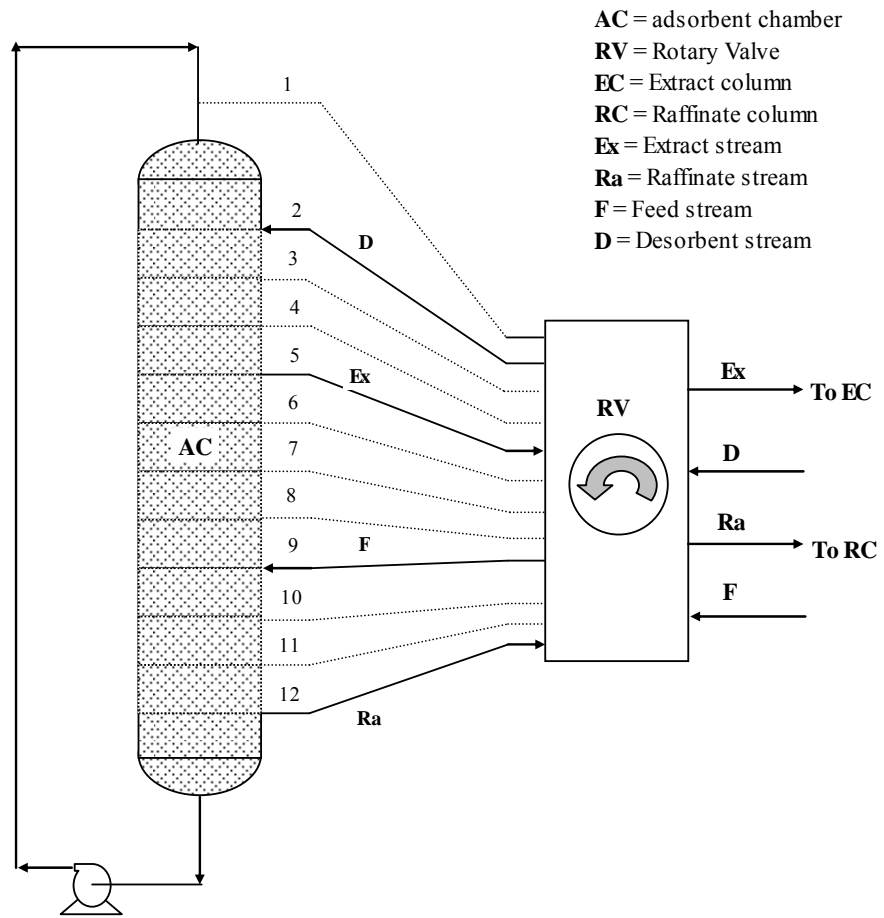
Figure 3.2 A Schematic flow diagram showing the operation of Parex process
(Ruthven and Ching, 1989)

type zeolites have been studied extensively in the liquid phase (Santacesaria et al., 1982 a & b; Carra et al., 1982; Azevedo et al., 1998; Hsiao et al., 1989) as well as in the vapor phase (Santacesaria et al., 1985; Morbidelli et al., 1985; Storti et al., 1985; Ruthven and Goddard, 1986; Goddard and Ruthven, 1986; Paludetto et al., 1987; Cavalcante et al., 1997). A detailed analysis of the design and optimization of a four-section SMB unit for separation of this C_8 aromatic mixture operating at liquid and vapor phases has been presented by Storti et al. (1989), in which appropriate flow-rate ratio for each section was established from equilibrium theory. Simulation studies on an industrial-scale SMB unit for the separation of the same were performed by Minceva and Rodrigues (2002).

In spite of being such an old and established industrial process, there is no work reported in the open literature that deals with rigorous optimization of the Parex process. The performance of SMB (as well as its modifications such as Varicol) process strongly depends on the complex interplay of different operating as well as design parameters. The optimization problem is complicated by the relatively large number of decision variables, including continuous variables, such as flow rates and length of the columns, as well as discontinuous/discrete ones, such as column number and configuration. Moreover, it is important to reformulate the optimization problem as multi-objective (Bhaskar et al., 2000), since usually the factors affecting the economy of a given separation process are multiple and are often in conflict with each other. A typical example of such conflicting objectives is maximizing recovery of *p*-xylene while minimizing solvent consumption. As discussed earlier, the principle of multi-criterion optimization with conflicting objectives is different from that of single objective optimization. Instead of trying to find the unique and best (global) optimum design solution, the goal of multi-objective optimization is to find a set of equally

good solutions that are known as Pareto optimal solutions (Bhaskar et al., 2000, Deb, 2001). A Pareto set is such that, when one moves from any one point to another within the set, at least one objective function improves while at least one other deteriorates. The importance of multi-objective optimization and the improvement in performance achieved in SMB and Varicol processes for various applications have been systematically studied in the literature (Zhang et al., 2002b, Subramani et al., 2003a & b, Yu et al., 2003).

In this chapter, multi-objective optimization study is carried out for the Parex process. The industrial data provided by Minceva and Rodrigues (Minceva and Rodrigues, 2002) was used for verification of the mathematical model. The feed is considered to be a typical C_8 aromatics mixture containing 23.6% *p*-xylene, 49.7% *m*-xylene, 12.7% *o*-xylene, and 14% ethylbenzene. In this system (Minceva and Rodrigues, 2002), completely potassium-exchanged Y-zeolite is used as the adsorbent while a solvent *p*-diethyl benzene (*p*DEB) is used as the desorbent. Toluene can also be used as a desorbent for this separation process. However, *p*DEB is less volatile than the C_8 aromatic isomers (Ruthven and Ching, 1989). This is very advantageous since then in the ancillary product separation, desorbent will be recovered as the bottom product. Since desorbent is generally in excess, this reduces the heat load on the distillation column. This leads to a more economical process operation. Details of the operating conditions and design parameters are listed in Table 3.1. The optimization study is aimed at increasing the recovery of *p*-xylene with a minimum solvent consumption. Furthermore, by comparing the performance of the Varicol process with an equivalent SMB process, this work tries to determine to what extent the operation of a SMB system can be improved by applying a non-synchronous switching pattern (characteristic of Varicol).

Table 3.1 Details of industrial Parex unit along with model parameters and operating conditions (Minceva and Rodrigues, 2002)

SMB Unit Geometry	Operating Conditions	Model Parameters
$N_{col} = 24$	T = 453 K, liquid phase	Pe = 2000
$L_{col} = 1.135$ m	$t_s = 1.16$ min	$k_a = 2$ min^{-1}
$d_{col} = 4.117$ m	$Q_F = 1.45$ m^3/min	$d_p = 9.2 \times 10^{-4}$ m
$\Omega = 6\,/\,9\,/\,6\,/\,3$	$Q_{Ex} = 1.65$ m^3/min	$\varepsilon = 0.39$
$V_{col} = 15.1$ m^3	$Q_{Ra} = 2.69$ m^3/min	$\rho = 1.39 \times 10^3$ kg/m^3
	$Q_D = 2.89$ m^3/min	$q_{mpX\,(mX;\,oX;\,EB)} = 0.1303$ kg/kg
	$Q_S = 5.39$ m^3/min	$K_{pX} = 1.0658$ m^3 /kg
		$K_{mX} = 0.2299$ m^3 /kg
		$K_{oX} = 0.1884$ m^3 /kg
		$K_{EB} = 0.3037$ m^3 /kg
		$q_{mpDEB} = 0.1077$ kg/kg
		$K_{pDEB} = 1.2935$ m^3/kg

3.2 Mathematical model

In SMB, as discussed earlier, the countercurrent motion between the fluid and solid phase is mimicked by a discrete shifting of injection and collection points in the direction of fluid flow. Also, SMB system consists of a set of identical fixed-bed columns that are connected in series. Model equations for SMB result from mass balance over a volume element of the bed and inside the particle. Axial dispersion for the bulk fluid phase is included and the linear driving force approximation is used to describe the intra-particle mass-transfer rate. The mathematical model used here is similar to the one described by Pais et al. (1998). The differential transient mass balance equations along with the boundary conditions are as follows.

$$\frac{\partial C_{i,k}}{\partial \theta} + \upsilon \frac{\partial q_{i,k}}{\partial \theta} = \frac{\psi_k}{Pe_k} \frac{\partial^2 C_{i,k}}{\partial \chi^2} - \psi_k \frac{\partial C_{i,k}}{\partial \chi} \qquad (3.1)$$

$$\frac{\partial q_{i,k}}{\partial \theta} = \alpha \left(\overset{*}{q}_{i,k} - q_{i,k} \right) \qquad (3.2)$$

The non-stoichiometric Langmuir isotherm is used to describe the multi-component adsorption equilibria.

$$\overset{*}{q}_{i,k} = \frac{q_{mi} K_i C_{ik}}{1 + \sum\limits_{l=1}^{NC} K_l C_{lk}} \qquad (3.3)$$

where $\chi = z / L_{col}$ and $\theta = t / t_s$

The boundary conditions are:

$$C_{i,\chi}^{in} = C_{i,k}(0,\theta) - \frac{1}{Pe_k} \frac{\partial C_{i,k}}{\partial \chi} \qquad (3.4)$$

$$\frac{\partial C_{i,k}}{\partial \chi}(1,\theta) = 0 \qquad (3.5)$$

The initial conditions are:

$$C_{i,k}(\chi,0) = C_{i,k}^0(\chi) \text{ and } \bar{q}_{i,k}(\chi,0) = q_{i,k}^0(\chi) \qquad (3.6)$$

The dimensionless parameters used in the above equations are:

$$\psi_k = U_{F_k} t_s / L_{col} \;, \alpha = k_a t_s \text{ and } Pe_k = U_{F_k} L_{col} / D_{ax_k} \qquad (3.7)$$

The mass balance at the node is then,

$$C_{i,k}^{in} = C_{i,k-1}(1,\theta) \qquad (3.8)$$

except if the column follows feed or desorbent port. In that case,

$$C_{i,k}^{in} = \left[Q_F C_{i,F} + Q_Q C_{i,k-1}(1,\theta) \right] / Q_R \text{ and } C_{i,k}^{in} = Q_S C_{i,k-1}(1,\theta) / Q_P \qquad (3.9)$$

respectively. Details pertaining to the adsorption isotherms are summarized in Table 3.1. The equilibrium data for *o*-, *m*-, and *p*-xylene, ethylbenzene and *p*-dimethylbenzene at 453 K were taken from Azevedo et al. (1998).

Two different numerical solution approaches were used to solve these set of Partial Differential Equations (PDEs) along with their boundary conditions. In the first method, the PDEs were discretized in space using the Finite Difference Method (FDM) to convert them into a system of coupled Ordinary Differential Equations-Initial Value Problem (ODE-IVP) (Method of Lines). The number of plates used in this case was 50. These stiff initial value ODEs were solved using the subroutine, DIVPAG (based on Gear's method), in the IMSL library. In the second approach, an orthogonal collocation method on finite elements (OCFE) was used to discretize the axial domain. In this case, each column was divided into six equal finite elements and each element was discretized with two internal collocation points to convert them again into a system of coupled ODE-IVPs as before. These were again solved using the DIVPAG subroutine in the IMSL library. Since periodic switching is imposed on the system, the separators always work under transient conditions. However, a cyclic (periodic) steady state with a period equal to the global switching time is eventually reached after several switching. For both SMB and Varicol, the periodic steady state was attained after about 40 switching cycles around the unit. Table 3.2 compares the simulation results obtained using the two numerical approaches used in this study, with the results reported in Minceva and Rodrigues (2002). Table 3.2 also shows the computational time taken for one simulation run by each method. The simulations in our study were performed on a CRAY J916 supercomputer. From the table it is clear that the OCFE method works much faster than the Method of Lines, which is understandable because of the drastic reduction in the total number of equations in the

former case. Figure 3.3 compares the steady-state internal concentration profiles obtained using the two numerical methods for the operating conditions listed in Table 3.1. The separation performance was evaluated by calculating the recovery (Rec) and purity (Pur) of *p*-xylene achieved at the extract port which is the objective of the Parex process. These quantities are defined as:

Purity of *p*-xylene in the extract

$$Pur\_pX = \frac{C_{Ex}^{pX}}{C_{Ex}^{pX} + C_{Ex}^{mX} + C_{Ex}^{oX} + C_{Ex}^{EB}} \times 100 \qquad (3.10)$$

Recovery of *p*-xylene in the extract

$$Rec\_pX = \frac{C_{Ex}^{pX} Q_{Ex}}{C_{F}^{pX} Q_{F}} \times 100 \qquad (3.11)$$

Table 3.2 Comparison of simulation results obtained with literature reported
(Minceva and Rodrigues, 2002)

Methods	Rec_pX (%)	Pur_pX (%)	CPU time (min)	Platform
MOL[#]	98.16	98.96	18.5	Cray J916
OCFE[‡]	98.29	99.51	1.2	Cray J916
gProms*	98.2	99.78	510	Pentium III

[#] This work using Method of Lines.
[‡] This work using Orthogonal Collocation on Finite Elements.
*   Results reported by Minceva and Rodrigues (2002) using gPROMS[®] (**g**eneral **PRO**cess **M**odelling **S**ystem), a general purpose process modeling, simulation and optimization software.

A = p-xylene; **B** = m-xylene; **C** = o-xylene; **D** = Ethyl Benzene
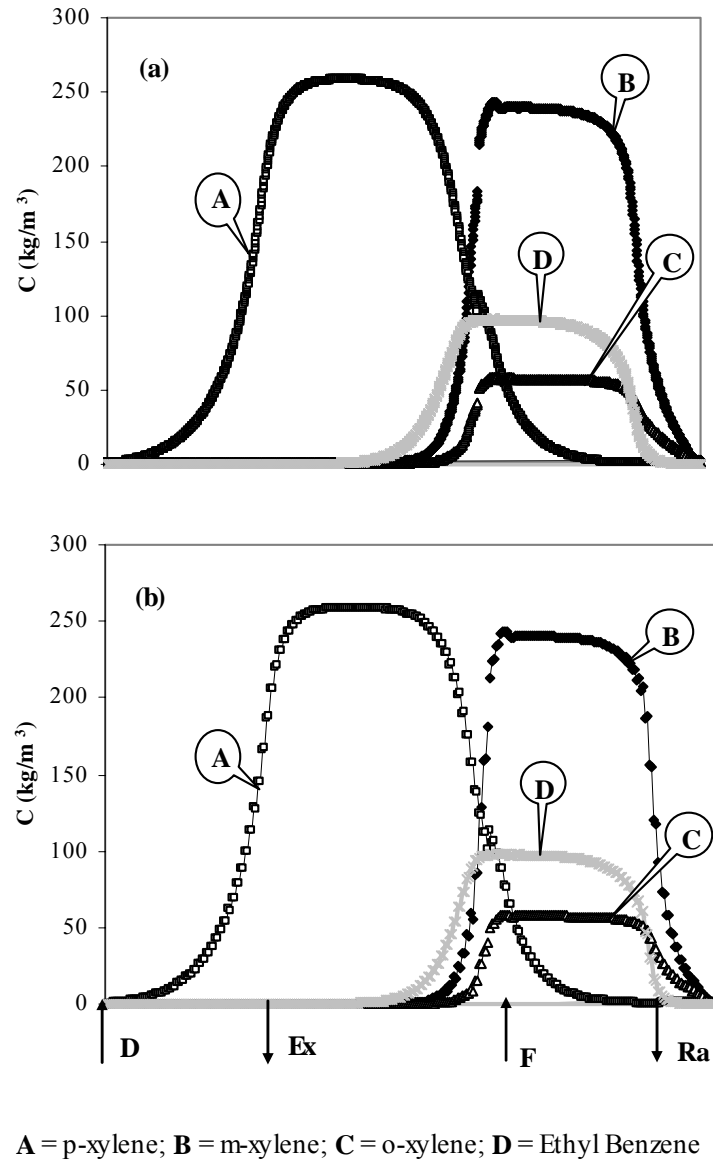
Figure 3.3 Comparison of steady-state concentration profiles of C$_8$ aromatics obtained by simulation of the industrial point (see Table 3.1 for data) **using (a)** method of lines (MOL) and **(b)** orthogonal collocation on finite elements (OCFE)

The emphasis of this study is on performing a rigorous multiobjective optimization of the Parex process to recover high purity of p-xylene from C_8 aromatic mixture using an adaptation of Genetic Algorithm. In order to obtain global Pareto optimal solution, one needs to perform large number of simulations (often over 2500 simulations consisting 50 chromosomes for 50 generations). In such a scenario, it is very important that we use a simulation method which is less time consuming. The results shown in the next section are obtained by using either of these methods. Method of Lines was used in solving Problem 1 while OCFE was used in solving optimization problems described in Problems 2 and 3.

3.3 Optimization of the SMB and Varicol systems

It is quite well known that one of the most serious problems associated with chromatographic processes is that though they are efficient in separation, the resultant product streams are dilute due to high desorbent requirements. Even if the desorbent is cheap it is desirable to get concentrated product streams since dilute streams result in higher operational cost (viz. heat requirement) in the subsequent downstream separation processes such as distillation. In Parex process, as can be seen from Table 3.1, the operating flow rates are very high as a result the downstream separation processes would have to handle high volumes of material and therefore would be very energy intensive. Reducing the desorbent consumption can therefore help in improving the economics of the overall process. Hence, one of the aims for optimization of Parex process is to improve the p-xylene recovery while reducing the total desorbent (pDEB) consumption.

In this work, a few double-objective optimization studies have been performed. It is to be emphasized that there is no end to the variety of multiobjective optimization problems that could be formulated and studied, and in this work only a few simple examples have been dealt with to illustrate the concept, technique and interpretation of results. One can, of course, consider more than two-objective functions but the analysis of those results becomes cumbersome as one has to deal with Pareto surfaces. In this study, a new state-of-the-art optimization technique based on genetic algorithm called as the non-dominated sorting genetic algorithm with jumping genes (NGSA-II-JG) (Kasat and Gupta, 2003) is utilized. NGSA-II-JG is an add-on novelty in the field of evolutionary algorithms and allows handling of these complex optimization problems. In addition to the sorting and sharing mechanism introduced in the Elitist Non-dominated Sorting Genetic Algorithm, NSGA-II (Kasat et al., 2002), the recent modification with jumping genes improves the diversity of mating pool leading to a much better spreading of the solution at an increased convergence speed. The jumping gene operations are performed by a modified mutation operator and the concept is borrowed from the working principle of the jumping genes (or transposons) in natural genetics. In natural genetics, jumping genes are DNAs that could jump in and out of chromosomes and can generate genetic diversity in natural populations. This concept is exploited in NSGA-II-JG. Details of methodology and applications of different adaptations of NSGA in chemical engineering can be obtained elsewhere (Nandasana et al., 2003). A short note on the optimization technique used in this study (NSGA-II with JG) is given in Appendix I.

In all the optimization runs presented in this chapter, 50 chromosomes (solutions) were considered and results are presented after 50 generations. It should be noted that optimization problems involved continuous variables such as column

length, flow rates and switching time and discrete variables such as number of columns and their distribution in various sections. Table 3.3 describes the list of the optimization problems formulated and solved in this study to determine the optimal operating conditions of SMB for this *p*-xylene separation.

3.3.1 Problem 1a: Determination of optimal column length (L_{col})

The first multi-objective optimization problem solved is maximization of the recovery of *p*-xylene (Rec_pX) with simultaneous minimization of the desorbent consumption (Q_D). To compare our results with those of Minceva and Rodrigues (2002), we fixed the diameter (d_{col}) and total number of columns (N_{col}), number of columns in each section ($\Omega = p/q/r/s$), feed flow rate (Q_F) and its concentration, flow rate in section S (Q_S) and temperature (T) as given in Table 3.1. Four decision (manipulative) variables are used, namely, the raffinate (Q_{Ra}) and the desorbent (Q_D) flow rates, the switching time (t_s), and length of each column (L_{col}). Since only four flow rates can be selected freely, while the other four are determined by mass balance around nodes A-D (see Figure 3.1), the remaining two flow rates were used as decision variables, namely the raffinate (Q_{Ra}) and the desorbent (Q_D) flow rate. The third decision variable is the switching time t_s, which clearly has a strong influence on the performance of SMB system. The bounds for t_s lie between the breakthrough times of the two components for the specific adsorbent. The fourth decision variable used is the length of each column (L_{col}) since it is impossible to determine the optimal column length merely through simulations. The optimization formulation and the bounds of decision variables are summarized in Table 3.3 (see Problem 1a). It is to be noted that a very narrow range is used for the bounds. This is required due to the existence of narrow "windows" for the decision variables in order to get meaningful

optimum solutions. Such boundaries can be estimated very conveniently using equilibrium theory and some preliminary sensitivity analysis of the model. The formulation can be mathematically represented as

Maximize	$J_1 = \text{Rec\_pX} [t_s, Q_{Ra}, Q_D, L_{col}]$	(3.12a)
Minimize	$J_2 = Q_D [t_s, Q_{Ra}, Q_D, L_{col}]$	(3.12b)
Subject to	$\text{Rec\_pX} \geq 92\ \%$	(3.12c)
	$\text{Pur\_pX} \geq 98\%$	(3.12d)
Decision variables	$1 \leq t_s \leq 2$ min	(3.12e)
	$2 \leq Q_{Ra} \leq 3\ \text{m}^3/\text{min}$	(3.12f)
	$2 \leq Q_D \leq 3.5\ \text{m}^3/\text{min}$	(3.12g)
	$1 \leq L_{col} \leq 1.15$ m	(3.12h)
Fixed parameters	$d_{col} = 4.117$ m, $N_{col} = 24$, $\Omega = 6/9/6/3$	(3.12i)
	$Q_F = 1.45\ \text{m}^3/\text{min}, Q_S = 5.39\ \text{m}^3/\text{min}, T = 453$ K	(3.12j)

SMB Model Equations given by Eqs. (3.1-3.9)

The inequality constraints (Eq. 3.12c-d) on recovery and purity were imposed to restrict optimal solutions that satisfy at least the minimum (industrial) acceptable recovery and purity values. The Pareto optimal solution along with the set of optimal values of the decision variables are shown in Figure 3.4. The figure clearly shows that the points do, indeed, constitute a Pareto set, i.e., as the recovery of *p*-xylene (Rec_pX) increases (desirable), the requirement for solvent (Q_D) also increases (undesirable). All points on this curve are equally good (non-dominated) optimal solutions. The optimum length of each column (L_{col}) was found out to be 1.086 m, lower than the industrial operating point (1.134 m). For $Q_D = 2.89\ \text{m}^3/\text{min}$, L_{col} reduced by 0.048 m, which amounts to circa 15.34 m^3 of total adsorbent savings for

24-column SMB system. The optimum t_s were found to be smaller, about 1.11 min, due to the reduction in the optimal column length while the optimal value of Q_{Ra} was obtained as 2.7 m^3/min. The purity of *p*-xylene (Pur_pX) was found to be almost same as that obtained for the industrial operating point, about 98.93% for a recovery of 98.18%.

Table 3.3 Description of the multi-objective optimization problems solved in this study

Problem No.	Objective Function	Decision Variables	Constraints	Fixed Parameters
1a (SMB)	Max Rec_pX Min Q_D	$1 \leq t_s \leq 2$ min $2 \leq Q_{Ra} \leq 3$ m^3/min $2 \leq Q_D \leq 3.5$ m^3/min $1 \leq L_{col} \leq 1.15$ m	Rec_pX $\geq$92 % Pur_pX $\geq$ 98%	$d_{col} = 4.117$ m $N_{col} = 24$, Ω (p/q/r/s) = 6/9/6/3 $Q_F = 1.45$ m^3/min $Q_S = 5.39$ m^3/min
1b (SMB)		Same as Problem 1a except $5 \leq p, r \leq 8, 1 \leq s \leq 4$		Same as Problem 1a except p, r, s are decision variables
1c (SMB)		Same as case Problem 1a except $6 \leq p, r \leq 9, 2 \leq s \leq 5$		Same as Problem 1b except $N_{col} = 28$
2 (Varicol)		Same as Problem 1a except Ω (32 possible combinations)		Same as Problem 1b
3 (SMB)	Max Rec_pX Max Pur_pX	Same as Problem 1b		Same as Problem 1b
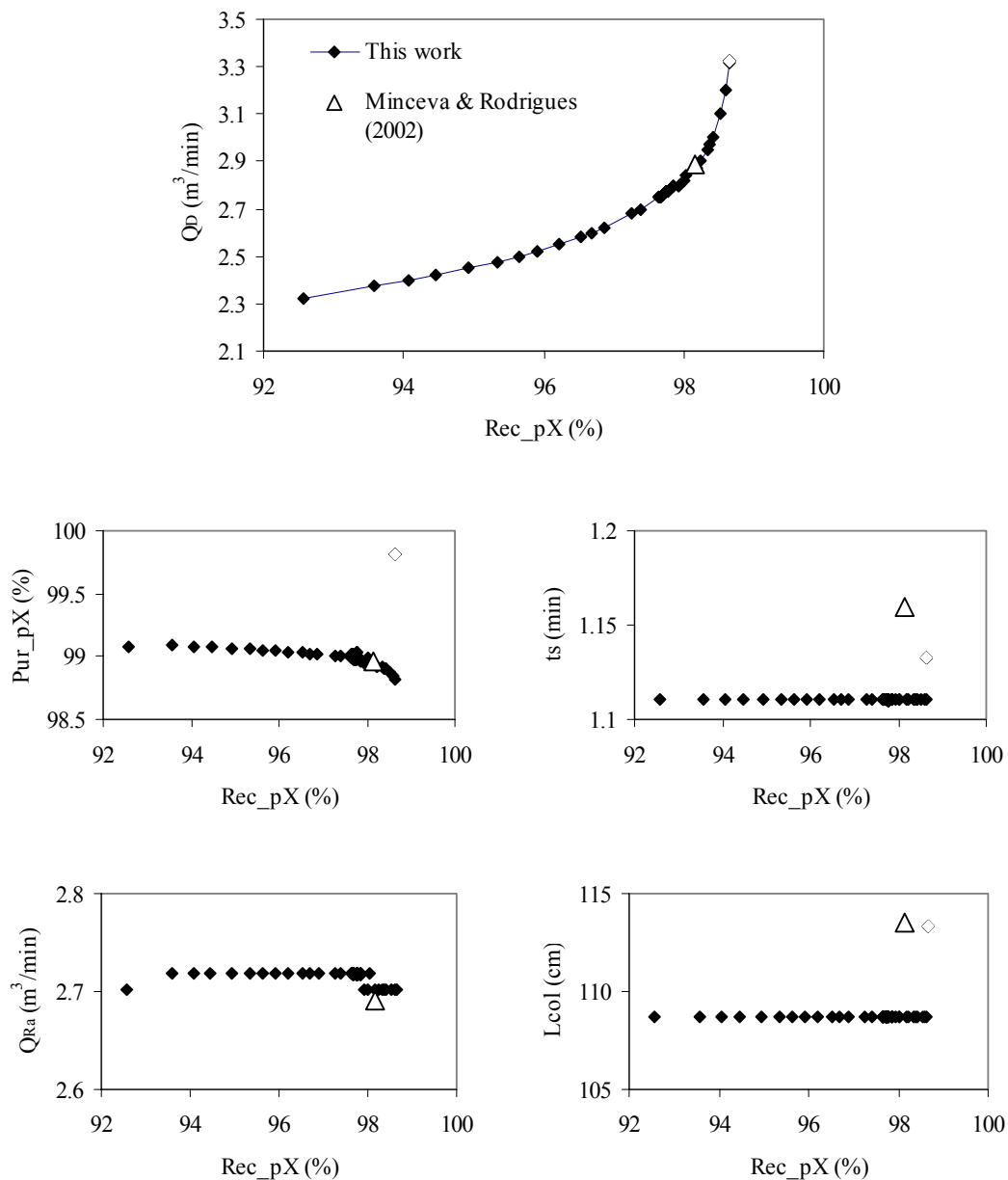
Figure 3.4 Pareto optimal solution and corresponding decision variables for Problem 1a (Determination of optimal column length)

Analysis of the optimal values of the decision variables shows that since some of them choose almost a single value for all the points on the Pareto curve, all the decision variables chosen may not be totally independent. However, it should be

noted that the relation between these parameters depend on various factors such as the adsorption selectivity, non-linearity of the adsorption isotherm, feed composition, mass transfer rates, column dispersion, etc. These interdependencies can be analytically obtained for linear separation systems with near equilibrium conditions. However, for difficult separation systems such as the present system, which is a multi-component mixture and is described by non-linear adsorption isotherms and with low adsorption selectivity, obtaining such analytical relations is very difficult. Hence, in order to obtain the optimal values of these parameters we were forced to consider them as independent variables for the remaining problems.

3.3.2 Problem 1b: Determination of optimal column configuration (Ω)

The optimal column distribution (configuration) that is the number of columns (p, q, r and s) in each section viz., P, Q, R and S (see Figure 3.1) determine the amount of adsorbent allocated for each section to carry out the required adsorption (or desorption) phenomenon. Hence, it is quite apparent that they also play a very important role in improving the recovery and purity of the desirable product. Optimal column distribution was determined by keeping N_{col} = 24 for the same optimization problem as in Problem 1a except that three additional decision variables, p, r, and s, number of columns in sections P, R and S respectively were used. Figure 3.5 compares the Pareto optimal solution obtained from Problems 1a-1b. The figure shows the shift in Pareto when 24 columns are distributed optimally, yielding better recovery while using less desorbent. Moreover, the optimal column length was further reduced by 0.021 m, which amounts to a further reduction of 6.71 m^3 of total adsorbent. The purity obtained in this case is slightly better as shown in Figure 3.5. The optimum column configuration (Ω) found out to be 7/6/7/4 for lower Q_D
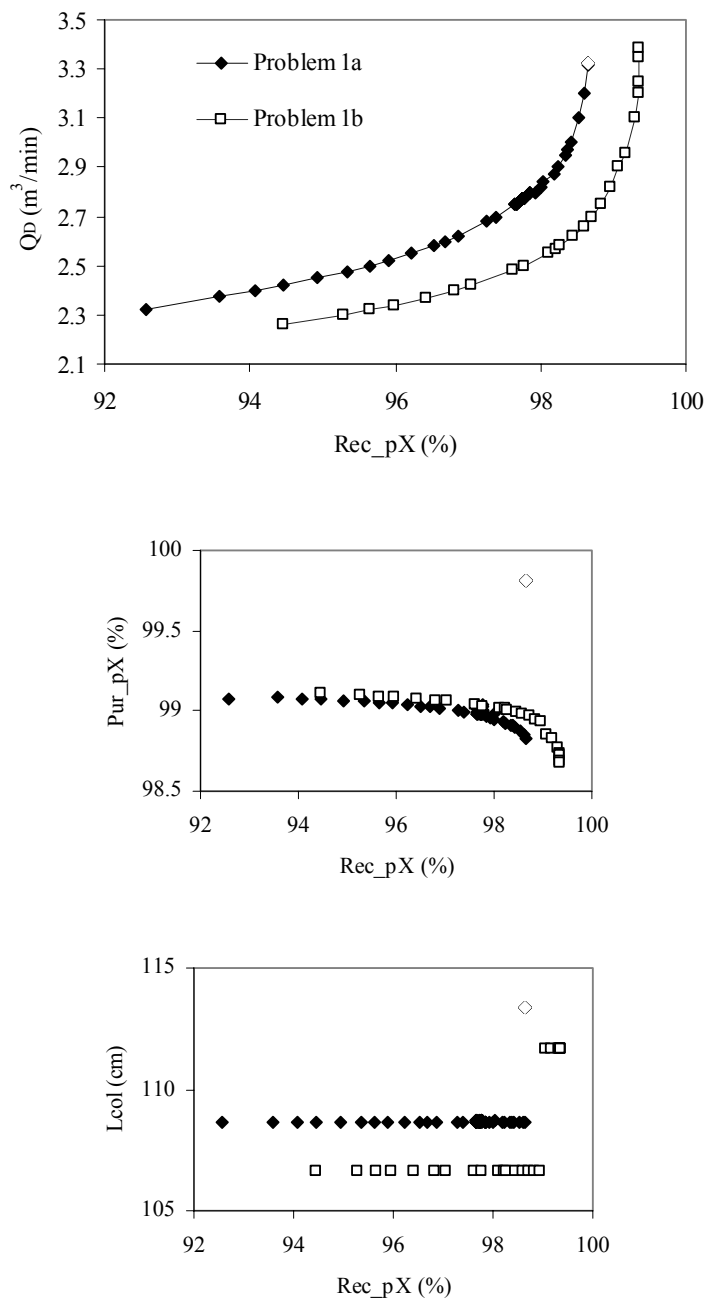
Figure 3.5 Comparison of Pareto optimal solution and corresponding decision variables for Problems 1a and 1b (Determination of optimal column configuration)

range while it is 8/6/8/2 for higher values of Q_D compared to $\Omega = 6/9/6/3$ used for the industrial operating point (Minceva and Rodrigues, 2002). The choice of these optimal configurations implies that more adsorbent is needed in the sections P and R. Sections P and R deal with desorption and adsorption of the strongly adsorbing component, *p*-xylene, respectively. Hence for higher recovery and purity of the desired product (*p*-xylene) at lower desorbent flow rate (Q_D), more solid adsorbent is required in these sections.

3.3.3 Problem 1c: Determination of optimal number of columns (N_{col})

In some cases there is a possibility to achieve better performance by increasing the total number of columns (N_{col}) while having a reduced length (L_{col}). This is possible because more columns would provide an additional flexibility for the operation. Hence, a new optimization problem with $N_{col} = 28$ was formulated and solved to see if better performance can be achieved compared to 24 columns used in problems 1a-1b. Figure 3.6 compares the Pareto optimal solution obtained. The figure shows a marginal shift (improvement) in Pareto although there is slight increase of purity of *p*-xylene (for example, Pur_pX = 99.12 % when $N_{col} = 28$ compared to 98.96 % for 24-column SMB system for the same Rec_pX = 98.7%). However, results show that probably 24 is the optimum number of columns and with further addition of columns, improvement in the system performance is insignificant.
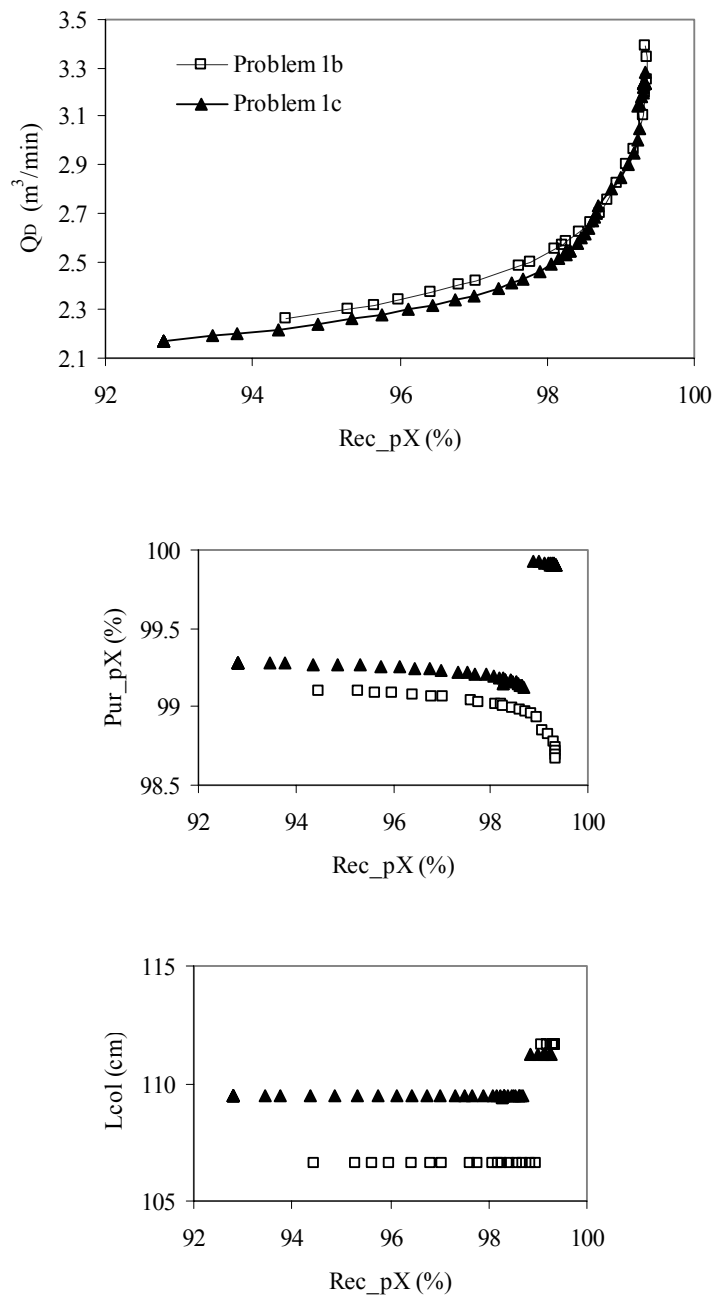
Figure 3.6 Comparison of Pareto optimal solutions and corresponding decision variables for Problems 1b and 1c (Determination of optimal column number)

3.3.4 Problem 2: Comparison between performance of SMB and Varicol Systems

Ludemann-Hombourger et al. (2000), showed experimentally that Varicol system can perform better than its equivalent SMB system due to the flexibility in its operation. It could even aid in reduction of total volume of the adsorbent required. Hence, the optimization study was extended to four-subinterval 24-column Varicol system to determine the extent of improvement that can be achieved over an equivalent 24-column SMB system. With $N_{col} = 24$ in the Varicol unit, there would be a very large number of possible column configurations. In order to reduce the computation time, extensive simulation studies were performed to determine the configurations that would lead to better performance of the system. From the results of these simulation studies 32 possible configurations were selected for the optimization exercise which could lead to better values of the objective functions. The optimization formulation is provided in Table 3.3 (Problem 2).

The Pareto-optimal solution of the 24-column Varicol system is compared with the equivalent 24-column SMB system in Figure 3.7. The figure clearly shows that 100% recovery of *p*-xylene is possible using reasonable amount of desorbent and it evidently elucidates the performance improvement in Varicol due to the increased flexibility compared to the more rigid SMB system. For example, for $Q_D = 2.57$ m^3/min Varicol shows almost 100% recovery while SMB shows only 98.21% recovery of *p*-xylene. Furthermore, the optimal L_{col} is further reduced by 0.054 m which helps in achieving further reduction of around 17.36 m^3 of adsorbent, which is remarkably high. The optimum switching time, t_s, obtained is 1.05 min. The optimal column configuration for the entire range of Pareto for Varicol system was found to be grouping of five different combination of column distribution as listed in Table 3.4.
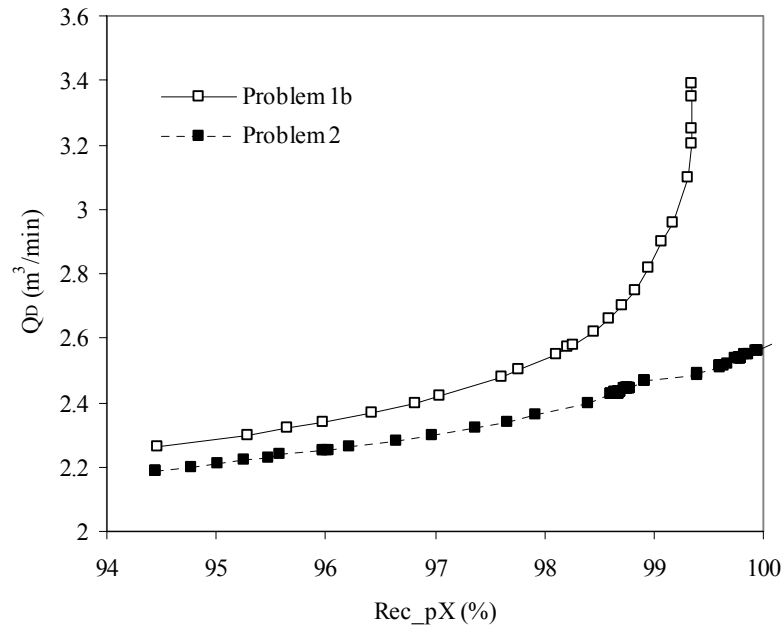
Figure 3.7 Comparison of Pareto optimal solution for Problem 1b (SMB) **and Problem 2** (Varicol)

Three different optimal column configurations for the 4-sub-interval 24-column Varicol system were obtained. For the lower desorbent flow rate region ($Q_D < 2.23$ m^3/min), the optimal configuration obtained was B-D-A-E, which means for the first sub-time interval (0-$t_s/4$), column distribution is B [$\equiv 5/8/8/3$]; for the second sub-time interval ($t_s/4$- $t_s/2$), column distribution is D [$\equiv 8/5/8/3$]; for the third time interval ($t_s/2$-$3t_s/4$), optimal column distribution is A [$\equiv 8/5/7/4$], and for the last sub-time interval ($3t_s/4$-t_s), optimal column distribution is E [$\equiv 8/4/8/4$]. For $2.23 < Q_D$ (m^3/min) < 2.43, the optimal configuration obtained was B-A-A-E, while for $Q_D >$

2.43 (m^3/min), the optimal configuration obtained was B-A-C-E. These configurations imply that to increase the recovery of *p*-xylene while satisfying the desired purity constraint, sections P and R always require more columns. This can be easily understood by recalling the earlier discussion for problem 1b that these sections deal with the adsorption and desorption of *p*-xylene and hence require more solid adsorbents.

Table 3.4 Optimum column configurations[#] (distribution) for N_{col} = 24

Ω	Column Configuration
A	8 / 5 / 7 / 4
B	5 / 8 / 8 / 3
C	7 / 6 / 8 / 3
D	8 / 5 / 8 / 3
E	8 / 4 / 8 / 4

\#   Column distribution Ω = A implies number of columns in sections P, Q, R and S are respectively 8, 5, 7 and 4 for the SMB. Column distribution Ω = B/D/A/E implies column distribution for Varicol process is B for t/t_s = 0-0.25, D for t/t_s = 0.25-0.5, A for t/t_s = 0.5-0.75 and E for t/t_s = 0.75-1. Note that only optimal column configuration is shown here out of many possible column distributions for N_{col} = 24.

3.3.5 Problem 3: Simultaneous maximization of purity and recovery of *p*-xylene

In problems 1 and 2, recovery of *p*-xylene was maximized while minimizing the desorbent. In this problem, both recovery and purity of *p*-xylene were maximized simultaneously. Such type of multiobjective problems have been solved earlier (Subramani et al., 2003a) and it has been observed that these two objective functions always contradict each other. The decision variables and their bounds used for this case are same as that considered for problem 1b. Mathematical description for this problem is given in Table 3.3. The Pareto optimal solution is shown in Figure 3.8.

The figure shows that the Pareto is very sensitive near the region of high *p*-xylene recovery. For recovery of *p*-xylene from 92% to around 98.8%, the purity of *p*-xylene remains very high around 100%. Beyond this the purity decreases very sharply and drops to as low as 98.6% for recovery of *p*-xylene at 99.5%. The corresponding optimal decision variables are also shown in Figure 3.8. Optimal Q_{Ra} values are constant at low recovery values but Q_{Ra} slowly decreases at higher values of *p*-xylene recovery. The optimal values of Q_D steadily increase as recovery of *p*-xylene increase but become insensitive to the maximization of objective functions thereafter. Hence, the plot of Q_D shows scattered points at higher values of *p*-xylene recovery.

Optimum column length varies with the recovery of *p*-xylene but the most dominating L_{col} chosen was around 1.05 m and the optimum t_s chosen was according to the L_{col} chosen. The optimum column configurations obtained were $\Omega = 5/7/8/4$ for the lower recovery values and $\Omega = 8/4/8/4$ for the higher range of *p*-xylene recovery. The desorbent consumption in this case is certainly higher than in earlier cases (Problems 1-2) as Q_D is not one of the objective functions in this problem and certainly to maximize purity one needs higher desorbent flow rates. For example, for problem 1b, the desorbent requirement was only 2.58 m^3/min for a recovery of 98.26%, while for this case Q_D needed was 2.93 m^3/min for the same recovery. However, the purity is now 99.95% as compared to 99.0% for problem 1b for the same recovery. Figure 3.9 compares the concentration profile between Case 1b and 3 for recovery of *p*-xylene equal to 98.26%.
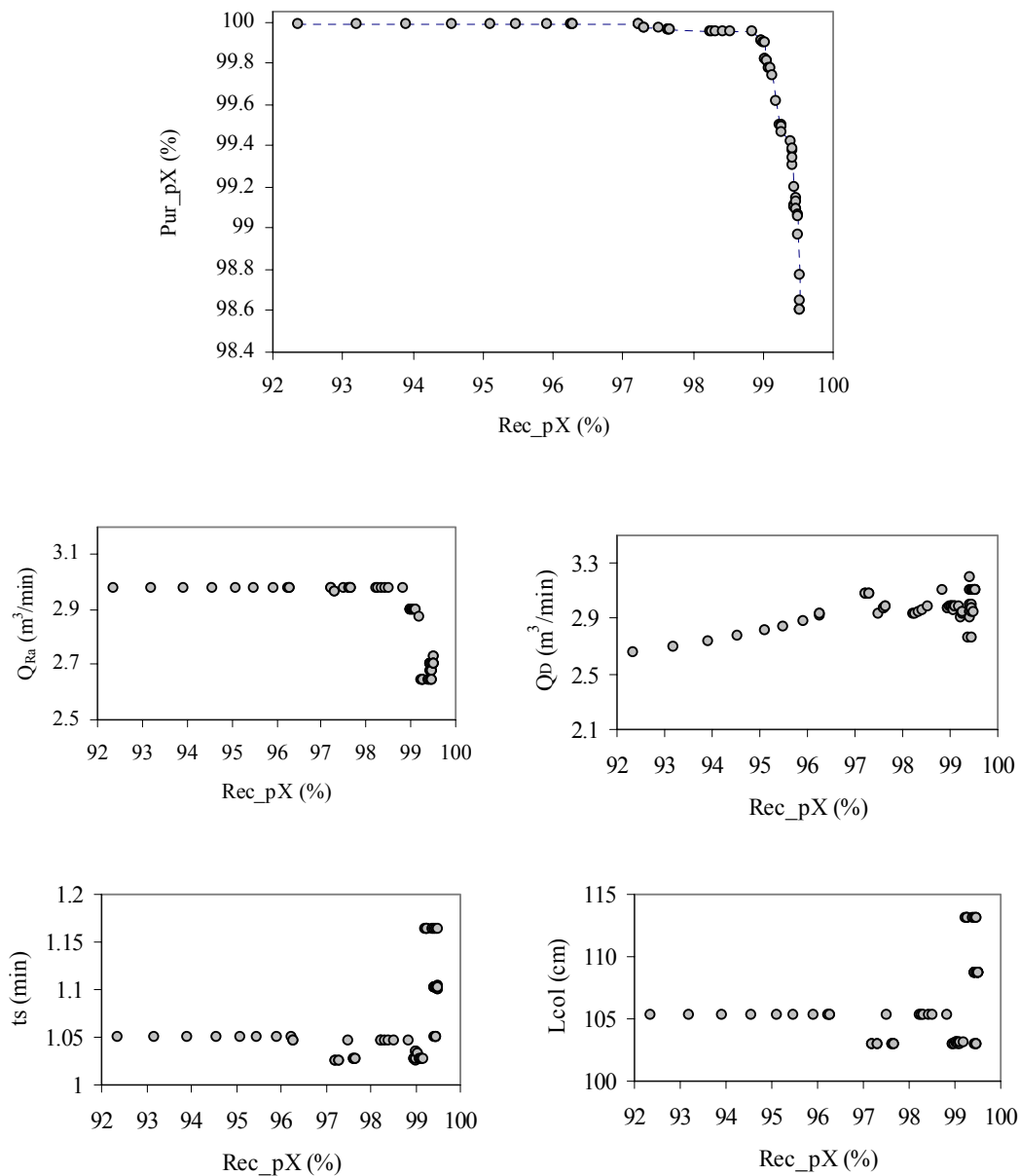
Figure 3.8 Pareto optimal solution and corresponding decision variables for Problem 3 (Simultaneous maximization of purity and recovery of *p*-xylene)
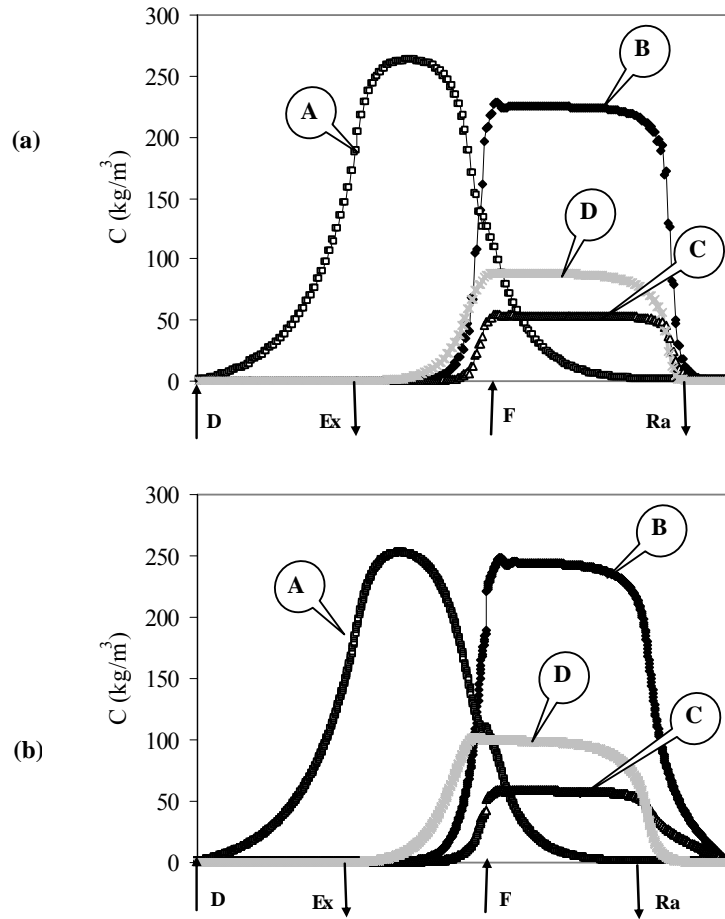
Figure 3.9 Comparison of steady-state concentration profiles for optimum points corresponding to Rec_pX = 98.26% shown in Figure 3.8 (Problem 3) (a) and in Figure 3.5 (Problem 1b) (b)

3.4 Prediction of separation regions and process performance using equilibrium Triangle theory

In order to understand the reliability of the optimization results it is worthwhile to discuss the results using equilibrium triangle theory (Storti et al., 1995) applied to countercurrent chromatography. Storti et al. showed that the counter current chromatographic unit behavior can be explained in terms of the flow rate ratio parameters relative to the four zones of the unit (see Figure 3.1):

$$ m_\varphi = \frac{Q_\varphi^{SMB} t_s - V_{col}\varepsilon}{V_{col}(1-\varepsilon)}, \quad \varphi = P, Q, R, S \tag{3.13}$$

According to this theory, the flow rate ratio parameter for section P, m_P, has to be larger than a critical value in order to achieve complete regeneration of the solid phase from the strongly adsorbed component, while m_S has to be smaller than a critical value in order to achieve complete regeneration of the liquid phase from the weakly adsorbed component. Once both these conditions are satisfied, it is possible to identify in the $m_Q - m_R$ parameter plane, a triangular region that includes all pairs of values leading to complete separation or where both the components are recovered pure in the extract and in the raffinate respectively. It is also worth pointing out that the distance from the diagonal of a point in the $(m_Q - m_R)$ plane is directly proportional to productivity and inversely proportional to desorbent requirement. The vertex of the complete separation triangular region thus gives the optimal operating point with respect to such process performance. This region depends only on the adsorption isotherms and on feed concentrations.

In order to interpret the optimization results, we have re-plotted the optimal values of the decision variables in Figure 3.4 for problem 1b in terms of the four flow rate ratio parameters, m_φ (calculated from Eq. 3.13) as shown in Figure 3.10. This

figure shows that as the objective function, that is the recovery of *p*-xylene, increases, desorbent flow rate increases and m_P is seen to increase. This is due to the necessity for improving the solid regeneration in zone P in order to avoid the heavier component entering zone S and then polluting the raffinate. This also indicates that zone P is critical in controlling the recovery of *p*-xylene. One needs to better control the regeneration of the solid from the heavy component in zone P. On the other hand, m_S seems to be almost constant, indicating that zone S meets the constraint that for regeneration of the desorbent m_S should be below a critical value. Also since it is constant it seems to be not so critical in achieving the desired separation performance for the particular case under examination. As can be recalled from the discussion for Problem 1b, two optimal configurations were chosen for these Pareto results. The configuration for results greater than $Q_D = 2.9$ m^3/min was different from those below this desorbent flow rate. Due to this we can see a shift in the values of m_Q, m_R and m_S from this value onwards. In the respective sets of these configurations, we can see that the values of m_Q and m_R obtained remain almost constant as the recovery rate increases. This is consistent with the equilibrium theory according to which the optimal operating point (the vertex of the triangle) is independent of the feed and desorbent flow rates. Moreover according to equilibrium theory, the values of m_Q and m_R should not vary a lot but should be constant corresponding to the vertex of the complete separation region.

After explaining the optimization results using the equilibrium theory, it was decided to construct the separation region for this process using the triangle theory. Figure 3.11 shows the m_Q-m_R plot. The diagonal $m_Q = m_R$ corresponds to a zero feed flow rate; therefore, m_R must be higher than m_Q when the feed enters the system. The horizontal branch $m_R = 0.042$ (see Figure 3.10) corresponds to a zero raffinate flow
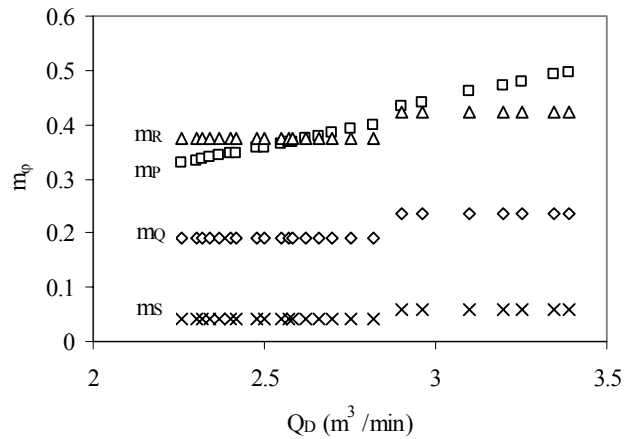
Figure 3.10 Calculated m_φ values corresponding to Pareto optimal solutions shown in Figure 3.5 (Problem 1b)

rate. Hence, to obtain a point on the m_Q – m_R plane, the SMB model was successively solved for several values of m_Q and m_R within the region between the diagonal $m_Q = m_R$, the horizontal line $m_R = 0.042$, and the m_R axis. The increment in m_Q used was 0.0125, and was chosen to be sufficiently small to provide precise determination of the separation region. For each pair of (m_Q, m_R), the purity and recovery of *p*–xylene in the extract were estimated. A high recovery of *p*-xylene in the extract implies high raffinate purity. The values which satisfy the constraint Pur_pX > 98% and Rec_pX > 92% were selected to build the region of pure separation. The values that did not fulfill this requirement were discarded. The region of pure separation calculated in this fashion is shown in Figure 3.11(a). The vertex of the triangle provides the optimal operating conditions for the system. It corresponds to the point $m_Q = 0.1875$ and $m_R = 0.4625$ with Pur_pX = 98.9% and Rec_pX = 94.94. Figure 3.11(a) was re-plotted (shown in Figure 3.11(b)) by further constraining the recovery of *p*-xylene and only those points were chosen that correspond to Rec_pX > 98%. As can be seen in Figure

3.11b, the pure separation region further narrows. The vertex of the triangle now corresponds to the point $m_Q = 0.1875$ and $m_R = 0.3875$ with Pur_pX = 98.7% and Rec_pX = 98.5%. It is worth noting that this point is very close to the values obtained from our optimization study ($m_Q = 0.19$ and $m_R = 0.38$).
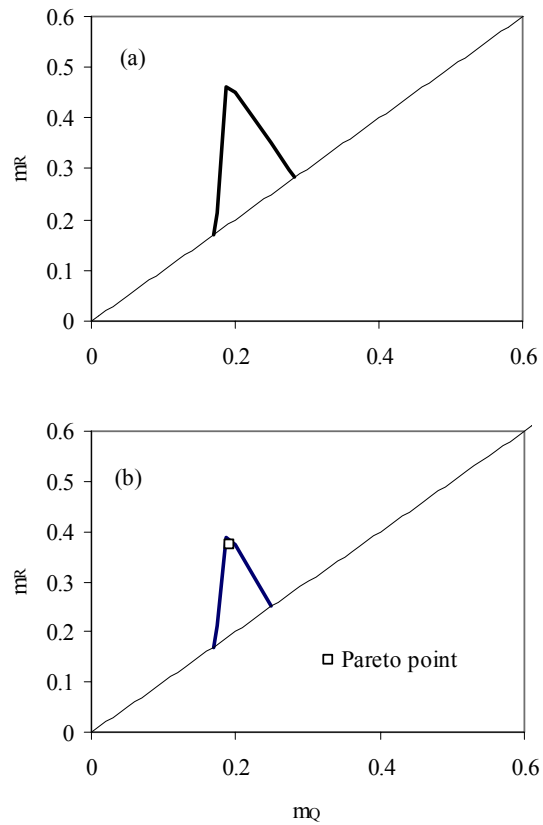
Figure 3.11 Optimal operating regimes in m_Q-m_R plane calculated from triangular theory for optimal solutions shown in Figure 3.10 (Problem 1b). (a) relaxed constraint, (b) stringent (restricted) constraint

3.5 Conclusions

Continuous large-scale chromatographic separations of C_8 aromatic mixture to recover *p*-xylene using simulated moving bed (SMB) technology have been of great interest for many years. In this work, we have presented a systematic study for optimal operation of SMB and Varicol process for recovery of *p*-xylene based on Parex process. The selection of operating parameters such as length and number of columns, switching time interval (in SMB) and sequence (in Varicol), and liquid flow rates in different sections are not straightforward. In most cases, conflicting requirements and constraints govern the optimal choice of the decision (operating or design) variables. In addition, SMB (and Varicol) systems for *p*-xylene recovery operate at high feed concentrations leading to non-linear competitive adsorption behaviors.

The economical operation of SMB (and Varicol) process is governed by many factors depending on the objective and product quality. One may be interested in higher recovery of the desired component using minimum solvent (desorbent) or may be interested in simultaneous maximization of recovery and purity of the desired product streams. In this work, we considered two multi-objective optimization problems that involve simultaneous optimization of more than one objective functions. Optimal design and operating conditions were found out for two cases: (a) simultaneous maximization of recovery of *p*-xylene with minimization of desorbent consumption, and (b) simultaneous maximization of productivity and purity of *p*-xylene. A Pareto optimal curve was obtained for both SMB and Varicol systems. It was found that significant improvement could be obtained for SMB performance when column length and its distribution in various sections are selected appropriately. Moreover, Varicol process operation could lead to 100% *p*-xylene recovery which

Chapter 3   Optimal Operation of an Industrial-Scale Parex Process for p-xylene recovery

was not possible with an equivalent SMB system. Systematic optimization resulted in better operating points in terms of recovering more *p*-xylene while using less desorbent over the current industrial operating point. It should be noted that it is the first time Varicol is applied to this industrially important separation system. Optimization results were also explained using equilibrium theory.

92

Chapter 4   Optimization of Reactive SMB and Varicol for Sucrose Inversion

4.1 Introduction

Chromatographic reactors are systems that are used to convert one or more components (partially or totally) and simultaneously separate one or more of the products that are being formed. Reaction occurs either in the mobile or stationary phase. In the latter case, the catalyst is supported or immobilized on the solid adsorbent that promotes the separation of the reaction products. In-situ separation of the products drives the reversible reaction to completion beyond thermodynamic equilibrium and at the same time helps in obtaining products of high purity. Chromatographic reactor based on SMB technology, namely Simulated Moving Bed Reactor (SMBR), provides economic benefit for equilibrium limited reversible reactions, such as, many hydrogenation, isomerization, and esterification reactions (Ray et al., 1990). They are also unique in applications where the removal of inhibitors, acceptor products or poisons improves the overall reaction yield. This is particularly true for bioreactors catalyzed by microorganisms since, in such cases the systems seem to be very efficient when operated with product concentration within a certain physiological range (Cen and Tsao, 1993). Besides, a build-up of product concentration may also lead to inhibition of the process concerned and thus, limit the productivity.

The application of chromatographic reactors in the biochemical field was initiated in the early 1980s by Barker and co-workers (Barker and Ganetsos, 1987; 1988). Other ingenious arrangements that implement the principle of continuous chromatographic reaction-separation principle have been reported (Ganestos et al., 1993; Barker et al., 1992 Hashimoto et al., 1983; 1993; Sarmidi & Barker, 1993;

Meurer et al., 1996). The inversion of sucrose, the isomerization of glucose to fructose and the biosynthesis of dextran from sucrose were the test reactions in all these works. It was observed that financial and operational benefits were achieved through such process intensification.

Invert sugar syrup, an equimolecular mixture of glucose and fructose, is a valuable sweetener and is required by the food and pharmaceutical industries. Fructose is 1.3 times sweeter than sucrose and about 1.7 times sweeter than glucose. Furthermore, it has functionally more desirable properties like low carcinogenicity, high osmotic pressure, high solubility, source of instant energy and prevents crystallization of sugar in food products. Hence, high fructose syrups are in great demand as food and soft drink sweeteners. There are different methods to conduct the Inversion reaction, among which acid inversion and bio-inversion are more popular. Bio-inversion though expensive, is a better alternative, as it does not produce any polymerized byproducts as seen in case of acid inversion. Hydrolysis of sucrose by the enzyme Invertase leads to the production of invert sugar syrup. Yeast cells are commonly used as a source of Invertase. The inversion of sucrose takes place as follows:

$$\text{Sucrose} \xrightarrow{\text{invertase}} \text{Glucose + Fructose} \tag{4.1}$$
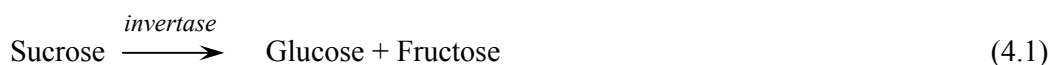
As seen in Eq. (4.1), inversion of sucrose is an irreversible reaction, and thus, the reaction rate is not influenced by the product accumulation. However, it has been shown that even for irreversible reactions, the use of a simulated moving bed reactor (SMBR) increases conversion and product purity as compared to the performance of an equivalent chromatographic reactor-separator in batch mode (Ray et al., 1994; Meurer et al., 1996). Barker et al. (1992) have also shown that simultaneous inversion and product separation makes it possible to overcome problems associated with

substrate inhibition. This further justifies the use of SMBR systems in the industrial production of high fructose sugar solutions from the cane sugar (sucrose). Furthermore, use of SMB technology, helps in reducing total amount of water in the product stream. The major expense in these sugar industries is incurred from the concentration of products that are diluted with water. Water from the product streams is generally removed by evaporation (sometimes in combination with reverse osmosis) and has a major effect on design, investment and operation costs of these sugar industries.

Industrial processes aim at maximizing their production capacities while simultaneously improving the product quality and reducing operating costs. Usually, there exists a trade-off between these requirements. This is particularly true in the production of high fructose syrups (HFS) using SMB (or Varicol) systems where high productivity at reduced desorbent consumption is the most important issue. Thus, in this case the design and operation of SMB (and Varicol) systems need to be optimized using multiple objective functions and constraints.

There are a number of publications focusing on the design of reactive SMB (Ray et al., 1990, 1994, 1995; Fricke et al., 1999a; Migliorini et al., 1999b). Except for the works of Zhang et al. (2002a) and Yu et al. (2003) there are no optimization studies reported in the literature. In this work, an elaborate optimization study on the applicability of SMBR (and reactive Varicol) for the inversion of sucrose in the presence of the enzyme Invertase and in-situ separation of the products, viz., glucose and fructose, is discussed at length. An existing model that can predict published pilot-scale experimental results of the system is used in the optimization. The model was verified first with published experimental results (Azevedo and Rodrigues, 2001b) and thereafter, few multi-objective optimization studies were carried out to

obtain the Pareto-optimal solutions to provide a clear distinction between the performances of the SMB and Varicol process. The concept of employing a variable feed flow mode was also explored. The optimal operating parameters (such as the feed and desorbent flow rates, the flow rates in the different sections, the switching time and amount of catalyst) and geometric parameters (such as number and length of columns, and its switching sequence) are determined.

4.2 Enzymatic Inversion of Sucrose in SMBR

In the last couple of decades a substantial amount of research has been conducted for the separation of fructose and glucose in SMB systems (Hashimoto et al., 1983; Ching and Ruthven, 1985a; 1985b; 1985c; Ching and Lu, 1997; Ruthven and Ching, 1989; Ma and Wang, 1997; Azevedo and Rodrigues, 2000; 2001a; Subramani et al., 2003a). Both glucose and fructose have linear isotherms over a wide concentration range. Hence these are excellent experimental mixtures used in developing analytical and numerical simulations for the performance prediction and design purposes. Recently, inversion of sucrose in presence of Invertase has also been studied for the design of bio-reactive SMB systems (Azevedo and Rodrigues, 2001b). The separation is performed using ion-exchange resins with warm water as the desorbent. The preferred implementation consists of using polystyrene cation-exchange resins in the calcium form in which the fructose forms a complex with the calcium ions and is retarded, while glucose and other oligosaccharides are eluted with the desorbent.

In the work of Azevedo and Rodrigues (2001b), the SMBR set-up had 3, 2, 5 and 2 columns in sections P, Q, R and S respectively as shown in Figure 4.1. The feed was a diluted sucrose solution (80×10^3 kg/m^3), since the Michaelis-Menten equation

has been shown to apply at this concentration. The enzyme Invertase was fed to the

SMBR diluted in the desorbent (warm water). Its maximum activity was observed at

328K and at pH 4.5. Therefore, the desorbent consisted of a pH 4.5 buffer prepared

from acetic acid (0.28% v/v) and calcium acetate (0.5% w/v) (Azevedo & Rodrigues,
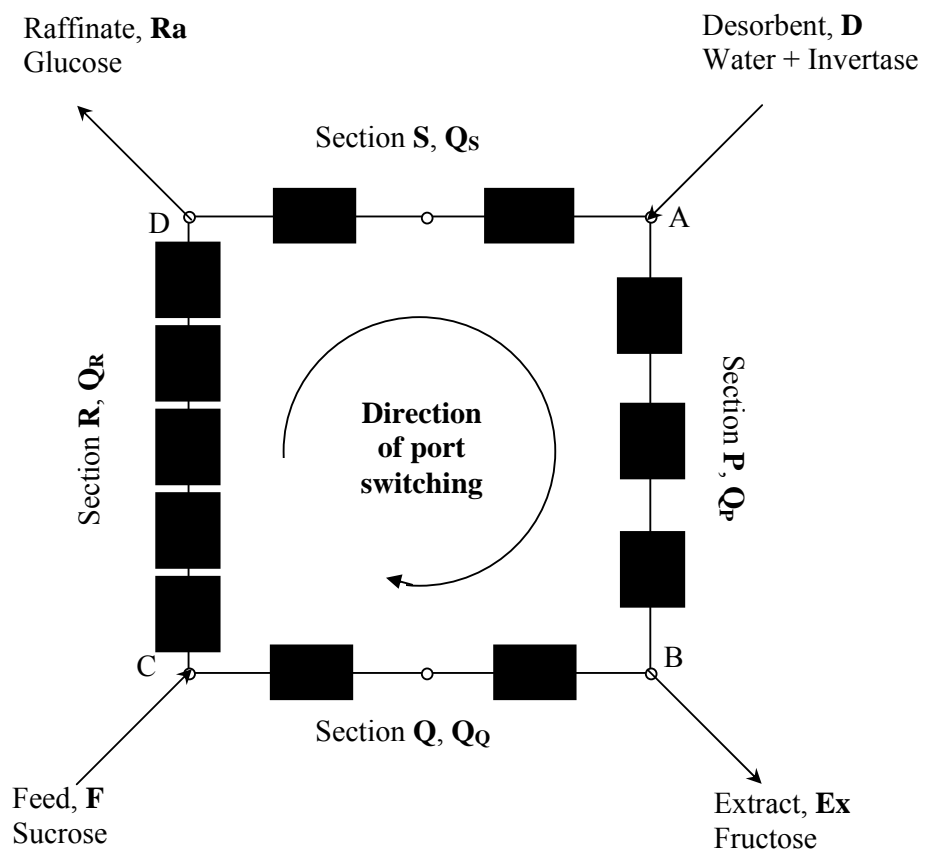
2001b).

Figure 4.1 Schematic diagram of a 12-column SMBR pilot plant.
(Azevedo & Rodrigues, 2001b)

4.3 Mathematical Model

The mathematical model together with the initial and boundary conditions that completely define the SMBR system for the inversion of sucrose were reported by Azevedo and Rodrigues (2001b). This model was based on the True Moving Bed Reactor (TMBR). However, in this work in the optimization study the SMBR model is used, as it is more realistic representation of the experimental set-up. The differential mass balance equations, overall as well as in the solid phase for species i in the kth column are as follows (Azevedo and Rodrigues, 2001a):

For glucose and fructose,

$$\frac{\partial C_{i,k}}{\partial \theta} + \upsilon \frac{\partial \bar{q}_{i,k}}{\partial \theta} = \frac{\psi_k}{Pe_k} \frac{\partial^2 C_{i,k}}{\partial \chi^2} - \psi_k \frac{\partial C_{i,k}}{\partial \chi} + k_r t_s \left(1 + \nu K_e\right)\left(\frac{\sigma_i R_j}{k_r}\right) \tag{4.2}$$

$$\frac{\partial \bar{q}_{i,k}}{\partial \theta} = \alpha_i \frac{Bi_{m_k}}{5 + Bi_{m_k}} \left(\bar{q}^*_{i,k} - \bar{q}_{i,k}\right) \tag{4.3}$$

$$\bar{q}^*_{i,k} = K'_i C_{i,k} \tag{4.4}$$

For Sucrose,

$$\frac{\partial C_{i,k}}{\partial \theta} = \frac{\psi_k}{Pe_k} \frac{\partial^2 C_{i,k}}{\partial \chi^2} - \psi_k \frac{\partial C_{i,k}}{\partial \chi} + k_r t_s \left(1 + \nu K_e\right)\left(\frac{\sigma_i R_j}{k_r}\right) \tag{4.5}$$

where $\sigma_I = 0.526$ for glucose and fructose, while $\sigma_I = -1$ for sucrose

$$R_j = k_r \left(\frac{C_{Suc,j} \times C_{Enz,j}}{K_{mm} + C_{Suc,j}}\right) \tag{4.6}$$

For the enzyme, Invertase,

$$\frac{\partial C_{i,k}}{\partial \theta} = \frac{\psi_k}{Pe_k} \frac{\partial^2 C_{i,k}}{\partial \chi^2} - \psi_k \frac{\partial C_{i,k}}{\partial \chi} \tag{4.7}$$

where $\chi = z / L_{col}$ and $\theta = t/t_s$

The boundary conditions are:

$$C_{i,\chi}^{in} = C_{i,k}(0,\theta) - \frac{1}{Pe_k}\frac{\partial C_{i,k}}{\partial \chi} \tag{4.8}$$

$$\frac{\partial C_{i,k}}{\partial \chi}(1,\theta) = 0 \tag{4.9}$$

The initial conditions are:

$$C_{i,k}(\chi,0) = C_{i,k}^0(\chi) \text{ and } \bar{q}_{i,k}(\chi,0) = \bar{q}_{i,k}^0(\chi) \tag{4.10}$$

The dimensionless parameters used in the above equations are:

$$\psi_k = U_{F_z} t_s / L_{col} \text{ and } \alpha_i = k_{h_z} t_s \tag{4.11}$$

$$\text{where, } k_{h_z} = \left(\frac{K + \varepsilon_p}{k_p} + \frac{K}{k_\mu(K + \varepsilon_p)} \right)^{-1}$$

$$K' = K + \varepsilon_p, \quad Pe_k = U_{F_z} L_{col} / D_{ax_k} \text{ and } Bi_{m_k} = k_{f_k} R_p / D_{pe}$$

The mass balance at the node is then, $C_{i,k}^{in} = C_{i,k-1}(1,\theta)$, except if the column follows feed or desorbent port. In that case,

$$C_{i,k}^{in} = \left[Q_F C_{i,F} + Q_Q C_{i,k-1}(1,\theta) \right] / Q_R \text{ and } C_{i,k}^{in} = Q_S C_{i,k-1}(1,\theta) / Q_P \text{ respectively.}$$

The details pertaining to the adsorption isotherms and the experimental set-up are summarized in Table 4.1. Sucrose is assumed to react in the inter-particle fluid phase and at the surface of the resin (Azevedo and Rodrigues, 2001b). This is accounted for by the term $(1+\nu K_e)$, present in the Eqs. (4.2) and (4.5). The reaction products, viz., glucose and fructose are assumed to have linear isotherms (Hashimoto et al., 1983; Lee and Lee, 1992; Viard and Lameloise, 1992). The diffusion within the adsorbent particle is described by means of a bi-linear driving force approximation (Azevedo and Rodrigues, 1999).

The PDEs were discretized in space using the Finite Difference method to convert them into a system of coupled ODE-IVPs (Method of Lines). Since periodic switching is imposed on the system, the reactor-separator works under transient conditions. However, a cyclic (periodic) steady state with a period equal to the global switching time is eventually reached after several switching. For both SMBR and Varicol process, the periodic steady state was always attained after about 10 switching cycles around the unit. The simulated values predicted by the above mathematical model matched very well with the experimental values reported by Azevedo and Rodrigues (2001b). The SMBR performance was evaluated based upon the productivity and purity achieved at both the extract and the raffinate ports. These quantities are defined as:

PR_F = kg of fructose at extract port/(m^3 adsorbent)/hour (4.12)

PR_G = kg of glucose at raffinate port/(m^3 adsorbent)/hour (4.13)

Pur_F = kg of fructose/(kg of fructose and glucose at extract port) (4.14)

Pur_G = kg of glucose/(kg of fructose and glucose at raffinate port) (4.15)

X_{Suc} = kg of sucrose reacted/kg of sucrose fed (4.16)

Table 4.2 compares the simulation results obtained from the current study with those reported in the literature for a particular experimental run (Azevedo and Rodrigues, 2001b). It is worth noting that all the values reported in the literature were based on the TMBR model, while the results from the present work are all based on the SMBR model. We can see that the prediction of experimental results with the SMBR model is much better than that with the TMBR model.

Table 4.1 Experimental operating conditions and model parameters: Data extracted from Azevedo and Rodrigues (2001b)

a. Experimental Set-up

Parameter	Value
Number of columns, N_{col}	12
Length of the column, L_{col} (m)	0.29
Diameter of the column, d_{col} (m)	0.026
Operating temperature, T (K)	328
pH	4.5
Maximum allowable pressure, P (bar)	120

b. Experimentally measured model parameters (at T = 328 K)

Parameter	Glucose	Fructose
Pe	1500	1500
Bi_m	500	500
ε	0.4	0.4
ε_p	0.1	0.1
K	0.17	0.43
$K' = K + \varepsilon_p$	0.27	0.53
$K' \dfrac{(1-\varepsilon)}{\varepsilon}$	0.405	0.795
$10^2\, k_p$ (s^{-1})	4.17	4.17
$10^2\, k_\mu$ (s^{-1})	2.17	2.17
$10^2\, k_h$ (s^{-1})	3.15	2.217
$10^2\, k_r$ (s^{-1})	83.87	
K_e	5.0	

Table 4.2 Comparison of the SMBR model predicted results (this work) with the experimental and TMR model results (Azevedo and Rodrigues, 2001b)

Operating Variables		Performance of the SMBR			
Parameter	Value	Parameter	Experi-mental Value[+]	Predicted Value[*]	Our Prediction[#]
Q_P (x 10^3 m^3/h)	2.1228	Pur_F (%)	90.0	92.6	90.7
Q_Q (x 10^3 m^3/h)	1.5762	Pur_G (%)	96.3	96.1	96.5
Q_R (x 10^3 m^3/h)	1.7934	PR_F (kg/m^{3}h)	7.78	7.55	7.65
Q_S (x 10^3 m^3/h)	1.44	PR_G (kg/m^{3}h)	7.07	7.40	7.20
Q_F (x 10^3 m^3/h)	0.2172	PR_{Enz} (kg/g)	0.102	0.102	0.102
Q_{Ra} (x 10^3 m^3/h)	0.3534	$C_{F, Ex}$ (x 10^{-3} kg/m^3)	15.78	15.3	15.52
Q_D (x 10^3 m^3/h)	0.6828	$C_{G, Ra}$ (x 10^{-3} kg/m^3)	22.18	23.2	22.59
Q_{Ex} (x 10^3 m^3/h)	0.5466	X_{Suc} (%)	100	--	100
t_s (min)	3.4				
C_{SucF} (x 10^{-3} kg/m^3)	80.0				
C_{Enz} (x 10^{-3} kg/m^3)	0.25				

[+] Azevedo and Rodrigues (2001b)
[*] Azevedo and Rodrigues (2001b) based on TMBR model
[#] This work based on SMBR model

4.4 Optimization of the SMBR and Varicol Systems

The experimental conditions used by Azevedo and Rodrigues (2001b) were selected from the SMB operation triangle based on equilibrium theory. They also performed optimization studies using an optimization algorithm that is an extension of that developed by Biressi et al. (2000). However, the optimization technique was carried out with a single objective function. The purity and productivity of the two products resulting from the Inversion of sucrose, viz., fructose and glucose, were found to change in conflicting ways with changes in the operating parameters. In real life problems, such as the SMBR system considered in this work, there are often more than one objective functions which are equally significant and need to be considered simultaneously. In such cases, a more thorough multi-objective optimization study has to be done so that the design of the SMBR set-up could be more accurate, comprehensive and economical. Throughout this study the focus is given on maximizing the productivity of fructose while minimizing the water consumption. Decreasing the water consumption, as discussed earlier, is a major concern for most of the sugar industries.

Two distinct types of problems may be considered in the multi-objective optimization of the reactive SMB (and Varicol) systems. One is the performance enhancement of existing set-up by suitably determining the optimal operating parameters. The other one is optimization at design stage (the design of a new SMBR unit) for efficiently handling sucrose inversion by enzymatic action and simultaneous separation of fructose-glucose. The design strategy for the SMBR (and Varicol) proposed in this work consists of determining the optimal geometric parameters (such as length, number and sequence of columns) and the operating conditions (flow rates, switching time, etc) that allow a desired substrate conversion and purity at the outlet

streams with maximum productivity using minimum desorbent at the same time without exceeding pressure drop limits imposed by the packing material. A few two-objective functions optimization has been reported in this work which fall under both the categories of the optimization problems mentioned above. In this chapter, only a few simple examples have been dealt with, to illustrate the concepts, techniques and interpretation of results obtained by such a multi-objective optimization exercise.

In all the optimization runs presented in this work, 50 chromosomes (solutions) were considered and results are presented after 50 generations. The CPU time taken to generate one Pareto set is about 24-36 hours on the CRAY J916 supercomputer.

4.4.1 Problem 1: Performance enhancement of the existing set-up

Azevedo and Rodrigues (2001b) reported single objective function optimization results for maximization of enzyme productivity subject to conversion greater than 99%, and both extract and raffinate purity greater than 95% as the constraints. However, as explained in the earlier chapter, the optimization of SMBR (and Varicol) operation is complex and is influenced by relatively large number of parameters and requires multi-objective optimization study. A majority of the sugar plants which deal with this Inversion of sucrose supply the high fructose syrups produced to soft drink manufacturing units. In such cases, the primary objective of these industries is to maximize production of at least 60% concentrated fructose using minimum solvent. Water consumption in these separation processes is usually very large (circa 50 liters of water is required per kg of fructose product) and therefore, reduction of water consumption is one of the primary objectives in industry. Thus, the first multi-objective optimization problem solved is the maximization of fructose

productivity using minimum solvent (water) for an existing set-up. The formulation can be represented mathematically as

Maximize $\qquad J_1 = PR_F [t_s, Q_{Ra}, Q_D]$ $\hfill$ (4.17a)

Minimize $\qquad J_2 = Q_D [t_s, Q_{Ra}, Q_D]$ $\hfill$ (4.17b)

Subject to $\qquad Pur_F$ and $Pur_G \geq 60\%$ $\hfill$ (4.17c)

$\qquad\qquad\qquad PR_F$ and $PR_G \geq 7.0$ kg/m^3 solid/h $\hfill$ (4.17d)

The choice of these two objectives enable the production of fructose using minimum water subject to target purities of extract and raffinate streams (greater than 60%) and productivities greater than experimental reported values of Azevedo and Rodrigues (2001b). Three decision variables were used for this optimization study as indicated in Eq. (4.19): switching time, t_s, raffinate stream flow rate, Q_{Ra}, and desorbent flow rate, Q_D. To compare our results with those of an existing set-up used by Azevedo and Rodrigues (2001b), we fixed (see Table 4.3) the values of length, diameter and number of columns in each section, feed flow rate and flow rate in section S, concentration of sucrose in feed and enzyme concentration in desorbent and temperature corresponding to their experimental values. Since only four flow rates could be selected independently, while the other four are determined by mass balance equations at points A-D (see Figure 4.1), the remaining two flow rates (in this case, Q_D and Q_{Ra}) were used as decision variables. The third decision variable is the switching time t_s, which clearly has a strong influence on the purity of the outlet streams. The bounds for t_s lie between the breakthrough times of the two components for the resin used as adsorbent.

Figure 4.2 shows the Pareto-optimal solution and the decision variables corresponding to each of the points on the Pareto for the optimization problem formulated as Problem1. The figure clearly shows that the points do, indeed,

constitute a Pareto set, i.e., as the productivity of fructose increases (desirable), it requires more solvent (undesirable). The optimum values of switching time and raffinate flow rate obtained are 3.5 min and 0.33 x 10^{-3} m^3/h respectively. Although, constraint on purity was only 60%, the purity of fructose achieved was 90%, same as in the experimental study. The conversion of sucrose achieved was 100%. The optimal values of fructose productivity obtained were observed to be only slightly better, PR_F = 7.67 kg/m^{3}solid/h for the desorbent flow rate 0.68 m^3/h (about 0.3 % increase as compared with the performance with existing parameters). This is due to the fact that only three decision variables were used and therefore the scope for improvement was considerably restricted.

Table 4.3 Description of the multi-objective optimization problems solved for the SMBR systems

Problem No.	Objective Function	Decision Variables	Constraints	Fixed Parameters
1 (Existing)		$2 \le t_s \le 6$ min $0.24 \le Q_{Ra} \le 0.42$ x10^{-3} m^3/h $0.3 \le Q_D \le 0.9$ x10^{-3} m^3/h	$PR_F \ge 7.0$ kg/m^{3}solid/h $PR_G \ge 7.0$ kg/m^{3}solid/h	L_{col} = 0.29 m, d_{col} = 0.026 m N_{col} = 12, p/q/r/s = 3/2/5/2, T = 323 K Q_F = 0.2172 x 10^{-3} m^3/h, C_{SucF} = 80 x 10^3 kg/m^3 C_{Enz} = 0.25 x 10^3 kg/m^3, Q_S = 1.44 x 10^{-3} m^3/h
	Max PR_F Min Q_D			
2 (Design)		$0.5 \le t_s \le 4$ min $0.06 \le Q_{Ra} \le 0.3$ x10^{-3} m^3/h $0.3 \le Q_D \le 1.2$ x10^{-3} m^3/h $0.1 \le L_{col} \le 0.3$ m $1 \le$ p, q, r≤ 5	$Pur_F \ge 60\%$ $Pur_G \ge 60\%$	Same as Problem 1 Except N_{col} = 8, 10 or 12, & p, q, r and L_{col} are decision variables
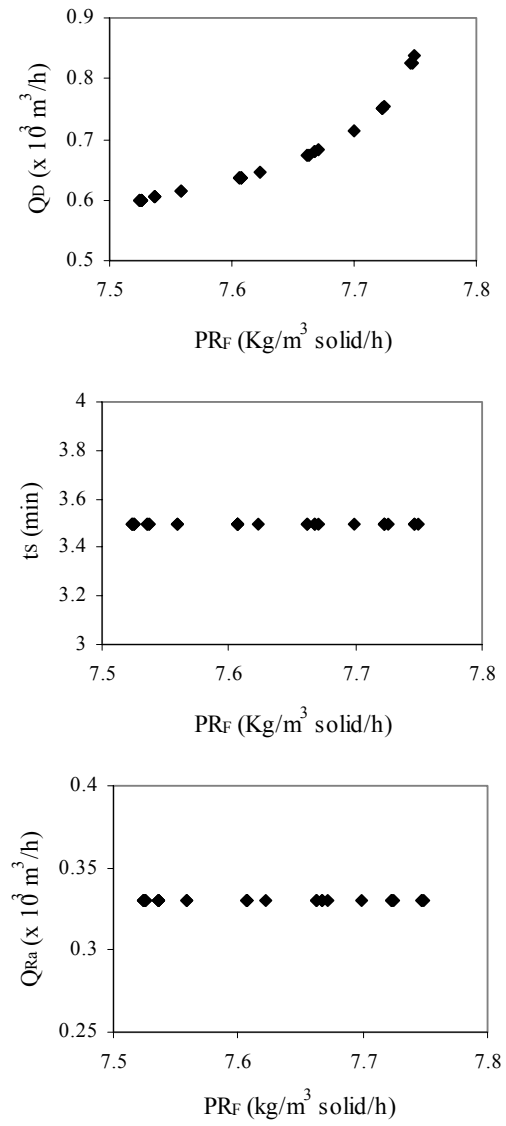
Figure 4.2 Pareto-optimal solutions and decision variables for the 12-column SMBR (Problem 1)

4.4.2 Problem 2: Optimization at the design level - Optimal column length and configuration

Optimization at the design stage provides far more freedom than when one is constrained to optimize the performance with an existing set-up. At the design stage, several additional decision variables become available for optimization. A meaningful optimization problem would be same as in problem 1 except additional decision variables as length, number and distribution of columns in different sections p, q, r and s. The cost of adsorbent is always one of the key deciding factors for the implementation of SMB units. The existing set-up considered in Problem 1 consisted of 12 columns each 0.29 m long. In this case, optimization problem was formulated to determine optimal column length and distribution of columns in different sections for different total number of columns, N_{col}, equal to 8, 10 and 12. The complete optimization formulation is given in Table 4.3. The Pareto sets for this problem is shown in Figure 4.3. When compared with problem 1, the performance of reactor is seen to have considerably improved. For equivalent 12-column SMBR system and for the same desorbent consumption of 0.6 x 10^{-3} m^3/h, the productivity has dramatically increased from 7.52 to 17.46 kg/m^3-solid/h. This was achieved primarily by optimizing column length and by optimally distributing the columns in different sections. The optimum column length and configuration (distribution) obtained for the design stage are 0.113 m and Ω = 3/1/4/4 compared to 0.29 m and 5/2/3/2 used for the existing set-up. Note that although in the optimization formulation we have used only two objectives (PR$_F$ and Q$_D$), but in reality it involves three objectives due to the manner in which productivity (amount of fructose produced in kg/h per unit volume of total adsorbent used) is defined. Obviously, the optimum amount of glucose produced (Q$_{Ra}$) is reduced from 0.33 to 0.129 x 10^{-3} m^3/h
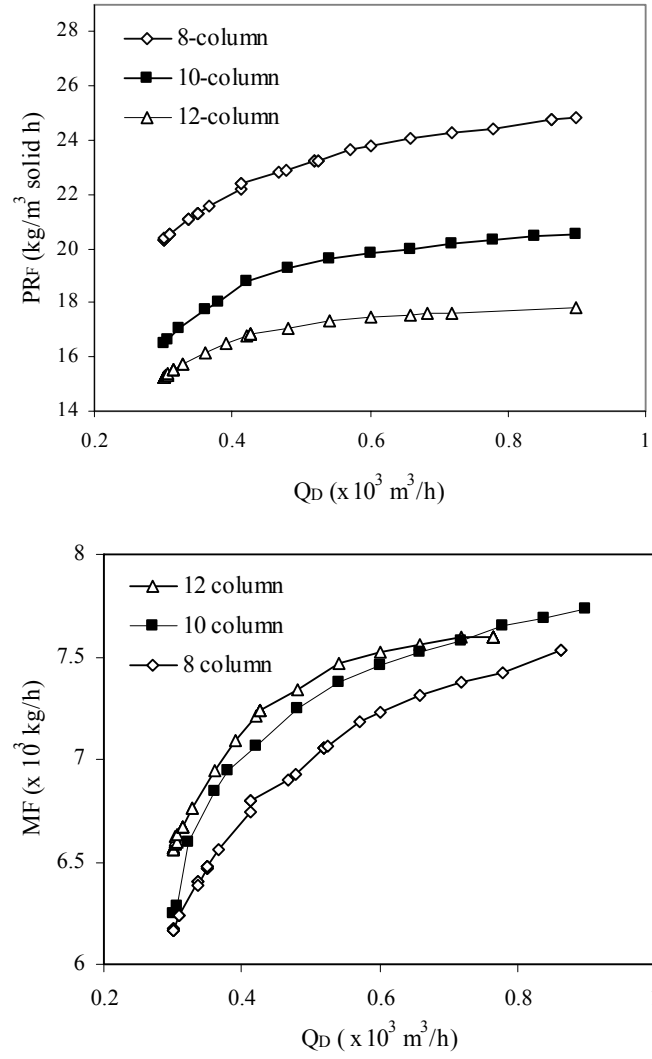
Figure 4.3 Comparison of PR$_F$ and M$_F$ between 8 column, 10 column and 12 column SMBR

due to the increased production of fructose. The optimum switching time has reduced to 1.51 min (from 3.5 min) as the column length is reduced. Even though the actual productivity (in kg/m^3-solid/h) is increased but the mass flow rate of fructose (M_F, kg/h) has actually decreased compared to problem 1. However, the reduction in M_F is only 9.5% compared to total reduction in V_{solid} by 61% in the case of design optimization compared to the existing set-up for the 12-column SMBR system. Hence, the present optimization formulation helps to design the SMBR system for efficient utilization of adsorbent in producing fructose using minimum solvent.

In order to determine whether 12 columns were necessary, optimization was carried out for 10 and 8 total columns. The Pareto-optimal solution for the 8 and 10-column SMBR unit are also shown in Figure 4.3. The Pareto set of Q_D with PR_F followed the similar trend as in the earlier cases, but yielding even higher values of fructose productivity at a particular desorbent flow rate. For example, for a given Q_D of 0.6 x 10^{-3} m^3/h, an improvement in PR_F from 17.46 (for a 12-column SMBR) to 19.84 (for a 10-column SMBR) to 23.8 kg/m^3-solid/h (for a 8-column SMBR) was possible. The optimum column length, configuration, switching time and raffinate flow rate for all the points in the Pareto set for a particular set-up was found to be constant and are respectively L_{col} = 0.113 m, Ω = 4/4/3/1, t_s = 1.51 min, Q_{Ra} = 0.129 x 10^{-3} m^3/h for 12-column; L_{col} = 0.118 m, Ω = 4/1/2/3, t_s = 1.48 min, Q_{Ra} = 0.1464 x 10^{-3} m^3/h for 10-column; and L_{col} = 0.119 m, Ω = 2/2/2/2, t_s = 1.51 min, Q_{Ra} = 0.1425 x 10^{-3} m^3/h for 8-column SMBR system. Once again, even though PR_F increased when N_{col} is reduced from 12 to 8 columns, the values of M_F also decreased. This is also shown in Figure 4.3. It clearly shows that by adding 2 columns to the 8-column system, the improvement is considerable but further addition of 2 columns to make it a 12-column system, the increase is not significant. For example, for a particular Q_D

of 0.6 x 10^{-3} m^3/h, reduction in M_F is only 1.12% against a total reduction in V_{solid} by

13% for the 10 column system when compared to the 12 column SMBR system at

design stage optimization. Similarly, reduction in M_F is 4.3% with a V_{solid} reduction of

30% for 8 column SMBR system compared to the 12 column SMBR system. Table

4.4 gives the comparison between these three systems in terms of the amount of

fructose produced, V_{solid} needed and the efficiency of the systems defined as

productivity of fructose per unit desorbent consumption. The comparison is also done

with the performance obtained with the existing set up (optimized). From this table

we can say that design stage optimization provides operating parameters which can

lead to production of 2.91×10^4 kg of concentrated fructose per m^3 of solid adsorbent

per m^3 of water consumption compared 1.25×10^4 kg-fructose/m^3-solid/m^3-water for a

12-column SMBR set-up. The efficiency increases to 3.97×10^4 kg-fructose/m^3-

solid/m^3-water for the 8-column SMBR set-up.

Table 4.4 Comparison of results obtained for 8, 10 and 12 column SMBR

	Existing	Design		
N_{col}	12	12	10	8
L_{col} (m)	0.29	0.113	0.118	0.119
$10^4 \times V_{solid}$ (m^3)	11.09	4.32	3.76	3.03
$10^4 \times Q_D$ (m^3/h)	6	6	6	6
PR_F (kg/ m^3/h)	7.52	17.46	19.84	23.81
$10^3 \times M_F$ (kg/h)	8.34	7.56	7.44	7.2
$10^{-4} \times$ Efficiency[#] (kg/m^3-solid/m^3-water)	1.25	2.91	3.31	3.97

Efficiency is defined as productivity of fructose (kg/h/m^3-solid
used) per unit desorbent consumption (m^3/h).

4.4.3 Problem 3: Modification of SMBR: Variable Feed Flow Rates

The advantages of using variable flow rates in the operation of SMB have been already explained in the second chapter. It is worthwhile to see the applicability and the advantages achieved when this concept is applied for SMBR. In this study, only the feed flow rate was decided to be allowed to vary during the operation. However, as explained earlier such changes in flow rates would affect the concentration profiles and may even lead to decreased productivity unless a rigorous optimization study is performed taking into consideration the complex interplay of all these process parameters.

In order to evaluate the efficacy of this variable flow mode and to determine the extent to which the performance of SMBR could be improved by using this mode, three different optimization problems were formulated as described in Table 4.5. In all the formulations, maximization of mass flow rate of fructose (M_F, g/h) is used as one of the objective functions instead of maximization of productivity as used in the previous problems. In the first problem (Problem 3, Table 4.5), optimal Pareto solutions are obtained at the design stage for a 8-column SMBR system in which feed flow rate was maintained constant at 0.2172×10^{-3} m^3/h. Subsequently, two more optimization problems were solved with variable (distributed) feed flow rate. In Problem 3a, the switching interval was divided into four sub-intervals. The feed flow rate was not kept constant at $Q_F = 0.2172 \times 10^{-3}$ m^3/h for the entire switching interval, instead was allowed to vary according to the following equations

$$0.18 \leq Q_{F1}, Q_{F2}, Q_{F3} \leq 0.6 \times 10^{-3} \ m^3/h \tag{4.18a}$$

$$Q_{F4} = 4Q_F - (Q_{F1} + Q_{F2} + Q_{F3}) \tag{4.18b}$$

where, Q_{F1}, Q_{F2}, Q_{F3} and Q_{F4} are the feed flow rates in the sub-interval 1, 2, 3 and 4 respectively. Equation (4.18b) is used to ensure that total feed flow rate is same as

that of the constant feed flow case (Problem 3) in order to facilitate the comparison between the optimum results obtained. In the second sub-case (Problem 3b), instead of using discrete values, the feed flow rate was allowed to vary continuously throughout the switching interval according to the equation

$$Q_F = a - bt - ct^2 \qquad (4.19)$$

where *a, b* and *c* are constants and *t* is the time such that $0 \leq t \leq t_s$. The constants *b* and *c* were chosen as decision variables while *a* was calculated by equating the integrated value of the above equation over the integral 0 to t_s (Eq. 4.20) to the total feed flow rate. This again ensures that the total feed remains constant (0.2172 x 10^{-3} m^3/h),

$$a = Q_F + \frac{b}{2}t_s + \frac{c}{3}t_s^2 \qquad (4.20)$$

In these two problems (Problem 3a and 3b), length of each column (L_{col}), switching time (t_s) and column configuration (Ω) were kept fixed at the optimum values for Problem 3. The detailed optimization formulation is described in Table 4.5. Figure 4.4 shows the Pareto optimal solution obtained when the feed flow rate was constant (Problem 3). The optimal values for t_s, L_{col} were found to be 2.58 min and 0.2 m respectively and the optimal configuration was found to be 4/1/1/2. With these fixed parameters Problems 3a and 3b were solved. Figure 4.4 compares the Pareto-optimal solutions for the three cases. The results show that a significant improvement is possible when one uses variable feed flow rate instead of constant feed flow rate and further improvement is possible if one uses continuous variation in contrast to discrete variation of the feed flow rate. The optimum flow rate of glucose at the raffinate port (Q_{Ra}) was found out to be 0.126 x 10^{-3} m^3/h for all three cases. Typical optimal feed flow rates for these cases within a switching period is shown in Figure

4.4 for a pareto point corresponding to $Q_D = 0.42$ x 10^{-3} m^3/h. The figure shows that the optimal trend when continuous variation in feed was allowed is to have lower Q_F at the beginning of the switching interval and gradual increase in Q_F as time progresses. Almost similar trend is observed when Q_F was allowed to vary in four discrete steps. At the beginning of any switching period, feed rate required is low due to recycle from section S to P and it gradually increases towards the end of the switching period.

Table 4.5 Description of the multi-objective optimization problems solved for the modified SMBR

Problem No.	Objective Function	Decision Variables	Constraints	Fixed Parameters*
3 SMBR (Fixed feed)		$0.09 \le Q_{Ra} \le 0.3$ x 10^{-3} m^3/h $0.24 \le Q_D \le 1.2$ x 10^{-3} m^3/h $0.5 \le t_s \le 4$ min $0.1 \le L_{col} \le 0.3$ m $1 \le p, q, r \le 5$		$N_{col} = 8$, $d_{col} = 0.026$ m, T = 323 K $Q_F = 0.2172$ x10^{-3} m^3/h, $C_{SucF} = 80$ x10^3 kg/m^3
	Max M_F Min Q_D		Pur$_F \ge 60\%$ Pur$_G \ge 60\%$	$C_{Enz} = 0.25$ x10^3 kg/m^3, $Q_S = 1.44$ x10^{-3} m^3/h
3a SMBR (Discrete feed)		$0.09 \le Q_{Ra} \le 0.3$ x10^{-3} m^3/h $0.24 \le Q_D \le 1.2$ x10^{-3} m^3/h $0.18 \le Q_{F1}, Q_{F2}, Q_{F3} \le 0.3$ x10^{-3} m^3/h		Same as Problem 3 & $t_s = 2.58$ min, $L_{col} = 0.2$ m, $\Omega = 4/1/1/2$
3b SMBR (Continu-ous feed)		$0.09 \le Q_{Ra} \le 0.3$ x10^{-3} m^3/h $0.3 \le Q_D \le 1.2$ x10^{-3} m^3/h $0.5 \le b, c \le 5.0$		Same as Problem 3a
4 (Varicol)		$0.09 \le Q_{Ra} \le 0.3$ x10^{-3} m^3/h $0.3 \le Q_D \le 1.2$ x10^{-3} m^3/h $0.5 \le t_s \le 4$ min $0.1 \le L_{col} \le 0.3$ m Ω (32 combinations)		Same as Problem 3

Figure 4.4 Comparison of 8-column SMBR with fixed feed and variable feed (discrete & continuous)

The improvement in the performance achieved can be easily explained by recalling the earlier discussion about the possibility of performance improvement by deliberately increasing (or decreasing) the flow rates. Due to the special purity requirements in this case (60%), probably during the start of the switching period the solids are saturated and therefore can process lesser feed, while due to the flushing away of the solids during the switching period the feed that can be processed increases. For fixed values of Q_{Ra} and Q_D, Q_{Ex} would increase when Q_F is increased, thereby increase the amount of fructose collected. In other words, the system tends to operate such that higher quantity of fructose is collected when the concentration of fructose is higher while when the concentration is lower lesser quantities are collected, thus keeping the mean flow rates over the switching time constant. Note that the productivity is not just a mean of the intermediate values, but is the integral of the product of flow rate and concentration over the switching period.

4.4.4 Problem 4: Modification of SMBR: Varicol System

It has been reported as discussed earlier that Varicol system can perform better than the SMBR due to the flexibility in its operation. It could aid in reducing the volume of adsorbent required, or for a fixed total adsorbent can increase throughput or productivity of the process. Hence, optimization study was performed for a four sub-time interval 8-column reactive Varicol system to determine the extent of improvement that can be obtained over an equivalent SMBR system. With 8 total columns in the Varicol unit, there could be a large number of possible column configurations (Ω). The mathematical formulation of the optimization problem is given in Table 4.5 (Problem 4).

The Pareto-optimal solution of the 8-column Varicol system is illustrated in Figure 4.5. The optimal Q_D-M_F trend line obtained was similar to Problem 3 (Figure 4.4). Figure 4.5 clearly shows that mass flow rate of fructose produced per unit time is significantly higher for a fixed desorbent flow rate or same amount of fructose could be produced using less desorbent. This is possible in Varicol process due to the non-synchronous switching compared to synchronous switching in SMBR system. However it was observed that the length of column chosen is much higher (0.26 m as compared to 0.2 m for SMBR). The purpose of still keeping L_{col} as one of the decision variables was to see if an optimal L_{col} could be obtained for the Varicol. Table 4.6 shows the comparison between the performances of SMBR and Varicol. Three different optimal column configurations for the 4 sub-interval 8-column Varicol system were obtained. Most part of the Pareto optimal curve was dominated by the configuration 4/1/2/1, 4/1/2/1, 3/1/3/1, 3/1/3/1 which means that the configuration chosen for the first two sub-intervals was 4/1/2/1 and for the last two sub-intervals was 3/1/3/1. For the middle points on the Pareto (Q_D = 0.48 to 0.54 x 10^{-3} m^3/h) the configuration chosen was 4/1/2/1, 3/2/2/1, 3/1/3/1, 3/1/3/1. The trend clearly shows that more number of columns is needed in section P in the beginning of the subinterval while more are needed in section R in the end of the subinterval. This probably can be explained by understanding that fructose is more strongly adsorbed than glucose and tends to diffuse very slowly. Sections P and R being the zones for desorption and adsorption of the more strongly compound respectively, for the productivity of fructose to increase while consuming lesser desorbent, more solids (adsorbent) are required in these sections. The switching time and the Q_{Ra} values chosen are 3.2 min and 0.21 x 10^{-3} m^3/h respectively. Figure 4.6 elucidates the concentration profiles for glucose and fructose for the 8-column SMBR with fixed

and variable feed (discrete) and the 4-subinterval Varicol system corresponding to the

optimal point with desorbent flow rate 0.48 x 10^{-3} m^3/h.

Table 4.6 Comparison of results obtained for 8 column SMBR and Varicol

	SMBR	Varicol
N_{col}	8	8
L_{col} (m)	0.2	0.27
$10^4 V_{solid}$ (m^3)	5.1	6.88
$10^4 Q_D$ (m^3/h)	6	6
$10^3 M_F$ (kg/h)	7.61	8.51
10^{-4}Efficiency (kg/m^3-solid/m^3-water)	2.49	2.06
10^2 Volume of water /kg fructose (m^3/kg)	7.88	7.05
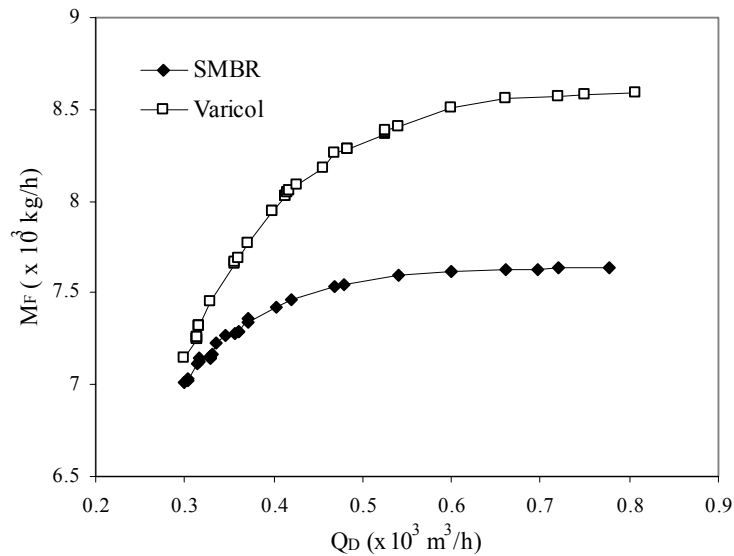
Figure 4.5 Comparison of Varicol with 8 column SMBR
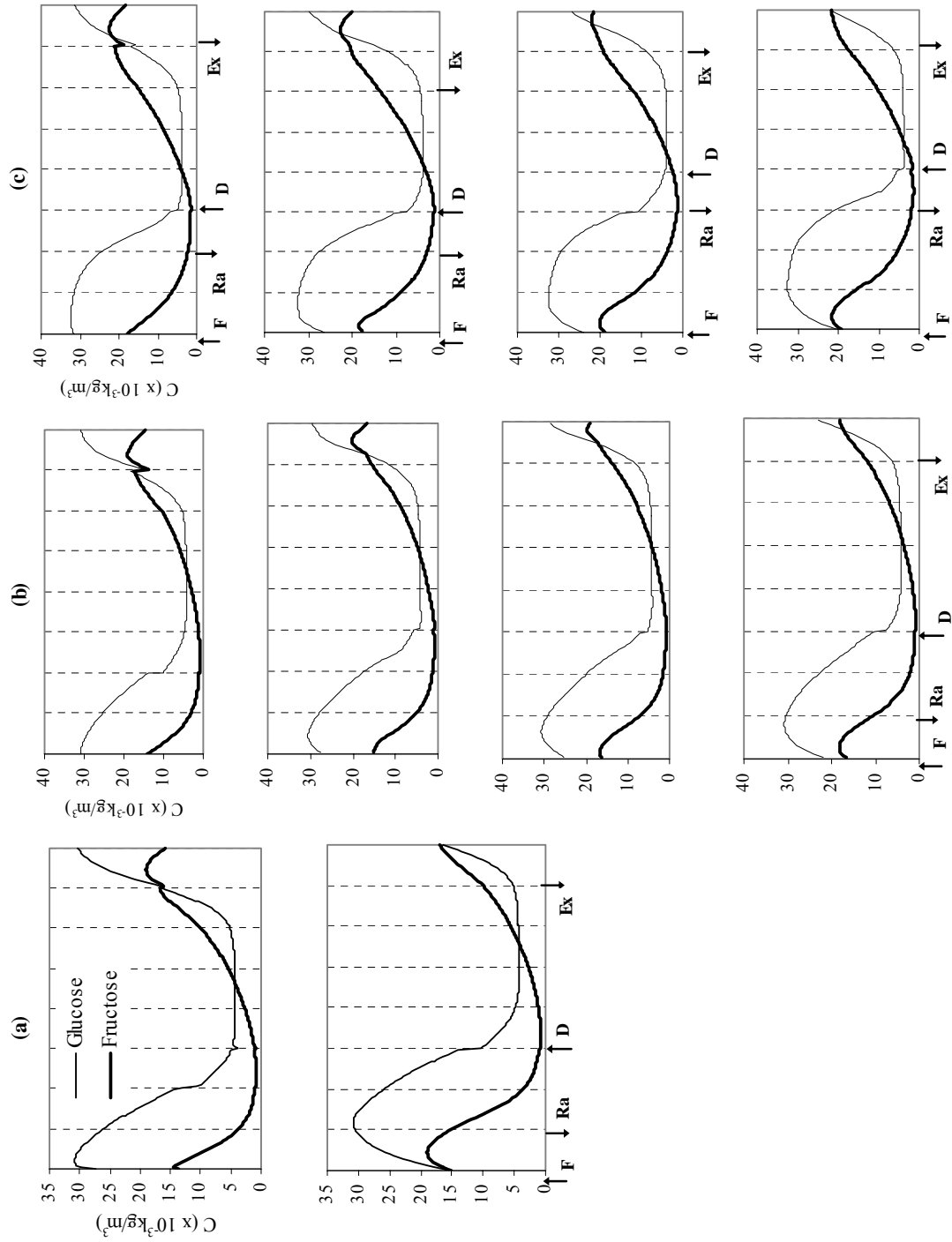
Figure 4.6 Concentration profiles for 8-column SMBR (a), variable feed (discrete) (b) and Varicol (c) for the point, $Q_D = 0.48 \times 10^{-3}$ m^3/h

4.5 Conclusions

Simulated Moving Bed Reactor an outstanding example of the Chromatographic Reactor-Separator systems have been studied in this work and we have performed multi-objective optimization studies for the Inversion of Sucrose to produce fructose and glucose and simultaneously separate fructose from the mixture of glucose and fructose to produce fructose rich sugar syrups. The goal of this study was to obtain the optimal operating conditions that provide performance enhancement for an existing system as well as for the design of new SMBR systems. Minimization of water consumption while maximizing the productivity of fructose were always the objectives in this study since these are the problems regularly faced by the sugar industries. Several decision variables were used that include length of columns and column configuration in addition to switching time and the desorbent and raffinate flow rates. The optimization was performed using a very robust, non-traditional, state-of-the-art AI-based technique, Non-dominated Sorting Genetic Algorithm (NSGA-II with Jumping Genes). Pareto optimal curves were obtained and comparisons were done in the performance improvement achieved as compared to increase in the adsorbent requirement. It is to be emphasized that there is no end to the variety of multi-objective optimization problems, which could be formulated and studied, and we have presented here, only a few simple examples, to illustrate the concepts, techniques and interpretation of results.

Variable feed flow systems were also studied and there performance as compared to the constant feed flow SMBR systems was done. It was found that SMBR in the variable feed flow mode (both discrete and continuous) shows better performance in terms of higher amounts of fructose produced for the same desorbent consumption. Finally, optimization was performed for the Varicol system and again it

was observed that performance of the reactive Varicol is much better than SMBR but

at the cost of increase in the adsorbent consumption.

Chapter 5   Modified SMB systems for Ternary Separation
- A Comparative Study under Non-ideal conditions

5.1 Introduction

Simulated Moving Bed system, as mentioned earlier, has been implemented successfully as a separation technique in the petrochemical, biochemical and fine chemical industries. The SMB is a well established separation technology, particularly for separation of binary mixtures which are otherwise difficult (or nearly impossible). The four-zone SMB for binary separation (see Figure 5.1) has been extensively studied by many groups and is now well understood (Ruthven and Ching, 1989; Hashimoto et al., 1993; Fish et al., 1993; Storti et al., 1993; Charton et al., 1995). However, the use of SMB systems for multi-component separations has not been studied extensively. As discussed in the second chapter of this dissertation, the major limitation of SMB is the inability to purify a ternary mixture into three different pure fractions in a single unit. As a consequence, several concepts have been proposed to achieve this goal through various modifications keeping the advantages of SMB. A discussion about the same is presented in the second chapter. Amongst these concepts, in the work of Kim et al. (2003), three cases of single cascades, similar to the approach described by Nicoud (2000) and Beste and Arlt (2002), were developed and the favorable conditions to achieve good separations using equilibrium theory were determined for these designs. Kim et al. (2003) simulated the system using Aspen Chromatography and studied the effect of different feed compositions and mass transfer rates. However, they only considered linear isotherms.

In this study, we have extended the work of Kim et al. (2003), by comparing the systems in presence of several non-idealities such as high mass-transfer resistance,
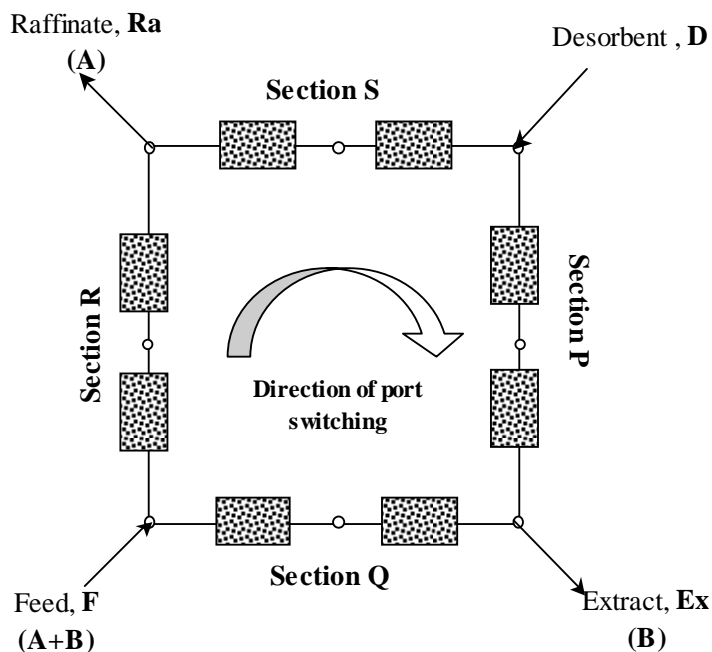
Figure 5.1 Simulated Moving Bed system for binary separation

low adsorption selectivity, non-linearity in adsorption isotherm etc. In this study, the performances of these systems are compared at optimal conditions. Furthermore, the optimization studies are carried out to satisfy multiple objectives (Chankong and Haimes, 1983; Bhaskar et al., 2000; Deb, 2001). There are several SMB systems in the open literature for ternary separations, however, to the best of our knowledge there does not seem to be any detailed study to see their behavior in presence of non-ideal conditions, which are more often found in industries. Also, these systems, due to the addition of more sections and / or product streams (compared to conventional SMB used for binary separation), tend to be more complicated and have more design variables. As a result the design and consequently optimization, particularly multi-objective optimization, of these systems becomes rather difficult. It is needless to

emphasize the importance of optimization of systems at the design stage (Bhaskar et al., 2000). In such a scenario, non-traditional optimization techniques such as the Evolutionary Algorithms (Deb, 2001) prove to be very useful. In this study similar to the earlier studies, we have used NSGA-II –JG as the optimization algorithm. NSGA has already been successfully applied for binary separation (Zhang et al., 2002b; Subramani et al., 2003a; Wongso et al., 2004) with SMB systems as well as with reactive SMB (Subramani et al., 2003b; Yu et al., 2003) and here we have attempted to apply it on SMB systems designed for ternary separation.

5.2 Conventional and Modified SMB systems

The general concept of a classical four-zone SMB unit for binary separation can be recollected from the earlier chapters and is illustrated in Figure 5.1. It consists of a number of columns with uniform cross-section connected in a circular array, each of length (L_{col}) and packed with adsorbent. There are two incoming streams: the feed mixture (F) containing components A (weakly adsorbed) and B (strongly adsorbed) to be separated, and the desorbent (D). Two streams leave the unit, one enriched with less adsorbable component (A), raffinate (Ra), and one enriched with the more adsorbable component (B), extract (Ex). The four streams divide the unit into four sections (P, Q, R and S). Each zone contains at least one fixed column (bed) and has to fulfill distinct tasks, i.e., in the sections Q and R countercurrent separation takes place, while in section P and S, the solid and the fluid phases are regenerated, respectively. The movement of the solid bed is simulated by switching of ports (or columns) in specific time interval, t_s. The separation is achieved by a simulated countercurrent contact between the mobile fluid phase and the stationary adsorbent phase.

The two configurations of SMB systems chosen from the three configurations described by Kim et al. (2003) for ternary separation are shown in Figure 5.2a and 5.2b. The third configuration described by Kim et al. (2003) (shown in Figure 2.9b of Chapter 2) is very similar to the configuration shown in Figure 5.2a except that it has two raffinate streams and hence in this study, only the other two configurations are chosen. If we assume that the feed consists of a ternary mixture of components, A, B and C, of which component A is the least adsorbed while component C is the most adsorbed and B has an intermediate adsorption affinity. The first modified configuration, MC1 (Figure 5.2a), is a five-zone cascade system. It is very similar to the conventional four-zone SMB (Figure 5.1) except that there are five zones due to the addition of an extra product outlet port in the Section Q for the collection of the intermediate component B. Hence, one can consider section Q of conventional SMB to be split into two sections, Q_1 and Q_2, due to the additional port. Once again, in MC1 (Figure 5.2(a)), similar to conventional SMB, each zone contains at least one fixed column (bed) and has to fulfill distinct tasks to facilitate the separation, i.e., in the sections Q_1, Q_2 and R countercurrent separation takes place, while in section P and S, as usual the solid and the fluid phases are regenerated, respectively. To achieve separation between the components, the internal flow rates of the fluid phases have to be specified such that there is countercurrent separation between B and C in section Q_1 and separation between A and B in sections Q_2 and R.

The second modified configuration, MC2 (Figure 5.2(b)), is a four-zone system similar to conventional SMB system (Figure 5.1). However, it differs from the traditional four-zone SMB due to the break between sections P and Q and use of an additional desorbent stream, D_2. This system is more like a batch chromatographic

a)

b)
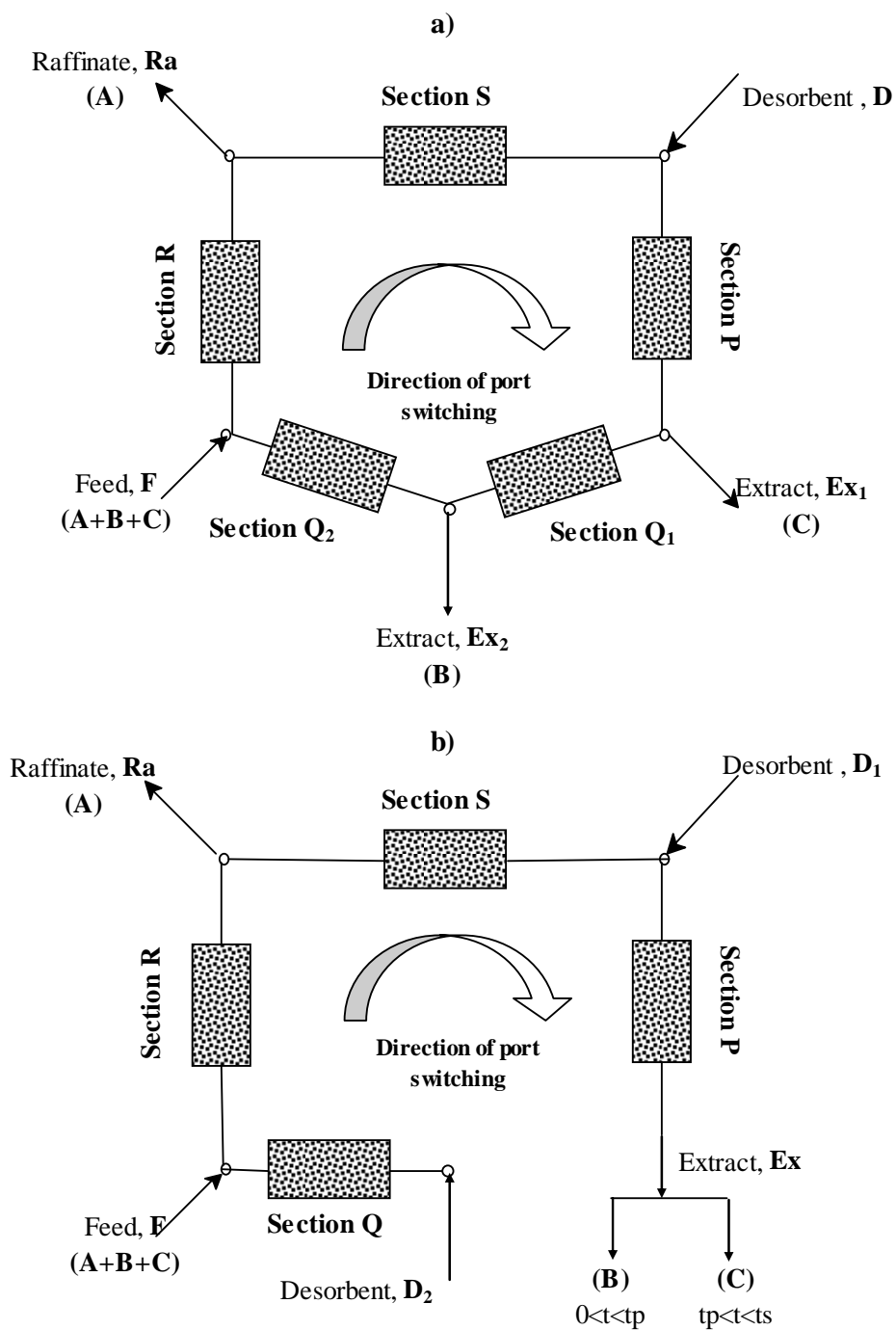
Figure 5.2 Schematic diagrams of modified simulated moving bed systems for ternary separation. (a) Modified configuration 1 **(MC1)**, and **(b)** Modified configuration 2 **(MC2)**

column since there is no recycle of desorbent within the system. However, even in this configuration, the solids do still move counter-currently due to the switching of the ports similar to the conventional SMB. The component with the least adsorption affinity, A, is collected as usual at the raffinate port. However, the product collection at the extract port is such that the component with intermediate adsorption capacity, B, is collected for some period ($0 < t < t_p$) while the most strongly adsorbed component, C, is collected for the remainder of the switching time ($t_p < t < t_s$) (as shown in Figure 5.2b). The collection time of intermediate product B, t_p, is decided based on the breakthrough time of C, i.e., the time the most strongly adsorbed component C starts to desorb. This process is repeated for every switching of the ports.

5.3 Mathematical model

The mathematical model used in this study is given below. The modeling approach assumes constant selectivity axial dispersion for the fluid flow and linear driving force for the intra-particle mass-transfer. The differential mass balance equations along with the boundary conditions are as follows:

$$\frac{\partial C_{i,k}}{\partial \theta} + \upsilon \frac{\partial q_{i,k}}{\partial \theta} = \frac{\psi_k}{Pe_k} \frac{\partial^2 C_{i,k}}{\partial \chi^2} - \psi_k \frac{\partial C_{i,k}}{\partial \chi} \tag{5.1}$$

$$\frac{\partial q_{i,k}}{\partial \theta} = \alpha \left(q_{i,k}^* - q_{i,k} \right) \tag{5.2}$$

where $\chi = z/L_{col}$ and $\theta = t/t_s$. The boundary conditions are:

$$C_{i,\chi}^{in} = C_{i,k}(0,\theta) - \frac{1}{Pe_k} \frac{\partial C_{i,k}}{\partial \chi} \tag{5.3}$$

$$\frac{\partial C_{i,k}}{\partial \chi}(1,\theta) = 0 \tag{5.4}$$

The initial conditions are:

$$C_{i,k}(\chi,0)= C_{i,k}^0(\chi) \text{ and } q_{i,k}(\chi,0)= q_{i,k}^0(\chi) \qquad (5.5)$$

The dimensionless parameters used in the above equations are:

$$\psi_k = U_{F_z}t_s/L_{col} \;\;, \alpha = k_a t_s \text{ and } Pe_k = U_{F_k} L_{col}/D_{ax_k} \qquad (5.6)$$

Three different adsorption equilibria were used in this study.

Linear adsorption isotherm: $\qquad\qquad q_{i,k}^* = K_i C_{i,k} \qquad\qquad\qquad (5.7)$

Langmuir isotherm (single-component): $\quad q_{i,k}^* = \dfrac{q_m B_i C_{i,k}}{1+ B_i C_{i,k}} \qquad\qquad (5.8)$

Langmuir isotherm (multi-component): $\quad q_{i,k}^* = \dfrac{q_m B_i C_{i,k}}{1+\sum\limits_{l=1}^{NC} B_l C_{l,k}} \qquad\qquad (5.9)$

The difficulty of separations can be classified on the basis of selectivity

$$\phi_{ik} = K_i / K_k \geq 1.0 \qquad\qquad\qquad (5.10)$$

No separation between component i and k is possible when $\phi_{ik} = 1$. A separation is considered difficult when ϕ_{ik} is around 1.1 while it is moderate when ϕ_{ik} is around 1.5, and is an easy separation when ϕ_{ik} is around 4. The governing PDEs described in Eqn. (5.1-2) were discretized in space using the Finite Difference Method (FDM) to convert them into a system of coupled ODE-IVPs. The number of plates used in this study was 50. The resultant stiff IVP-ODEs were solved using the subroutine, DIVPAG, in the IMSL library. Separate computer codes were written for the above two modified SMB (MC1 and MC2) systems. In order to validate the mathematical model, simulation results were compared with reported results (Kim et al., 2003). The system and operating parameters used are summarized in Table 5.1. Only one column was assumed in each section. High mass-transfer rates were assumed and the dispersion coefficient was estimated from the available correlation (Chung and Wen,

1968). The effect of low mass-transfer rates are discussed later. The various performance parameters used for comparisons between the systems are defined in Table 5.2. The simulation results are compared in Table 5.3 for feed composition η = 0.33/0.34/0.33 (0.33% A, 0.34% B and 0.33% C). Table 5.3 shows that the simulation results obtained in this study are comparable with the reported results. The slight difference in performance is most likely due to the discrepancies in the model. Note that Kim et al. (2003) used Aspen Chromatography to simulate the systems whereas in this study a general purpose computer code was developed, which was subsequently interfaced with NSGA-II-JG for multi-objective optimization study. The above model is used for all the subsequent optimization studies.

In order to study the sensitivity of these systems, two additional simulations were performed with conditions as mentioned earlier, except that the mass transfer coefficient (k_a) was assumed to be 5 min^{-1}, which is a more realistic value for practical systems. For MC1, desorbent flow rate was increased from 300 cm^3/min to 360 cm^3/min, while for MC2 the ratio t_P/t_s was changed from 0.33 to 0.36 as separate simulation studies showed that desorbent flow rate is not very sensitive for MC2. The simulation results are shown in Table 5.4. For MC1, as Q_D increases PurB decreases. At low Q_D, flow rates in the sections responsible for the desorption of B (viz., section Q_1 for MC1) are low enough so that only part of B gets desorbed and results in higher purity for B since it is not contaminated with C, and the undesorbed B gets eluted in the section P and contaminates Ex1 decreasing PurC. Also, Q_P being low, section P is not regenerated fully and PurA decreases. Higher Q_D results in high flow rate in section Q_1 (since the Q_{Ex} is fixed) desorbing both B and some amount of C which decreases PurB but since the solids in section P in this case are devoid of B, Ex1 contains only C and thus PurC is high. Also due to high flow rates section P is fully

regenerated and PurA is high. Figure 5.3 shows the concentration profile for components A, B and C for MC1 after the cyclic steady-state has reached for the two different desorbent flow rates. Cyclic steady-state for both the systems reached after around 100 switchings around the columns. Table 5.4 shows PurB has a conflicting trend with respect to both PurA and PurC. While the PurA and PurC increase consistently, PurB decreases. For MC2, it is seen that as t_p/t_s increases, PurA remains constant (which is expected), but PurB decreases while PurC increases. This is also quite logical since as t_p/t_s increases, B is collected for a longer time than probably required and as a result gets contaminated by C, while C collected is purer since most of the B gets removed.

Table 5.1 Model, operating and system parameters for the modified SMB systems (Kim et al., 2003)

SMB unit geometry	Operating conditions	Model parameters
Modified SMB configuration 1 (MC1)		
$L_{col} = 166.67$ cm	$t_s = 7.5$ min	$k_a = 1.0 \times 10^5$ min^{-1}
$d_{col} = 1.38$ cm	$Q_F = 60$ cm^3/min	$d_p = 0.002$ cm, $\varepsilon = 0.4$
$N_{col} = 5$	$Q_{Ex1} = 240$ cm^3/min	$\phi_{BA} = 4.0$, $\phi_{CB} = 4.0$
$\Omega = 1/1/1/1/1$	$Q_{Ex2} = 60$ cm^3/min	$\rho_B = 0.67$ g/cm^3
	$Q_{Ra} = 60$ cm^3/min	$\rho_f = 1.0$ g/cm^3
	$Q_D = 300$ cm^3/min	$\eta = 0.33/0.34/0.33$
	$Q_S = 33.33$ cm^3/min	
Modified SMB configuration 2 (MC2)		
$L_{col} = 166.67$ cm	$t_s = 7.5$ min, $t_P/t_s = 0.33$	Same as MC1
$d_{col} = 1.38$ cm	$Q_F = 60$ cm^3 /min	
$N_{col} = 4$	$Q_{Ex} = 300$ cm^3 /min	
$\Omega = 1/1/1/1$	$Q_{Ra} = 60$ cm^3 /min	
	$Q_{D1} = 33.33$ cm^3 /min	
	$Q_{D2} = 266.67$ cm^3 /min	

Table 5.2 Definition of the performance parameters used in this study

	Purity	Recovery
Component	Modified SMB configuration 1 (MC1)	
A	$\text{PurA} = \dfrac{C_{Ra}^{A}}{C_{Ra}^{A} + C_{Ra}^{B} + C_{Ra}^{C}} \times 100$	$\text{RecA} = \dfrac{C_{Ra}^{A} Q_{Ra}}{C_{F}^{A} Q_{F}} \times 100$
B	$\text{PurB} = \dfrac{C_{Ex2}^{B}}{C_{Ex2}^{A} + C_{Ex2}^{B} + C_{Ex2}^{C}} \times 100$	$\text{RecB} = \dfrac{C_{Ex2}^{B} Q_{Ex2}}{C_{F}^{B} Q_{F}} \times 100$
C	$\text{PurC} = \dfrac{C_{Ex1}^{C}}{C_{Ex1}^{A} + C_{Ex1}^{B} + C_{Ex1}^{C}} \times 100$	$\text{RecC} = \dfrac{C_{Ex1}^{C} Q_{Ex1}}{C_{F}^{C} Q_{F}} \times 100$
Component	Modified SMB configuration 2 (MC2)	
A	$\text{PurA} = \dfrac{C_{Ra}^{A}}{C_{Ra}^{A} + C_{Ra}^{B} + C_{Ra}^{C}} \times 100$	$\text{RecA} = \dfrac{C_{Ra}^{A} Q_{Ra}}{C_{F}^{A} Q_{F}} \times 100$
B	$\text{PurB} = \dfrac{C_{Ex}^{B}}{C_{Ex}^{A} + C_{Ex}^{B} + C_{Ex}^{C}} \times 100$; $(0 < t < t_{p})$	$\text{RecB} = \dfrac{C_{Ex}^{B} Q_{Ex} t_{p}}{C_{F}^{B} Q_{F} t_{s}} \times 100$
C	$\text{PurC} = \dfrac{C_{Ex}^{C}}{C_{Ex}^{A} + C_{Ex}^{B} + C_{Ex}^{C}} \times 100$; $(t_{p} < t < t_{s})$	$\text{RecC} = \dfrac{C_{Ex}^{C} Q_{Ex} (t_{s} - t_{p})}{C_{F}^{C} Q_{F} t_{s}}$ x 100

Table 5.3 Comparison of simulation results with reported values in literature

	PurA	PurB	PurC
Modified SMB configuration 1 (MC1)			
Simulation*	88.93	95.27	90.16
Simulation (This work)	91.02	96.59	92.96
Modified SMB configuration 2 (MC2)			
Simulation*	84.48	92.14	93.42
Simulation (This work)	84.86	92.63	97.73

*Reported in Kim et al. (2003)

Table 5.4 Sensitivity analysis: Effect of desorbent flow rate in MC1 and effect of product collection time in MC2

Modified SMB configuration 1 (MC1)			
Q_D (cm^3/min)	PurA	PurB	PurC
300	84.4	93.6	87.6
360	87.4	89.1	96.6
Modified SMB configuration 2 (MC2)			
t_p /t_s	PurA	PurB	PurC
0.33	79.6	88.6	91.4
0.36	79.6	87.6	92.8
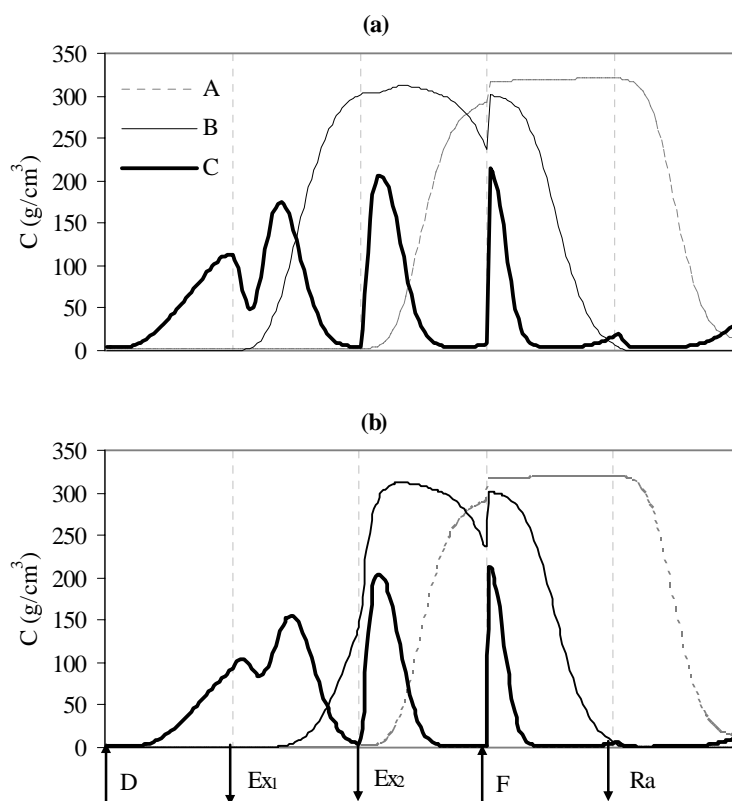
Figure 5.3 Concentration profile for components A, B and C along the sections of MC1 after steady-state was reached: (a) Q_D = 300 cm^3/min, (b) Q_D = 360 cm^3/min

5.4 Formulation of the multi-objective optimization problems

Comparison of these two modified systems is inappropriate if the performances are not compared at optimal conditions. As mentioned in the earlier chapters, for SMB systems, the optimization objectives can be numerous and sometimes it is essential to satisfy two or more objectives simultaneously. There are recently some publications on using genetic algorithm to perform such multi-objective optimization on SMB / SMBR (reaction-separation coupled) systems (Zhang et al., 2002; Subramani et al., 2003; Wongso et al., 2004; Subramani et al., 2003; Yu et al., 2003). However, all these deal with binary systems. In this study, multi-objective optimization study has been extended to ternary systems.

In this study, our aim is to simultaneously maximize purities of all the three components at their respective collection ports. One can define a three-objective function problem maximizing purities of all three streams simultaneously. However, in this case Pareto *surfaces* in a multidimensional decision variable space would be generated, which is usually difficult to analyze. In the sensitivity study, we have seen that PurB has a conflicting trend with respect to both PurA and PurC. Hence, one can formulate a two-objective function problem, defining maximization of summation of PurA and PurC as one objective function while maximization of PurB as the second objective function without losing any optimal solutions but at the same time being able to analyze only Pareto curves. Detailed mathematical formulation of the optimization problems solved is described in Table 5.5.

Table 5.5 Description of the multi-objective optimization problems solved

Configuration	Objective Function	Decision variable	Fixed parameters
MC1	Max (PurA + PurC)	$1 \leq t_s \leq 8$ min $30 \leq Q_{Ra} \leq 80$ cm^3/min $280 \leq Q_D \leq 1000$ cm^3/min $100 \leq Q_{Ex1} \leq 260$ cm^3/min	$L_{col} = 166.67$ cm, $d_{col} = 1.38$ cm, $N_{col} = 5$ $\Omega = 1/1/1/1/1$, $\eta = 0.33/0.34/0.33$ $Q_F = 60$ cm^3/min, $Q_S = 33.33$ cm^3/min
MC2	Max PurB	$1 \leq t_s \leq 8$ min $0.19 \leq t_p/t_s \leq 0.82$ $30 \leq Q_{Ra} \leq 80$ cm^3/min $20 \leq Q_{D1} \leq 200$ cm^3/min $270 \leq Q_{D2} \leq 1000$ cm^3/min	$L_{col} = 166.67$ cm, $d_{col} = 1.38$ cm, $N_{col} = 4$ $\Omega = 1/1/1/1$, $\eta = 0.33/0.34/0.33$ $Q_F = 60$ cm^3/min

Furthermore, in this work, we have endeavored to observe the effect of various non-idealities on the performances of the two modified systems, MC1 and MC2. The first parameter studied was the variation in adsorption selectivity of the components A, B and C. The degree of difficulty for separations is classified on the basis of selectivity, ϕ_{ik} (see Eq. 5.10). We considered three optimization problems: (1a) $\phi_{BA} = 1.8$, $\phi_{CB} = 2.58$; (1b) $\phi_{BA} = 4.0$, $\phi_{CB} = 4.0$; (1c) $\phi_{BA} = 8.0$, $\phi_{CB} = 3.0$. The first case (1a) implies degree of difficulty for separation is moderate while the second case (1b) can be considered as easy separation. The last set (1c) was studied to see the mathematical maximum of the performance of the two systems. In all these problems, the linear mass transfer coefficient, k_a, was assumed to be 5.0 min^{-1}. The various optimization problems solved were described as MC1-P1a to MC1-P1c for modified configuration

1 problems 1a to 1c, while MC2-P1a to MC2-P1c designate similar problems solved for modified configuration 2 (see Table 5.6). The second parameter studied was the effect of mass-transfer rates. Two problems were considered: (2a) $k_a = 100.0$ min^{-1} and (2b) $k_a = 0.1$ min^{-1} for the separation factor of $\phi_{BA} = 4.0$, $\phi_{CB} = 4.0$. Along with case (1b) with $k_a = 5.0$ min^{-1} it covers the regime from very high mass transfer rates to very low rates. Next we considered the effect of non-linearity in the adsorption isotherm. Single-component Langmuir isotherm was used. Once again three problems were solved with different values of the adsorption parameters. In order to compare the results, the isotherm parameters were adjusted such that the performance of the system tends towards the results obtained with linear adsorption isotherm. It was observed that the adsorption isotherm with $q_m = 5000$ g/cm^3 almost behaves like linear while with $q_m = 1000$ g/cm^3 it is highly non-linear. Finally, the effect of competitive multi-component Langmuir isotherm was studied to see the performance change when concentrations of the components affect the adsorption of each other. The detailed optimization formulation of these problems is described in Table 5.5 while parameter values used for all these problems are described in Table 5.6. The optimization studies were carried out with a population size of 50 for 50 generations. Average computational time in obtaining a Pareto set was circa 36 hrs on a 2.4GHz Pentium 4 computer with 512MB of SDRAM.

Table 5.6 Model parameters for different optimization problems studied

Effect of linear adsorption isotherm					
Configuration-Problem No.		K_A	K_B	K_C	k_a
MC1-P1a	MC2-P1a	1.0	1.8	4.65	5.0
MC1-P1b	MC2-P1b	1.0	4.0	16.0	5.0
MC1-P1c	MC2-P1c	1.0	8.0	24.0	5.0
Effect of linear mass-transfer coefficient					
Configuration-Problem No.		K_A	K_B	K_C	k_a
MC1-P2a	MC2-P2a	1.0	4.0	16.0	100.0
MC1-P2b	MC2-P2b	1.0	4.0	16.0	0.1
Effect of Langmuir adsorption isotherm parameter					
Configuration-Problem No.		q_m	B_A	B_B	B_C
MC1-P3a	MC2-P3a	5000	0.0002	0.0008	0.0032
MC1-P3b	MC2-P3b	2000	0.0005	0.002	0.008
MC1-P3c	MC2-P3c	1000	0.001	0.004	0.016
Effect of multi-component Langmuir adsorption isotherm parameter					
Configuration-Problem No.		q_m	B_A	B_B	B_C
MC1-P4	MC2-P4	1000	0.001	0.004	0.016

5.5 Results and discussion

The effect of selectivity, mass-transfer rate and non-linearity in adsorption isotherm parameters in the performance of the two modified SMB configurations at optimal conditions are studied. The Pareto optimal solutions are discussed below.

5.5.1 Effect of linear adsorption isotherm parameters

When separation factor (selectivity) was varied from moderately difficult separation to easy separation (see Table 5.6), there was seen a shift in the Pareto

curves as can be seen from Figure 5.4(a) & (b) which elucidate the Pareto optimal

solution and the plots of decision variables respectively for MC1. Figure 5.5 shows

similar results for MC2. Figure 5.4a shows that as PurB increases purities of both A

and C decreases. This is primarily due to decreased desorbent consumption (as

explained earlier) as the purity of B increases. Moreover, there is a very drastic

change in the performance as the separation task becomes easier (Problem 1b) from a

moderately difficult separation (Problem 1a). The maximum PurB achievable by Run

MC1-P1a is only ~55% at the cost of PurA being as low as ~70% while PurC about

~89% as compared to that for Run MC1-P1b where PurB achieved is about 95% with

still reasonably high purities of A (~ 84%) and C (~ 97%). However, improvement in

purity was marginal when the separation task was made the easiest possible separation

(Run MC1-P1c). Similar trends were observed for the modified configuration 2

(MC2) as shown in Figure 5.5. Maximum PurB achieved is about 57% (PurA ~72%

and PurC ~80%) for Run MC2-P1a while for Run MC2-P1b, PurB is about 92%

(PurA ~ 90% and PurC ~94%). Once again, insignificant improvement was observed

when degree of difficulty for separation was made easier (Run MC2-P1c) similar to

the one observed for MC1.

The results shown in Figure 5.4 (for MC1) can also be explained using the

parameter σ defined in the second chapter (Eqn. 2.3) as shown below:

$$\sigma_i = \frac{1-\varepsilon}{\varepsilon} NK_i \frac{u_s}{u_g} \tag{5.11}$$

where, in this case NK_i can be replaced by just K_i. To achieve countercurrent

separation between two components, one must set σ greater than 1 for one component

and less than 1 for the other. When $\sigma_i < 1$, species move with the fluid phase, and

when $\sigma_i > 1$, species move with the solid phase. Table 5.7 shows the calculated values
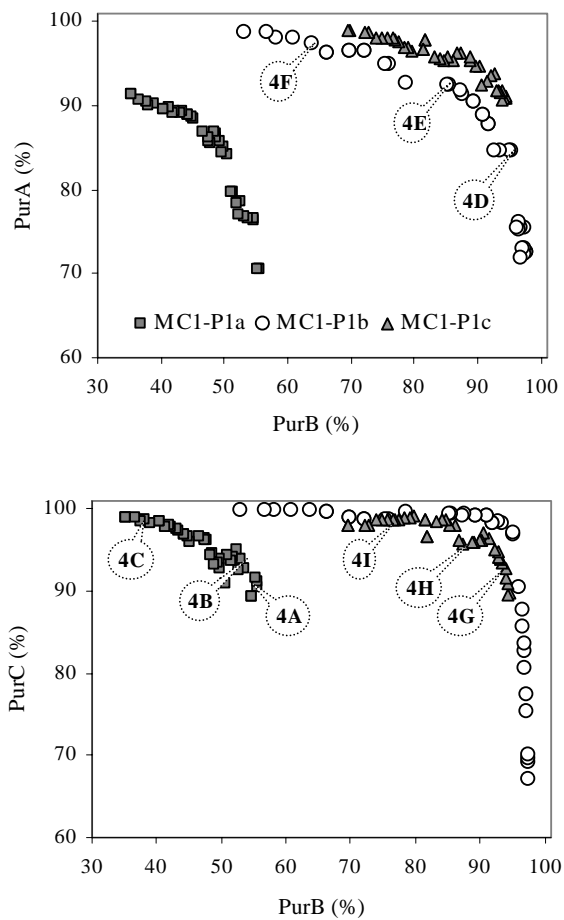
Figure 5.4(a) Pareto optimal solutions for MC1 – effect of varying linear adsorption isotherm parameters
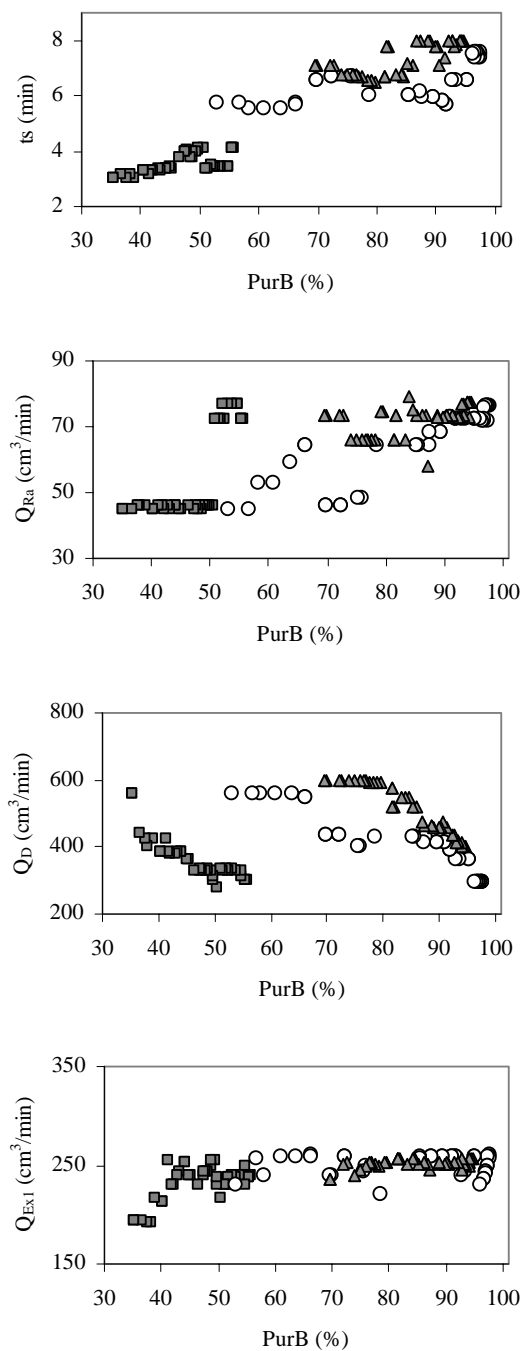
Figure 5.4(b) Corresponding decision variables for MC1 – effect of varying linear adsorption isotherm parameters
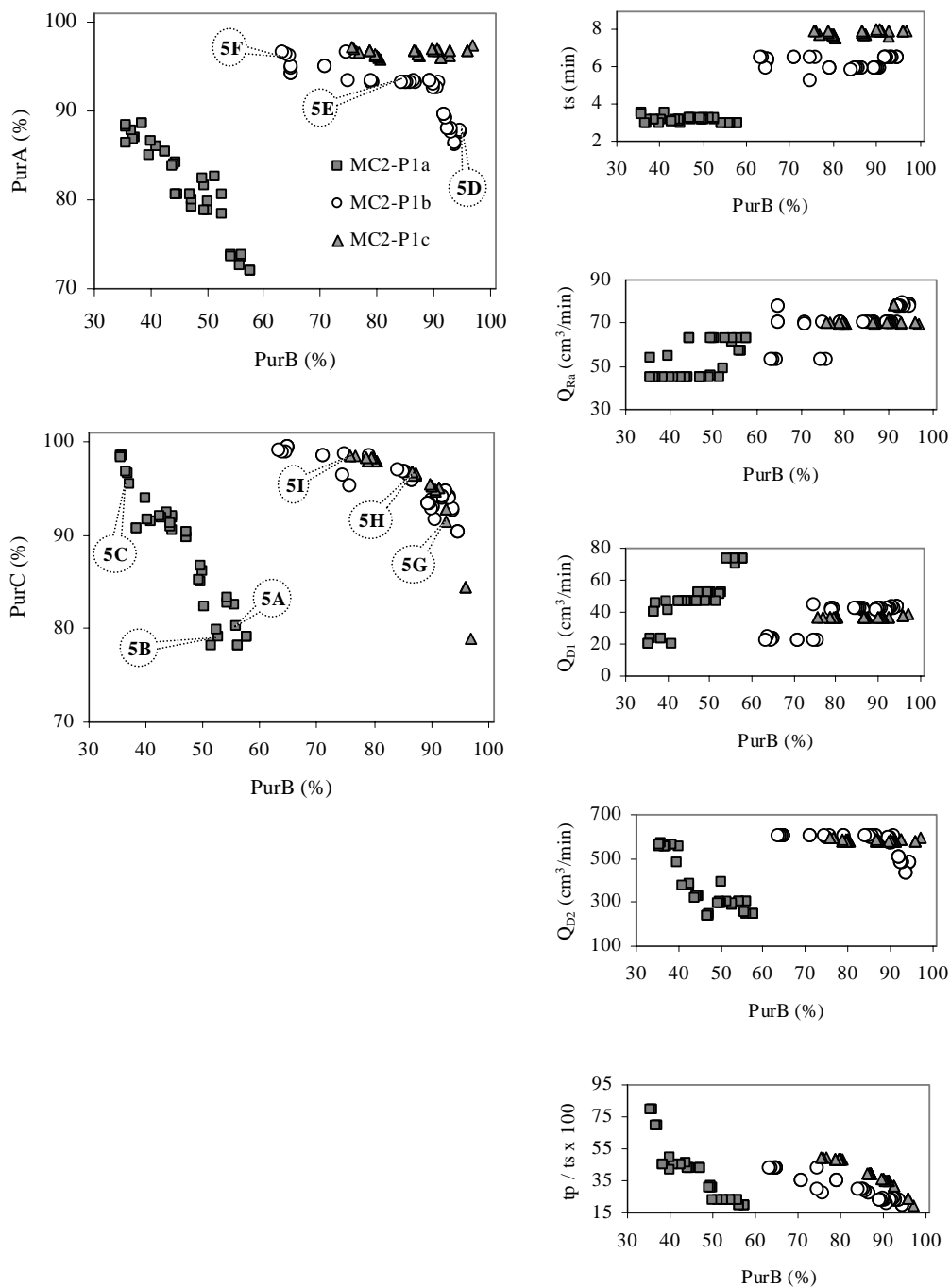
Figure 5.5 Pareto optimal solutions and corresponding decision variable plots for MC2 - effect of varying linear adsorption isotherm parameters

of σ's for the three components A, B and C for few selected points shown in Figure 5.4. Also shown in the table are the desired values of σ's in different sections. The following conclusions can be drawn when close scrutiny is done for values shown in Table 5.7 for the points 4A, 4B and 4C shown in Figure 5.4: (a) the most strongly adsorbed component C is not completely desorbed in Section P, since σ_C is not less than 1, and therefore, the adsorbent is not regenerated totally, (b) for the first two points (4A and 4B), σ_B is not less than 1 in section Q_1, resulting in poor countercurrent separation between components B and C. Consequently, PurB and PurC at the respective extract ports Ex2 and Ex1 are low, (c) in section Q_2, desired condition is satisfied for point 4A. However, for points 4B and 4C, σ_A is greater than 1, resulting in low PurB, and (d) desired conditions are satisfied for all three points in sections R and S. It should be noted that desired conditions could be achieved if enough flexibility is rendered to the system by increasing number of columns in each section. With only one column in each section, it is difficult (rather impossible) to achieve desired task in each section of the SMB system.

Similar observations can be made for points 4D-4F when degree of difficulty for separation is changed from moderately difficult to an easy separation. All points in the Pareto satisfy the desired condition in section P. Obviously, when separation task is easy, it is easier to regenerate solid in section P. Likewise, in section Q_1, except for the point 4D, effective countercurrent separation between component B and C can be achieved resulting in high purity values except for PurC for point 4D. In section Q_2, the first two points (4D and 4E) satisfy the desired conditions while for point 4F, component A is not desorbed efficiently thereby contaminating B resulting in low PurB in port Ex_2. In section R, for the points 4D and 4E, component B was not

Table 5.7 Comparison of σ values of the three components in different sections for various optimal solutions in Figure 5.4

Point	Section P			Section Q$_1$			Section Q$_2$			Section R			Section S			Purity		
	σ_A	σ_B	σ_C	σ_A	σ_B	σ_C	σ_A	σ_B	σ_C	σ_A	σ_B	σ_C	σ_A	σ_B	σ_C	PurA	PurB	PurC
4A	0.11	0.43	1.74	0.38	1.53	6.13	0.80	3.18	12.73	0.34	1.37	5.50	1.09	4.36	17.43	70.4	55.7	90.4
4B	0.10	0.41	1.63	0.31	1.23	4.93	2.02	8.08	32.32	0.47	1.89	7.56	1.11	4.44	17.77	85.6	47.9	96.1
4C	0.08	0.34	1.35	0.13	0.50	2.01	2.72	10.88	43.54	0.64	2.55	10.19	1.50	5.99	23.94	91.3	35.3	98.8
4D	0.06	0.25	0.98	0.30	1.20	4.79	0.40	1.61	6.44	0.18	0.73	2.92	0.60	2.41	9.62	72.5	97.7	67.2
4E	0.06	0.23	0.93	0.14	0.55	2.22	0.56	2.24	8.95	0.24	0.97	3.89	0.77	3.10	12.40	89.0	91.0	99.3
4F	0.04	0.18	0.71	0.07	0.29	1.16	1.43	5.71	22.84	0.33	1.34	5.35	0.79	3.14	12.57	98.9	53.1	99.8
4G	0.04	0.17	0.69	0.11	0.43	1.71	0.37	1.47	5.90	0.17	0.68	2.70	0.56	2.25	8.99	90.9	94.6	89.8
4H	0.04	0.15	0.61	0.07	0.28	1.11	0.45	1.79	7.17	0.20	0.78	3.14	0.63	2.51	10.04	95.8	85.2	97.9
4I	0.03	0.13	0.54	0.05	0.21	0.85	0.45	1.81	7.25	0.20	0.79	3.17	0.63	2.54	10.15	98.9	69.5	97.9
Desired	<1	<1	<1	<1	<1	>1	<1	>1	>1	<1	>1	>1	>1	>1	>1			
	Regeneration of solid			Separation of B & C			Purification of B			Purification of A			Regeneration of fluid					

adsorbed efficiently and thus lowering PurA, while in section S, component A is not adsorbed fully thus contaminating C at port Ex_1. When the separation task was made even easier (MC1-P1c), similar observations can be made. Desired conditions can be easily satisfied in sections P and Q_2. In section Q_1, point 4I does not satisfy the condition for countercurrent separation, thereby contaminating component B at port Ex_2 lowering its purity. In section R, component B is not adsorbed efficiently resulting in low PurA while in section S, A is not adsorbed fully thus contaminating C at port Ex_1.

5.5.2 Effect of linear mass-transfer rate

Figure 5.6 shows the shift in the Pareto optimal solution together with the corresponding decision variables plots for MC1 while Figure 5.7 shows similar results for MC2 when the mass-transfer rate parameter was varied. Once again, similar to the previous problems, a very drastic change in performance was observed when the mass-transfer rate was changed. When $k_a = 100$ min^{-1} (MC1-P2a and MC2-P2a), the separation task is very easy as the system tends to reach equilibrium quickly due to negligible mass transfer resistance. The figure shows that very high purities of all three components can be achieved. For example, for MC1 when PurB is as high as ~97 %, PurA and PurC are still as high as ~96% and ~99% respectively. However, when the mass-transfer rate, k_a, was decreased to 0.1 min^{-1}, as expected the performance of the system deteriorated significantly. For example, for Run MC1-P2b, purities obtained are quite low (PurA ~ 47%, PurB ~ 45% and PurC ~ 59%). This is expected since as the mass-transfer resistance increases, the adsorption of the components becomes more difficult, consequently reducing the separation efficiency. Similar trends were observed in MC2-P2a and MC2-P2b.
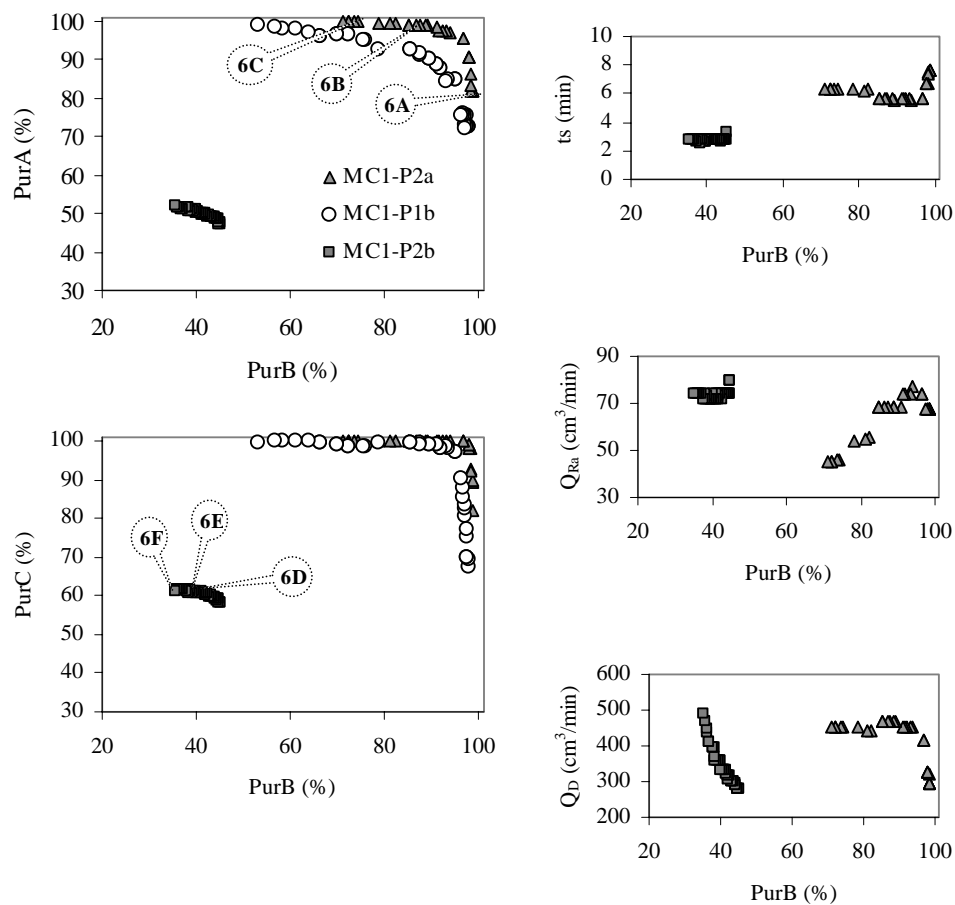
Figure 5.6 Pareto optimal solutions and corresponding decision variable plots for MC1 – effect of varying mass-transfer rates
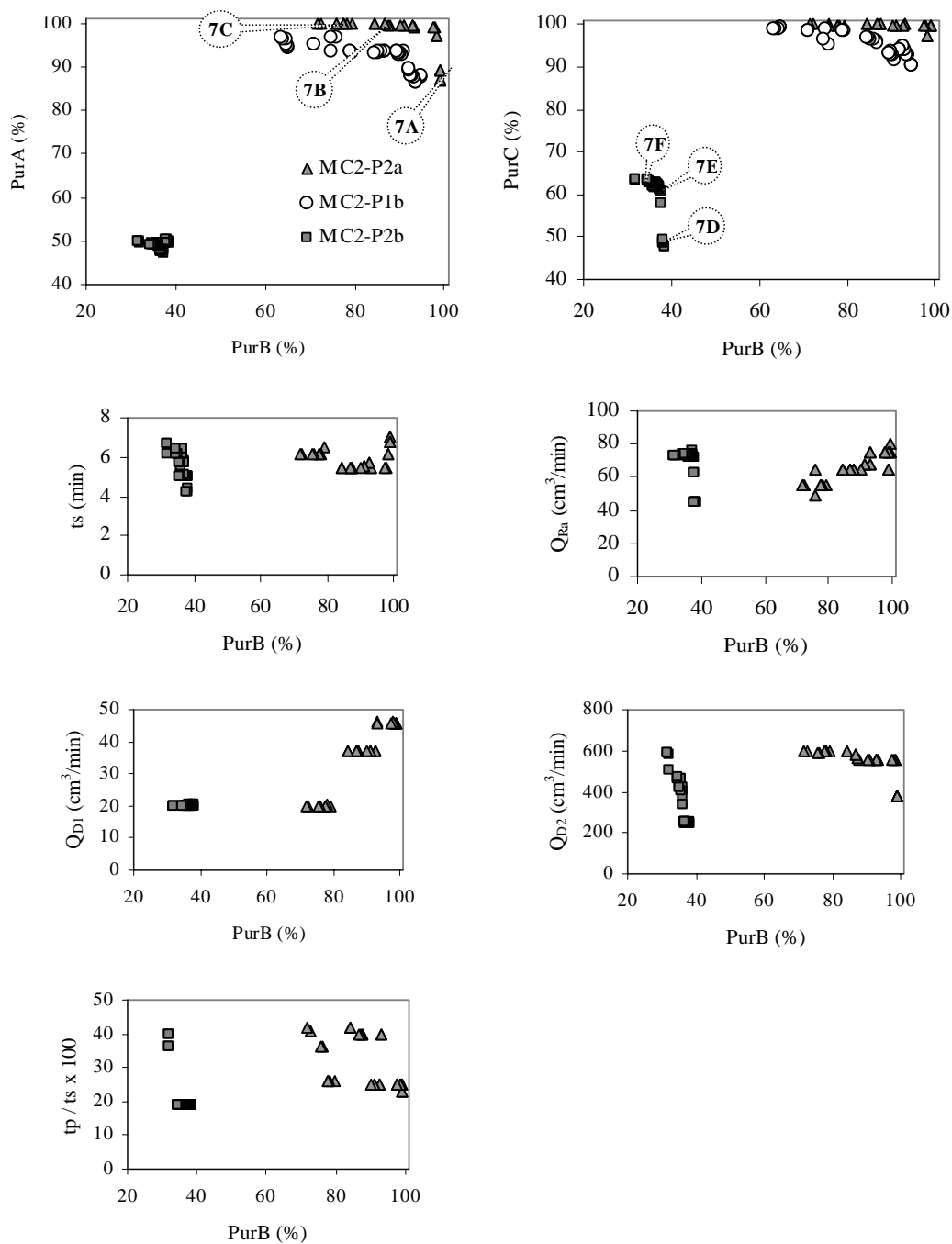
Figure 5.7 Pareto optimal solutions and corresponding decision variable plots for MC2 – effect of varying mass-transfer rates

Recoveries of components A, B and C are listed in Table 5.8 for few selected points from each of the Pareto results shown in Figures 5.4-5.7 for MC1 and MC2. The results in the table show that high purity with good recoveries for all the three components are possible when the separation task is easy for both MC1 and MC2. Similar observation can be made when the mass-transfer rate was set very high. However, as the separation task becomes difficult, either when adsorption selectivity was decreased or mass-transfer resistance was increased, purity and recovery values drop significantly. Another important observation that can be made from Table 5.8 is that recovery of each component follows a conflicting trend with that of its purity. When PurA and PurC are low, RecA and RecC values are high, and vice versa. Same holds true for PurB and RecB.

5.5.3 Effect of non-linearity in adsorption isotherm

The objective of these optimization runs was to see the effect of non-linearity in the adsorption isotherm on the performance of the two modified SMB systems. The adsorption isotherm parameters are given in Table 5.6. Three different sets of runs (MC1-P3a, MC1-P3b, MC1-P3c for MC1 and MC2-P3a, MC2-P3b, MC2-P3c for MC2) are based on increasing non-linearity for the adsorption isotherm. The Pareto optimal solutions together with the corresponding decision variables plots are shown in Figure 5.8 for MC1 and Figure 5.9 for MC2. For MC1-P3a, value for t_s was found to be 5.5 min for the initial part of the Pareto while 4.2 min for the later part. Similar values for MC1-P3b are 4.2 and 2.6 min and for MC1-P3c are 3.2 and 2.6 min. We can see that for MC1-P3a and MC2-P3a the system almost behaves like that of a linear isotherm. The performance steadily decreases as the isotherm becomes more non-linear due to the tailing effect of the components, which results in interference of

Table 5.8 Purity and Recovery values for few selected optimal points

Modified configuration 1 (MC1)								Degree of difficulty for separation	Modified configuration 2 (MC2)							
Configuration Problem no.	Point	Purity (%)			Recovery (%)				Configuration Problem no.	Point	Purity (%)			Recovery (%)		
		A	B	C	A	B	C				A	B	C	A	B	C
MC1-P1a	4A	70.4	55.7	90.4	75.7	61.7	72.5	Moderate	MC2-P1a	5A	72.7	55.7	82.5	77.6	56.5	71.4
	4B	78.5	52.6	92.6	56.6	79.8	67.9			5B	78.3	52.7	79.1	56.9	65.2	76.2
	4C	90.6	36.7	98.9	11.0	98.3	12.9			5C	87.8	36.7	96.8	30.5	93.0	5.4
MC1-P1b	4D	84.6	95.2	97.0	98.0	85.8	91.5	Easy	MC2-P1b	5D	87.8	94.8	90.4	98.1	75.7	95.3
	4E	92.5	85.3	99.4	91.4	95.1	87.8			5E	93.3	85.1	96.8	94.6	88.6	87.2
	4F	97.3	63.8	99.8	79.6	97.5	61.2			5F	96.4	63.8	98.9	75.7	95.0	64.2
MC1-P1c	4G	93.7	92.7	94.7	95.1	97.8	88.0	Very easy	MC2-P1c	5G	96.8	92.7	92.8	98.4	92.0	91.3
	4H	96.3	86.8	96.2	95.1	98.9	83.4			5H	96.9	86.6	96.8	98.4	96.5	83.6
	4I	98.0	75.8	98.6	95.5	99.7	69.0			5I	97.1	75.7	98.6	98.4	98.3	67.3
MC1-P2a	6A	82.1	98.6	82.1	97.2	63.1	96.6	Easy & no mass-transfer resistance	MC2-P2a	7A	89.2	98.9	99.8	100.1	86.7	98.6
	6B	99.0	86.5	100.0	94.4	98.3	88.9			7B	99.7	86.8	100.0	85.5	97.4	95.4
	6C	99.8	72.1	99.9	64.4	99.6	94.5			7C	99.9	71.7	100.0	65.9	98.8	89.4
MC1-P2b	6D	51.5	37.8	61.1	83.5	29.3	35.6	Easy but significant mass-transfer resistance	MC2-P2b	7D	48.9	44.1	37.5	51.2	17.8	63.8
	6E	51.1	36.8	61.7	84.7	29.6	32.2			7E	50.9	53.7	36.6	71.0	17.4	59.5
	6F	51.9	35.4	61.3	84.4	32.8	26.5			7F	46.4	66.5	34.7	90.6	11.0	50.0
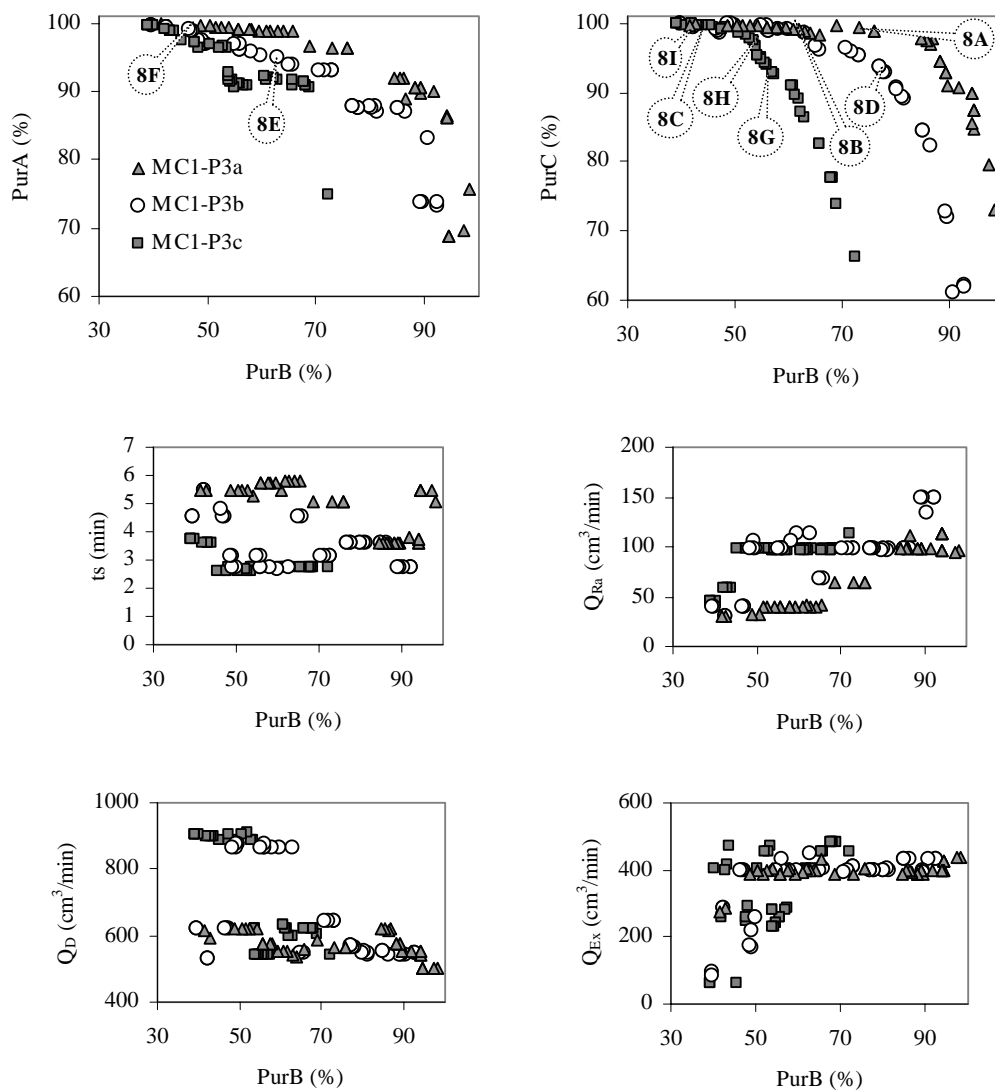
Figure 5.8 Pareto optimal solutions and corresponding decision variable plots for MC1 - effect of non-linearity in adsorption isotherm
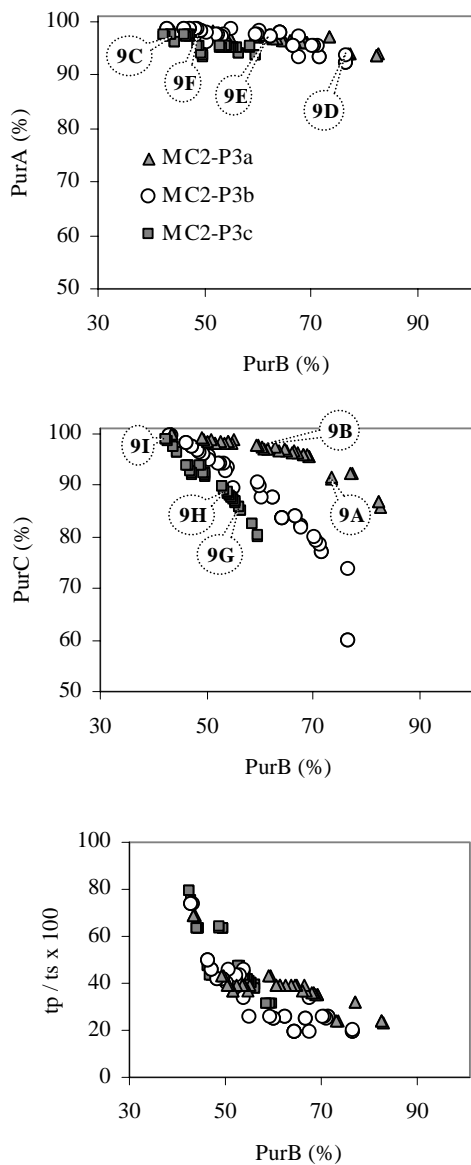
Figure 5.9 Pareto optimal solutions and corresponding decision variable plots for MC2 – effect of non-linearity in adsorption isotherm

the adsorption bands of components. For MC1, the purities for both A and C decrease with the increasing non-linearity, however for MC2, PurA remains almost unaffected except for the last run (P3c), while PurC decreases.

5.5.4 Effect of multi-component competitive Langmuir adsorption isotherm

These runs were performed to see the effect of competitive multi-component adsorption isotherm on the performance of these systems. Instead of single-component Langmuir isotherm, multi-component Langmuir isotherm was used. The parameters used are given in Table 5.6. The Pareto optimal solution and corresponding decision variable results for both MC1 and MC2 are shown in Figures 5.10 and 5.11 respectively. It was interesting to see that the performance of the system improves slightly for both the cases. In case of competitive multi-component isotherm all the components compete for the same adsorption sites and as a result we can see improved separations and higher purities. PurA for MC1-P4 and MC2-P4 remains the same for both the cases but PurB and PurC increase as compared to MC1-P3c and MC2-P3c (single-component Langmuir isotherm) respectively. This is most probably because the adsorption constants for B and C are 4 times and 16 times greater than that of A and hence these components have more probability for adsorption.
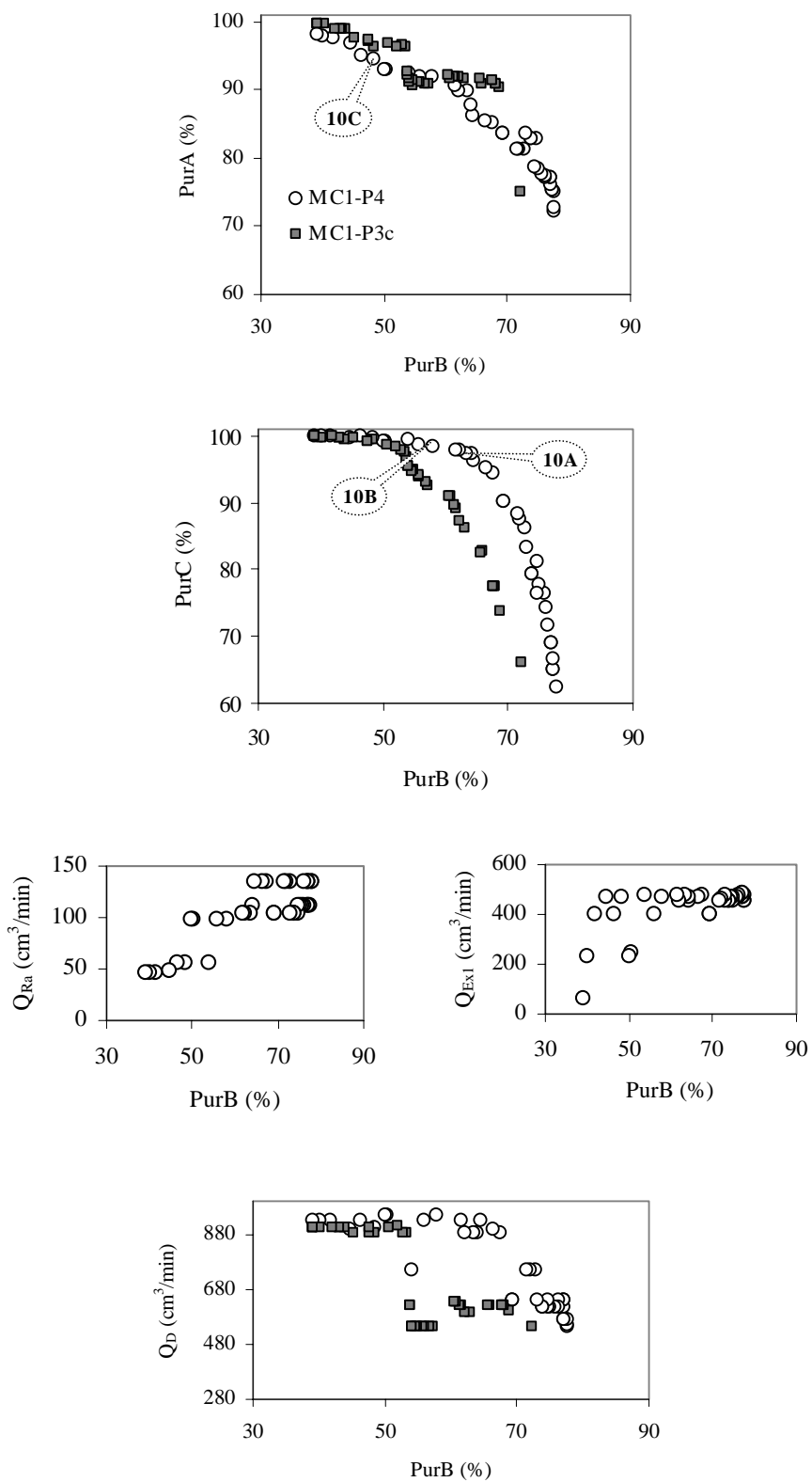
**Figure 5.10 Pareto optimal solutions and corresponding decision variable plots
for MC1 - effect of multi-component competitive Langmuir adsorption isotherm**
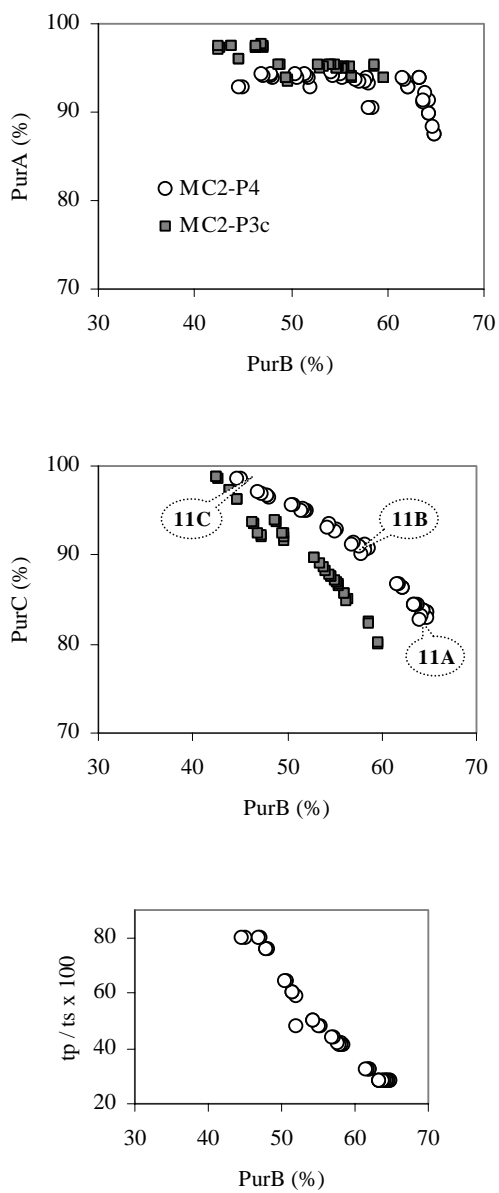
Figure 5.11 Pareto optimal solutions and corresponding decision variable plots for MC2 - effect of multi-component competitive Langmuir adsorption isotherm

5.6 Comparison between MC1 and MC2

After individually studying the sensitivity of Pareto solutions for MC1 and MC2, the above results could be used to compare the performance between MC1 and MC2. Three points were chosen from each of the Pareto curve with identical PurB values for both MC1 and MC2, and the purities of A and C were compared. Table 5.9 shows the purity values along with the values of desorbent consumption for each of the points. For MC2, since there are two desorbent flow rates, Q_{D1} and Q_{D2}, the total desorbent ($Q_D = Q_{D1} + Q_{D2}$) is tabulated. The following conclusions were made for each run (see Table 5.9):

(a) When separation task is difficult, MC1 performs better than MC2 as PurA and PurC are slightly higher also with comparatively lesser consumption of desorbent. When separation task is easier, both MC1 and MC2 perform equally well.

(b) When the mass-transfer rate is high with good adsorption selectivity (MC1-P2a and MC2-P2a), MC2 performs better than MC1 as higher PurC can be achieved. However, when mass-transfer resistance is high (MC1-P2b and MC2-P2b), MC1 performs better than MC2.

(c) When non-linearity in adsorption isotherm is increased, PurA is lower but PurC is always higher for MC1 compared to MC2.

(d) When competitive multi-component Langmuir isotherm is used, similar trend is observed. When desired PurB is high, PurA is lower but PurC is higher for MC1 compared to MC2.

(e) For all the optimization results it was observed that MC2 consumes more desorbent compared to MC1. But, it should be noted that MC2 has only four columns and hence has less total adsorbent compared to MC1, which has five columns.

Kim et al. (2003) have reported that MC2 would perform better or at least same as that of MC1. They have mentioned that as the desorbent to feed flow rate ratio D/F increases from minimum D/F (~5 as reported in Kim et al., 2003), the purity of C for MC1 increases rapidly while for MC2 it does not increase that drastically, and hence have recommended that for larger D/F values MC1 is preferable. Their conclusions were based on equilibrium theory and were validated with simulations, which were also performed mostly at near equilibrium conditions. The same observations were seen in this study when the system is operating near the equilibrium region. Also in this study, the D/F ratio was always maintained far from the minimum D/F, as a result it was generally observed that MC1 performs better than MC2. For easier separations, however, both MC1 and MC2 perform equally well. Nevertheless, from the industrial point of view, MC2 seems to be less complicated in terms of operation, compared to MC1. MC1 needs more outlet ports and more complications arise as the number of zones increase. On the contrary, MC2 can be very easily modified from a conventional 4-zone SMB with little additional cost compared to MC1, but requires more desorbent due to the absence of recycle.

Table 5.9 Comparison of optimal solutions of MC1 and MC2

Separation characteristic	PurB	Point	Problem	PurA	PurC	Q_D (cm³/min)	Point	Problem	PurA	PurC	Q_D (cm³/min)
				Modified configuration 1 (MC1)					Modified configuration 2 (MC2)		
Moderate	56	4A	MC1-P1a	70.4	90.4	301	5A	MC2-P1a	72.7	82.5	329
	53	4B		78.5	92.6	331	5B		78.3	79.1	337
	37	4C		90.6	98.9	440	5C		87.8	96.8	598
Easy	95	4D	MC1-P1b	84.6	97.0	360	5D	MC2-P1b	87.8	90.4	524
	85	4E		92.5	99.4	430	5E		93.3	96.8	641
	64	4F		97.3	99.8	558	5F		96.4	98.9	623
Very easy	93	4G	MC1-P1c	93.7	94.7	433	5G	MC2-P1c	96.8	92.8	620
	87	4H		96.3	96.2	474	5H		96.9	96.8	620
	76	4I		98.0	98.6	600	5I		97.1	98.6	630
Easy & no mass transfer resistance	99	6A	MC1-P2a	82.1	82.1	294	7A	MC2-P2a	89.2	99.8	421
	87	6B		99.0	100	470	7B		99.7	100	619
	72	6C		99.8	99.9	450	7C		99.9	100	618
Easy but significant mass transfer resistance	38	6D	MC1-P2b	51.5	61.1	397	7D	MC2-P2b	48.9	44.1	260
	37	6E		51.1	61.7	411	7E		50.9	53.7	354
	35	6F		51.9	61.3	491	7F		46.4	66.5	260
Slightly non-linear adsorption isotherm	73	8A	MC1-P3a	96.4	99.3	566	9A	MC2-P3a	97.2	91.4	1034
	61	8B		98.7	99.1	555	9B		97.6	97.1	974
	43	8C		99.7	99.8	595	9C		98.4	99.9	946
Moderately non-linear adsorption isotherm	77	8D	MC1-P3b	87.7	93.6	572	9D	MC2-P3b	92.1	59.9	1059
	63	8E		95.0	98.7	867	9E		97.1	87.6	763
	47	8F		99.1	99.2	623	9F		98.6	97.5	945
Highly non-linear adsorption isotherm	56	8G	MC1-P3c	91.0	94.1	544	9G	MC2-P3c	95.1	86.4	995
	53	8H		96.5	97.8	885	9H		95.3	89.7	1033
	42	8I		99.0	99.8	901	9I		97.4	98.7	984
Competitive adsorption isotherm	65	10A	MC1-P4	86.3	96.2	928	11A	MC2-P4	88.2	83.0	839
	58	10B		92.0	98.2	951	11B		93.4	90.9	987
	45	10C		96.8	99.8	894	11C		92.9	98.6	1010

5.7 Conclusions

An attempt has been made to study the separation effectiveness of modified SMB systems for ternary mixtures. Two different modified SMB configurations, MC1 and MC2, were considered and separation effectiveness was studied under different conditions, such as adsorption selectivity, mass-transfer rates, and non-linear adsorption isotherm. Rigorous multi-objective optimization was performed in each case and the optimal results were compared. It was observed that performance of MC1 and MC2 are comparable, MC2 performing slightly better than MC1 when the separation task is very easy while as the separation task tends towards more difficult ones MC1 performs better than MC2. Also, MC2 needs more desorbent but requires less solid adsorbent compared to MC1. However, MC2 is a less complicated set-up compared to MC1.

These observations can be used as a guideline if more realistic applications such as separation of C_8 aromatics are considered using these modified configurations. The suitable choice of a particular configuration will obviously depend on the ternary system so that it can then be clear whether the desorbent is more affordable or the adsorbent. Moreover, the feed compositions would have a major effect on the performance of these systems. The next study, therefore, should deal with the application of a more realistic industrial application on these two modified SMB systems.

Chapter 6   Modified SMB systems with multiple columns
- Ternary separation of C$_8$ aromatics

6.1 Introduction

In the previous chapter, we discussed and compared the performance of two modified configurations of SMB for ternary separation. The modified configurations were compared in the presence of several non-idealities such as high mass-transfer resistance, low adsorption selectivity, non-linearity in adsorption isotherm, etc. Besides, the comparisons were done at optimal conditions considering multiple objectives. However, the studies were done by assuming just one column in each section. In the application of SMB systems for industrial processes, one generally requires more than one column in each section. The reasons for having multiple columns can be numerous. Ruthven and Ching (1989) claimed that at least two columns per section are required to provide enough flexibility in achieving the countercurrent separation. Moreover, having more columns in each section helps in revamping the performance deterioration caused by the presence of non-idealities in real systems, such as low mass transfer rates, high degree of non-linearity in adsorption isotherms, etc.

In the previous chapter, the two modified configurations of SMB for ternary separation systems, MC1 (Figure 5.2a) and MC2 (Figure 5.2b) were studied at optimal conditions for a hypothetical separation problem in which degree of separation difficulty, adsorption isotherm and mass-transfer rates were assumed arbitrarily. In this chapter, we first extend our earlier study on modified SMB systems under non-ideal conditions to include more than one column per section for the hypothetical separation problem. It is important to see the effect of having multiple

columns in different sections on the performance of the modified configurations. Subsequently, further modifications to one of the modified configurations are proposed to revamp its inability to perform in presence of multiple columns in the sections. These modified systems are then investigated for the separation of C$_8$ aromatics at optimal conditions.

C$_8$ aromatic mixture consists of ethyl benzene and three xylene isomers all having the same molecular weight but differing structurally from one another. The separation of these four isomers from one another is difficult by conventional distillation because their boiling points are very close to each other. The Parex™ and Ebex™ are industrial separation processes based on SMB technology for the recovery of *p*-xylene and ethyl benzene respectively from mixed C$_8$ aromatic isomers. In Chapter 3 of this dissertation which deals with the multi-objective optimization studies on the Parex process we have already mentioned the use of *p*-xylene which goes in the production of fibers, films and resins that are used for household fabrics, carpets, and clothing. Ethyl benzene is also another important chemical that can be recovered from the C$_8$ aromatic mixture. It is used for the production of styrene that is one of the most manufactured monomers in the world with an annual turnover of US$ 60 billion. Styrene is the raw material for the production of polystyrene, acrylonitrile-butadiene-styrene resins (ABS) and a variety of miscellaneous polymers, which are the basic materials of the plastic revolution. Most of the conventional processes till now have focused only on the recovery of either *p*-xylene or ethyl benzene from this mixture. Though there are some patents, there is no report in the open literature which deals with the simultaneous recovery of both *p*-xylene and ethyl benzene from the mixture of C$_8$ aromatics. After studying the performance of various modified SMB configurations for a hypothetical ternary separation problem, it is important to observe

the performance of a practical system that not only exhibits non-ideal behavior but also requires more than one column in each section. Hence, it will be quite interesting to see if it is possible to recover both *p*-xylene as well as ethyl benzene from this C$_8$ aromatic mixture using a single modified SMB unit. To further enhance the separation efficiency, the effect of adding a reflux stream purely containing one of the components, as explained by Nicoud (1998), is also studied.

The optimization studies were performed considering multiple objectives. It is needless to emphasize the importance of multi-objective optimization either at the operating stage or at the design stage for any SMB system.

6.2 Modified SMB Systems

In order to achieve separation between the components in the conventional four-section SMB system (Figure 5.1), the internal flow rates of the fluid phases within the four sections, and the switching time, t$_s$ (that defines the imaginary solid-phase velocity) have to be specified appropriately. The two modified configurations of SMB systems described by Kim et al. (2003) and studied under optimal conditions for non-ideal systems for ternary separation in the earlier chapter are shown in Figure 5.2a and 5.2b. Throughout this chapter, again we have assumed that the feed consists of a ternary mixture of components A, B and C with A being the least adsorbed component, C being the most adsorbed component and B being the component with an intermediate adsorption affinity compared to A and C.

It is easy to understand that having more columns in each section in MC1 will have similar effect to that of having multiple columns in the four-zone conventional SMB. When designed properly, MC1 with multiple columns should either give better or at least equal performance in terms of purity (or recovery) of the desired product

streams when compared with MC1 having only one column in each section. However, this does not necessarily hold true for the configuration MC2. When there is only one column in section P, the functioning of this section is equivalent to a single column chromatographic fixed bed system within the time of one switching. The desorbent elutes the two components that have peaks separated along the length of the column. However, when multiple columns are present these peaks are spread along the section across different columns. Since the switching operation is done by moving the ports by each column (and not by section), one can see that component C (the most strongly adsorbed component) in this case cannot be collected in the similar fashion as described for configuration MC2 with one column in each section. Hence, it is necessary to modify configuration MC2 slightly to facilitate collection of component C at the location where higher purities of C can be obtained. Two modifications are proposed and are shown in Figure 6.1 (a) and (b) as MC2A and MC2B respectively. Both the modifications are based on the fact that when there are multiple columns, it is improper to have the same outlet stream for both components B and C, and C must be collected upstream of the collection port for component B. The presence of this additional outlet port for C splits section P into two sub-sections, P_1 and P_2. The modified configuration MC2A (Figure 6.1(a)) is almost similar to MC1 baring the fact that section P and section Q are disconnected. However, the modified configuration MC2B (Figure 6.1(b)) is more alike MC2. In this case, B is collected from the end of section P for time until t_p ($\equiv$ < t_s, i.e., 0 < t < t_p) similar to MC2. When t = t_p, the extract port is switched in the backward direction to a point upstream (of flow direction) and component C is collected for the remainder of the switching time ($t_p \leq t < t_s$). However, it is worth noting that in these two cases an additional port is

(a)

(b)
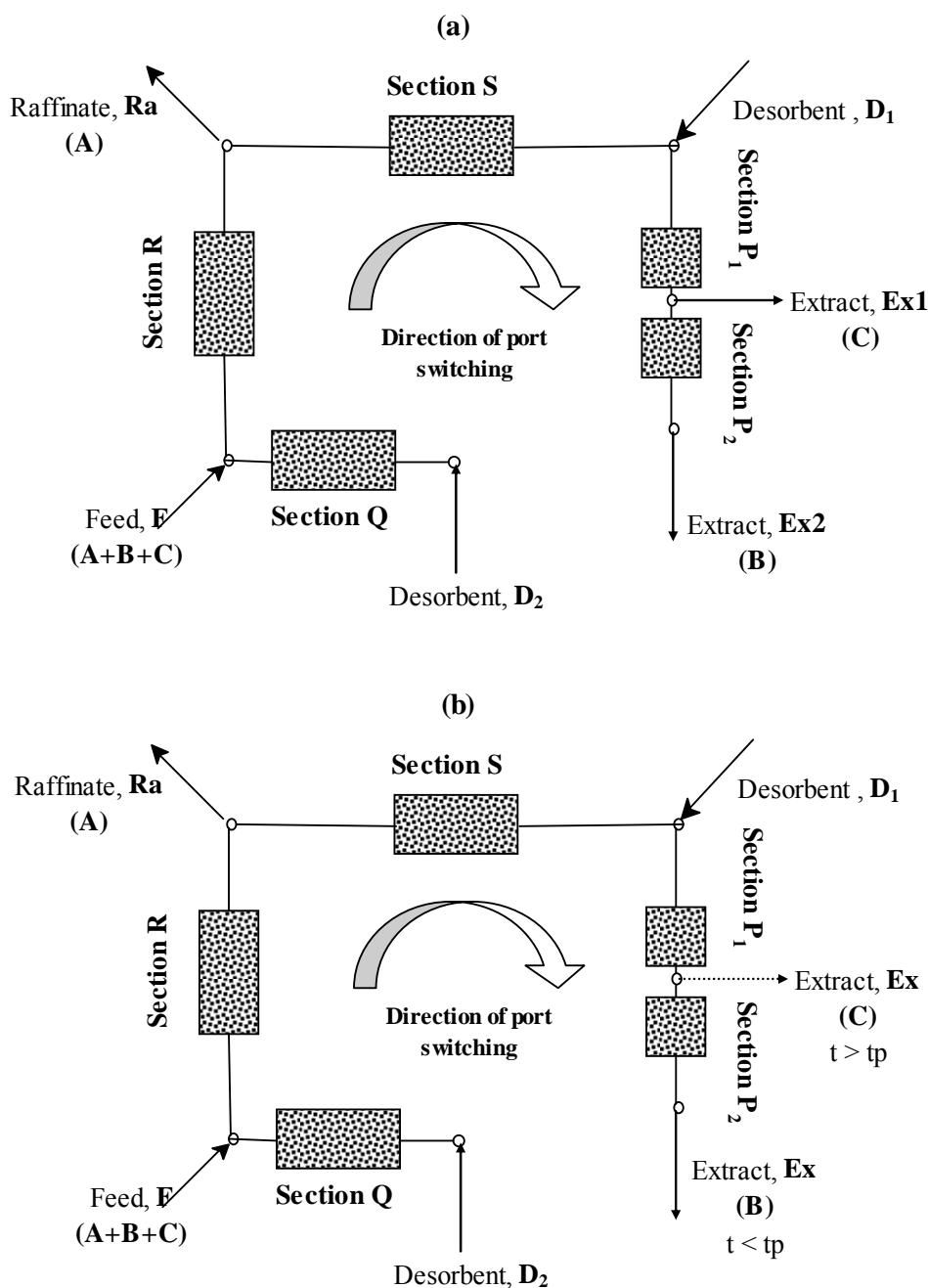
Figure 6.1 Schematic diagrams for further modifications of MC2
(a) Modified configuration MC2A & (b) Modified configuration MC2B

needed, and thus the advantage of MC2 over MC1 of being a less complicated system is lost. Nevertheless, it is important to test the performance of these two modifications (MC2A and MC2B) on both the hypothetical separation example studied in the earlier chapter as well as for the practical and industrial ternary separation example of C$_8$ aromatic mixture.

In this chapter, multi-objective optimization studies were performed on the proposed modifications (MC2A and MC2B) to determine their credibility in improving the performances of the system for the hypothetical ternary separation problem. Subsequently, suitability of the three modified configurations (MC1, MC2A and MC2B) at optimal conditions were studied for the separation of C$_8$ aromatics to recover simultaneously *p*-xylene (*p*-X) and ethyl benzene (EB) with the aim of achieving purities of both streams as high as possible. Furthermore, the effect of adding a reflux stream, containing only the intermediate component on the performances of modified systems, MC1 and MC2, was also investigated.

6.3 Mathematical model

The mathematical model describing the dynamic behavior of the modified SMB system is described in detail in the previous chapter. The same is not discussed here for brevity. Two different numerical solution approaches were used to solve the sets of partial differential equations (PDEs) along with their boundary conditions. For the first problem, the hypothetical ternary separation example, the PDEs were discretized in space using the Finite Difference Method to convert them into a system of coupled ODE-IVPs and solved using Method of Lines. The number of plates used was 50. The resultant stiff ODE-IVPs were solved using the subroutine, DIVPAG (based on Gear's method), in the IMSL library. The system and operating parameters

used are given in the earlier chapter wherein, the mathematical model was validated by comparing simulation results with reported results of Kim et al. (2003), who used Aspen Chromatography simulator to simulate the system. Details of comparative studies are reported in the earlier chapter. The second problem, the ternary separation of C$_8$ aromatics, was solved using the orthogonal collocation method on finite elements (OCFE). Each column was divided into six equal finite elements and each element was discretized with two internal collocation points to convert the PDEs into a system of coupled ODE-IVPs as before. These were again solved using the subroutine DIVPAG of the IMSL library. The mathematical model for this case was validated with the simulation results reported by Minceva and Rodrigues (2002), who used gPROMS (a general purpose process modeling, simulation and optimization software) as simulator. The details of the operating conditions used and model validation are reported in chapter 3. All simulations in this study were performed on a CRAY J916 supercomputer.

6.4 Formulation of the multi-objective optimization problems

In this chapter, few double-objective optimization problems for ternary separation were formulated. First set of problems solved are an extension of our earlier study reported in chapter 5 for hypothetical ternary separation in MC1 and MC2 configuration to include multiple columns per section. Subsequently, systematic investigation was performed to study the ternary separation of C$_8$ aromatics containing mixtures of xylene isomers. In order to obtain global Pareto optimal solution, one needs to perform large number of simulations, often over 2500 simulations consisting 50 chromosomes for 50 generations. In such a scenario, it is very important that we use a numerical simulation method which is less time

consuming. The results shown in the next section are obtained using method of lines in solving the first separation problem (hypothetical case) while orthogonal collocation on finite elements is used in solving the second separation problem (C$_8$ aromatics).

6.5 Results and Discussion

The Pareto results obtained by solving the various multi-objective optimization problems are explained in the following sub-sections.

6.5.1 Problem 1: Separation of a hypothetical ternary mixture

Few two-objective function optimization problems are solved for modified configurations MC1 and MC2. The adsorption selectivity for the components used are Φ_{BA} ($\equiv K_B/K_A$) = 4 and Φ_{CB} ($\equiv K_C/K_B$) = 4 while the linear mass-transfer rate (k_a) was assumed a moderate value of 5.0 min^{-1}. Since, the presence of more columns in section P can have an adverse effect on the performance of MC2, 3 columns were used in section P while the other sections were kept fixed with one column each. It was necessary to provide three columns in section P for flexibility between sub-sections P_1 and P_2 of the MC2 configuration. The other operating parameters used are similar to the one used in the earlier chapter. The details of the optimization formulation are shown in Table 6.1.

6.5.1.1 Problem MC1-P1: Effect of multiple columns in section P of MC1

This run deals with the effect of multiple columns in section P for modified configuration 1, MC1 (see Figure 5.2(a)). This run was necessary to have a fair comparison between configurations MC1 and MC2, both with multiple columns in

**Table 6.1 Description of the multi-objective optimization problems for the
hypothetical ternary separation problem**

Problem No.	Objective Function	Decision Variables	Fixed Parameters
MC1-P1		$3 \leq t_s \leq 8$ min $30 \leq Q_{Ra} \leq 150$ cm³/min $280 \leq Q_D \leq 700$ cm³/min $50 \leq Q_{Ex1} \leq 500$ cm³/min	$d_{col} = 1.38$ cm, $L_{col} = 166.67$ cm $N_{col} = 7$, $p/q_1/q_2/r/s = 3/1/1/1/1$ $Q_F = 60$ cm³/min $Q_S = 33.33$ cm³/min
MC2-P1	Max (PurA + PurC) Max (PurB)	$3 \leq t_s \leq 8$ min $0.19 \leq t_p/t_s \leq 0.82$ $30 \leq Q_{Ra} \leq 150$ cm³/min $20 \leq Q_{D1} \leq 100$ cm³/min $240 \leq Q_{D2} \leq 600$ cm³/min	Same as MC1-P1 except $N_{col} = 6$, $p/q/r/s = 3/1/1/1$, & Q_S is not fixed.
MC2A-P1		$3 \leq t_s \leq 8$ min $30 \leq Q_{Ra} \leq 150$ cm³/min $20 \leq Q_{D1} \leq 100$ cm³/min $240 \leq Q_{D2} \leq 600$ cm³/min $1 \leq p_1 \leq 2$	Same as MC2-P1 except $p_2 = 3 - p_1$, $q/r/s = 1/1/1$
MC2B-P1		Same as MC2A-P1 & $0.19 \leq t_p/t_s \leq 0.82$	Same as MC2A-P1

section P. The mathematical formulation of the optimization problem is described in Table 6.1 as MC1-P1. The Pareto optimal solutions are compared in Figure 6.2 while the corresponding decision variables are shown in Figure 6.3. Due to the presence of more columns in section P in MC1-P1, the overall performance increases, as expected, when compared to problem MC1-P1b in our earlier study (chapter 5) in which one column each was assumed in all sections. This is obvious, since the presence of more columns in P facilitate better desorption of strongly adsorbed component C.
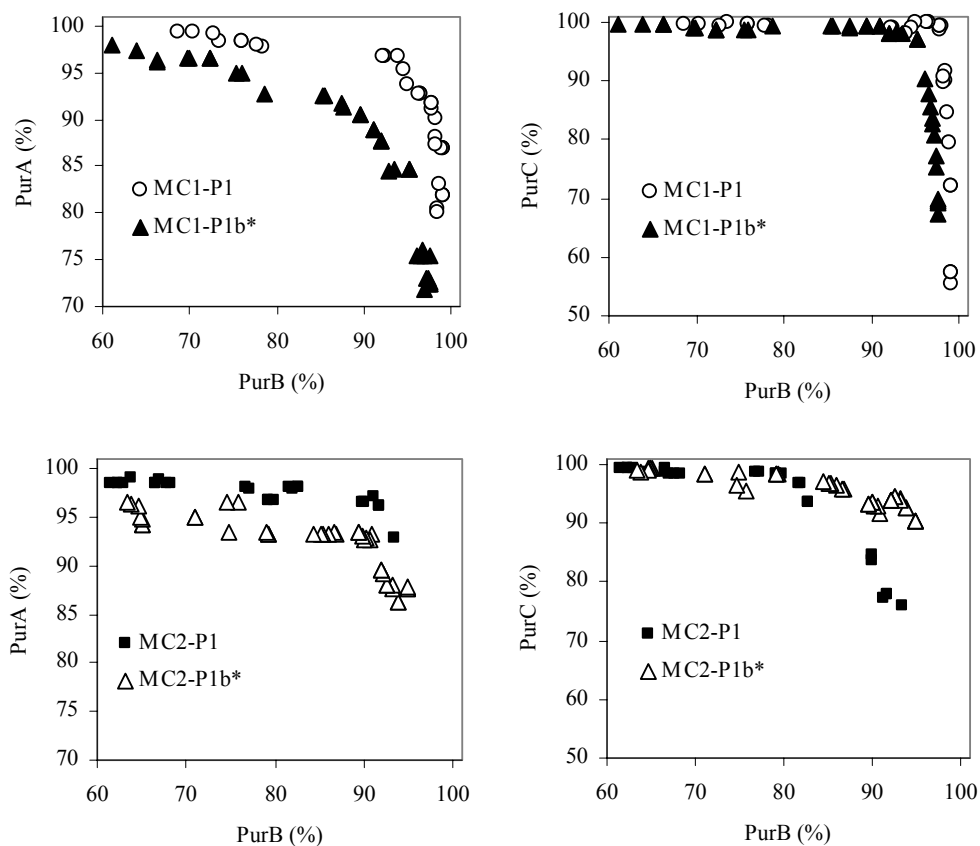
* Reported in chapter 5 as MC1-P1b and MC2-P1b

Figure 6.2 Comparison of Pareto optimal solutions when multiple columns are present in section P (problems MC1-P1 and MC2-P1) **with modified configuration when only one column is present** (problems MC1-P1b and MC2-P1b)
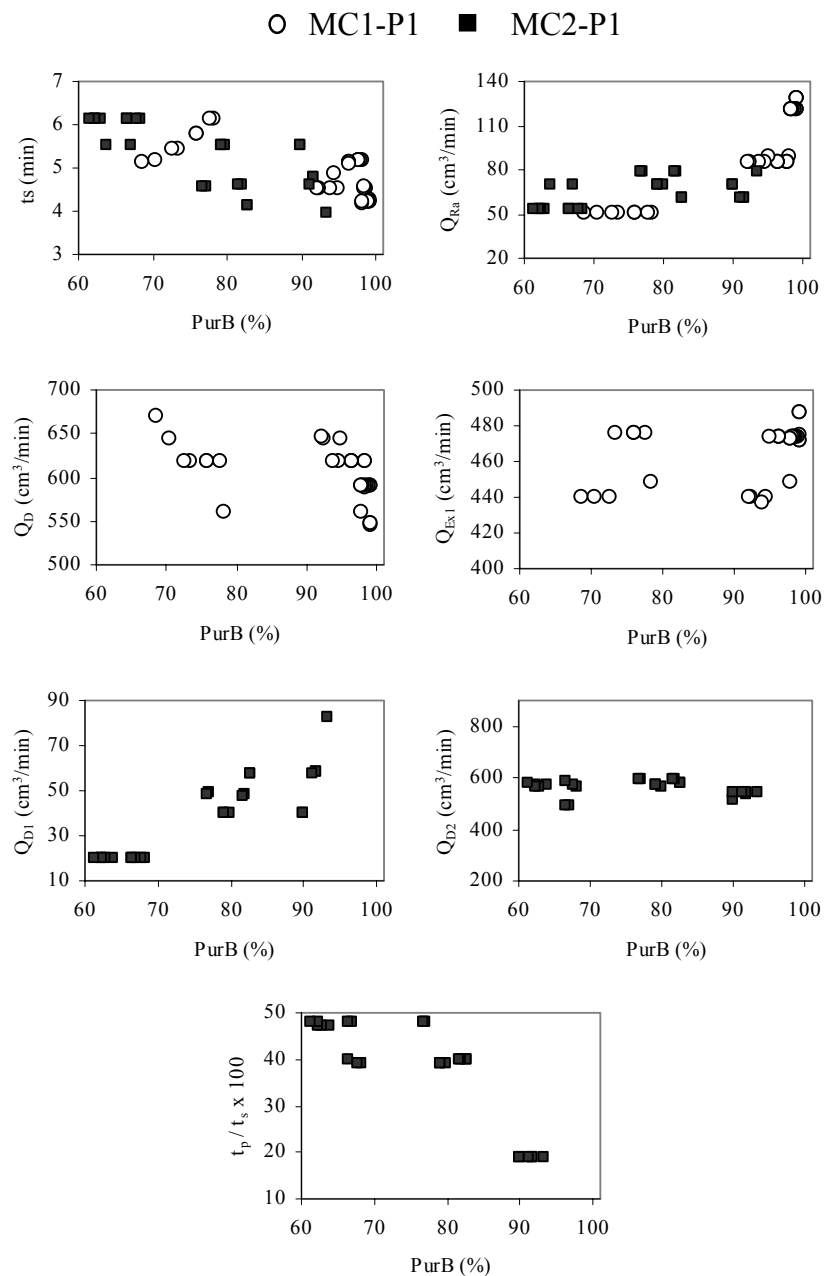
Figure 6.3 Decision variables corresponding to Pareto solutions in Figure 6.2

6.5.1.2 Problem MC2-P1: Effect of multiple columns in section P of MC2

Similar optimization run was performed to study the effect of multiple columns in section P for MC2. The mathematical formulation of the optimization problem is shown in Table 6.1 as MC2-P1. The Pareto optimal solutions for MC2-P1 together with solutions for MC2-P1b (when one column is present in each section) are also shown in Figure 6.2 while the corresponding decision variable plots given in Figure 6.3. The results reveal that the performance of MC2 with multiple columns is not as good as that obtained with MC1. It was seen that the performance decreases with the addition of columns in section P for MC2. This effect, as explained earlier, is due to the improper collection of strongly adsorbed component C. The results clearly show that for the separation processes which need more number of columns in section P due to the presence of non-idealities (such as non-linearity in adsorption isotherm, low mass transfer rates, etc.), the configuration shown in MC2 as such cannot be used for efficient operation. The decrease in performance will be more pronounced as the number of columns increase. Hence, it is necessary to further modify configuration MC2 to configurations like MC2A or MC2B described in Figure 6.1.

It should be noted that the Pareto curves obtained for the above two problems and the remaining problems in this chapter as well as the later chapters (as will be seen later) are not as smooth as those obtained in the chapters 3 and 4. This is because instead of the actual objective function (PurA + PurC), the values of PurA and PurC individually are plotted against PurB, which is more meaningful. One can also observe the presence of gaps between the points on the curve which can be overcome by running the same problem with various optimization (NSGA-II with JG) parameters such as random seed. Nevertheless, the results obtained clearly indicate the trend followed by the performance of these configurations and in this study

optimization is used as a mere tool for comparing the performances of the different configurations.

6.5.1.3 Problem MC2A-P1 and MC2B-P1: Effect of multiple columns in section P of MC2A and MC2B

The two modifications suggested and described for MC2 (MC2A and MC2B) when multiple columns have to be used are studied next. The mathematical formulation is described in Table 6.1 as MC2A-P1 and MC2B-P1. All the decision variables are the same as in the problem MC2-P1 except that p_1, the number of columns in sub-section P_1, is also added as a decision variable and p_2 (the number of columns in sub-section P_2) is chosen such that $p_1 + p_2 = 3$. In case of MC2A-P1, an additional decision variable Q_{Ex1} is used. The optimization results are shown in Figure 6.4. The figure shows that although there is no further improvement in purity of component A (PurA), the performance is much better when purity of strongly adsorbed component C (PurC) is considered for both MC2A and MC2B compared to MC2. Improvement in PurC is substantial for both MC2A and MC2B. For example, for PurB of about 93.3%, PurC is equal to circa 76.0% for MC2 while it is equal to circa 99.9% for MC2A. It is also observed that MC2B is slightly better than MC2A in terms of slight increase in PurB that can be achieved. Thus, the new modifications suggested in this study do further improve the performance of MC2 when more than one column is present. Note that for all these three problems, total number of columns used was six.
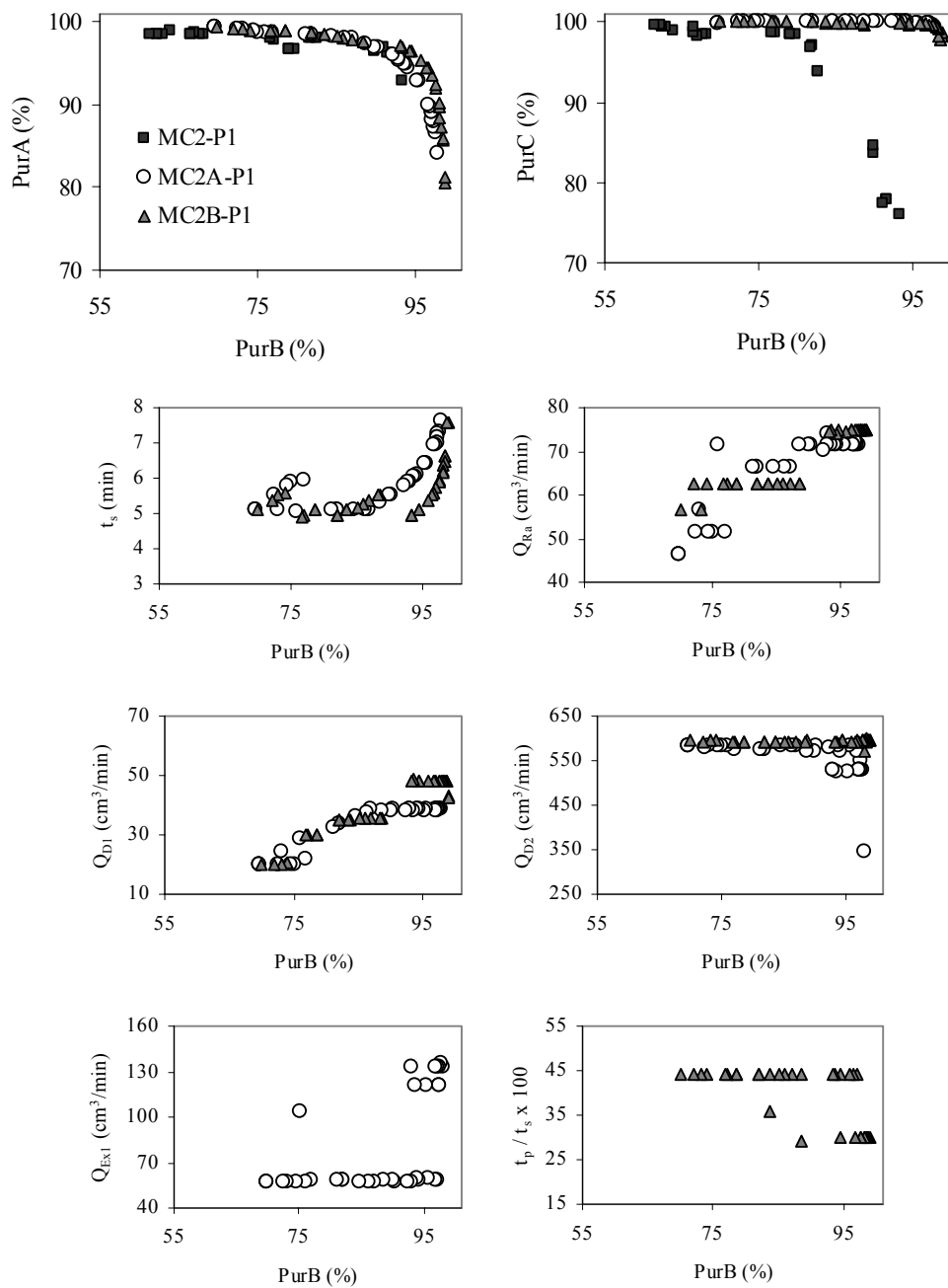
Figure 6.4 Pareto optimal solutions and the corresponding decision variables for the problems MC2-P1, MC2A-P1 and MC2B-P1

6.5.2 Problem 2: Separation of C$_8$ aromatic mixtures

After studying the performance of these modified configurations on a hypothetical separation problem it is important to see their performance when applied to a real industrial scale separation problem such as the separation of the C$_8$ aromatics. In this case the feed is considered to be a typical C$_8$ aromatic mixture containing 23.6% *p*-xylene, 49.7% *m*-xylene, 12.7% *o*-xylene, and 14% ethyl benzene. Completely potassium-exchanged Y-zeolite is considered to be the adsorbent while *p*-diethyl benzene (*p*DEB) solvent as the desorbent. Toluene can also be used as a desorbent for this separation process but *p*DEB is preferred as it is less volatile than the C$_8$ aromatics (Ruthven and Ching, 1989). This is very useful since in the ancillary product separation the desorbent is recovered as the bottom product and since the desorbent is generally in excess, this reduces the heat load on the distillation column. This leads to a more economical process operation. The details of the other operating conditions and design parameters are summarized in Table 6.2. The equilibrium data for *o*-, *m*-, and *p*-xylene, ethyl benzene and *p*DEB at 453 K were taken from Azevedo et al. (1998).

As mentioned earlier, the motive of this study is simultaneous recovery of both *p*-xylene and ethyl benzene from the mixture of C$_8$ aromatics, with best achievable purity. The feed flow rate in the optimization study was fixed at 0.3 m^3/min. This feed flow rate was decided after systematic sensitivity analysis study. The system was designed by fixing the parameters such as L$_{col}$, t$_s$, number of columns in each section and the flow rates in section P and S. For MC1, many simulations were performed by changing the three middle zone flow rates (Q$_{Q1}$, Q$_{Q2}$, and Q$_R$) one at a time to obtain the operating regime. Similar exercises were done for MC2A and

MC2B. Based on these sensitivity studies, it was decided to fix the feed flow rate at 0.3 m^3/min in order to have a fair comparison between the systems.

Table 6.2 Operating and model parameters for the separation of C$_8$ aromatics.

SMB unit geometry	Model Parameters
L$_{col}$ = 1.135 m	Pe = 2000
d$_{col}$ = 4.117 m	k$_a$ = 2 min^{-1}
V$_c$ = 15.1 m^3	d$_p$ = 9.2 x 10^{-4} m
Operating conditions	ε = 0.39
T = 453 K, liquid phase	ρ = 1.39 x 10^3 kg/m^3
t$_s$ = 1.16 min	q$_{m, pX (mX; oX; EB)}$ = 0.1303 kg/kg
	B$_{pX}$ = 1.0658 m^3 /kg (see Eqn. 5.9)
	B$_{mX}$ = 0.2299 m^3 /kg
	B$_{oX}$ = 0.1884 m^3 /kg
	B$_{EB}$ = 0.3037 m^3 /kg
	q$_{m, pDEB}$ = 0.1077 kg/kg
	B$_{pDEB}$ = 1.2935 m^3/kg

As in Problem 1, similar two-objective function optimization problems were formulated. Details of the mathematical formulation are shown in Table 6.3. The adsorption selectivity of these isomers is in the order of *p*-xylene (strongly adsorbed) > ethyl benzene > *m*-xylene > *o*-xylene (least strongly adsorbed). Following the earlier convention for the hypothetical ternary separation example, one can identify (*m*-xylene + *o*-xylene) as component A (component with least affinity for adsorption), ethyl benzene as component B (component with intermediate affinity) and *p*-xylene as component C (most strongly adsorbed component). The purity and recovery of the stream collecting *m*-xylene plus *o*-xylene were named as Pur_moX and Rec_moX respectively. Similarly the purities and recoveries for ethyl benzene and *p*-xylene were named as Pur_EB, Rec_EB and Pur_pX, Rec_pX respectively. Based on similar

sensitivity studies as in Problem 1, it was observed that both Pur_moX and Pur_pX are conflicting with respect to Pur_EB. When high Pur_moX and high Pur_pX can be achieved, Pur_EB is low. Moreover, it is easier to obtain high Pur_moX and high Pur_pX, but it is difficult to obtain very high Pur_EB. Hence, the optimization problem was formulated similar to the one discussed earlier in Problem 1, viz., maximizing the total purity of streams containing *m*-xylene plus *o*-xylene (Pur_moX) and *p*-xylene (Pur_pX) as one objective function while simultaneously maximizing Pur_EB as the other objective function. However, it was observed that due to the difficulty in separation between *m*-xylene and ethyl benzene, the stream collecting ethyl benzene was contaminated with *m*-xylene. It is important that ethyl benzene stream be devoid of *m*-xylene and *o*-xylene. However, contamination of this stream with *p*-xylene may be acceptable since in that case one can still separate *p*-xylene from ethyl benzene by passing it through another SMB binary separation unit. Hence, two constraints were incorporated in the optimization formulation as $C_{moX, \, Ex2} \leq 1\%$ and Pur_moX ≥ 60 %. The second constraint is added with the intention that more of ethyl benzene should be pushed towards the extract stream thus increasing its recovery. The mathematical formulations of the different optimization problems explained above are summarized in Table 6.3. The various results obtained are discussed below. Note that configuration MC2 was not considered for this problem for obvious reasons as explained before with Problem 1. Instead application of modified configurations, MC2A and MC2B, are considered and discussed below.

6.5.2.1 Problem MC1-P2: Ternary separation of C$_8$ aromatics in MC1

Figure 6.5 shows Pareto optimal solution and corresponding decision variable plots for the separation of C$_8$ aromatics in configuration MC1. The figure shows that the

Table 6.3 Description of the multi-objective optimization problems for the ternary separation of C$_8$ aromatics

Problem No.	Objective Function	Decision Variables	Constraints	Fixed Parameters
MC1-P2	Max (Pur_moX + Pur_pX)	$1 \leq t_s \leq 2$ min $0.8 \leq Q_{Ra} \leq 3$ m^3/min $2.8 \leq Q_D \leq 5$ m^3/min $0.1 \leq Q_{Ex1} \leq 3$ m^3/min	Pur_moX ≥ 60 %	$d_{col} = 4.117$ m, $L_{col} = 1.135$ m $N_{col} = 27$, $p/q_1/q_2/r/s = 6/6/6/6/3$ $Q_F = 0.3$ m^3/min $Q_S = 5.39$ m^3/min
MC2A-P2	Max (Pur_EB)	Same as MC1-P2 & $5.5 \leq Q_{D1} \leq 7$ m^3/min $2.8 \leq Q_{D2} \leq 6$ m^3/min $0.5 \leq Q_{Ex1} \leq 6$ m^3/min	$C_{moX, Ex2}$ $\leq 1\%$	Same as MC1-P2 except $p_1/p_2/q/r/s = 6/6/6/6/3$ & Q_S is not fixed
MC2B-P2		Same as MC2A-P2 & $0.19 \leq t_p/t_s \leq 0.82$		Same as MC2A-P2

performance of the system is not very good compared to the results obtained with Problem 1. This is expected since in this case, the separation is difficult, as the adsorption selectivity is quite low, in addition to the non-linearity in the adsorption isotherm.

The maximum Pur_EB achievable is 85.2% when Pur_moX and Pur_pX are 94.7% and 90.3% respectively. The maximum Pur_moX and Pur_pX achievable are 98.11% and 99.4% respectively but then Pur_EB drops to 55.4%. One can also observe that along the Pareto curve, as Pur_EB increases, Q_D decreases. Similar observation was made in the earlier chapter. The optimum values for the decision variables, t_s, Q_{Ra} and Q_{Ex1} were found to be almost constant along the Pareto. The respective values are $t_s \sim 1.0$ min, $Q_{Ra} \sim 1.8$ m^3/min and $Q_{Ex1} \sim 2.2$ m^3/min. The respective recoveries of *m*-xylene and *o*-xylene, ethyl benzene and *p*-xylene for three representative points (shown in Figure 6.5) along the Pareto line are given in Table

6.4. Recovery of *p*-xylene at the extract stream Ex1 as well as total *p*-xylene recovery calculated by adding the amount of *p*-xylene recovered at both the extract streams (Ex1 and Ex2) is reported in Table 6.4. The tabulated data shows that although the recovery values of *p*-xylene may not look very attractive at Ex1, but the total *p*-xylene recovery is almost 100%. The extract stream (Ex2), which contains both ethyl benzene and *p*-xylene can be further separated into pure streams of ethyl benzene and *p*-xylene in another (four-zone) SMB binary unit. This is inevitable since it is impossible to achieve 100% purity of ethyl benzene at the extract port Ex2, and consequently this stream will always be contaminated with *p*-xylene. One should also recollect that the feed concentration of the C$_8$ aromatics is more biased towards not-so-desirable m-xylene (49.7%) while amount of *p*-xylene (23.6%) and ethyl benzene (14%) are present in much lower concentration. This obviously has an adverse effect on the overall separation process making the recovery of ethyl benzene and *p*-xylene more difficult. Figure 6.6 shows the internal concentration profiles of *p*-xylene, *m*-xylene, *o*-xylene and ethyl benzene for one of the points on the Pareto (Point 5A shown in Figure 6.5) where Pur_moX~ 94.8%, Pur_EB ~ 85.2% and Pur_pX ~ 90.3%. It can be seen that the collection stream for ethyl benzene, the extract port Ex2 is always contaminated with at least small amount of *p*-xylene. Considering these facts, the five-zone SMB configuration when coupled with another SMB in series can be a very attractive option for the simultaneous recovery of *p*-xylene and ethyl benzene from the mixture of C$_8$ aromatics.
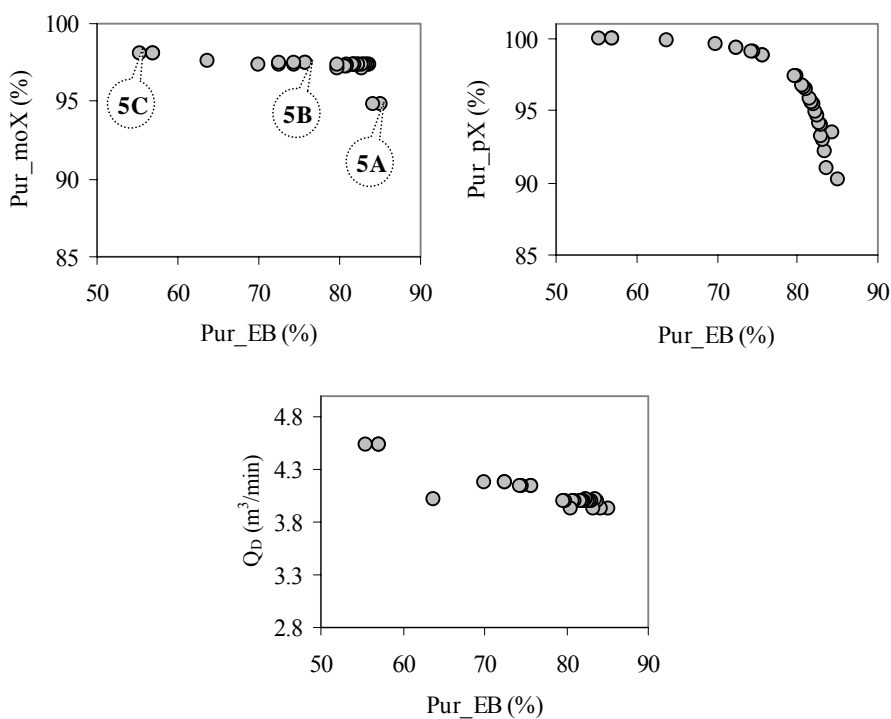
Figure 6.5 Pareto optimal solutions and the corresponding decision variables for the ternary separation of C$_8$ aromatics (Problem MC1-P2)

Table 6.4 Recovery and purity values for few selected points from the Pareto for MC1-P2

Point	Pur_EB	Pur_moX	Pur_pX	Rec_EB	Rec_moX	Rec_pX	Rec_pX$_T$[*]
5A	85.2	94.8	90.3	57.3	100	93.5	99.3
5B	75.7	97.4	98.8	85.9	100	83.5	99.4
5C	55.4	98.1	99.9	90.4	100	57.5	99.6

* Calculated by considering *p*-xylene from both extract streams, Ex1 and Ex2
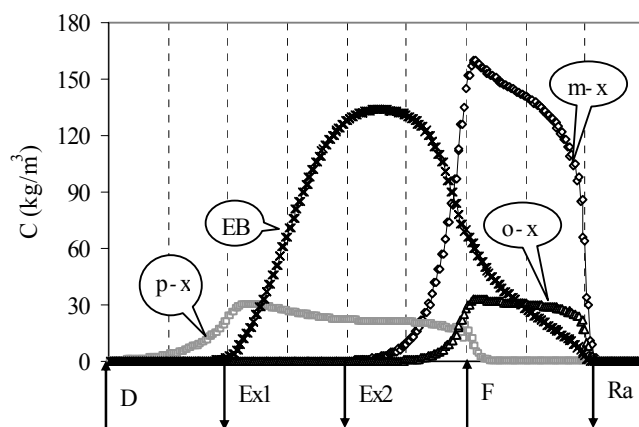
Figure 6.6 Concentration profiles of the four components of C$_8$ aromatics mixture in MC1 corresponding to the optimal point 5A shown in Figure 6.5

6.5.2.2 Problem MC2A-P2 and MC2B-P2: Ternary separation of C$_8$ aromatics in MC2A and MC2B

Similar two-objective optimization problems were formulated for the separation of C$_8$ aromatics in the proposed modified configurations MC2A and MC2B. The detailed mathematical formulations described as MC2A-P2 and MC2B-P2 are given in Table 6.3. The Pareto optimal solutions and the corresponding decision variables are shown in Figure 6.7. One can see that the performance achieved in this case is quite poor. It is seen that high Pur_EB cannot be achieved with this system, even though high values of Pur_moX and Pur_pX can be obtained. For example, the maximum Pur_EB achievable is only 39.4% with Pur_pX dropping to as low as 67.3% although Pur_moX remains more or less constant around 98% all along the Pareto. The highest Pur_pX achievable is 99.8 % (when Pur_moX ~ 98.3 %) but Pur_EB then reduces to as low as 36.9%. Once again, it can be observed that MC2B performs slightly better than MC2A when Pur_EB is considered. For both MC2A and

177
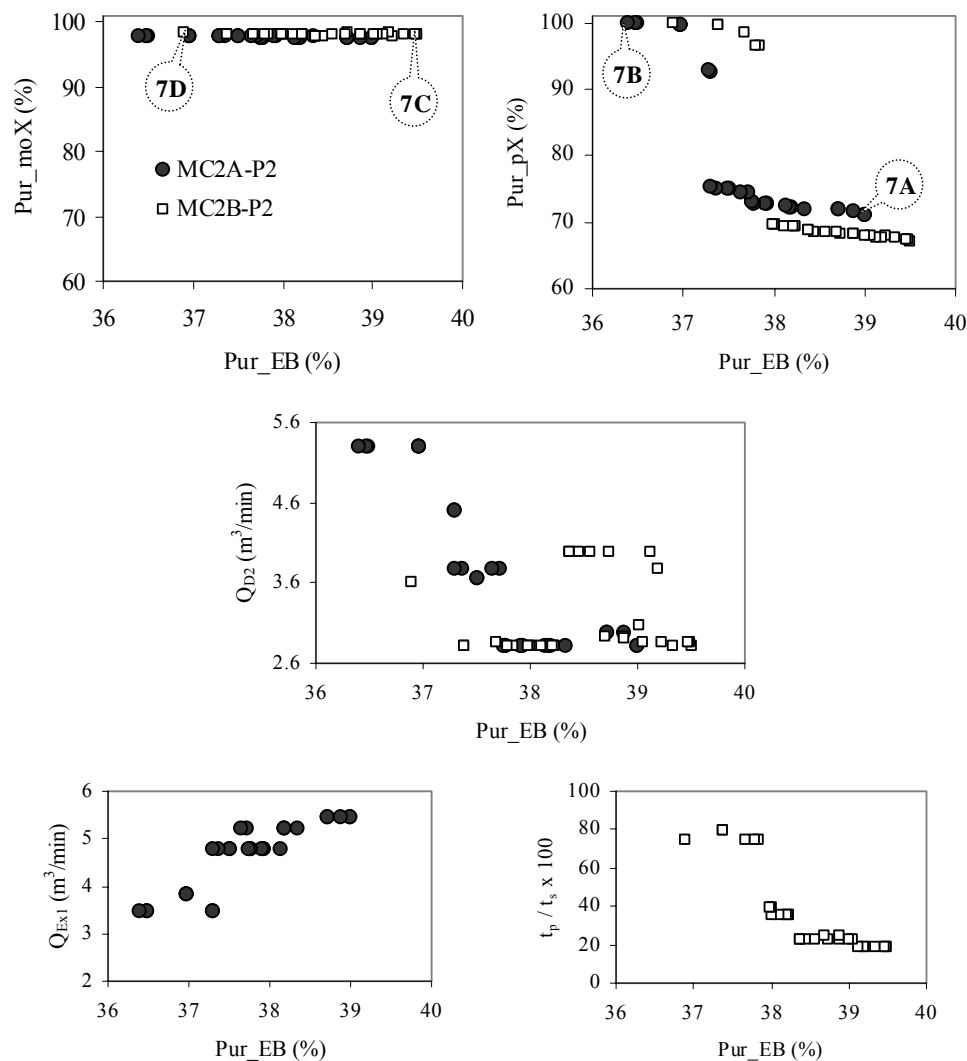
Figure 6.7 Pareto optimal solutions and the corresponding decision variables for the ternary separation of C₈ aromatics in MC2A and MC2B
(Problems MC2A-P2 and MC2B-P2)

MC2B, the optimum values for decision variables t_s, Q_{Ra} and Q_{D1} were found to be almost constant. The values for MC2A are t_s = 1.1 min, Q_{Ra} = 1.74 m³/min, Q_{D1} = 6.4 m³/min. The respective optimal values for MC2B are 1.1 min, 1.2 m³/min and 6.3 m³/min. The recoveries of *m*-xylene plus *o*-xylene, ethyl benzene and *p*-xylene for two extreme points on the Pareto for both MC2A and MC2B are given in Table 6.5. One can see that for lower values of purity of ethyl benzene, Rec_pX decreases very

drastically if one considers the *p*-xylene collection stream (Ex1) alone. However, recovery of *p*-xylene collectively in both extract streams (Rec_pX$_T$) is quite high (~99 %). Figure 6.8 shows the internal concentration profiles of the four components of C$_8$ aromatics for one of the optimal points for MC2A configuration on the Pareto (point 7A in Figure 6.7) where Pur_moX~ 97.4%, Pur_EB ~ 39.0% and Pur_pX ~ 71.1%. From the concentration profile one can see that the dilution of the components is very high for these systems when compared to Figure 6.6. From the optimal solutions, it is quite clear that modified five-zone SMB configuration, MC1, is a much better option for the separation of C$_8$ aromatics compared to MC2 and its modified version, MC2A and MC2B. MC1 results in much higher purities of ethyl benzene along with high values for Pur_moX and Pur_pX compared to MC2. This result is also in agreement with the observations made for Problem 1 discussed in the earlier chapter where it was found that as the separation becomes more difficult MC1 performs better than MC2 while at the same time consumes less amount of desorbent.

Table 6.5 Recovery and purity values for few selected points from the Pareto for MC2A-P2 and MC2B-P2

Config.	Point	Pur_EB	Pur_moX	Pur_pX	Rec_EB	Rec_moX	Rec_pX	Rec_pX$_T$
MC2A	7A	39.0	97.4	71.1	60.8	100	42.8	98.6
	7B	36.4	97.9	99.9	89.6	100	7.4	99.2
MC2B	7C	39.5	98.2	67.2	40.6	100	62.4	98.6
	7D	36.9	98.3	99.8	90.0	100	8.6	98.6
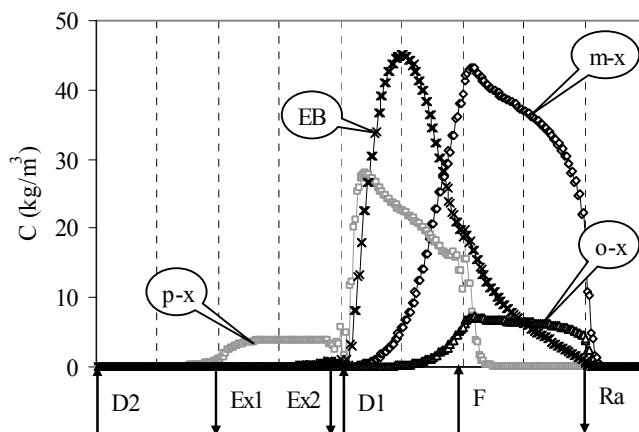
Figure 6.8 Concentration profiles of the four components of C₈ aromatics mixture in MC2A corresponding to the optimal point 7A shown in Figure 6.7

6.5.3 Effect of addition of a reflux stream containing pure ethyl benzene

Nicoud (1998) have explained the importance of introducing a reflux stream rich in one of the components to the conventional four-zone SMB for binary separation. For systems which involve competitive adsorption isotherms, low concentration of one of the components compared with the other, causes lowering of the adsorption selectivity. In such cases, it is difficult to obtain high purities and high recoveries. For example, we consider a binary system with components A and B (A is the weakly adsorbed component and is present in large amount in the feed mixture) that have to be separated in a conventional four-zone SMB system comprising of sections P, Q, R and S. If an additional section is created between section P and Q by introducing a reflux stream that is rich in component B, a drastic adjustment in the concentration profile takes place. The concentration of B increases at the extract withdrawal point and as a result component A is more diluted with regard to component B. Generally component B elutes component A better than the desorbent

does. Thus separation between A and B can be improved by adding this reflux stream facilitating the collection of B with high purity.

From the results obtained for modified configurations, MC2A and MC2B, it was observed that high purity and recovery of component B is very difficult to be obtained for non-ideal systems such as the mixture of C$_8$ aromatics. The feed composition for the C$_8$ aromatics is such that the component A (m-xylene + o-xylene) dominates the feed mixture. It will therefore be worthwhile to see the effect of addition of a reflux stream containing pure ethyl benzene. The configurations MC1, MC2A and MC2B were accordingly further modified to form new configurations, MC3, MC4A and MC4B respectively. The modified configurations MC3 and MC4A are shown in Figure 6.9 (a) and (b) respectively. The configuration MC4B is not shown, for brevity sake, as it is easy to visualize configuration MC4B based on MC4A (similar to the difference in configuration of MC2B from MC2A). Table 6.6 summarizes new optimization problems formulated similar to the optimization exercise performed earlier.

6.5.3.1 Problem MC3-P2: Ternary separation of C$_8$ aromatics in MC3

This problem (MC3-P2) was solved to see the effect of adding a reflux stream to the five-zone SMB system. Results obtained from the optimization study are shown in Figure 6.10. Three Pareto points (corresponding to minimum, middle and maximum Pur_EB values) obtained in problem MC1-P1 are also shown in Figure 6.10. One can see that by adding a reflux stream (as shown in Figure 6.9(a)), Pur_EB and Pur_pX can be improved. Rec_moX was seen to be almost 100%. The plots for Rec_EB and Rec_pX are also shown in Figure 6.10.

(a)

(b)
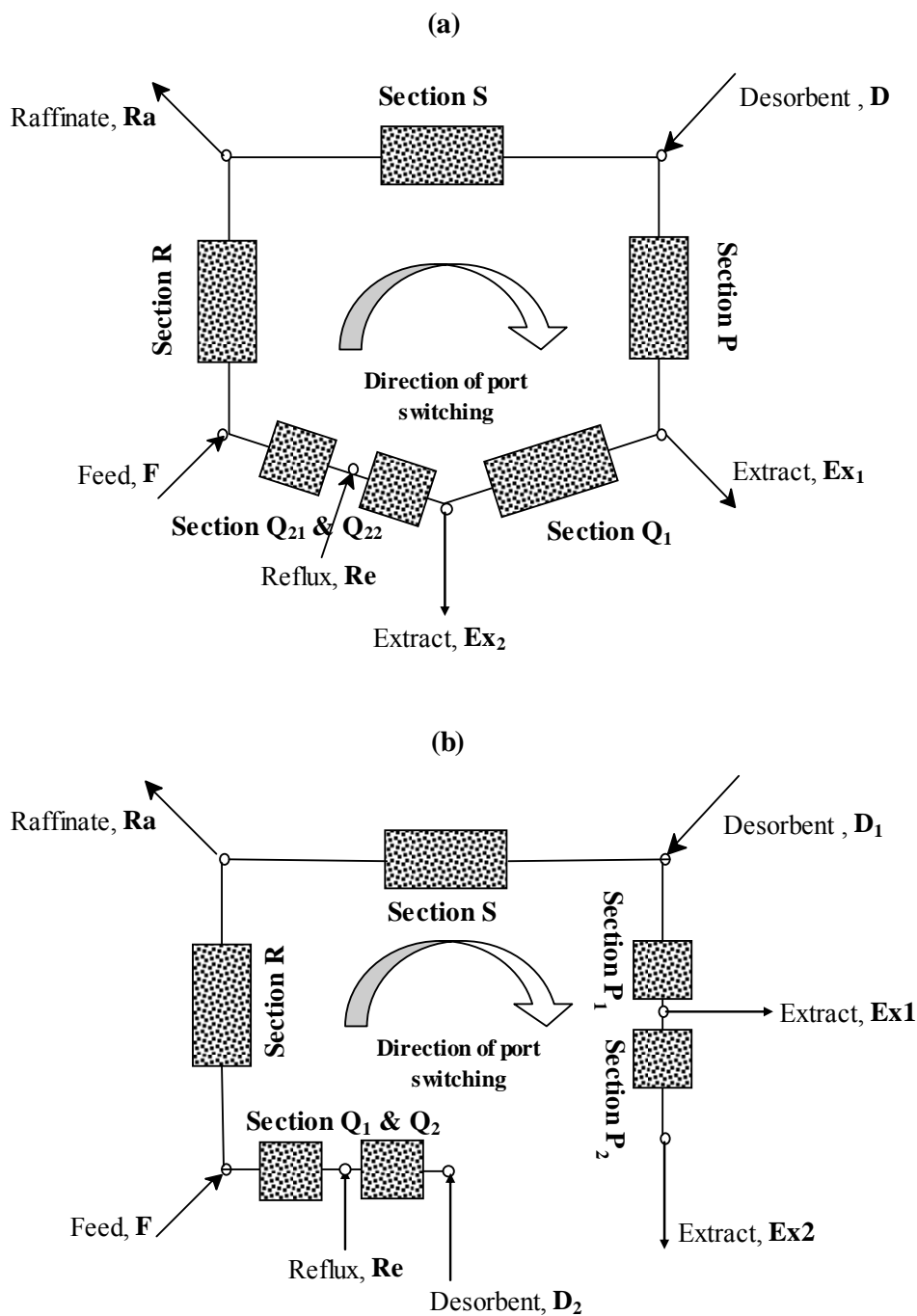
Figure 6.9 Schematic diagram of modified SMB configurations when a reflux stream is added, (a) Modified configuration 3 (MC3) and (b) Modified configuration 4 (MC4A)

Table 6.6 Description of the multi-objective optimization problems for the ternary separation of C$_8$ aromatics on modified configurations with reflux streams

Problem No.	Objective Function	Decision Variables	Constraints	Fixed Parameters
MC3-P2	Max (Pur_moX + Pur_pX)	$1 \leq t_s \leq 2$ min $0.8 \leq Q_{Ra} \leq 3$ m^3/min $2.8 \leq Q_D \leq 5$ m^3/min $0.1 \leq Q_{Ex1} \leq 3$ m^3/min $0.01 \leq Q_{Re} \leq 0.1$ m^3/min $1 \leq q_{21} \leq 4$	Pur_moX ≥ 60 %	Same as MC1-P2
MC4A-P2	Max (Pur_EB)	Same as MC3-P2 & $5.5 \leq Q_{D1} \leq 7$ m^3/min $2.8 \leq Q_{D2} \leq 6$ m^3/min $0.5 \leq Q_{Ex1} \leq 6$ m^3/min $1 \leq q_2 \leq 4$	C$_{moX, Ex2}$ $\leq 1\%$	Same as MC1-P2
MC4B-P2		Same as MC4A-P2 & $0.19 \leq t_p/t_s \leq 0.82$		Same as MC1-P2

When compared with the results obtained from the problem MC1-P1, the figure shows that Rec_EB has improved drastically due to the introduction of additional reflux stream. However, Rec_pX drops significantly when compared to MC1-P1 as Pur_EB decreases. Nevertheless, one will always tend to operate the system such that one can get both Pur_pX and Pur_EB as high as possible at which Rec_pX value seems to be reasonably good.
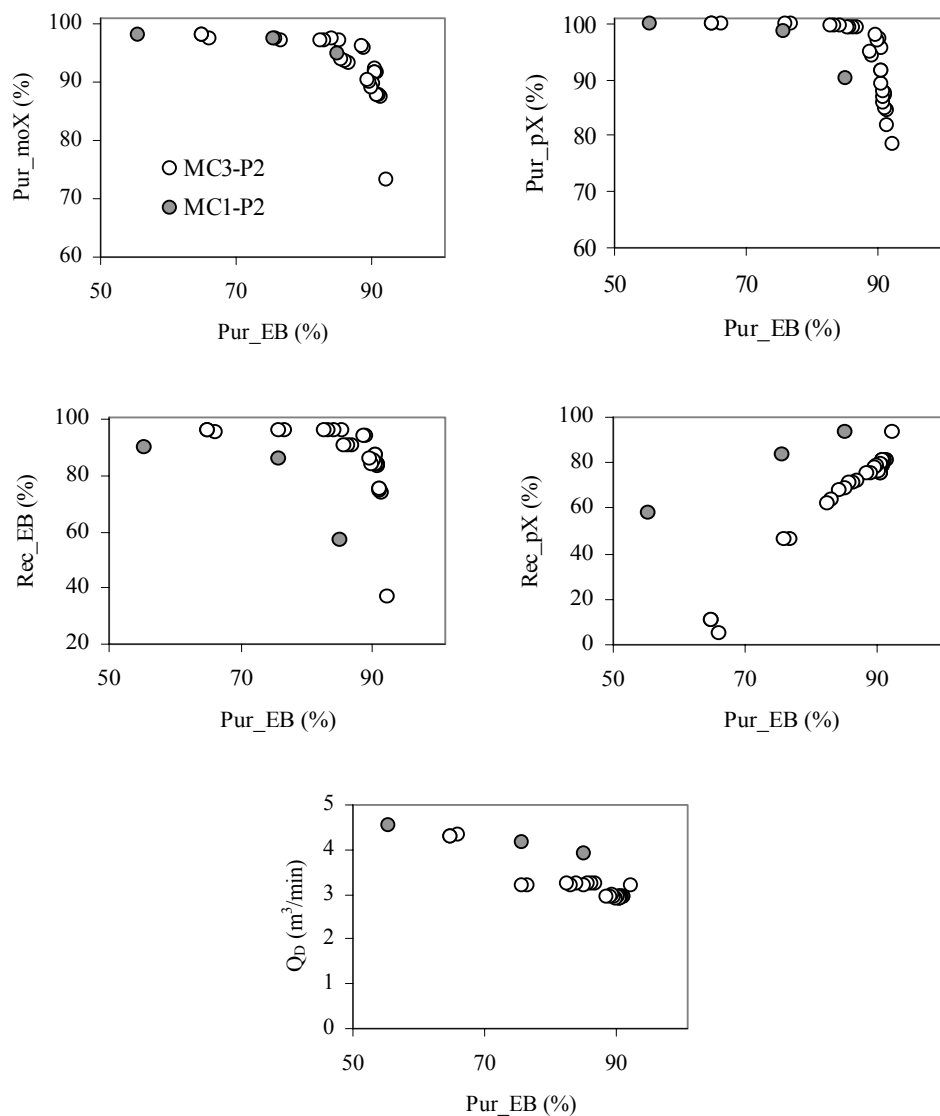
**Figure 6.10 Pareto optimal solutions and the corresponding decision variables
for the ternary separation of C$_8$ aromatics in configuration MC3** (Problem MC3-
P2) **when additional reflux stream is used**

The column configuration chosen was 6/6/4/2/6/3 for $p_1/p_2/q_1/q_2/r/s$, i.e., six columns
in section Q for MC1-P2 was divided between section Q_1 and Q_2 as 4 and 2 columns
respectively for MC3-P2. The reflux flow rate was found to be insensitive and the
values were chosen between 0.08 and 0.09 m^3/min. Optimum values for the decision

184

variables such as t$_s$ and Q$_{Ra}$ were found to be ~1.06 min and ~1.84 m^3/min respectively while the values of desorbent flow rate are shown in Figure 6.10.

6.5.3.2 Problem MC4A-P2 and MC4B-P2: Ternary separation of C$_8$ aromatics in MC4A and MC4B

Similar double-objective optimization problems were formulated for the separation of C$_8$ aromatics in the proposed modified configurations MC4A and MC4B to find out the effect of addition of the reflux stream. The detailed mathematical formulation described as MC4A-P2 and MC4B-P2 is given in Table 6.6. The Pareto optimal solutions and the corresponding decision variables are shown in Figure 6.11. The improvement in the system performance in terms of the product purity is more pronounced in this case than the previous optimization run. One can see that much higher Pur_EB can be obtained with the addition of reflux. The maximum Pur_EB is ~ 66% in MC4A and MC4B as compared to 40% in MC2A. Rec_moX is almost ~100% irrespective of whether additional reflux is used or not. The variation of Rec_EB and Rec_pX when reflux stream is used is also shown in Figure 6.11. As seen in the previous case, it is observed here too that although Rec_EB increases, Rec_pX decreases quite drastically. In the earlier case (MC3-P2), when Pur_EB was high the Rec_pX was seen to be comparable with the system without reflux stream (MC1-P2). However, in this case it is seen that even at high Pur_EB values, Rec_pX is much lower than the system without reflux stream (MC2A-P2). In such a situation, using this configuration may not be a good choice to recover both *p*-xylene and ethyl benzene simultaneously with the best possible purities.

The optimal values of the decision values such as t$_s$, Q$_{Ra}$ and Q$_{D1}$ were seen to be around 1.1 min, 1.41 m^3/min and 6.23 m^3/min respectively for MC4A-P2 and

around 1.08 min, 1.33 m³/min and 6.37 m³/min respectively for the problem MC4B-

P2. Q_{Ex1} for MC4A-P2 was seen to be 3.38 m³/min while t_p/t_s was found to be 0.62.

The optimal column configuration was seen to be 6/6/4/2/6/3 while the optimal reflux

flow rate was seen to be 0.09 m³/min.
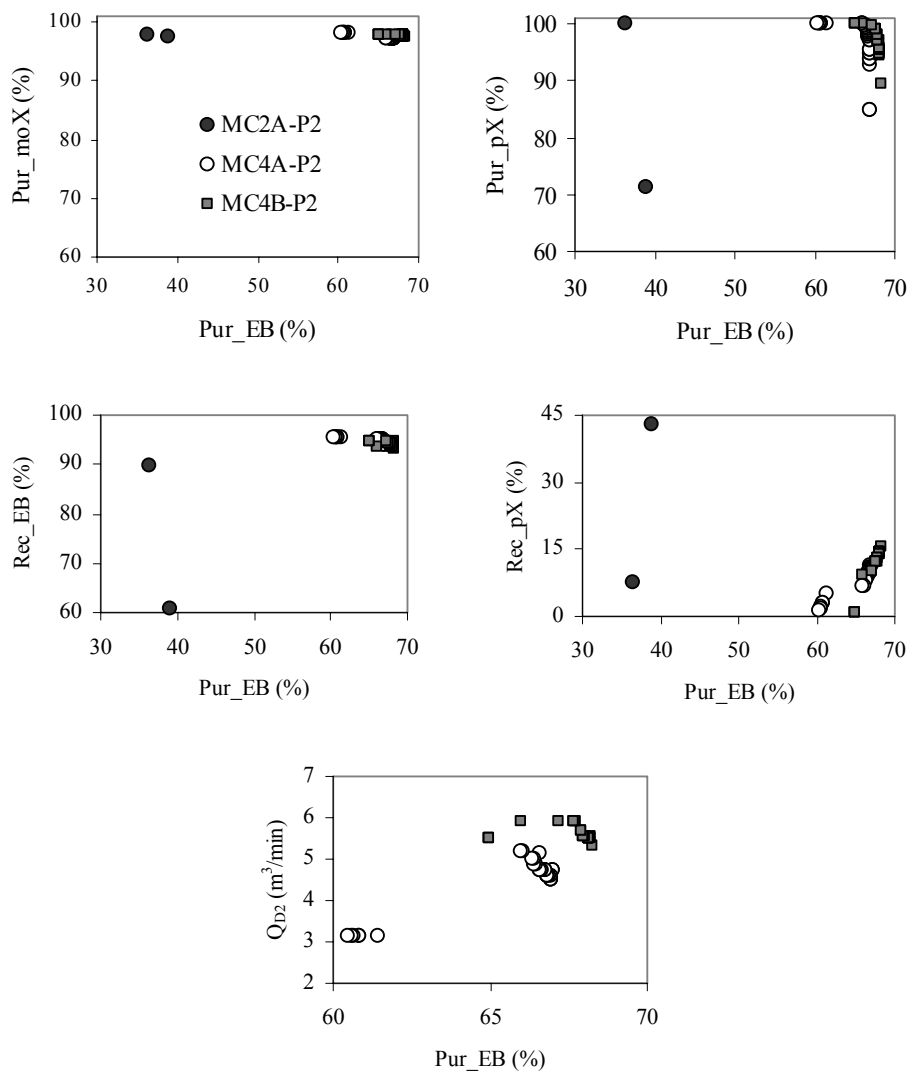
**Figure 6.11 Pareto optimal solutions and the corresponding decision variables
for the ternary separation of C_8 aromatics in configuration MC4A and MC4B**
(Problem MC4A-P2 and MC4B-P2) **when additional reflux stream is used**

6.6 Conclusions

In chapter 5, separation of ternary mixture using two different modified configurations of SMB system was studied and their performance were compared at optimal conditions for varying degrees of difficulty in separation (adsorption selectivity), mass-transfer resistance and non-linearity in adsorption isotherm. Performances of the systems were optimized using multiple-objectives and it was observed that in general MC1 performed better than MC2. However, studies were performed assuming only one column per section. In this chapter, we first extended our earlier study on modified SMB systems under non-ideal conditions to include more than one column per section for the hypothetical separation problem. It was found that when multiple columns are present in section P, configuration MC1 performs better than when only one column is present. However, performance for configuration MC2 deteriorates. Two new configurations (MC2A and MC2B) were proposed and its was found that both perform better, in terms of achieving better purity of the most strongly adsorbed component, for any particular value of purity of the intermediate component. Moreover, MC2B performs slightly better than MC2A. Subsequently, the modified systems were investigated for the separation of C_8 aromatics at optimal conditions to recover simultaneously *p*-xylene and ethyl benzene. It was found that modified five-zone SMB configuration, MC1, is a much better option for the separation of C_8 aromatics compared to MC2 and its modified version, MC2A and MC2B. MC1 results in much higher purities of ethyl benzene along with high values for Pur_moX and Pur_pX compared to MC2. It was observed that as the separation becomes more difficult MC1 performs better than MC2 while at the same time consumes less amount of desorbent.

An attempt was also made to enhance the performance of the modified systems by adding a reflux stream containing pure ethyl benzene. It was observed that though Pur_EB and Rec_EB can be improved, it results in a decrease in the recovery of *p*-xylene particularly for MC2. MC1 however seems to show high recovery of *p*-xylene when the Pur_EB is high. Thus it can be concluded that using a reflux stream containing pure ethyl benzene can improve the Pur_EB and Rec_EB with some loss of *p*-xylene into the stream collecting ethyl benzene.

Chapter 7   Pseudo-SMB system for ternary separation
- Ternary separation of C$_8$ aromatics

7.1 Introduction

In the earlier two chapters, we studied the comparison of two modified simulated moving bed systems (MC1 and MC2) to facilitate the simultaneous recovery of three components from the feed mixture. The comparisons were done in the presence of several non-idealities such as high mass-transfer resistance, low adsorption selectivity, non-linearity in adsorption isotherm etc. The performance of these configurations was also compared in the presence of more than one column in the SMB sections. These configurations were then applied to an industrial case study, ternary separation of the C$_8$ aromatics to recover both *p*-xylene and ethyl benzene from a single SMB unit with the best possible purities. It was observed that due to the difficult separation and due to the inherent limitation of the configurations, high purity of the ethyl benzene product stream is difficult to be achieved. This stream always seems to be contaminated with some amount of *p*-xylene. It was also concluded in the previous chapter that the configuration MC1 (as compared to MC2) seems to be an attractive option for such difficult separations when coupled with another SMB unit in series to further separate *p*-xylene and ethyl benzene.

Amongst the various concepts reported in the literature for ternary separation using SMB, a novel configuration which can be called as the Pseudo-SMB system seems to be quite interesting. As will be explained in the next section, in this system the feed is discontinuously added only during a part of the total cycle time during which it operates in the batch chromatographic mode. For the remaining cycle time the system is switched to the SMB mode of operation but with no feed. This system is

commercialized by the Japan Organo Company (Ando et al., 1990). Mata and Rodrigues (2001) have developed a pseudo SMB model to describe this system. This process can be called as the Pseudo-SMB system by the virtue of its operation mode which is semi batch chromatography and semi SMB.

In this study, we explore the efficacy of the Pseudo-SMB system for ternary separation in the presence of several non-idealities such as high mass-transfer resistance and non-linearity in the adsorption isotherm. Effect of variation in the feed composition is also studied. In each of these cases the system was optimized to satisfy multi-objective criteria using NSGA-II-JG as the optimization algorithm. It is needless to mention the importance of multi-objective optimization either at the operating stage or at the design stage for any type of SMB system. This special Pseudo-SMB system is further investigated for the ternary separation of C$_8$ aromatics. The primary aim of this work is to recover simultaneously high purities of ethyl benzene and *p*-xylene from the mixture of C$_8$ aromatic isomers.

7.2 Description of the Pseudo-SMB system

This system is invented by the Japan's Organo Company and is described as "JO chromatographic separation device". The system requires two additional features compared to the traditional simulated moving-bed system, a shut-off valve, which can cut the circulation flow and an extra outlet for collection of the intermediate component B. The operation of this system is in essence a cyclic process in which a cycle consists of the following two steps (see Figure 7.1):

(a) In the first step of the cycle (duration t = T$_{step1}$), the circulation flow is stopped (shut-off valve closed), feed mixture is fed in, and, in a similar way to the fixed-bed operation mode, the component having an intermediate affinity (which is component

B) to the adsorbent is withdrawn. During this process only the feed (F) and desorbent (D₁) streams enter the process while there is only one outlet called the intermediate stream (I).

(b) In the second step (duration t = T_{step2}), there is no feed flow (the shut-off valve is opened) and there is only one inlet flow that of the desorbent (D₂). In this step, the system operates in the same way as it does in the conventional simulated moving-bed mode, i.e., the desorbent feeding and the product withdrawal ports are periodically switched with switching time, t_{s2}, and component A (least strongly adsorbed) and component C (most strongly adsorbed) are continuously collected at the raffinate (Ra) and the extract port (Ex) respectively.

During the second step, when there is no feed inlet, the migration rate at each of the desorbent feeding and the component withdrawal points becomes approximately equal to the migration rate of intermediate component B. As a result, components A and C move towards the front and rear of the intermediate affinity component B, and gradually a zone with only component B is formed. When the desorbent and the product outlet ports have been moved periodically around until they are back to the same positions as in step 1, the circular flow is once again cut (shut-off valve closed), the feed mixture is fed, and component B is withdrawn. Through the repetition of this operation, components A and C can be simultaneously collected during step 2 while component B can be collected during step 1 thus enabling the continuous separation of a ternary mixture. In this study, all the internal flow rates (Q_P, Q_Q, Q_R, Q_S) for step 1 are represented with a suffix "1", while that for step 2 are represented with a suffix "2". The above operation can thus be described as "Pseudo-SMB" or "Quasi-SMB" process. This technique is being applied in the separation of

complex multi-component mixtures, e.g. sucrose, glucose and betains (Masuda et al.,

1993) and in the production of raffinose from beet molasses (Sayama et al., 1992).
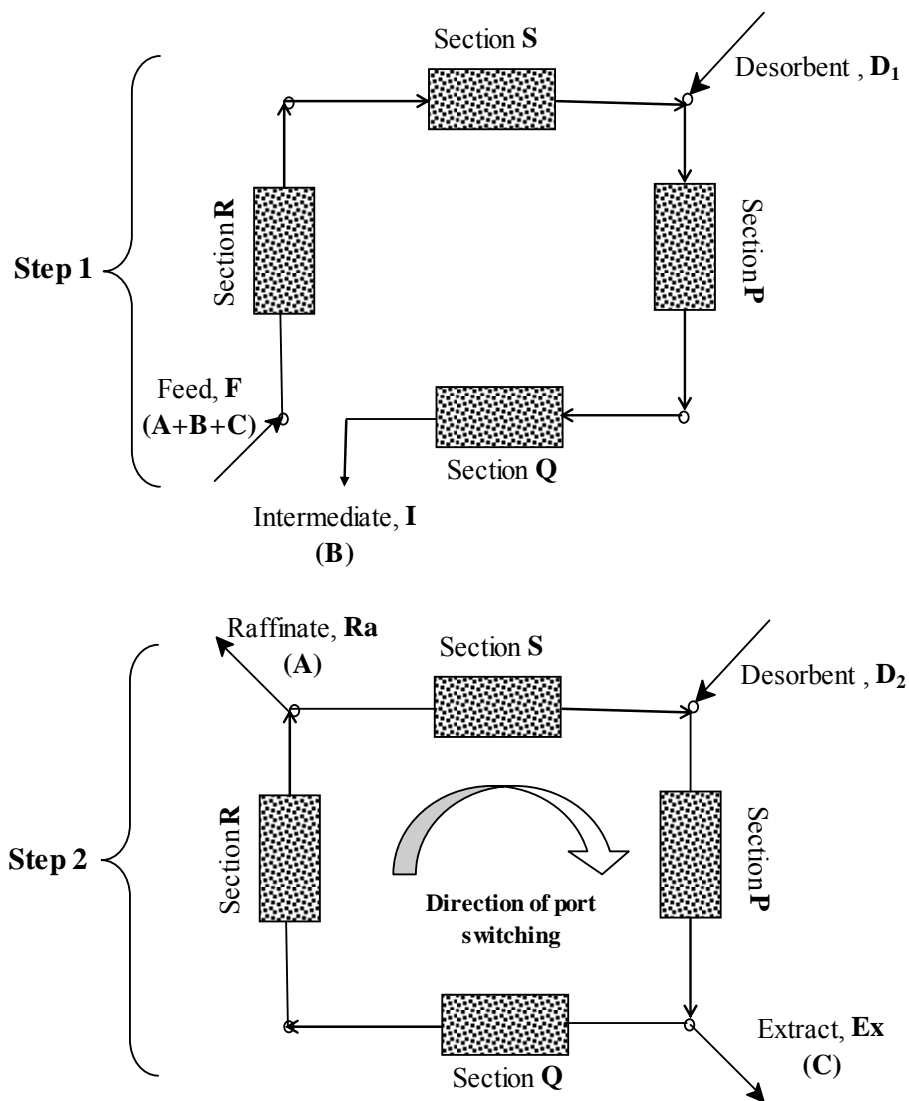
Figure 7.1 Schematic diagram showing the operation of the Pseudo-SMB system

7.3 Mathematical model

In the conventional four-zone SMB, the two incoming streams (the feed, F, and the desorbent, D) and the two outgoing streams (the raffinate, Ra, and the extract, Ex) divide the system into four sections (zones), namely P, Q, R and S, each of which comprises of p, q, r and s columns respectively. The columns are each of uniform cross-section and length packed with adsorbent and connected in a circular array. The flow rates in the section P, Q, R and S are designated as Q_P, Q_Q, Q_R and Q_S respectively while those of the feed, raffinate, desorbent and extract are designated as Q_F, Q_{Ra}, Q_D and Q_{Ex} respectively. The Pseudo-SMB system can also be considered as consisting of four sections. In step 1, section R and section S have fluid flow rates equivalent to the feed flow rate, Q_F. Section P and section Q have flow rates equal to the sum of the feed and the desorbent flow rate, Q_{D1}. In step 2, section Q and section R have the same flow rate since no feed is introduced during this step. Step 1 of Pseudo-SMB can be modeled as a series of chromatographic columns arranged in four sections with two inputs (Q_F and Q_{D1}) and one output (Q_I) as shown in Figure 7.1. Step 2 can be modeled as the conventional four-zone SMB but with only one input (Q_{D2}) and two outputs (Q_{Ra} and Q_{Ex}). It should be noted that the desorbent flow rates in step 1 and step 2 are designated as Q_{D1} and Q_{D2} respectively and these should not be confused with the Q_{D1} and Q_{D2} mentioned in the sixth chapter for the configuration MC2.

The mathematical model used in this study is given below. The modeling approach assumes constant selectivity axial dispersion for the fluid flow and linear driving force for the intra-particle mass-transfer. The governing differential mass balance equations along with the initial and boundary conditions are given below:

Differential mass balances, global and in solid phase for species *i* in column *k*:

$$\frac{\partial C_{i,k}}{\partial \theta} + \upsilon \frac{\partial q_{i,k}}{\partial \theta} = \frac{\psi_k}{Pe_k} \frac{\partial^2 C_{i,k}}{\partial \chi^2} - \psi_k \frac{\partial C_{i,k}}{\partial \chi} \tag{7.1}$$

$$\frac{\partial q_{i,k}}{\partial \theta} = \alpha \left(q_{i,k}^* - q_{i,k} \right) \tag{7.2}$$

$$q_{i,k}^* = K_i C_{i,k}, \text{ where, } \chi = z/L_{col} \text{ and } \theta = t/T_{step} \tag{7.3}$$

Initial conditions:

$$C_{i,k}(\chi, 0) = C_{i,k}^0(\chi) \tag{7.4}$$

$$q_{i,k}(\chi, 0) = q_{i,k}^0(\chi) \tag{7.5}$$

Boundary conditions:

$$C_{i,\chi}^{in} = C_{i,k}(0, \theta) - \frac{1}{Pe_k} \frac{\partial C_{i,k}}{\partial \chi} \tag{7.6}$$

$$\frac{\partial C_{i,k}}{\partial \chi}(1, \theta) = 0 \tag{7.7}$$

Dimensionless parameters:

$$\psi_k = U_{F_k} T_{step} / L_{col} \tag{7.8}$$

$$\alpha = k_a T_{step} \tag{7.9}$$

$$Pe_k = U_{F_k} L_{col} / D_{ax_k} \tag{7.10}$$

Node balances:

$$C_{i,k}^{in} = C_{i,k-1}(1, \theta) \tag{7.11}$$

except, if the column follows feed or desorbent port, In that case,

$$C_{i,k}^{in} = \left[Q_F C_{i,F} + Q_Q C_{i,k-1}(1, \theta) \right] / Q_R \text{ and } C_{i,k}^{in} = Q_S C_{i,k-1}(1, \theta) / Q_P \tag{7.12}$$

The governing partial differential equations were discretized in space using orthogonal collocation method on finite elements (OCFE) to convert them into a system of coupled ODE-IVPs. Each column was discretized into 20 finite elements

and each element had two internal collocation points. The transient model equations were numerically solved, starting from an initial condition where the columns are filled only with the desorbent until the cyclic steady state (CSS) is reached. Each cycle comprises of step 1 and step 2 operations as described earlier with respect to Figure 7.1. In step 2, since the system operates in the conventional SMB mode, there exists a switching pattern amongst the columns. The average concentration of components in extract and raffinate streams were calculated by integrating concentration over the total time of step 2 (T$_{step2}$), unlike the conventional SMB where the integration is done only during one switching period. In all the results explained later, it was seen that CSS is reached in circa 20 cycles. In order to ensure the validity of the mathematical model, simulation results were compared with that reported by Mata and Rodrigues (2001). The system and operating parameters are summarized in Table 7.1 while several performance parameters used are defined in Table 7.2. The simulations results are compared in Table 7.3, which shows that the predictions in this study are quite comparable with those reported. Figure 7.2 shows the evolution of concentration profiles of components A, B and C at the end of step 1 and step 2 after 1, 2 and 20 (when CSS is reached) cycles.

The influence of mass-transfer coefficient k$_a$ was studied to examine the sensitiveness of the model. Table 7.4 shows the effect of mass-transfer coefficient on the purities of A, B and C after 20 cycles. It can be seen that as the mass-transfer coefficient decreases, thus making the separation more difficult, the purities, as expected, decrease. The effect is not so significant till k$_a$ = 6 min^{-1}, after which the decrease is quite drastic when it is reduced further. It can also be seen that PurB and PurC are more affected, decreasing to as low as 95.7% and 95.5% respectively, as compared to PurA which is equal to 98.8% even when k$_a$ = 3 min^{-1}. This is probably

due to the fact that in this case the adsorption selectivity ratio between A and B (Φ_{BA} = K_B/K_A) is much greater than between B and C (Φ_{CB} = K_C/K_B). As a result, separation between B and C is more difficult than between A and B. Degree of difficulty in separation and increased mass-transfer resistance, causes reduced purities of both streams collected as B and C.

Table 7.1 Details of model and operating parameters used in this study
(Mata and Rodrigues, 2001)

SMB unit geometry	Model Parameters	Operating conditions		
			Step 1	Step 2
L_{col} = 120 cm	Pe = 2000			
d_{col} = 10.84 cm	k_a = 30 min^{-1}	T_{step} (min)	18.17	68.0
V_c = 11.1 × 10^3 cm^3	ε = 0.4	t_s (min)	-	5.67
N_{col} = 12	K_A = 0.19 cm^3/mg	Q_F (cm^3/min)	350.0	-
Ω = 3/3/3/3	K_B = 0.39 cm^3/mg	Q_{Ra} (cm^3/min)	-	177.4
	K_C = 0.65 cm^3/mg	Q_D (cm^3/min)	422.9	451.4
	$C_{A, feed}$ = 100 mg/cm^3	Q_{Ex} (cm^3/min)	-	274.0
	$C_{B, feed}$ = 100 mg/cm^3	Q_S (cm^3/min)	350.0	900.1
	$C_{C, feed}$ = 100 mg/cm^3			

Table 7.2 Definition of the performance parameters used in this study

Component	Purity	Recovery
A	$PurA = \dfrac{C_{Ra}^{A}}{C_{Ra}^{A} + C_{Ra}^{B} + C_{Ra}^{C}} \times 100$	$RecA = \dfrac{C_{Ra}^{A} Q_{Ra} T_{step2}}{C_{F}^{A} Q_{F} T_{step1}} \times 100$
B	$PurB = \dfrac{C_{I}^{B}}{C_{I}^{A} + C_{I}^{B} + C_{I}^{C}} \times 100$	$RecB = \dfrac{C_{I}^{B} Q_{I}}{C_{F}^{B} Q_{F}} \times 100$
C	$PurC = \dfrac{C_{Ex}^{C}}{C_{Ex}^{A} + C_{Ex}^{B} + C_{Ex}^{C}} \times 100$	$RecC = \dfrac{C_{Ex}^{C} Q_{Ex} T_{step2}}{C_{F}^{C} Q_{F} T_{step1}} \times 100$

**Table 7.3 Comparison of the simulation results with the
literature reported values** (Mata and Rodrigues, 2001)

Performance criteria	This work			Reported		
	A	B	C	A	B	C
Purity (%)	99.99	99.96	100.00	100.00	99.98	99.94
Recovery (%)	100.00	99.99	99.92	96.70	99.90	100.00
Average concentration (g/l)	57.72	45.28	37.18	52.10	45.30	36.70

Table 7.4 Sensitivity study with different mass-transfer rates

k_a (min^{-1})	PurA (%)	PurB (%)	PurC (%)
30	99.99	99.96	100.00
6	99.52	99.03	98.89
5	99.37	98.52	98.29
3	98.79	95.71	95.49

7.4 Optimization Problem Formulation

Similar to the earlier chapters, the performance of this novel separation system is studied by optimizing it using rigorous multi-objective optimization. In this work, a few two-objective optimization studies have been performed.

Simulation studies on this Pseudo-SMB system have revealed that with this system it is easier to achieve high purities and recoveries of the least strongly adsorbed component, A, and hence our aim in this study was to simultaneously maximize purities of components B and C. Initially, multi-objective optimization study was performed for the existing set-up (operation stage optimization) and this
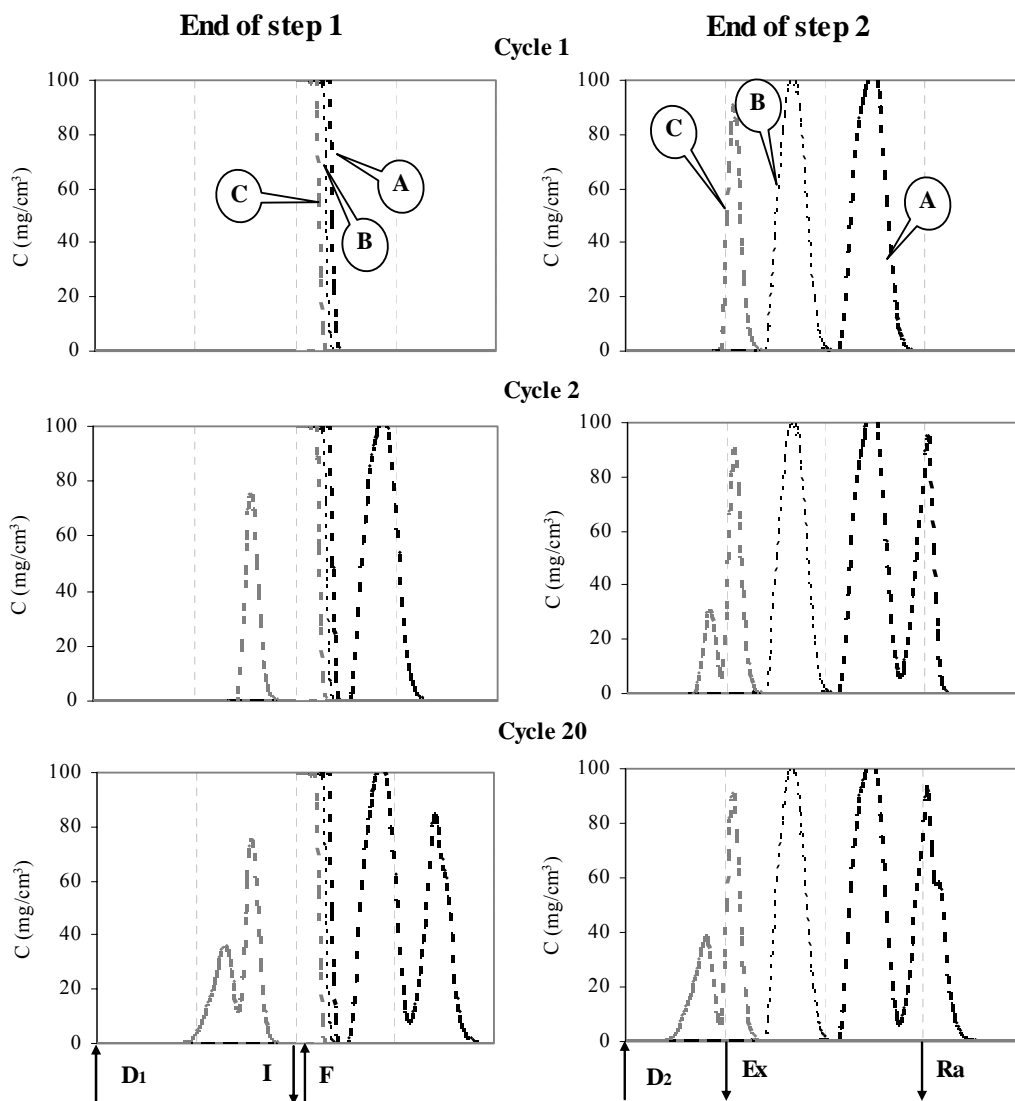
Figure 7.2 Concentration profiles for components A, B and C at the end of step 1 and step 2 after cycle 1, 2 and 20 (cyclic steady-state)

was followed by the design-stage optimization. The results obtained justify the importance of such optimization exercises. Next, the effect of non-linearity of adsorption isotherm on the performance of the system was studied. Two different problems with varying degrees of non-linearity in the adsorption isotherm were studied. Using one of these problems as the base case, the effect of feed composition was also studied. Subsequently, a problem in which the desorbent consumption was minimized while maximizing simultaneously the purities of all the three components was studied. Finally, similar optimization studies on the separation of C$_8$ aromatics were performed.

7.5 Results and discussion

The different problems as explained above were mathematically formulated and solved. The Pareto results and the values of the decision variables chosen for the different problems are explained below. It should be noted that for the sake of brevity all the plots of performance parameters and the decision variables are not shown in this study. Only a few important ones are shown.

7.5.1 Problem 1: Performance enhancement of the existing set-up

This problem aims at enhancing the performance of the existing Pseudo-SMB system. The mathematical formulation is described in Table 7.5 as Problem 1. Purities of components B (PurB) and C (PurC) are maximized subject to a constraint of achieving purity of component A (PurA) at least greater than 99%. Four decision variables, viz., desorbent flow rates in step 1 and 2, switching time in step 2 and raffinate flow rate, are used keeping all other parameters constant as shown in Table 7.5. Linear adsorption isotherm was used in this case, the values of which are shown

in Table 7.6. Effect of non-linearity in the adsorption isotherm is studied later to determine the sensitivity in the shift of the Pareto. Figure 7.3 shows the resulting Pareto for this two-objective optimization problem. It is seen that as PurB increases, PurC decreases. This figure also shows the simulated values of PurB and PurC when the system was operated at the original operating parameters listed in Table 7.1. All points on the Pareto, when the system is optimized, are well above the original simulated point (based on the reported operating parameters of Table 7.1), thus justifying the importance of optimization in such cases. Figure 7.3 also shows the values of RecC corresponding to the Pareto points for PurB. It can be seen that RecC shows almost a linear relationship with PurB, increasing as PurB increases (while PurC decreases). As discussed earlier, since the adsorption selectivity between B and C is much less than that of between A and B, the port collecting the intermediate component B (stream I in Figure 7.1) gets contaminated with component C uncollected during step 2. As a result when the system focuses on operating with higher PurB, then most of C has to be collected during step 2 and thus causing the increase in RecC. It was observed that PurA is always above 99% due to the constraint used in the formulation, and recovery of A (RecA) was almost equal to 100%. Moreover, RecB was always greater than 99%. The optimal switching time during the step 2, t_{s2}, was observed to be nearly constant taking a value of 5.6 min. Q_{D1} was found to be equal to 500 cm^3/min initially while afterwards decreases to 400 cm^3/min as PurB increases. Figure 7.3 also shows the variation of Q_{Ra} and Q_{D2} as PurB increases. It is seen that Q_{Ra} decreases as PurB increases. Due to mass balance, Q_{Ex} is inversely related to Q_{Ra}. Lower Q_{Ex} causes less collection of component C during step 2 and thus contaminates the intermediate stream during step 1 thereby

decreasing PurB. Similarly, it is quite obvious that Q_{D2} increases while PurB increases

since Q_{Ex} is directly proportional to Q_{D2}.

Table 7.5 Description of the multi-objective optimization problems solved

Prob. No.	Remarks	Objective Function	Decision Variables	Constraints	Fixed Parameters
1	Existing set-up linear isotherm		$400 \leq Q_{D1} \leq 600$ cm^3/min $3 \leq t_{s2} \leq 7$ min $100 \leq Q_{Ra} \leq 250$ cm^3/min $400 \leq Q_{D2} \leq 600$ cm^3/min	PurA ≥ 99 %	$d_{col} = 10.84$ cm, $L_{col} = 120$ cm $N_{col} = 12$, $\Omega = 3/3/3/3$, $k_a = 5$ min^{-1} $Q_F = 350$ cm^3/min, $Q_{S2} = 900$ cm^3/min, $T_{step1} = 18.17$ min
2a	Design-stage Linear isotherm	Max PurB Max PurC	Same as Problem 1 except $300 \leq Q_{D1} \leq 600$ cm^3/min $100 \leq L_{col} \leq 150$ cm		Same as Problem 1 except L_{col} is a decision variable Isotherm parameters (see Table 7.6)
2b, 2c	Design-stage Non-linear isotherm		Same as Problem 2a except $100 \leq L_{col} \leq 200$ cm	PurA ≥ 90 %	Same as Problem 2a Isotherm parameters (see Table 7.6)
3a, 3b	Design-stage Effect of feed composition		Same as Problem 2a		Same as Problem 2b Feed compositions (see Table 7.6)
4	Purity maximization Desorbent minimization	Max (PurA+ PurB+ PurC) Min $Q_{D, to}$	Same as Problem 2a	PurA ≥ 99 %	Same as Problem 2a

Table 7.6 Model parameters used in this study for different problems described in Table 7.5

Problem No.	C_F (mg/cm^3)			Adsorption parameters		
	$C_{F, A}$	$C_{F, B}$	$C_{F, C}$	K_A (cm^3/mg)	K_B (cm^3/mg)	K_C (cm^3/mg)
1, 2a and 4	100	100	100	0.19	0.39	0.65
Non-linear isotherm (see Eqn. 7.13)				q_m (mg/cm^3)	$10^3 B_A$ (cm^3/mg)	$10^3 B_B$ (cm^3/mg)	$10^3 B_C$ (cm^3/mg)
2b	100	100	100	100	1.9	3.9	6.5
2c	100	100	100	50	3.8	7.8	13.0
3a	150	75	75	50	3.8	7.8	13.0
3b	200	50	50	50	3.8	7.8	13.0
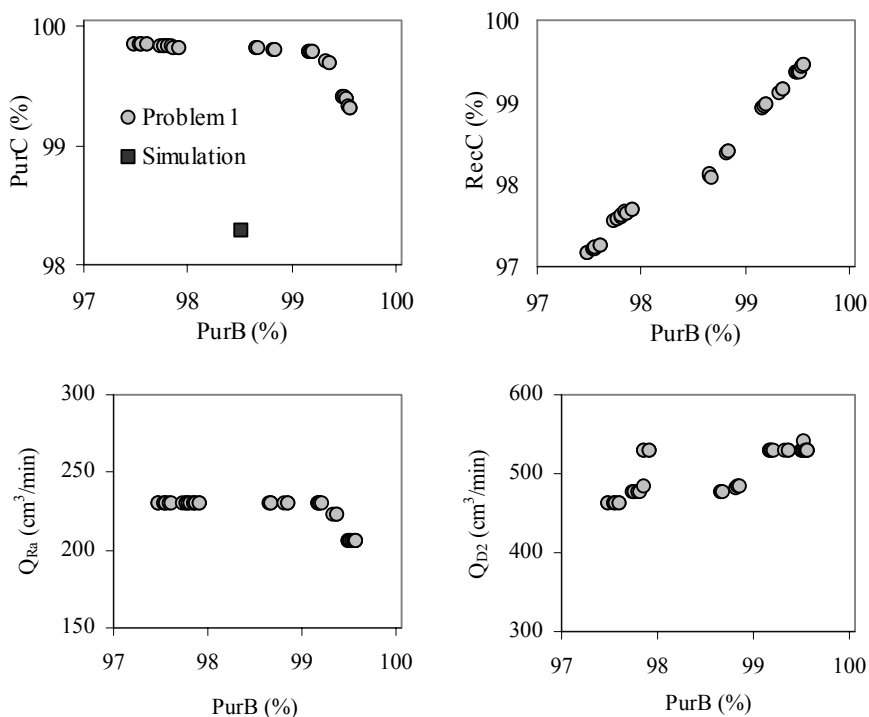
Figure 7.3 Pareto optimal solutions and corresponding decision variables for Problem 1 (existing set-up with linear adsorption isotherm)

7.5.2 Problem 2: Optimization at the design-stage

In Problem 1, the length of the column was fixed at 120 cm. In this case, L$_{col}$ was allowed to vary in order to see whether further performance improvement is possible.

7.5.2.1 Problem 2a: Determination of the optimal column length

The mathematical formulation is shown in Table 7.5 (Problem 2a). The same linear adsorption isotherm parameters as in the case of problem 1 are used. Figure 7.4 shows the comparison in the performance between the two cases. It can be seen that Pareto shifts upwards as both PurB and PurC are improved when L$_{col}$ was allowed to
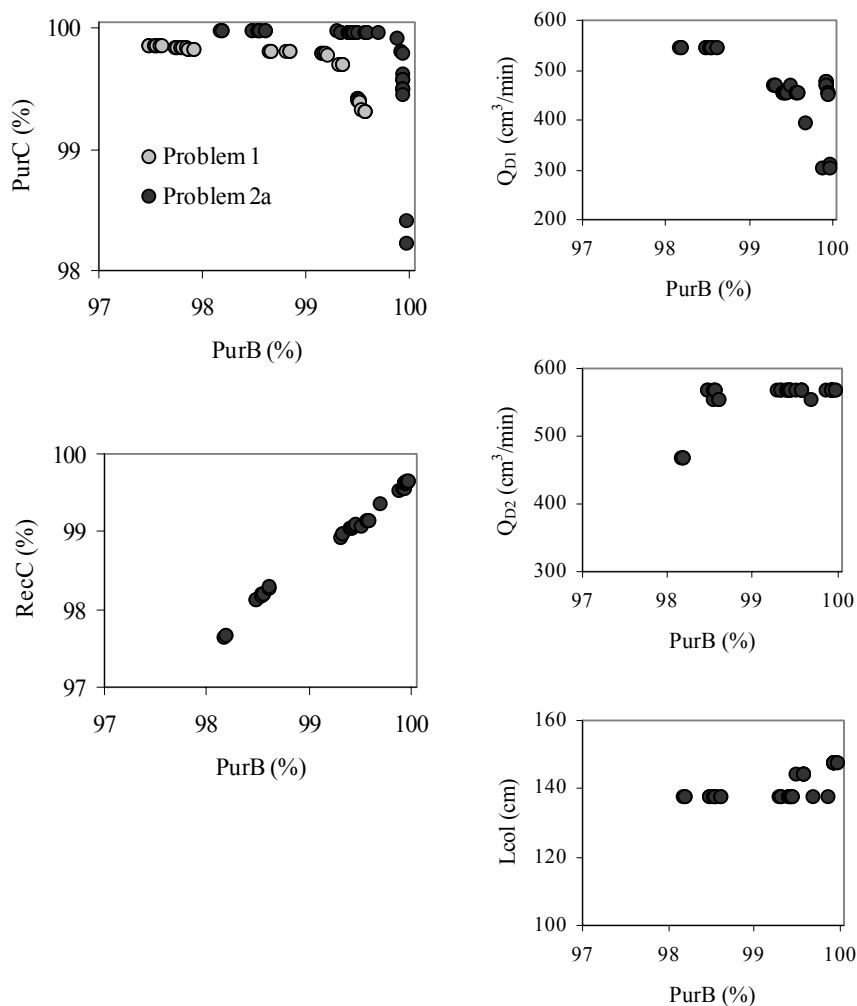
Figure 7.4 Comparison of Pareto optimal solution between design-stage
(Problem 2a) **and existing-stage** (Problem 1)

be selected optimally. For example, when L_{col} is 137.3 cm, both PurB and PurC are as high as 99.9%. Once again RecC was found to increase linearly as PurB increases (while PurC decreases). As in the earlier problem, in this case also PurA was found to be greater than 99% and RecA was equal to 100%. RecB obtained was around 98%. The optimal switching time in the second step, t_{s2}, was seen to take values 6.5 min for lower values of PurB while it is 6.9 min as PurB increases. The optimal value for Q_{Ra}

was equal to 250 cm³/min. Figure 7.4 shows that Q_{D1} decreases as PurB increases. It was observed in Figure 7.2 that during step 1, the peak for component C follows peak of component B in the direction of flow. When Q_{D1} is very high, the flow rate in section Q is high and as a result along with component B some amount of component C also gets collected thus contaminating stream I. As a result, when PurB increases, the values chosen for Q_{D1} are lower. As explained for Problem 1, Q_{D2} increases as PurB increases.

7.5.2.2 Problem 2b and 2c: Effect of non-linearity in the adsorption isotherm

Two additional problems (Problems 2b and 2c) were solved to determine the effect of non-linearity in the adsorption isotherm on the performance of the system. In problems 1 and 2a, adsorption isotherm considered was linear. In this case, a multi-component competitive Langmuir isotherm was used, which is described as below:

$$q^{*}_{i,k} = \frac{q_m B_i C_{i,k}}{1 + \sum_{l=1}^{NC} B_l C_{l,k}} \tag{7.13}$$

The model parameters for Problems 2b and 2c were changed increasing the degree of non-linearity in the adsorption isotherm. Table 7.6 shows the adsorption parameter values used in this case while the mathematical formulation is shown in Table 7.5. The constraint on PurA was relaxed to 90% in this case in order to get feasible optimal solutions. Figure 7.5 compares the Pareto optimal solutions. Note that the adsorption isotherm in case of problem 2a is linear while for problems 2b and 2c the model parameters are in the increasing order of non-linearity. The figure shows that the Pareto shifts downwards (both PurB and PurC decrease) quite drastically as the adsorption isotherm becomes more and more non-linear. For example, for Problem 2b the maximum value of PurB obtained is 99.3% at the cost of PurC which
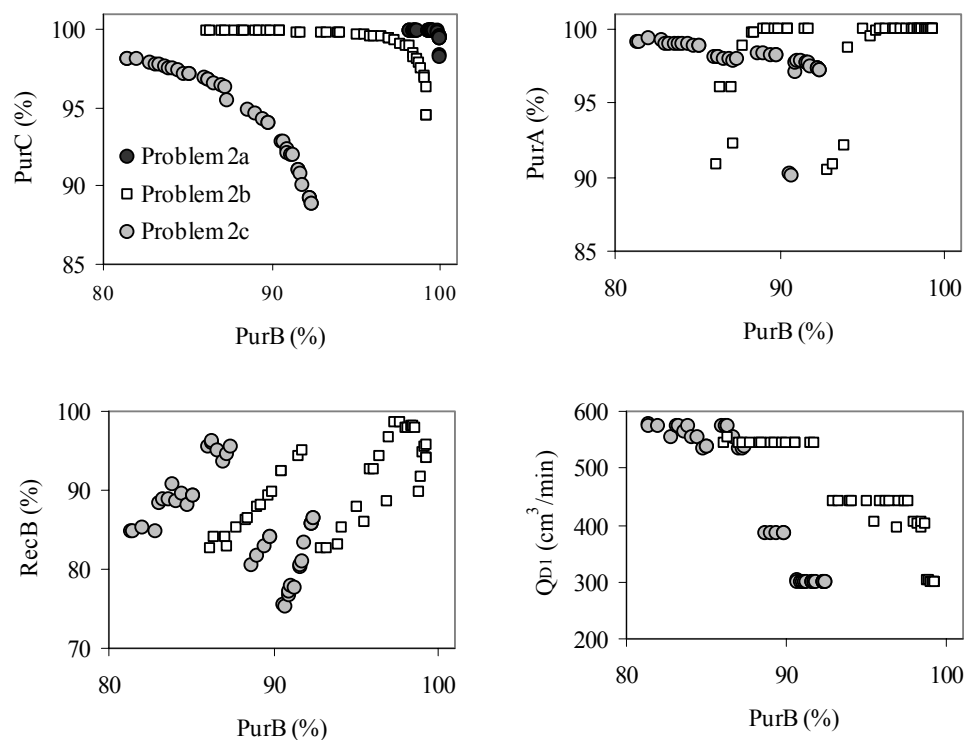
Figure 7.5 Effect of non-linearity in adsorption isotherm on the Pareto optimal solution for design-stage optimization (Problems 2a-2c)

is as low as 94.5%. For Problem 2c, the maximum PurB achievable is only 92.4 with

PurC equal to 88.9%. Figure 7.5 also shows the variation of PurA and RecB as PurB

increases. Recovery of A seemed not affected by the non-linearity of the isotherm as

it is observed that RecA is nearly 100% for all the problems. RecC also increased

linearly as PurB increases, however the values dropped with increasing non-linearity.

For example, it was found that for Problem 2b, when PurB was 86.1 and 99.3 %

(minimum and maximum PurB in the Pareto), RecC achieved was 86.7 and 99.1%

respectively, while for Problem 2c, when PurB was 81.5 and 92.4%, RecC was as low

as 80.3 and 91.1% respectively. The optimal switching time value, t_{s2}, chosen for both

problems was constant at about 6.9 min. Q_{Ra} was observed to decrease slightly from

120 to 101 cm^3/min for Problem 2b and for Problem 2c it was nearly constant at 180.0 cm^3/min. For Problem 2b, the optimal Q_{D2} was equal to 473 cm^3/min for low values of PurB and 575 cm^3/min as PurB increases, while for Problem 2c it is constant at 581 cm^3/min. The optimal L_{col} increases slightly for Problem 2b (between 147 and 149.5 cm) along the Pareto while for Problem 2c, optimal L_{col} is nearly constant at 170 cm. Q_{D1} decreases as PurB increases, as explained earlier.

7.5.3 Problem 3: Effect of feed composition

The effect of feed composition on the system performance was studied next to determine its effect on the shift in Pareto. Two problems (Problem 3a and 3b) were formulated as described in Table 7.5 with model parameters given in Table 7.6. As shown in Table 7.6, two sets of feed concentrations were considered such that component A dominates components B and C. Though, there are other sets possible where concentration of either B or C can be higher in the feed, in this study we considered only the above case, since as shown later, this system will be applied for the separation of C$_8$ aromatic mixture. In a typical C$_8$ aromatic cut, it is seen that component A (m-xylene + o-xylene) is present in higher concentration than either component B (ethyl benzene) or component C (*p*-xylene). The mathematical formulation of the problem is shown in Table 7.5. Note that the adsorption isotherm used for these two problems are same as that used for Problem 2c.

The Pareto optimal solution showing the plot of PurC and PurB is shown in Figure 7.6. The plot of RecB vs PurB is also shown in this figure. It was seen that RecB for Problem 3a was higher than that for Problem 3b. When PurB is 89.8%, RecB is 80.3% for Problem 3a, while for Problem 3b it is as low as 73%. It was observed that RecA for both the problems was 100%. PurA for Problem 3a was

greater than 95% while for Problem 3b it shows an increasing trend from 90 to 96% as PurB increases along the Pareto.
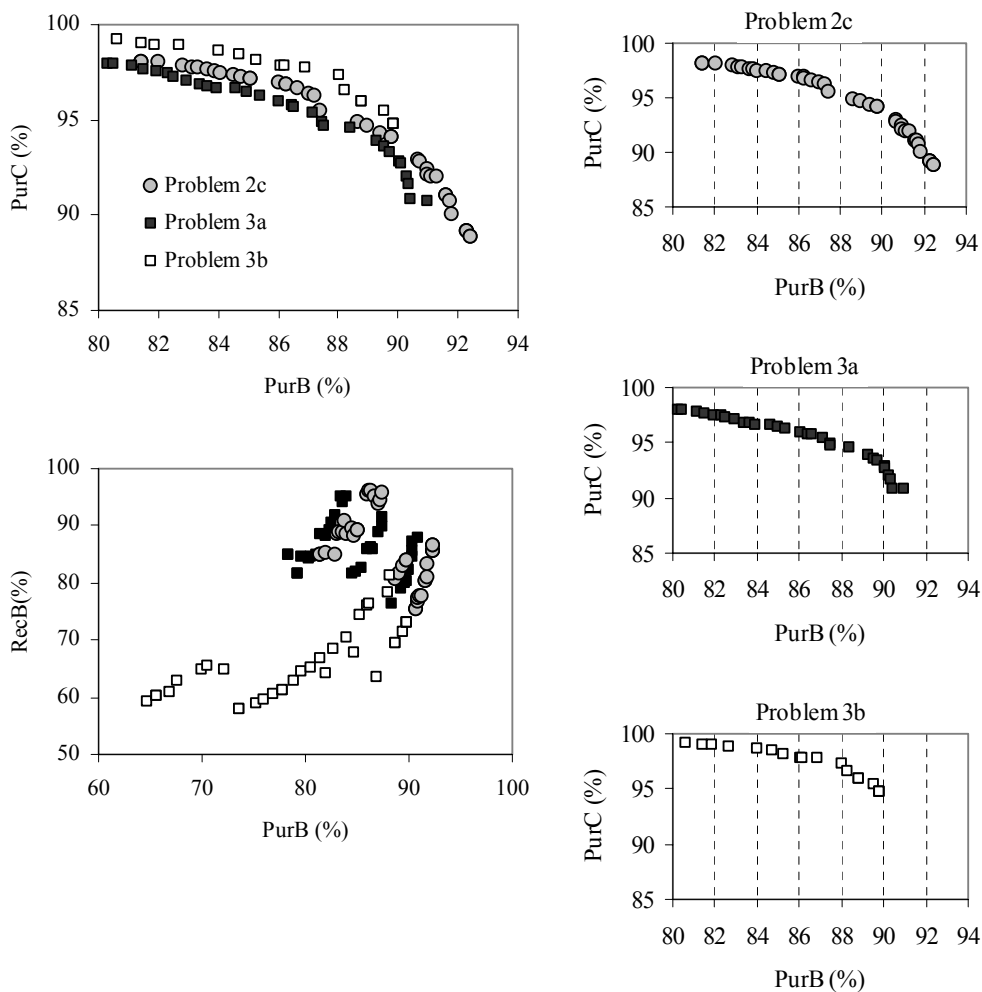
Figure 7.6 Effect of feed composition on Pareto optimal solution when adsorption isotherm is non-linear (Problems 2c, 3a and 3b)

From the results obtained from these two problems, it was observed that the effect of high concentration of A in the feed is more drastic on the recovery and purity of component B. The figure also reveals that as the concentration of A increases in the feed it becomes more difficult to get higher PurB. Moreover, the recovery of B drops significantly.

Similar to the observations made earlier, optimal Q_{D1} decreased as PurB increased. For Problem 3a, when PurB values were 78.3% and 91%, Q_{D1} was seen to be 746 and 300 cm³/min respectively. For Problem 3b, when PurB was 70.5% and 89.8%, Q_{D1} was 582 and 300 cm³/min respectively. The optimal switching time, t_{s2}, for Problem 3a was found to be 6.2 min while for Problem 3b it was 5.9 min. Q_{Ra} was seen to be constant along the Pareto for both problems. For Problem 3a, it was 136 cm³/min while for Problem 3b it was 202 cm³/min. Q_{D2} for Problem 3a was seen to be constant around 567 cm³/min while for Problem 3b it was 566 initially and then increased to 591 cm³/min as PurB increases. Optimal L_{col} chosen for Problem 3a was around 145 cm while for Problem 3b it was 140 cm.

7.5.4 Problem 4: Simultaneous maximization of purities of all three components while minimizing the desorbent consumption

In all the problems solved above the aim was to maximize purities for components B and C using desorbent consumption as one of the decision variables. However, it is worth to see if the desorbent consumption can also be minimized simultaneously. A new optimization problem (Problem 4) was solved with a linear adsorption isotherm similar to Problem 2a. The mathematical formulation is shown in Table 7.4. The two objective functions were minimization of the total desorbent consumed ($Q_{D1}+Q_{D2} = Q_{D, to}$) while maximizing the sum of purities of A, B and C. The optimization results obtained are compared with that of Problem 2a in Figure 7.7. The figure shows that for Problem 4, purities achieved for components A, B and C are comparable with that obtained in Problem 2a and can be achieved using significantly lower amount of desorbent. For example, for Problem 2a for total purity of A, B and C of about 299.7%, total desorbent consumed is 1035 cm³/min, while for Problem 4

for attaining the same total purity, desorbent consumption is only 887 cm^3/min. When compared with the plots of Q_{D1} and Q_{D2} for Problem 2a, one can see that Q_{D2} for Problem 4 remains nearly the same as that of Problem 2a, but optimal Q_{D1} is found to be much lower in Problem 4. Other performance parameters such as PurA and PurB were found to be almost 100%. PurC increases slightly as $Q_{D, to}$ (particularly Q_{D2}) increases from 98.8 to 99.9%. Recoveries of A, B and C were found to be 100, 99 and 100% respectively. The decision variables such as t_{s2}, Q_{Ra} and L_{col} were found to be nearly constant values and were equal to 6.9 min, 231 cm^3/min and 147 cm respectively.
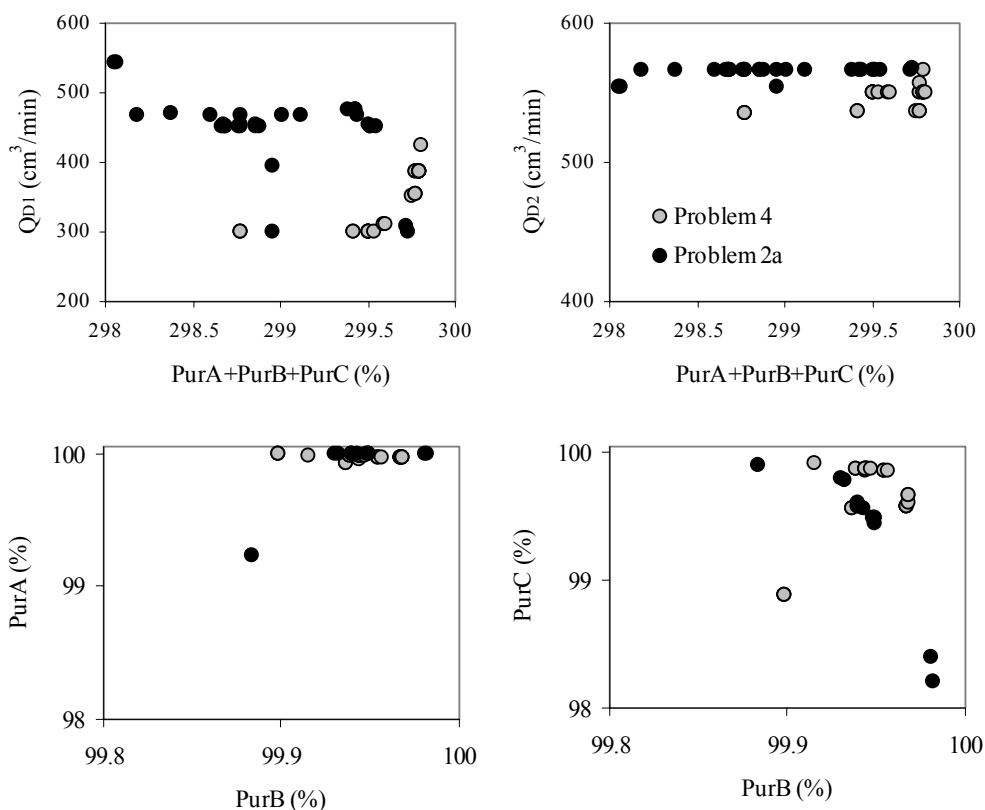
Figure 7.7 Pareto optimal solutions for Problem 4 when desorbent consumption was minimized with maximization of purities of all the three components

7.5.5 Separation of C$_8$ aromatic mixture

As discussed earlier the C$_8$ aromatic mixture consists of ethyl benzene and the three xylene isomers all having the same molecular weight but differing structurally from one another. After studying the performance of the Pseudo-SMB for a hypothetical ternary separation problem, it is important to examine the performance of a practical system that exhibits non-ideal behavior. Hence, it will be quite interesting to see if it is possible to recover both *p*-xylene as well as ethyl benzene with the best possible achievable purity from this C$_8$ aromatic mixture using a single modified SMB unit.

The feed is considered to be a typical C$_8$ aromatic mixture containing 23.6% *p*-xylene, 49.7% *m*-xylene, 12.7% *o*-xylene, and 14% ethyl benzene. Completely potassium-exchanged Y-zeolite is used as the adsorbent while *p*-diethyl benzene (*p*DEB) solvent as the desorbent. The details of the other operating conditions and design parameters are summarized in Table 7.7. The equilibrium data for *o*-, *m*-, and *p*-xylene, ethyl benzene and *p*DEB at 453 K were taken from Azevedo et al (1998).

Table 7.7 Operating and model parameters for the separation of C$_8$ aromatics

SMB unit geometry	Operating conditions
d_{col} = 4.117 m	T = 453 K, liquid phase
Model Parameters	
Pe = 2000	$q_{m, pX (mX; oX; EB)}$ = 0.1303 kg/kg
k_a = 2 min^{-1}	B_{pX} = 1.0658 m^3 /kg (see Eqn. 7.13)
d_p = 9.2 x 10^{-4} m	B_{mX} = 0.2299 m^3 /kg
ε = 0.39	B_{oX} = 0.1884 m^3 /kg
ρ = 1.39 x 10^3 kg/m^3	B_{EB} = 0.3037 m^3 /kg
	$q_{m, pDEB}$ = 0.1077 kg/kg
	B_{pDEB} = 1.2935 m^3/kg

As mentioned earlier, the motive of this study is simultaneous recovery of both *p*-xylene and ethyl benzene from the mixture of C$_8$ aromatics, with the best achievable purity. Based on the earlier studies reported in the Chapter 6, it was decided to fix the feed flow rate (Q$_F$) as 0.3 m^3/min and N$_{col}$ as 21 with configuration 6/6/6/3. This feed flow rate was decided after systematic sensitivity analysis study. The important design parameters for pseudo-SMB process are L$_{col}$, T$_{step1}$, t$_{s2}$, Q$_F$, Q$_{D1}$, Q$_{D2}$, Q$_{Ra}$, Q$_{S2}$ and the configuration p/q/r/s. During the step 2, the requirement of the system is to achieve the separation of components A, B and C, such that A moves towards the raffinate port, C towards the extract port and the intermediate component B remains stationery between sections Q and R. Initially, a typical L$_{col}$/t$_{s2}$ ratio was assumed (based on the studies in Chapter 6), Q$_S$ was fixed to a reasonable value (based on the guidelines of triangle theory) and by performing a systematic sensitivity study the flow rates, Q$_{D2}$ and Q$_{Ra}$, which guarantee countercurrent separation were obtained. A rigorous sensitivity study was performed by fixing these parameters and changing other parameters in step 1, such as T$_{step1}$ and Q$_{D1}$, and then the parameters L$_{col}$, t$_{s2}$ and T$_{step2}$ one at a time. Simulation studies revealed that for this ternary separation of C$_8$ aromatics, higher duration of T$_{step2}$ is needed. It was observed that two cycles is generally required to achieve high purities of component B which is ethyl benzene in this case. Hence for all the results later in this study, T$_{step2}$ = (N$_{col}$ × 2) t$_{s2}$. The results obtained from such a sensitivity study provide the direction of a suitable operating regime for further optimization exercises.

The adsorption selectivity of these isomers is in the order of *p*-xylene (strongly adsorbed) > *m*-xylene > *o*-xylene (least strongly adsorbed). Following the earlier convention for the hypothetical ternary separation example, one can identify (*m*-xylene + *o*-xylene) as component A (component with least affinity for

adsorption), ethyl benzene as component B (component with intermediate affinity) and *p*-xylene as component C (most strongly adsorbed component). It can be recollected from the sixth chapter, the purity and recovery of the stream collecting *m*-xylene plus *o*-xylene were named as Pur_moX and Rec_moX respectively. Similarly the purities and recoveries for ethyl benzene and *p*-xylene were named as Pur_EB, Rec_EB and Pur_pX, Rec_pX respectively. Based on the sensitivity studies, it was observed that both Pur_moX and Pur_pX are conflicting with respect to Pur_EB. When high Pur_moX and high Pur_pX can be achieved, Pur_EB is low. Moreover, it is easier to obtain high Pur_moX and high Pur_pX, but it is difficult to obtain very high Pur_EB. Hence, the optimization problem formulated was maximizing the total purity of streams containing *m*-xylene plus *o*-xylene (Pur_moX) and *p*-xylene (Pur_pX) as one objective function while simultaneously maximizing Pur_EB as the other objective function. However, it was observed that due to the difficulty in separation between *m*-xylene and ethyl benzene, the stream collecting ethyl benzene was contaminated with *m*-xylene. It is important that ethyl benzene stream be devoid of *m*-xylene and *o*-xylene. However, contamination of this stream with *p*-xylene may be acceptable since in that case one can still separate *p*-xylene from ethyl benzene by passing it through another SMB binary separation unit. Hence, two constraints were incorporated in the optimization formulation as $C_{moX, I} \leq 1\%$ and Pur_moX ≥ 60 %. The second constraint is added with the intention that more of ethyl benzene is pushed towards the extract stream thus increasing its recovery. Details of the mathematical formulation are shown in Table 7.8. The results obtained are discussed below.

Table 7.8 Description of the multi-objective optimization problems for the ternary separation of C$_8$ aromatics

Problem	Objective function	Decision variables	Constraints	Fixed parameters
5	Max (Pur_moX + Pur_pX)	$2.8 \leq Q_{D1} \leq 3.5$ m^3/min $1.5 \leq t_{s2} \leq 2.5$ min $0.7 \leq Q_{Ra} \leq 1.2$ m^3/min $2.89 \leq Q_{D2} \leq 3$ m^3/min	$C_{moX, I} \leq 1\%$ Pur_moX $\geq 60\%$	$d_{col} = 4.117$ m, $L_{col} = 2$ m $N_{col} = 21$, $\Omega = 6/6/6/3$ $T_{step1} = 5.0$ min, $Q_F = 0.3$ m^3/min $Q_{S2} = 5.39$ m^3/min
6a	Max (Pur_EB)	Same as problem 5 except $6 \leq p, q, r \leq 7$ $3 \leq s \leq 4$		Same as problem 5
6b		Same as problem 5 except $5 \leq p, q, r \leq 8$ $1 \leq s \leq 4$		Same as problem 5

7.5.5.1 Problem 5: Design of Pseudo-SMB system for the separation of C$_8$ aromatics

The results obtained are shown in Figure 7.8. The figure shows that very high Pur_EB can be obtained (~99.6%). Pur_moX decreases as Pur_EB increases. When Pur_EB is 98.9%, Pur_moX is 91.1 while Pur_moX is as low as 85.1% when Pur_EB is 99.6 %. It was observed that Pur_pX achieved are always greater than 99.5%. Moreover, Rec_moX was almost 100% and Rec_pX was greater than 99.5%. However, with this existing set-up it was observed that a higher value of Rec_EB is difficult to achieve. The best possible Rec_EB achieved is only 55.8% when Pur_EB is 98.9%. This is probably due to the dominance of m-xylene + o-xylene in the feed mixture. Similar decrease in the recovery of ethyl benzene was observed earlier with respect to the problems 2b and Problem 2c. Figure 7.8 also shows the plot of Q_{D1}

against Pur_EB. As seen for the earlier examples, it is seen that Q_{D1} decreases as Pur_EB increases. The switching time, t_{s2}, was seen to be constant at around 2.02 min while Q_{D2} was seen to be insensitive and showed values between 2.95 and 2.99 m^3/min. Q_{Ra} increased from 0.84 to 0.94 m^3/min as Pur_EB increased.
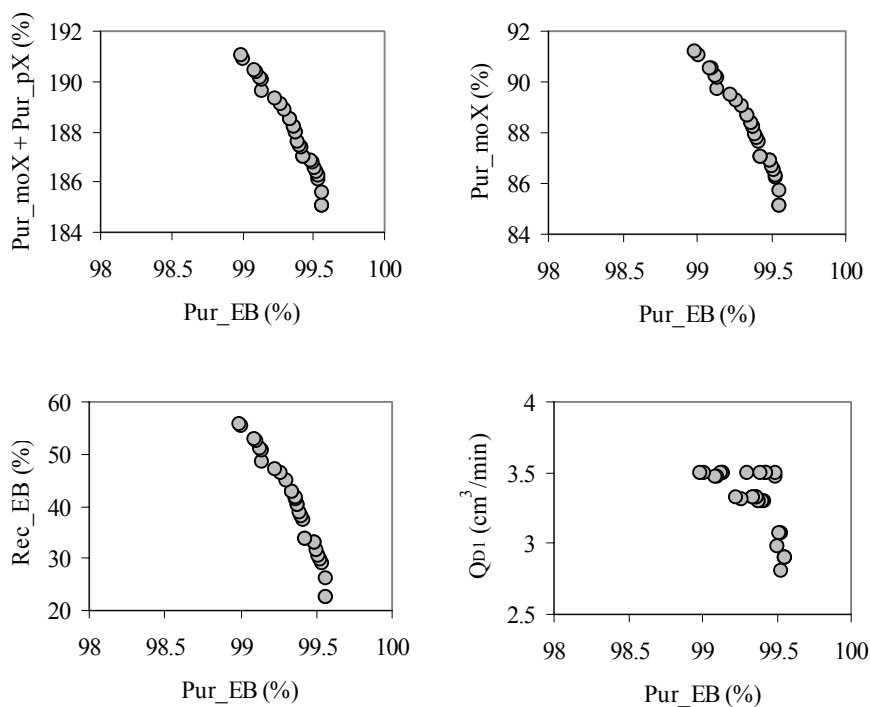
Figure 7.8 Pareto optimal solutions for the separation of C$_8$ aromatics (Problem 5)

7.5.5.2 Problems 6a and 6b: Optimal number of columns (N$_{col}$) and configuration (Ω)

In Problem 5 the number of columns in section P, Q, R and S was fixed as 6/6/6/3. It was decided to see if further performance improvement is possible if more columns are allowed to be selected for these sections. In Problem 6a, p, q, r and s (the number of columns in sections P, Q, R and S) were allowed to vary ±1 column in

each section from the reference value (Ω = 6/6/6/3). In Problem 6b more flexibility was allowed. An optimization problem was formulated to see if one can obtain an entirely different column configuration. The mathematical formulations for both problems are shown in Table 7.8 and the results obtained are compared in Figure 7.9. The figure shows that maximum Pur_EB achievable for Problem 6a is ~ 99.87%, which is much higher than the value obtained in Problem 5. Even higher values of Pur_EB (maximum = 99.93%) is achievable for Problem 6b. Another important observation that can be made is that Rec_EB achieved increases as the total adsorbent volume increases. Rec_EB for Problem 6b is as high as 84.1% when Pur_EB is 99.1%. For both problems, Pur_pX was greater than 99.5%, Rec_moX was equal to 100% and Rec_pX was greater than 99.5%.

The decision variables such as t_{s2}, Q_{D1} and Q_{D2} were found to be constant and for both the problems the values were 2.02 min, 3.5 m^3/min and 2.9 m^3/min respectively. The optimal values for Q_{Ra} was found to increase slightly along the Pareto curve. For Problem 6a, it increased from 0.87 to 0.95 m^3/min while for Problem 6b it increased from 0.83 to 0.92 m^3/min. It was seen that for both the problems, the configuration with the highest possible number of columns was selected. For Problem 6a, it was 7/7/7/4 and for Problem 6b it was 8/8/8/4. Figure 7.10 shows the concentration profile for o-xylene, m-xylene, ethyl benzene and p-xylene for one of the points (point 10A shown in Figure 7.9) on the Pareto for Problem 6b. Through these optimization studies one can recognize that Pseudo-SMB system can result in very good separation as almost pure *p*-xylene and ethyl benzene can be obtained from the C$_8$ aromatic mixture in just one unit. There is no need to further purify the ethyl benzene stream from *p*-xylene as was observed for other modified SMB systems in chapter 6. The system can be further optimized by
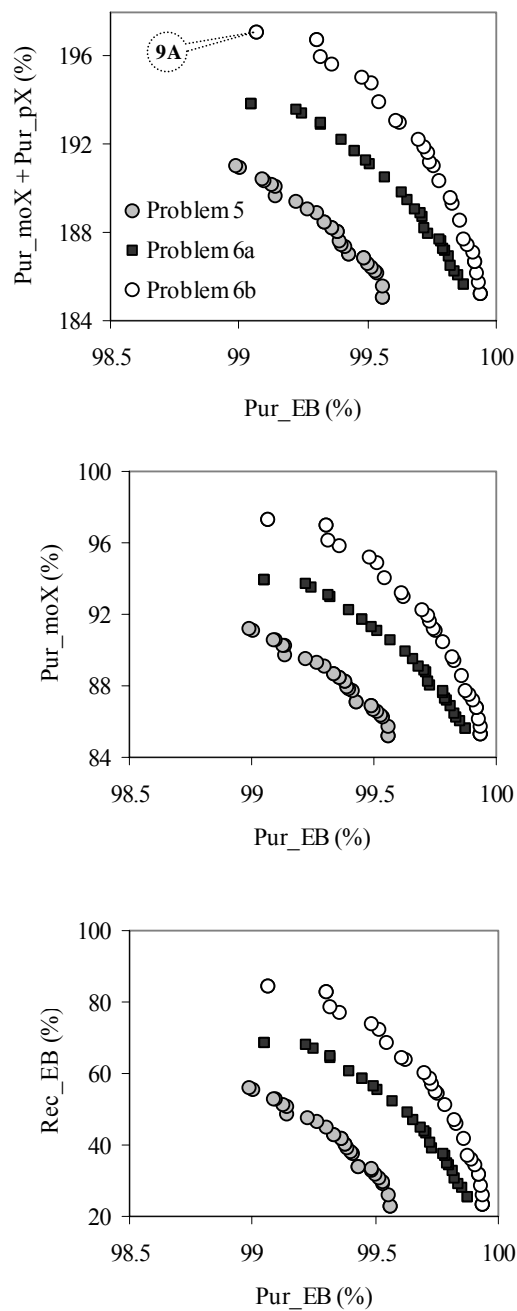
Figure 7.9 Pareto optimal solutions for the separation of C₈ aromatics determining optimum number of columns and configurations (Problems 6a and 6b)
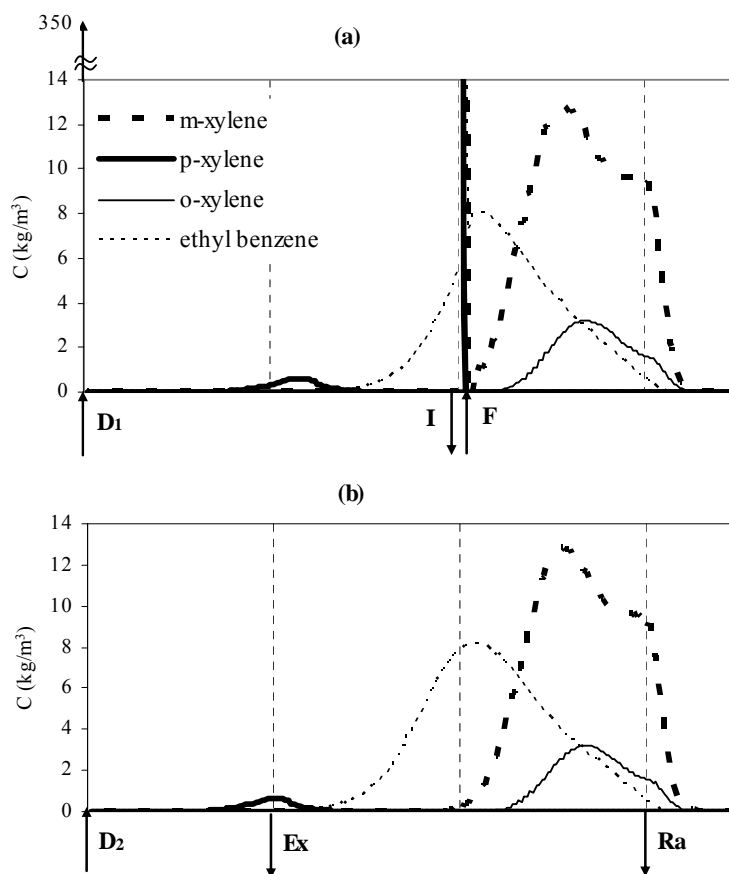
Figure 7.10 Concentration profiles for *o*-xylene, *m*-xylene, *p*-xylene and ethyl benzene for the point 9A shown in Figure 7.9 (a) end of step 1 and (b) end of step 2

considering other decision variables such L_{col}, which were kept fixed in problems 5 and 6 as the present problems are highly computational intensive. There are five components along with their respective solid phase concentrations, which makes ten PDEs for each column. Total number of columns for this separation is more than 21, which further increases the number of equations. Moreover, in obtaining one global Pareto set one need to perform computations using at least 50 chromosomes for circa 50 generations. Hence, in this present study the optimization studies were restricted to only the above few cases.

7.5.6 Comparison of performances between different modified SMB systems

In Table 7.9, the performance of Pseudo-SMB is compared at optimal conditions with that of other modified SMB configurations (MC1 and MC2) for the separation of C$_8$ aromatic isomers described in detail in Chapter 6. The first modified configuration, MC1, is the five-zone cascade system described in Chapter 6. The second modified configuration, MC2, is a four-zone SMB system that differs from the traditional four-zone SMB due to the break between sections P and Q and uses an additional desorbent stream. MC2 was further modified to MC2A and MC2B when multiple columns are present in the sections. Details of MC1, MC2A and MC2B configurations are not discussed in detail for brevity and are available in Chapter 5 and 6.

The first row of Table 7.9 lists the maximum and minimum optimal values for purity of ethyl benzene (Pur_EB) for all the modified SMB systems. In all cases, one of the objective functions was maximization of Pur_EB while the other was maximization of sum of purities of o-, m- and p-xylene (Pur_moX + Pur_pX). The subsequent values in the Table (i.e., the values for Pur_moX, Pur_pX, Rec_EB, Rec_moX and Rec_pX) are the corresponding values obtained with respect to Pur_EB listed in the first row. It is clearly seen that the Pseudo-SMB can result in very high values of Pur_EB, which is quite impossible to be obtained from the other modified SMB configurations. This improvement in Pseudo-SMB is possible with virtually same number of columns (27 or 28) although Pseudo-SMB requires much longer column length (2 m) compared to the other modified SMB systems in which the optimum L$_{col}$ is 1.135 m. It should be noted that although feed flow rate is same (Q$_F$ = 0.3 m^3/min) for all cases, the average feed flow rate for Pseudo-SMB is much lower as for some duration (during step 2) it operates with no feed flow. As a result,

productivity, PR (defined as average feed treated per unit volume of adsorbent) is significantly lower for Pseudo-SMB. Moreover, desorbent requirement, DR (desorbent required per unit volume of feed treated) is also very high in Pseudo-SMB. Hence, significant improvement in the performance of a Pseudo-SMB unit in terms of recovering all three components in very pure form is achieved at the cost of lower productivity and higher desorbent requirement. Nevertheless, Pseudo-SMB process can be very useful for ternary separation of systems where high capacity is not necessary, such as purification of drugs.

Table 7.9 Comparison of performances between different modified SMB configurations for the ternary separation of C$_8$ aromatics

	MC1		MC2A		MC2B		Pseudo-SMB[#]	
Pur_EB (%)	85.2	55.4	39.0	36.4	39.5	36.9	99.9	99.1
Pur_moX (%)	94.8	98.1	97.4	97.9	98.2	98.3	85.3	97.3
Pur_pX (%)	90.3	99.9	71.1	99.9	67.2	99.8	100.0	99.8
Rec_EB (%)	57.3	90.4	60.8	89.6	40.6	90.0	23.3	84.1
Rec_moX (%)	100	100	100	100	100	100	100	100
Rec_pX (%)	93.5	57.5	42.8	7.4	62.4	8.6	99.5	99.7
N_{col} (-)	27	27	27	27	27	27	28	28
L_{col} (m)	1.135	1.135	1.135	1.135	1.135	1.135	2.0	2.0
Q_D (m^3/min)	3.93	4.53	9.22*	11.94*	9.11*	9.91*	2.93[†]	2.93[†]
$AR^{\S}$ (m^3)	408	408	408	408	408	408	746	746
$10^4\,PR^{\&}$ (min^{-1})	7.35	7.35	7.35	7.35	7.35	7.35	0.17	0.17
$DR^{\ddagger}$ (-)	13.1	15.1	30.7	39.8	30.4	33.0	232.7	228.4

[#] For this process, $Q_F = Q_{F, avg} = (Q_F\,T_{step1}) / (T_{step1} + T_{step2})$
† $Q_D = Q_{D, avg} = (Q_{D1}\,T_{step1} + Q_{D2}\,T_{step2}) / (T_{step1} + T_{step2})$
* Q_D (m^3/min) $= Q_{D1} + Q_{D2}$;
§ Adsorbent Requirement, AR (m^3) $= N_{col} \times V_{col}$;
& Productivity, PR (m^3/min-feed per m^3-solid) $= Q_F$ / AR
‡ Desorbent Requirement, DR (m^3/min per m^3/min-feed) $= Q_D / Q_F$

7.6 Conclusions

A modified SMB system for ternary separation called the pseudo-SMB (or Quasi-SMB) system was studied. This process is different from the conventional four-zone SMB as it is partly operated as a fixed-bed chromatographic set-up and partly as a conventional SMB without any feed inflow. It was observed that this system performs extremely well when used for simpler systems with near equilibrium conditions such as linear adsorption isotherms and high mass-transfer rates. In the presence of non-idealities such as low mass-transfer rates and non-linear adsorption isotherms, it was observed that the performance of the system measured in terms of purities and recoveries of the three components decreases. Moreover, when the concentration of the least adsorbed component in the feed was increased, the performance of the system deteriorated.

The feasibility of this Pseudo-SMB system was studied for an industrial separation problem, the separation of C_8 aromatics containing xylene isomers. It was observed that one can simultaneously recover both *p*-xylene and ethyl benzene with nearly 100% purity. This is commendable since all the other modified SMB systems such as the five-zone SMB (MC1) or discontinuous four-zone SMB (MC2) cannot assure near 100% purity of both *p*-xylene and ethyl benzene in a single SMB unit. This can probably be achieved only by using the eight-zone or even higher-zone SMB systems. But, increasing the number of zones in SMB leads to increased complication in the process operation. In four-zone Pseudo-SMB system, high purities of all the three components is possible but in order to achieve high recovery of the middle (intermediate) component the adsorbent required is very high. Nevertheless, this system seems to be very attractive due to its simplicity in operation (a conventional

four-zone SMB can be changed with very less modification) and can be used for

separating non-ideal ternary systems involving low adsorption selectivity.

Chapter 8   Conclusions & Recommendations

8.1 Conclusions

This dissertation, in the chapters 3 and 4, deals with systematic and comprehensive multi-objective optimization studies of non-reactive and reactive SMB systems and the modifications of SMB such as the Varicol and SMB with variable flow for binary separation systems. In the later three chapters, the application of SMB technology for ternary separation was studied. Few configurations were studied and compared for the separation of a hypothetical system and an industrial-scale separation of C_8 aromatic mixtures to recover both p-xylene and ethyl benzene. The conclusions from these studies are presented in the following sub-sections.

8.1.1 Non-reactive and Reactive Binary Separation

In chapter 3, a systematic study for the optimal operation of an industrial scale SMB and Varicol for the recovery of *p*-xylene based on Parex process has been presented. The aim was to obtain the optimal operating parameters such as the length and number of columns, switching time interval (in SMB) and sequence (in Varicol), and liquid flow rates in different sections, which otherwise is not very straightforward. In this chapter, simultaneous maximization of recovery of *p*-xylene while minimizing desorbent consumption, and simultaneous maximization of productivity and purity of *p*-xylene were considered. Pareto optimal curves were obtained for both SMB and Varicol systems. Significant improvement in SMB performance, in terms of higher recovery of *p*-xylene for the same desorbent consumption and reduced adsorbent requirement, as compared to the reported industrial operating point, could be obtained when column length and its distribution

in various sections were selected appropriately. It was also observed that almost 100% recovery of p-xylene was seen to be possible with Varicol process operation. It is for the first time that Varicol is applied to this important separation system. Optimization results were also explained using equilibrium theory.

Simulated Moving Bed Reactor, an outstanding example of the Chromatographic Reactor-Separator systems, has been studied in chapter 4. Multi-objective optimization studies for the Inversion of sucrose to produce fructose and glucose and simultaneously separate fructose from the mixture of glucose and fructose to produce fructose rich sugar syrups were performed. The study was aimed at obtaining the optimal operating conditions that provide performance enhancement of both an existing system and for the design of new SMBR systems. The objectives used in this study were minimization of the water consumption while maximizing the productivity of fructose, since these are the problems regularly faced by the sugar industries. Variable feed flow systems were also studied and comparison of their performance with the constant feed flow SMBR systems was done. It was found that SMBR in the variable feed flow mode (both discrete and continuous) shows better performance in terms of higher amounts of fructose produced for the same desorbent consumption. Finally, optimization was performed for the Varicol system and again it was observed that performance of the reactive Varicol is much better than SMBR but at the cost of increase in the adsorbent consumption.

8.1.2 Non reactive Ternary Separation

In chapter 5, the separation of ternary mixture using modified SMB systems was studied. Basically, two configurations called as MC1 and MC2, were studied under the effect of varying separation and kinetic conditions viz., varying mass

transfer rates, different adsorption selectivities and the presence of non-linearity in the adsorption isotherm. These configurations were compared by performing rigorous multi-objective optimization for each separation case.

It was observed that the performance of MC1 and MC2, in terms of the purities of the three product streams for components A, B and C, are comparable. However, it was observed that MC2 performs slightly better than MC1 only when the separation task is very easy and as the separation task tends towards more difficult ones, MC1 outperforms MC2. Also, MC2 needs more desorbent but requires less solid adsorbent compared to MC1. On the other hand it should be noted that, MC2 with only four sections is a relatively simpler set-up compared to MC1 with five sections.

In chapter 6, the study on modified SMB systems under non-ideal conditions was further extended by considering the effect of more than one column in the modified SMB sections for the hypothetical separation problem. It was observed that when multiple columns are present in section P, configuration MC1 performed better than when only one column is present. Performance for configuration MC2, on the contrary, deteriorated. Two new configurations (MC2A and MC2B) were proposed to revamp the inability of MC2 and it was found that both perform better in terms of achieving better purity of the most strongly adsorbed component for any particular value of purity for the intermediate component. Moreover, MC2B performed slightly better than MC2A.

Subsequently, the modified systems were investigated for the separation of C_8 aromatics at optimal conditions for the simultaneous recovery of *p*-xylene and ethyl benzene. It was found that MC1 is a much better option for the separation of C_8 aromatics compared to MC2 and its modified version, MC2A and MC2B. MC1

resulted in much higher purities of ethyl benzene along with high values for Pur_moX and Pur_pX compared to MC2. In this chapter, the effect of adding a reflux stream containing pure ethyl benzene on the performance of these configurations was also studied. However, it was observed that although Pur_EB and Rec_EB can be improved by the addition of the reflux stream, it resulted in a decrease in the recovery of *p*-xylene particularly for MC2. MC1, however, seemed to show high recovery of *p*-xylene when the Pur_EB was high. It can be concluded that using a reflux stream containing pure ethyl benzene can improve the Pur_EB and Rec_EB, however causing some loss of *p*-xylene into the stream collecting ethyl benzene.

A novel SMB based ternary separation system called as the Pseudo-SMB was studied in chapter 7. It was observed that this system performed extremely well when used for simpler systems with near equilibrium conditions such as linear adsorption isotherms and high mass-transfer rates. However, it was observed that in the presence of non-idealities such as low mass-transfer rates and non-linear adsorption isotherms, the performance of the system, measured in terms of purities and recoveries of the three components, decreased. Studies with change in the feed composition showed that an increase in the concentration of the least adsorbed component in the feed resulted in decrease in performance of the system.

The performance of this system was also studied for the industrial scale separation of C_8 aromatics. These studies showed that with this system it was possible to simultaneously recover both *p*-xylene and ethyl benzene with nearly 100% purity. This is laudable, since the other modified SMB systems studied in the chapter 5 and 6, MC1 and MC2 could not assure such high purities of both these industrially important products in a single SMB unit. For attaining such high purities, probably SMB with higher sections such as the eight-zone or more should be used. However, it should be

noted that increasing the number of zones in SMB leads to increased complication in the process operation. In the four-zone Pseudo-SMB system, high purities of the product streams was possible but in order to achieve high recovery of the middle (intermediate) component the adsorbent required was very high. Nevertheless, this system seems to be very attractive due to its simplicity in operation. A conventional four-zone SMB can be changed with few minor modifications into the Pseudo-SMB system. The most remarkable feature of this system is that it can be used for separating even non-ideal ternary systems involving low adsorption selectivity such as the mixture of C_8 aromatics but with high consumption of adsorbent and the desorbent. Nevertheless, this system can be probably used for small scale separation systems such as the chiral drugs.

8.2 Directions for future work

The simulation and the optimization results will always be very fruitful when there are enough experimental evidences to support the prediction. In this work, the multi-objective optimization studies on the different SMB systems have been performed elaborately. However, these optimal solutions obtained were not verified with experiments, owing to the lack of adequate equipments and the complexity of operation of the SMB set-up. It will be worthwhile to perform experiments based on these simulation and optimization results and validate the results obtained. The same can be said about the modified SMB systems used for ternary separation. In this study though we have compared the individual performance of these systems by performing rigorous optimization and by considering even non-ideal conditions, it is important that these comparisons should be validated with experimental results. In reality, the performance may be affected by many other parameters not studied here.

In this investigation, as has been mentioned earlier, the multi-objective optimization was performed using NSGA-II with JG and the pareto-optimal solutions were predicted. Whilst this algorithm is adequate for solving the multi-objective optimization problems in this study, its robustness may be affected when the complexity of the problem increases, i.e., increase in the number of the objective functions and/or decision variables. Also, constraints in these optimization exercises are incorporated using penalty functions which might have an influence on the results obtained since they tend to modify the objective functions. Hence, a better multi-objective optimization method with a better constraint handling technique is required to deal with such scenarios.

Due to the cyclic switching of the inlet and outlet ports, the SMB process features a complex hybrid (mixed discrete/continuous) dynamics. It has high sensitivities to disturbances and a tendency to instability when the operating condition is close to the economic optimum. Hence, the development and implementation of a suitable control framework for SMB process is necessary in order to exploit the full economic potential of the process.

In the case of ternary separation, due to the limitation of time only a few simple (in terms of easy up-gradations from the conventional SMB) configurations are studied and compared. There are of course some other attractive and relatively simple techniques that need to be explored, such as the concept of variable flow rates, temperatures or pressures applied to the conventional SMB or even the modified SMB systems to effect ternary separation. Similarly, as we have seen that the application of Varicol operation mode to SMB can improve the performance for binary separation, the same effect may be possible in case of ternary separation too. In this case, it might be very attractive to check the improvement in performance of these modified SMB

systems that can be obtained due to the Varicol operation mode, since the implementation of this can be done with no additional fixed costs.

References

Adam, P., R.-M. Nicoud, M. Bailly and O. Ludemann-Hombouger. Process and Device for Separation with Variable-Length, US Patent, 6,136,198. 1998.

Ando, M., M. Tanimura and M. Tamura. Method of chromatographic separation, US Patent, 4,970,002. 1990.

Azevedo, D.C.S., S.B. Neves, S.P. Ravagnani, C.V. Cavalcante and A.E. Rodrigues. The influence of dead zones on simulated moving bed units. In Fundamentals of adsorption 6, ed. by F. Meunier, pp. 521- 526, Amsterdam, The Netherlands: Elsevier. 1998.

Azevedo, D.C.S. and A.E. Rodrigues. Bi-linear driving force approximation in the modeling of simulated moving bed using bidisperse adsorbents, Ind. Eng. Chem. Res., *38*, pp. 3519-3529. 1999.

Azevedo, D.C.S. and A.E. Rodrigues. Obtainment of High-Fructose Solutions from Cashew (Anacardium occidentale) Apple Juice by Simulated Moving-Bed Chromatography, Separ. Sci. Technol., *35*(16), pp. 2561-2581. 2000.

Azevedo, D.C.S. and A.E. Rodrigues. Fructose-Glucose Separation in a SMB Pilot Unit: Modeling, Simulation, Design and Operation, AIChE J., *47*(9), pp. 2042-2051. 2001a.

Azevedo, D.C.S. and A.E. Rodrigues. Design methodology and operation of a simulated moving bed reactor for the inversion of sucrose and glucose-fructose separation, Chem. Eng. J., *82*, pp. 95-107. 2001b.

Barker, P.E. and D.H. Huntington. A Circular Chromatography Machine for the Preparative Separation of Liquid or Gaseous Mixtures. In Gas Chromatography, ed. by A.B. Littlewood, pp. 135-149. London: Institute of Petroleum. 1966.

Barker P.E. and G. Ganetsos. The Development and Applications of Preparative-Scale Continuous Chromatography, Separ. Sci. Technol., *22*(8-10), pp. 2011-2035. 1987.

Barker P.E. and G. Ganetsos. Chemical and Biochemical Separations Using Preparative and Large-Scale Batch and Continuous Chromatography, Separ. Purif. Methods, *17*(1), pp. 1-65. 1988.

Barker, P.E., G. Ganetsos, J. Ajongwen and A. Akintoye. Bioreaction-separation on continuous chromatographic systems, Chemical Engineering Journal and the Biochemical Engineering Journal, *50*(2), pp. B23-B28. 1992.

Barker, P.E. and G. Ganetsos. Continuous Moving-Column Chromatographic Systems. In Preparative and Production Scale Chromatography, ed by G. Ganetsos and P.E. Barker, pp. 173-186. New York: Marcel Dekker. 1993.

Berg, C. Hypersorption Process for Separation of Light Gases, Trans. Am. Inst. Chem. Eng., *42*, pp. 665-680. 1946.

Beste, Y.A. and W. Arlt. Side-Stream Simulated Moving-Bed Chromatography for Multicomponent Separation, Chem. Eng. Technol., *25*, pp. 956-962. 2002.

Bhaskar, V., S.K. Gupta and A.K. Ray. Applications of Multiobjective Optimization in Chemical Engineering, Rev. Chem. Eng., *16*, pp. 1-54. 2000.

Biressi, G., O. Ludemann-Hombourger, M. Mazzotti, R.-M. Nicoud and M. Morbidelli. Design and Optimisation of a Simulated Moving Bed Unit: Role of Deviations from Equilibrium Theory, J. Chromatogr. A., *876*, pp. 3-15. 2000.

Blehaut, J. and R.-M. Nicoud. Recent Aspects in Simulated Moving Bed, Analusis, *26*(7), pp. M60-M70. 1998.

Broughton, D.B. and C.G. Gerhold. Continuous Sorption Process Employing Fixed Bed of Sorbent and Moving Inlets and Outlets, US Patent 2,985,589. 1961.

Broughton, D.B. and S.A. Gembicki. Adsorptive Separations by Simulated Moving Bed Technology: the Sorbex Process. In Fundamentals of Adsorption, ed by A.L. Myers and G. Gelfort, pp. 115-124. New York: The Foundation. 1984.

Broughton, D.B. Molex: Case History of a Process, Chem. Eng. Prog., *64*(8), pp. 60-65. 1968.

Broughton, D.B., R.W. Neuzil, J.M. Pharis and C.S. Breasley. The Parex Process for Recovering P-xylene, Chem. Eng. Prog., *66*(9), pp. 70-75. 1970.

Buckley, M. and G. Norton. Experiences with a New Molasses Separation Plant at Mallow, Int. Sugar J., *93*, pp. 204-209. 1991.

Carra, S., E. Santacesaria, M. Morbidelli, G. Storti and D. Gelosa. Separation of Xylenes on Y-Zeolite. 3. Pulse curves and their interpretation, Ind. Eng. Chem. Process Des. Dev., *21*, pp. 451-457. 1982.

Cauley, F.G., Y. Xie and N.H.-L. Wang. Optimization of SMB Systems with Linear Adsorption Isotherms by the Standing Wave Annealing Technique, Ind. Eng. Chem. Res., *43*(23), pp. 7588-7599. 2004.

Cavalcante, C.L., Jr., V.E. Lima, L.G. Sousa and O.L.S. Alsina. Sorption kinetics of aromatics in Y-zeolite pellets using the gravimetric method, Braz. J. Chem. Eng., *14*(3), pp. 191-197. 1997.

Cen, P. and G.T. Tsao. Recent advances in the simultaneous bioreaction and product separation processes, Separ. Technol. *3*, pp. 58-75. 1993.

Chankong, V. and Y.Y. Haimes. Multiobjective Decision Making—Theory and Methodology, New York: Elsevier. 1983.

Charton, F. and R.-M. Nicoud. Complete Design of a Simulated Moving-Bed, J. Chromatogr A., *702*, pp. 97-112. 1995.

Chiang, A.S.T. Continuous Chromatographic Process Based on SMB Technology, AIChE J., *44*(8), pp. 1930-1932. 1998.

Ching, C.B. and D.M. Ruthven. Separation of glucose and fructose by simulated counter-current adsorption, AIChE Symp. Ser., *81*(242), pp. 1-8. 1985a.

Ching, C.B. and D.M. Ruthven. Experimental study of a simulated counter-current adsorption system – I. Isothermal steady state operation, Chem. Eng. Sci., *40*, pp. 877-885. 1985b.

Ching, C.B. and D.M. Ruthven. Experimental study of a simulated counter-current adsorption system – IV. Non-isothermal operation, Chem. Eng. Sci., *41*, pp. 3063-3071. 1985c.

Ching, C.B. and Z.P. Lu. Simulated Moving Bed Reactor: Application in Bioreaction and Separation, Ind. Eng. Chem. Res., *36*, pp. 152-159. 1997.

Chung, S.F. and Y. Wen. Longitudinal Dispersion of Liquid Flowing Through Fixed and Fluidized Beds, AIChE J., *14*, pp. 857-866. 1968.

Deb, K. Optimization for Engineering Design: Algorithms and Examples. pp. 290-320, New Delhi: Prentice-Hall of India, India. 1995.

Deb, K. Multi-Objective Optimization using Evolutionary Algorithms. UK: Wiley, Chichester. 2001.

Deb, K., A. Pratap, S. Agarwal and T. Meyarivan. A Fast and Elitist Multi-Objective Genetic Algorithm: NSGA-II. IEEE Transactions on Evolutionary Computation, *6*(2), pp. 182-197. 2002.

Dünnebier, G. and K.U. Klatt. Optimal Operation of Simulated Moving Bed Chromatographic Processes, Comput. Chem. Eng., *23*, pp. S195-S198. 1999.

Dünnebier, G., J. Fricke and K.U. Klatt. Optimal Design and Operation of Simulated Moving Bed Chromatographic Reactors, Ind. Eng. Chem. Res., *39*, pp. 2290-2304. 2000.

Fabri, J., U. Greaser, and T.A. Simo. Xylenes-Production, Separation and Further Processing. Ullmann's Encyclopedia of Industrial Chemistry, Weinheim, Germany: Wiley-VCH GmbH. 2001.

Fish, B., R.W. Carr and R. Aris. The continuous countercurrent moving bed chromatographic reactor, Chem. Eng. Sci., *41*(4), pp. 661-668. 1986.

Fish, B., R.W. Carr and R. Aris. Design and performance of a simulated countercurrent moving bed separator, AIChE J., *39*(11), pp. 1783-1790. 1993.

Fitch, G.R., M.E. Probert and P.F. Tiley. Preliminary Studies of Moving-Bed Chromatography, J. Chem. Soc., pp. 4875-4881. 1962.

Fonseca, C.M. and P.J. Fleming. Multiobjective Optimization and Multiple Constraint Handling with Evolutionary Algorithms I: A Unified Formulation, IEEE Trans. Syst. Man. Cy. A, *28*, pp. 26-37. 1998.

Fricke, J., M. Meurer and H. Schmidt-Traub. Design and Layout of Simulated-Moving Bed Chromatographic Reactors, Chem. Eng. Technol., *22*, pp. 835-839. 1999a.

Fricke, J., M. Meurer, J. Dreisorner and H. Schmidt-Traub. Effect of process parameters on the performance of a Simulated Moving Bed chromatographic reactor, Chem. Eng. Sci., *54*, pp. 1487-1492. 1999b.

Ganetsos, G. and P.E. Barker (ed). Preparative and Production Scale Chromatography, pp. 3-782, New York: Marcel Dekker. 1993.

Gentilini, A., C. Migliorini, M. Mazzotti and M. Morbidelli. Optimal Operation of Simulated Moving-bed Units for Non-linear Chromatographic Separations II. Bi-Langmuir Isotherm, J. Chromatogr. A., *805*, pp. 37-44. 1998.

Glasser, D. A New Design for a Continuous Gas Chromatography. In Gas Chromatography, ed by A.B. Littlewood, pp. 119-134. London: Institute of Petroleum. 1966.

Goddard, M. and D.M. Ruthven. Sorption and diffusion of C_8 aromatic hydrocarbons in Faujasite type Zeolites. II. Sorption kinetics and intracrystalline diffusivities, Zeolites. *6*(4), pp. 283-289. 1986.

Goldberg, D.E. Genetic Algorithms in Search, Optimization, and Machine Learning. pp. 1-379, Reading, Mass.: Addison-Wesley. 1989.

Hashimoto, K., S. Adachi, H. Noujima and Y. Ueda. A New Process Combining Adsorption and Enzyme Reaction for Producing Higher Fructose Syrup, Biotechnol. Bioeng., *25*, pp. 2371-2393. 1983.

Hashimoto, K., S. Adachi and Y. Shirai. Development of New Bioreactors of a Simulated Moving-Bed Type. In Preparative and Production Scale Chromatography, ed by G. Ganestos and P. E. Barker, pp. 395-420. New York: Marcel Dekker. 1993.

Holland, J.H. Adaptation in Natural and Artificial Systems: An Introductory Analysis with Applications to Biology, Control and Artificial Intelligence. pp. 1-183, Ann Arbor : University of Michigan Press. 1975.

Hongisto, H.J. Chromatographic Separation of Sugar Solutions, the Finnsugar Molasses Desugarization Process I, Int. Sugar J., *79*, pp. 100-104. 1977a.

Hongisto, H.J. Chromatographic Separation of Sugar Solutions, the Finnsugar Molasses Desugarization Process II, Int. Sugar J., *79*, pp. 131-134. 1977b.

Hotier, G., G. Terneuil, J.M. Toussaint and D. Lonchamp. Continuous process and apparatus for chromatographic separation of a mixture of at least three components into three purified effluents by means of two solvents, European Patent 1990-402334, 1990a.

Hotier, G., J.M. Toussaint, D. Lonchamp and G. Terneuil. Continuous process and apparatus for chromatographic separation of a mixture of at least three components into three purified effluents by means of one solvent at two different temperatures and/or pressures, European Patent 1990-402335. 1990b.

Hsiao, H.S., S.M. Yih and M.H. Li. Adsorption equilibrium of xylene isomers and p-diethylbenzene in the liquid phase on a Y-Zeolite, Adsorption Sci. Technol., *6*, pp. 64-82. 1989.

Huang, S. and R.W. Carr. A simple adsorber dynamics approach to simulated countercurrent moving bed reactor performance, Chem. Eng. J., *82*, pp. 87-94. 2001.

Karlsson, S., F. Pettersson and T. Westerlund. A MILP-Method for Optimizing a Preparative Simulated Moving Bed Chromatographic Separation Process, Comput. Chem. Eng., *23*, pp. S487-S490. 1999.

Kasat, R., D. Kunzru, D.N. Saraf and S.K. Gupta. Multiobjective optimization of industrial FCC units using elitist non-dominated sorting genetic algorithm, Ind. Eng. Chem. Res., *41*(19), pp. 4765-4776. 2002.

Kasat, R.B. and S.K. Gupta. Multiobjective optimization of an industrial fluidized bed catalytic cracking unit (FCCU) using genetic algorithm (GA) with the jumping genes operator, Comput. Chem. Eng., *27*(12), pp. 1785-1800. 2003.

Kehde, H., R.G. Fairfield, J.C. Frank and L.W. Zahnstecher. Ethylene Recovery, Commercial Hypersorption Operation, Chem. Eng. Prog., *44*(8), pp. 575-582. 1948.

Kim, J.K., Y. Zang and P.C. Wankat. Single-Cascade Simulated Moving Bed Systems for the Separation of Ternary Mixtures, Ind. Eng. Chem. Res., *42*, pp. 4849-4860. 2003.

Klatt, K.U., F. Hanisch, G. Dünnebier and S. Engell. Model-based Optimization and Control of Chromatographic Processes, Comput. Chem. Eng., *24*, pp. 1119-1126. 2000.

Kloppenburg E. and E.D. Gilles. A New Concept for Operating Simulated Moving-Bed Processes, Chem. Eng. Technol., *22*(10), pp. 813-817. 1999.

Kruglov, A. Methanol synthesis in a simulated countercurrent moving-bed adsorptive catalytic reactor, Chem. Eng. Sci., *49*(24a), pp. 4699-4716. 1994.

Lee, K.N. and W.K. Lee. A theoretical model for the separation of glucose and fructose mixtures by using a semicontinuous chromatographic refiner, Separ. Sci. Technol., *27*, pp. 295-311. 1992.

Lefevre, L.J. Separation of Fructose from Glucose Using Cation Exchange Resin Salts, US Patent 3,044,905. 1962.

Lode, F., M. Houmard, C. Migliorini, M. Mazzotti and M. Morbidelli. Continuous reactive chromatography, Chem. Eng. Sci., *56*, pp. 269-291. 2001.

Ludemann-Hombourger, O., R.-M. Nicoud and M. Bailly. The "VARICOL" Process: A New Multicolumn Continuous Chromatographic Process, Separ. Sci. Technol., *35*(12), pp. 1829-1862. 2000.

Ludemann-Hombourger, O., G. Pigorini, R.-M. Nicoud, D.S. Ross and G. Terfloth. Application of the VARICOL process to the separation of the isomers of the SB-553261 racemate, J. Chromatogr. A., *947*, pp. 59-68. 2002.

Luft, L. Mine Safety Appliances Co., US Patent 3,016,107. 1962

Ma, Z. and N.-H.L. Wang. Standing Wave Analysis of SMB Chromatography: Linear Systems, AIChE J., *43*(10), pp. 2488-2508. 1997.

Mallmann, T., B.D. Burris, Z. Ma and N.-H.L. Wang. Standing Wave Design of Nonlinear SMB Systems for Fructose Purification, AIChE J., *44*(12), pp. 2628-2646. 1998.

Masuda, T., T. Sonobe, F. Matsuda, and M. Horie. Process for fractional separation of multi-component fluid mixture, US Patent 5,198,120. 1993.

Mata, V.G. and A.E. Rodrigues. Separation of ternary mixtures by pseudo-simulated moving bed chromatography, J. Chromatogr. A., *939*, pp. 23-40. 2001.

Mazzotti, M., G. Storti and M. Morbidelli. Robust Design of Countercurrent Adsorption Separation Processes: 2. Multicomponent Systems, AIChE J., *40*(11), pp. 1825-1842. 1994.

Mazzotti, M., G. Storti and M. Morbidelli. Robust Design of Countercurrent Adsorption Separation: 3. Nonstoichiometric Systems, AIChE J., *42*(10), pp. 2784-2796. 1996a.

Mazzotti, M., R. Baciocchi, G. Storti and M. Morbidelli. Vapor-phase SMB Adsorptive Separation of Linear/Nonlinear Paraffins, Ind. Eng. Chem. Res., *35*(7), pp. 2313-2321. 1996b.

Mazzotti, M., G. Storti and M. Morbidelli. Optimal Operation of Simulated Moving Bed Units for Nonlinear Chromatographic Separations, J. Chromatogr. A., *769*, pp. 3-24. 1997a.

Mazzotti, M., G. Storti and M. Morbidelli, Robust Design of Countercurrent Adsorption Separation Processes: 4. Desorbent in the Feed, AIChE J., *43*(1), pp. 64-72. 1997b.

McCoy, M. SMB Emerges as Chiral Technique, Chem. Eng. News, *78*, pp. 17-19. 2000.

Meurer, M., U. Altenhoner, J. Strube, A. Untiedt and H. Schmidt-Traub. Dynamic simulation of a Simulated-Moving-Bed Chromatographic Reactor for the Inversion of Sucrose, Starch/Starke, *48*, pp. 452-457. 1996.

Meurer, M., U. Altenhoner, J. Strube and H. Schmidt-Traub. Dynamic simulation of simulated moving bed chromatographic reactors, J. Chromatogr. A., *769*, pp. 71-79. 1997.

Migliorini, C., A. Gentilini, M. Mazzotti and M. Morbidelli. Design of Simulated Moving Bed Units under Nonideal Conditions, Ind. Eng. Chem. Res., *38*, pp. 2400-2410. 1999a.

Migliorini, C., M. Fillinger, M. Mazzotti and M. Morbidelli. Analysis of Simulated Moving-Bed Reactors, Chem. Eng. Sci., *54*, pp. 2475-2480. 1999b.

Minceva, M. and A.E. Rodrigues. Modeling and simulation of a simulated moving bed for the separation of p-xylene, Ind. Eng. Chem. Res., *41*(14), pp. 3454-3461. 2002.

Morbidelli, M., E. Santacesaria, G. Storti and S. Carra. Separation of Xylenes on Y Zeolite in the Vapour Phase. 2. Breakthrough and pulse curves and their interpretation. Ind. Eng. Chem. Process Des. Dev., *24*, pp. 83-88. 1985.

Nandasana, A.D., A.K. Ray and S.K. Gupta. Applications of the non-dominated sorting genetic algorithm (NSGA) in chemical reaction engineering, Int. J. Chem. Reactor Eng., 1(R2). 2003.

Navarro, A., H. Caruel and L. Rigal. Continuous Chromatographic Separation Process: Simulated Moving Bed Allowing Simultaneous Withdrawal of Three Fractions, J. Chromatogr. A., *770*, pp. 39-50. 1997.

Nicolaos, A., L. Muhr, P. Gotteland, R.-M. Nicoud and M. Bailly. Application of equilibrium theory to ternary moving bed configurations (four+four, five+four, eight and nine zones) I. Linear case, J. Chromatogr. A., *908*, pp. 71-86. 2001a.

Nicolaos, A., L. Muhr, P. Gotteland, R.-M. Nicoud and M. Bailly. Application of the equilibrium theory to ternary moving bed configurations (4+4, 5+4, 8 and 9 zones) II. Langmuir case, J. Chromatogr. A., *908*, pp. 87-109. 2001b.

Nicoud, R.-M. Simulated Moving Bed (SMB) - Some Possible Applications for Biotechnology. In Bioseparation and Bioprocessing Handbook, ed. By G. Subramanian, pp. 3-39, New York: Wiley-VCH. 1998.

Nicoud, R.-M. Simulated Moving-Bed Chromatography for Biomolecules. In Handbook of Bioseparations, ed. by S. Ahuja, pp. 475-511, California: Academic Press. 2000.

Pais, L.S., J.M. Loureiro and A.E. Rodrigues. Modeling strategies for the enantiomers separation by SMB chromatography, AIChE J, *44*(3), pp. 561-569. 1998.

Paludetto, R., G. Storti, G. Gamba, S. Carra, and M. Morbidelli. On multicomponent adsorption equilibra of Xylene mixture on zeolites, Ind. Eng. Chem. Res., *26*(11), pp. 2250-2258. 1987.

Perrut, M., R.-M. Nicoud and G. Hotier. Method and device for fractionating a mixture in a simulated fluidized bed in the presence of a compressed gas, a supercritical fluid or a subcritical fluid, French Patent FR419, 1993.

Petroulas, T., R. Aris and R.W. Carr. Analysis and Performance of a Countercurrent Moving-Bed Chromatographic Reactor, Chem. Eng. Sci., *40*, pp. 2233-2240. 1985.

Pirkle, W.H., D.W. House and J.M. Finn. Broad Spectrum Resolution of Optical Isomers Using Chiral High-Performance Liquid Chromatographic Bonded Phases, J. Chromatogr. A., *192*, pp. 143-158. 1980.

Proll, T. and E. Kusters. Optimization strategy for simulated moving bed systems, J. Chromatogr. A., *800*, pp. 135-150. 1998.

Ray, A.K., A. Tonkovich, R.W. Carr and R. Aris. The Simulated Countercurrent Moving-Bed Chromatographic Reactor, Chem. Eng. Sci., *45*, pp. 2431-2437. 1990.

Ray, A.K. The Simulated Countercurrent Moving Bed Chromatographic Reactor: A Novel Reactor-Separator. Ph.D. Dissertation, University of Minnesota. 1992.

Ray, A.K., R.W. Carr and R. Aris. The simulated countercurrent moving-bed chromatographic reactor – a novel reactor separator, Chem. Eng. Sci., *49*, pp. 469-480. 1994.

Ray, A.K. and R.W. Carr. Numerical simulation of a simulated countercurrent moving bed chromatographic reactor, Chem. Eng. Sci., *50*, pp. 3033-3041. 1995.

Rosset, A.J. de, R.W. Neuzil and D.J. Korous. Liquid Column Chromatography as a Predictive Tool for Continuous Countercurrent Adsorptive Separations, Ind. Eng. Chem. Proc. Des. Dev., *15*, pp. 261-266. 1976.

Ruthven, D.M. The axial dispersed plug flow model for continuous counter-current adsorbers, Can. J. Chem. Eng., *61*, pp. 881-883. 1983.

Ruthven, D.M. Principles of Adsorption and Adsorption Processes. pp. 1-433, New York: John Wiley & Sons. 1984.

Ruthven, D.M. and M. Goddard. Sorption and diffusion of C_8 aromatic hydrocarbons in Faujasite type zeolites. I. Equilibrium isotherms and separation factor, Zeolites, *6*(4), pp. 275-282.1986.

Ruthven, D.M. and C.B. Ching. Counter-Current and Simulated Counter-Current Adsorption Separation Processes, Chem. Eng. Sci., *44*(5), pp. 1011-1038. 1989.

Santacesaria, E., M. Morbidelli, P. Danise, M. Mercenari, and S. Carra. Separation of Xylenes on Y-Zeolite. 1. Determination of the adsorption equilibrium parameters, selectivities and mass transfer coefficients through finite bath experiments, Ind. Eng. Chem. Process Des. Dev., *21*, pp. 440-446. 1982a.

Santacesaria, E., M. Morbidelli, A. Servida, G. Storti, and S. Carra. Separation of Xylenes on Y-Zeolite. 2. Breakthrough curves and their interpretation, Ind. Eng. Chem. Process Des. Dev., *21*, pp. 446-451. 1982b.

Santacesaria, E., D. Geloza, P. Danise and S. Carra. Separation of Xylenes on Y-Zeolite in the vapor phase 1. Determination of the adsorption equilibrium parameters and of the kinetic regime, Ind. Eng. Chem. Process Des. Dev., *24*, pp. 78-83. 1985.

Sarmidi, M.R. and P.E. Barker. Simultaneous biochemical reaction and separation in a rotating annular chromatograph, Chem. Eng. Sci., *48*(14), pp. 2615-2623. 1993.

Sayama, K., T. Kamada, S. Oikawa and T. Masuda. Production of raffinose: a new byproduct of the beet sugar industry, Zucherind., *117*(11), pp. 893-899. 1992

Schiesser, W.E. The Numerical Method of Lines. pp. 1-326, New York: Academic Press. 1991.

Schulte, M. and J. Strube. Preparative enantioseparation by simulated moving bed chromatography, J. Chromatogr. A., *906*, pp. 399-416. 2001.

Seko, M., H. Takeuchi and T. Inada. Scale-up for Chromatographic Separation of p-Xylene and Ethylbenzene, Ind. Eng. Chem. Prod. Res. Dev., *21*, pp. 656-661. 1982.

Shibata, T., I. Okamoto and K. Ishii. Chromatographic Optical Resolution on Polysaccharides and their Derivatives, J. Liq. Chromatogr., *9*, pp. 313-340. 1986.

Srinivas, N. and K. Deb. Multiobjective Function Optimization using Non-dominated Sorting Genetic Algorithms, Evolutionary Computing, *2*, pp. 221-248. 1995.

Storti, G., E. Santacesaria, M. Morbidelli and S. Carra. Separtion of Xylenes on Y-Zeolite in the vapor phase. 3. Choice of the suitable desorbent, Ind. Eng. Chem. Process Des. Dev., *24*, pp. 89-92. 1985.

Storti, G., M. Masi, R. Paludetto, M. Morbidelli and S. Carra. Adsorption Separation Processes: Countercurrent and Simulated Countercurrent Operations, Comput. Chem. Eng., *12*, pp. 475-482. 1988.

Storti, G., M. Masi, S. Carra, and M. Morbidelli. Optimal design of multi-component countercurrent adsorption separation processes involving nonlinear equilibria, Chem. Eng. Sci., *44*(6), pp. 1329-1345. 1989.

Storti, G., M. Mazzotti, M. Morbidelli and S. Carra. Robust Design of Binary Countercurrent Adsorption Separation Processes, AIChE J., *39*, pp. 471-492. 1993.

Storti, G., R. Baciocchi, M. Mazzotti and M. Morbidelli. Design of optimal operating conditions of simulated moving bed adsorptive separation units, Ind. Eng. Chem. Res., *34*(1), pp. 288-301. 1995.

Subramani, H.J., K. Hidajat and A.K. Ray. Optimization of simulated moving bed and Varicol processes for glucose-fructose separation, Chemical Engineering Research and Design. *81*(A5), pp. 549-567. 2003a.

Subramani, H.J., K. Hidajat and A.K. Ray. Optimization of reactive SMB and Varicol systems, Comput. Chem. Eng. *27*(12), pp. 1883-1901. 2003b.

Tonkovich, A.L., R.W. Carr and R. Aris. Enhanced C_2 yields from methane oxidative coupling by means of a separative chemical reactor, Science, *262*, pp. 221-223. 1993.

Toumi, A., F. Hanisch and S. Engell. Optimal Operation of Continuous Chromatographic Processes: Mathematical Optimization of the VARICOL Process, Ind. Eng. Chem. Res., *41*(17), pp. 4328-4337. 2002.

Viard, V. and M.L. Lameloise. Modeling glucose-fructose separation by adsorption chromatography on ion exchange resins, J. Food Eng., *17*, pp. 29-48. 1992.

Wankat, P.C. Simulated Moving Bed Cascades for Ternary Separations, Ind. Eng. Chem. Res. *40*, pp. 6185-6193. 2001.

Wongso F., K. Hidajat and A. K. Ray. Optimal operating mode for enantioseparation of SB-553261 racemate based on simulated moving bed technology, Biotechnology and Bioengineering, *87*(6), pp. 704-722. 2004.

Wooley, R., Z. Ma and N.–H.L. Wang. A Nine-Zone Simulated Moving Bed for the Recovery of Glucose and Xylose from Biomass Dydrolyzate, Ind. Eng. Chem. Res., *37*(9), pp. 3699-3709. 1998.

Wu, D.–J., Z. Ma and N.–H.L. Wang. Optimization of Throughput and Desorbent Consumption in Simulated Moving-Bed Chromatograph for Paclitaxel Purification, J. Chromatogr. A., *855*, pp. 71-89. 1999.

Yashima, E. and Y. Okamoto. Chiral Discrimination on Polysaccharides Derivatives, B. Chem. Soc. Jpn., *68*, pp. 3289-3307. 1995.

Yu, W., K. Hidajat and A.K. Ray. Application of Multiobjective Optimization in the Design and Operation of Reactive SMB and Its Experimental Verification, Ind. Eng. Chem. Res., *42*(26), pp. 6823-6831. 2003.

Zang, Y. and P.C. Wankat. Three-Zone Simulated Moving Bed with Partial Feed and Selective Withdrawal, Ind. Eng. Chem. Res., *41*(21), pp. 5283-5289. 2002a.

Zang, Y. and P.C. Wankat. SMB operation strategy - partial feed, Ind. Eng. Chem. Res., *41*(10), pp. 2504-2511. 2002b.

Zang, Y. and P.C. Wankat. Variable Flow Rate Operation for Simulated Moving Bed Separation Systems: Simulation and Optimization, Ind. Eng. Chem. Res., *42*(20), pp. 4840-4848. 2003.

Zhang, Z., K. Hidajat and A.K. Ray. Multiobjective Optimization of Simulated Countercurrent Moving Bed Chromatographic Reactor (SCMCR) for MTBE Synthesis, Ind. Eng. Chem. Res., *41*, pp. 3213-3232. 2002a.

Zhang, Z., K. Hidajat, A.K. Ray and M. Morbidelli. Multi-objective Optimization of Simulated Moving Bed system and Varicol process for Chiral Separation, AIChE J., *48*(12), pp. 2800-2816. 2002b.

Zhang, Z., M. Mazzotti and M. Morbidelli. Continuous chromatographic processes with a small number of columns: Comparison of simulated moving bed with Varicol, PowerFeed, and ModiCon, Korean Journal of Chemical Engineering, *21*(2), pp. 454-464. 2004.

Publications

Kurup, A. S., H. J. Subramani, K. Hidajat & A. K. Ray. Optimal design and operation of SMB bioreactor for Sucrose Inversion, Chem. Eng. J., *108*, pp.19-33. 2005.

Kurup, A. S., K. Hidajat & A. K. Ray, Optimal operation of an industrial scale Parex process for the recovery of p-xylene from a mixture of C_8 aromatics, Ind. Eng. Chem. Res., *44*, pp. 5703-5714. 2005.

Kurup, A. S., K. Hidajat & A. K. Ray. A Comparative Study of Modified Simulated Moving Bed Systems at Optimal Conditions for the Separation of Ternary Mixtures under Non-ideal Conditions, Ind. Eng. Chem. Res., 2006 (in press).

Kurup, A. S., K. Hidajat & A. K. Ray. A Comparative Study of Modified Simulated Moving Bed Systems at Optimal Conditions for the Separation of Ternary Mixtures of C_8 aromatics, Ind. Eng. Chem. Res., 2006 (under revision).

Kurup, A. S., K. Hidajat & A. K. Ray. Optimal Operation of a Pseudo-SMB Process for Ternary Separation under Non-ideal Conditions, Sep. Purif. Technol., 2006 (in press).

Appendix A

A.1 A note on NSGA-II with Jumping Genes (Kasat and Gupta, 2003)

There are many classical optimization techniques available in the literature based on deterministic approach. Most of these methods require an initial guess that is updated at the every iteration and the rate of convergence in such cases often depends on the initial guess. Also they suffer from a serious disadvantage of the solution getting easily trapped into zones of local minima/maxima and there is no way of getting out of such traps. Evolutionary algorithms have several advantages over these conventional techniques. These algorithms are robust and are probabilistic in nature and moreover these being population based techniques the chances of the optimal solutions getting trapped into local zones are small. Moreover, all these techniques can find several optimal solutions in a single run.

A popular technique in this group is genetic algorithm (GA) first developed by Holland (1975). Goldberg (1989) further developed this algorithm and provided what is known as simple GA (SGA). However the need to solve more complex problems led to the development of many more efficient, multi-objective optimization techniques. One such effective technique is the Non-dominated Sorting GA (NSGA) (Srinivas and Deb, 1995). Meanwhile the concept of elitism in multi-objective evolutionary algorithm was being developed which increases the chances of getting better solutions. One such elitist multi-objective evolutionary algorithm is the elitist non-dominated sorting genetic algorithm (NSGA-II) (Deb et al., 2002). In NSGA-II, a different sorting and sharing method is used, which reduces the numerical complexity to MN_p^2 operations in contrast to MN_p^3 operations required for NSGA-I, where M is the number of objective functions, and N_p is the number of chromosomes in the population. A further improvement to this technique is reported in the work of Kasat

and Gupta (2003). They introduced a modified mutation operator, its concept being borrowed from the working of jumping genes (JG) in natural genetics. This algorithm is being called as NSGA-II-JG. The jumping genes operation is carried out after crossover and normal mutation in NSGA-II. A part of the binary strings in the selected chromosomes is replaced with a newly (randomly) generated string of the same length. Only a single jumping gene was assumed to replace part of any selected chromosome. This operation helps to save considerable amount of the computation time (sometimes, gives correct solutions, which are missed by other algorithms) and is important for compute-intense multi-objective problems like that of the SMB and Varicol process. The steps involved in the algorithm are shown in the flow chart (Figure A.1).
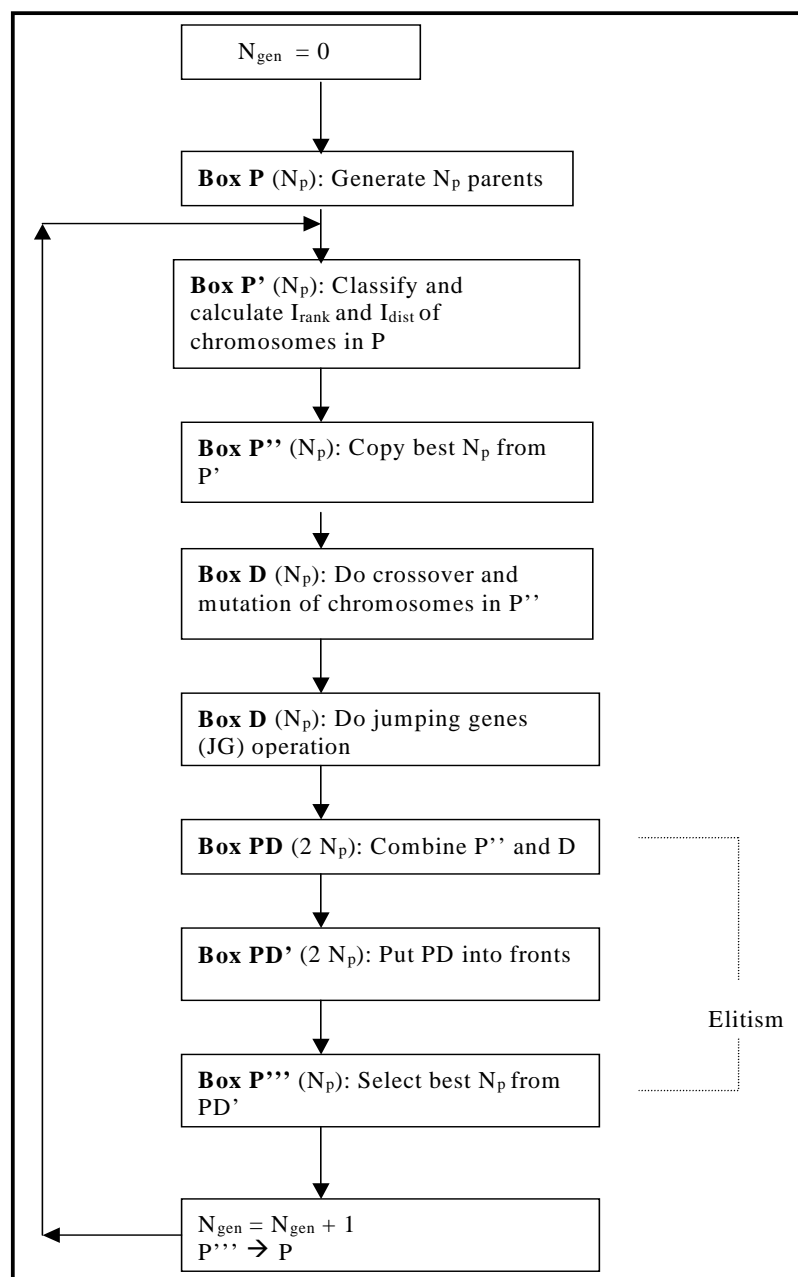
Figure A.1 Flow chart showing the steps involved in the optimization algorithm NSGA-II with JG (Kasat and Gupta, 2003)